MODELLING SUBMARINE LANDSCAPE EVOLUTION IN RESPONSE TO SUBDUCTION PROCESSES, NORTHERN HIKURANGI MARGIN, NEW ZEALAND

A thesis submitted in partial fulfilment of
the requirements for the degree of

Doctor of Philosophy in

Geology

at the University of Canterbury by

KATHERINE L PEDLEY

University of Canterbury
2010

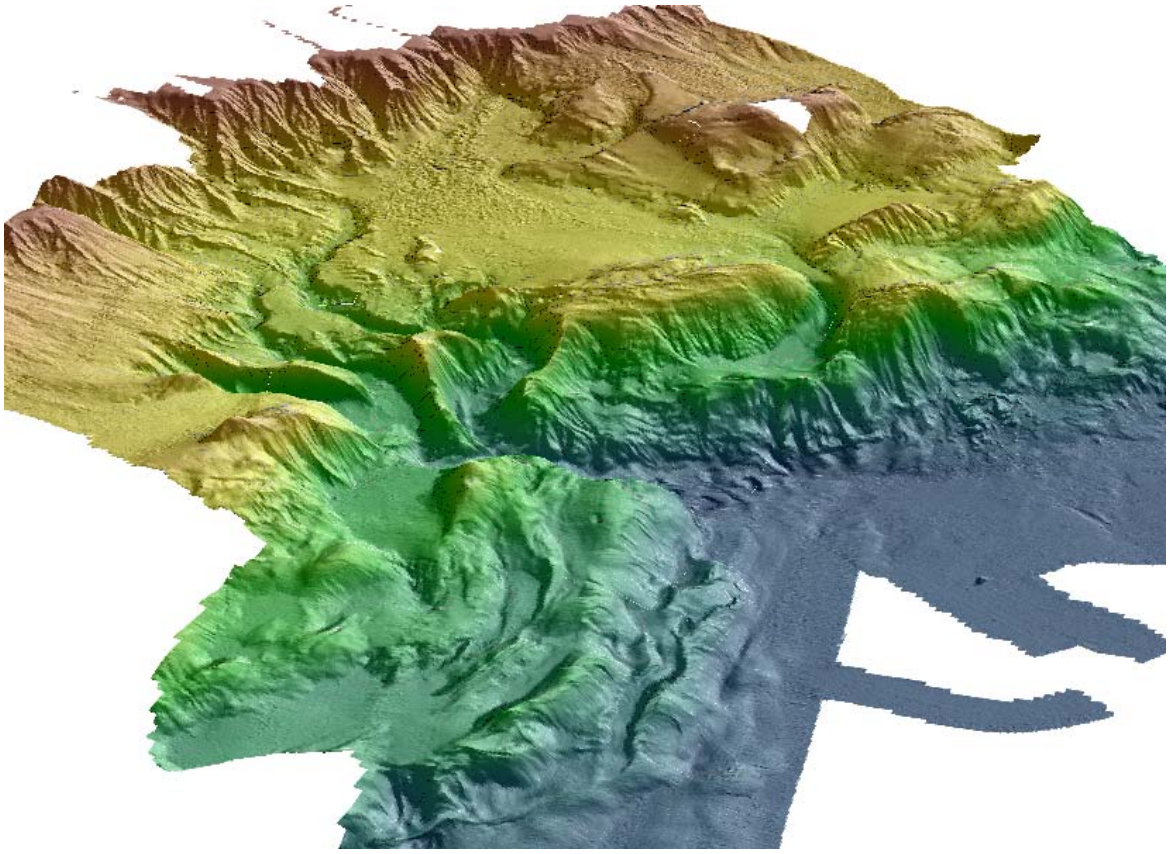

Oblique view of the Poverty Indentation digital elevation model (DEM), looking from south to north.

Table of Contents

APPENDICES

LIST OF FIGURES

LIST OF TABLES

Acknowledgements

First and foremost, thank you to my husband Dave, for all your love, support and encouragement. Thank you also to my very supportive parents, Pat and Nicky, and extra thanks Dad for proof-reading a couple of thesis chapters - your experience with theses and valuable suggestions made a huge difference. Thank you also to extended family and friends for your encouragement and friendship.

Thank you to my supervisory team of Professor Jarg Pettinga, Dr Phil Barnes and Dr Kari Bassett, and to our co-author Keith Lewis who has been an absolute mine of information and who lead the TAN0106 survey in 2001 that started this project. Thank you very much to Dr Kari Bassett for stepping in to help when most needed.

Thank you very much to Geoffroy Lamarche, Lionel Carter, Miles Dunkin, Mike Stevens, Claire Castellazzi, Arne Pallentin and Alan Orpin from the team at NIWA, Joshu Mountjoy (NIWA & UC), Clark Alexander, J.P. Walsh, and the crew, researchers and students aboard the RV Kilo Moana for the experience. Thank you also to Serge Lallemand (Montpellier Univ., France), Mike Finnemore (Southern Geophysical Ltd.), Bryan Davy (GNS Science), Callum Kennedy (Ministry of Economic Development, NZ), John Nicholson (DepthCon2000), Richard Jackson, Nicholas Christie-Blick (visiting researcher from Lamont-Doherty University, NY), and many others who have offered their advice, technical expertise and support. Much appreciation also goes to journal reviewers Bryan Davy and Gregory Moore for their comments and suggestions on the Marine Geology manuscript, and huge appreciation to my thesis examiners Dan Barker and Nina Kukowski - your feedback and suggestions were extremely constructive and helpful.

Thank you to the University of Canterbury Geological Sciences staff, particularly Pat Roberts, Janet Warburton, Anekant Wandres and John Southward for your technical support and advice. Last, but not least, thank you to the Geological Sciences department staff and students for making this a busy and exciting time and a wonderful place to be a part of. I look forward to the time ahead!

The steep forearc slope along the northern sector of the obliquely convergent Hikurangi subduction zone is characteristic of non-accretionary and tectonically eroding continental margins, with reduced sediment supply in the trench relative to further south, and the presence of seamount relief on the Hikurangi Plateau. These seamounts influence the subduction process and the structurally-driven geomorphic development of the over-riding margin of the Australian Plate frontal wedge.

The Poverty Indentation represents an unusual, especially challenging and therefore exciting location to investigate the tectonic and eustatic effects on this sedimentary system because of: (i) the geometry and obliquity of the subducting seamounts; (ii) the influence of multiple repeated seamount impacts; (iii) the effects of structurally-driven over-steeping and associated widespread occurrence of gravitational collapse and mass movements; and (iv) the development of a large canyon system down the axis of the indentation. High quality bathymetric and backscatter images of the Poverty Indentation submarine re-entrant across the northern part of the Hikurangi margin were obtained by scientists from the National Institute of Water and Atmospheric Research (NIWA) (Lewis, 2001) using a SIMRAD EM300 multibeam swath-mapping system, hull-mounted on NIWA's research vessel Tangaroa. The entire accretionary slope of the re-entrant was mapped, at depths ranging from 100 to 3500 metres. The level of seafloor morphologic resolution is comparable with some of the most detailed Digital Elevation Maps (DEM) onshore. The detailed digital swath images are complemented by the availability of excellent high-quality processed multi-channel seismic reflection data, single channel high-resolution 3.5 kHz seismic reflection data, as well as core samples. Combined, these data support this study of the complex interactions of tectonic deformation with slope sedimentary processes and slope submarine geomorphic evolution at a convergent margin.

The origin of the Poverty Indentation, on the inboard trench-slope at the transition from the northern to central sectors of the Hikurangi margin, is attributed to multiple seamount impacts over the last c. 2 Myr period. This has been accompanied by canyon incision, thrust fault propagation into the trench fill, and numerous large-scale gravitational collapse structures with multiple debris flow and avalanche deposits ranging in down-slope length from a few hundred metres to more than 40 km. The indentation is directly offshore of the Waipaoa River which is currently estimated to have a high sediment yield into the marine system. The indentation is recognised as the "Sink" for sediments derived from the Waipaoa River catchment, one of two target river systems chosen for the US National Science Foundation

(NSF)-funded MARGINS “Source-to-Sink” initiative. The Poverty Canyon stretches 70 km from the continental shelf edge directly offshore from the Waipaoa to the trench floor, incising into the axis of the indentation. The sediment delivered to the margin from the Waipaoa catchment and elsewhere during sea-level high-stands, including the Holocene, has remained largely trapped in a large depocentre on the Poverty shelf, while during low-stand cycles, sediment bypassed the shelf to develop a prograding clinoform sequence out onto the upper slope. The formation of the indentation and the development of the upper branches of the Poverty Canyon system have led to the progressive removal of a substantial part of this prograding wedge by mass movements and gully incision. Sediment has also accumulated in the head of the Poverty Canyon and episodic mass flows contribute significantly to continued modification of the indentation by driving canyon incision and triggering instability in the adjacent slopes.

Prograding clinoforms lying seaward of active faults beneath the shelf, and overlying a buried inactive thrust system beneath the upper slope, reveal a history of deformation accompanied by the creation of accommodation space. There is some more recent activity on shelf faults (i.e. Lachlan Fault) and at the transition into the lower margin, but reduced (~2 %) or no evidence of recent deformation for the majority of the upper to mid-slope. This is in contrast to current activity (approximately 24 to 47% shortening) across the lower slope and frontal wedge regions of the indentation. The middle to lower Poverty Canyon represents a structural transition zone within the indentation coincident with the indentation axis. The lower to mid-slope south of the canyon conforms more closely to a classic accretionary slope deformation style with a series of east-facing thrust-propagated asymmetric anticlines separated by early-stage slope basins. North of the canyon system, sediment starvation and seamount impact has resulted in frontal tectonic erosion associated with the development of an over-steepened lower to mid-slope margin, fault reactivation and structural inversion and over-printing.

Evidence points to at least three main seamount subduction events within the Poverty Indentation, each with different margin responses:

i) older substantial seamount impact that drove the first-order perturbation in the margin, since approximately ~1-2 Ma

ii) subducted seamount(s) now beneath Pantin and Paritu Ridge complexes, initially impacting on the margin approximately ~0.5 Ma, and

iii) incipient seamount subduction of the Puke Seamount at the current deformation front.

The overall geometry and geomorphology of the wider indentation appears to conform to the geometry accompanying the structure observed in sandbox models after the seamount has passed completely through the deformation front. The main morphological features correlating with sandbox models include: i) the axial re-entrant down which the Poverty Canyon now incises; ii) the re-establishment of an accretionary wedge to the south of the indentation axis, accompanied by out-stepping, deformation front propagation into the trench fill sequence, particularly towards the mouth of the canyon; iii) the linear north margin of the indentation with respect to the more arcuate shape of the southern accretionary wedge; and, iv) the set of faults cutting obliquely across the deformation front near the mouth of the canyon. Many of the observed structural and geomorphic features of the Poverty Indentation also correlate well both with other sediment-rich convergent margins where seamount subduction is prevalent particularly the Nankai and Sumatra margins, and the sediment-starved Costa Rican margin. While submarine canyon systems are certainly present on other convergent margins undergoing seamount subduction there appears to be no other documented shelf to trench extending canyon system developing in the axis of such a re-entrant, as is dominating the Poverty Indentation.

Ongoing modification of the Indentation appears to be driven by: i) continued smaller seamount impacts at the deformation front, and currently subducting beneath the mid-lower slope, ii) low and high sea-level stands accompanied by variations on sediment flux from the continental shelf, iii) over-steepening of the deformation front and mass movement, particularly from the shelf edge and upper slope.

CHAPTER 1: INTRODUCTION

1.1 PREAMBLE

The Poverty Indentation is a large (~4000 km^2) structural re-entrant in the Hikurangi Margin continental slope, directly off the coast of Poverty Bay, East Coast North Island (Figures 1.1 and 1.2). The formation of the indentation has previously been attributed to seamount collision and subduction into the margin, with ongoing responses from this impact including large-scale gravitational collapse and sedimentary erosion processes. The main aim of this research project is to improve our understanding of the tectonic processes operating in an accretionary margin setting when it is subjected to the collision of seamounts and how they may affect the stability and the structural geomorphology of the frontal wedge. In turn, we may gain further insight into the geohazards such as earthquakes, landslides, tsunamis, associated with this margin, their scale and genesis. The combined effects of these various morpho-structural processes shaping the frontal wedge, directly influence the sediment transport pathways from the continental shelf to the trench floor and these data sets provide an opportunity for innovative, detailed analysis of the interactive subduction driven tectonic processes with the sea floor geomorphic processes.

In recent years the acquisition of high quality swath bathymetry and multi-channel seismic data across the continental slope region are providing new insights into the off-shelf sediment transport, dispersal and storage system, and these in turn can be combined to underpin a structural geomorphic interpretation of the Poverty Bay Indentation. Based on this, we present in this project a morpho-structural evolutionary model for the indentation and address the role that the evolution of the indentation has played in influencing the sediment pathways from the continental shelf to the trench floor.

The indentation is recognised as the “Sink” for sediments derived from the Waipaoa River catchment (Figure 1.2), one of two target river systems chosen for the National Science Foundation (NSF)-funded MARGINS “Source-to-Sink” initiative (the other is Fly River System, Papua New Guinea - see Haq et al. 2004). The key objective of the source-to-sink (S2S) programme is to investigate the linked terrestrial source, fluvial and marine sediment transport/dispersal, and final sediment sequestration on the continental shelf, slope/structural

trench and extending across the Hikurangi Plateau (Figure 1.1). The Poverty Indentation represents an unusual, especially challenging, and therefore exciting location to investigate the tectonic and eustatic effects on this sedimentary system because of:

i) The obliquity of the subduction margin convergence

ii) The influence of multiple repeated seamount impacts

iii) The effects of structurally-driven over-steeping and associated widespread occurrence of gravitational collapse and mass movements

iv) The development of a large canyon system down the axis of the indentation

In combination all of these features significantly influence the location and effectiveness of sediment transport pathways through the indentation, and also function to entrap sediment locally in structurally formed basins on the shelf and slope of the margin.

To fully understand the Waipaoa S2S system, the structural, geomorphic and evolutionary components must first be comprehensively investigated and understood. The NZ and NSF S2S initiative has resulted in a series of coordinated projects investigating the various sectors from the terrestrial Waipaoa source to the offshore sink. A key outcome from this programme will be the development of an integrated understanding of the Waipaoa S2S system, in particular its response and sensitivity to the key tectonic and paleoclimatic drivers, in terms of sediment supply, transport, dispersal and sequestration respectively across the margin. In this study we recognise that the spatial and temporal evolution of the margin indentation has resulted in a very complex morpho-structural feature, and does not represent a simple closed sediment sink.

The project is a collaboration between the Active Tectonics and Earthquake Hazard Research Programme, University of Canterbury, and the National Institute of Water and Atmospheric Research (NIWA), with linkages to the United States National Science Foundation (NSF)-funded MARGINS Source-to-Sink initiative.

1.1.1 Project Objectives

Key project objectives include:

- Construct a detailed geomorphological map of the Poverty re-entrant and its associated features (identifying major and minor faults, folds, gullies, mass movement etc.).

- Undertake a detailed analysis of seismic reflection profiles of both high and low frequency data

- Integrate seismic and morpho-structural data to construct a model to identify the structure and tectonics of the region and help establish the processes that have influenced the tectonic and geomorphic setting.

- Investigate the geomorphological evolution of a shelf edge canyon system and how it may be affected by: i) the subduction of seamounts; ii) fault zone segmentation; and iii) mass failure.

- Investigate the major structures driving seafloor topography and identify their structural geometry and deformation styles.

- Quantitatively investigate the rates of deformation in the toe of slope accretionary wedge at the Poverty Indentation in order to establish the plate motion budget for the offshore sequence of the Hikurangi Margin.

- Compare analogue sandbox models of seamount collision and subduction effects on a convergent margin to the present day Poverty Indentation to generate 3D evolution models.

- Investigate how the processes of seamount collision and subduction contribute to the development and evolution of the Poverty Indentation and the effect on the sediment transport pathways from the continental shelf to the trench floor.

1.1.2 Thesis Organisation

This thesis is organised into eight chapters and four appendices. All figures for each chapter are presented at the back of each chapter, after each list of references. Chapters 4, 6 and 7 are organised as potential future publications.

Chapter 1 (this chapter) includes the introduction to the project and the study area, as well as addressing the processes of seamount subduction and collapse on convergent margins, the main focus for investigating the Poverty Indentation. Chapter 2 presents the methods used in

this project and a set of high quality data, collected over a number of voyages and combined in this project to enable detailed insights into the morphology, structures and processes acting on this continental slope environment. Chapter 3 is the main body of this thesis and presents a summary of the formation and evolution of the Poverty Indentation and how it compares globally. Groundwork for Chapter 3 is a published journal manuscript, the reprint for which is attached in Appendix 3. The following chapters thus expand on and provide much of the groundwork for this chapter so there is some repetition where appropriate. Chapter 4 presents an insight into the geomorphology and sedimentary processes ongoing in the Poverty Indentation, in particular the role of landslides and canyons in sediment transfer though the system. Chapter 5 presents the seismic data analyses and interpretations for this project and a presentation of the structural geomorphic map generated for the Poverty Indentation. Chapter 6 covers an investigation into the plate motion budget across the northern Hikurangi margin and the rates of horizontal shortening present in the frontal wedge. Chapter 7 is a globally focussed chapter on the effects of seamount subduction on convergent margins and compared to our observations in the Poverty Indentation. Chapter 8 outlines the main conclusions from this project and potential future work. Appendix 1 is the manuscript reprint for Pedley et al., 2009 and Appendix 2 is the manuscript reprint for Barnes et al., 2009, where I am ninth author. Appendix 3 presents some of the velocity data used for depth conversion, as well as correlations to the seismic profiles. Appendix 4 presents the uninterpreted seismic profiles from seismic arrays TAN0106, GeodyNZ and Mobil used in this project. Seismic profiles from the CM05 array are available to the general public from the MED Crown Minerals division at www.crownminerals.govt.nz.

1.2 THE MARGINS SOURCE-TO-SINK INITIATIVE

Sedimentary sequences accumulating at continental margins provide detailed records on paleo-climates, sea level change, tectonics/deformation, geomorphic evolution and even anthropogenic effects (e.g. Orange, 1999; Carter et al., 2002; Greene et al., 2002). Because of their proximity to, and the high sediment input from rivers, marine continental margins may preserve a far greater and more complete record of terrestrial erosional processes and the geological evolution of the margin than the sedimentary record of the more distal abyssal plain. The primary objective of the MARGINS Initiative is to understand the processes that

control the initiation and evolution of continental margins (Haq et al., 2004). Within that context, the primary research questions of the Source-to-Sink initiative are:

i) How do tectonics, climate, sea level fluctuations, and other forcing parameters regulate the production, transfer, and storage of sediments and solutes from their sources to their sinks?

ii) What processes initiate erosion and sediment transfer, and how are these processes linked through feedbacks?

iii) How do variations in sediment processes and fluxes and longer-term variations such as tectonics and sea level build the stratigraphic record to create a history of global change?

(Haq et al., 2004)

While a number of previously published studies have addressed the development of similar indentations along other subduction margins (e.g. Fryer and Smoot, 1985; Lallemand and Le Pichon, 1987; Dubois et al., 1988; Lallemand et al., 1989; Masson et al., 1990; Robertson, 1998; Hühnerbach et al., 2005), the oblique convergence occurring along the Hikurangi Margin provides for new insights into the effects of multiple seamount impacts on the morpho-structural development of the forearc slope as well as their influence on the associated sediment dispersal system. The northern sector of the Hikurangi Plateau, offshore the Gisborne/East Cape region, is studded with large seamounts (Figure 1.2). Episodic collision of these seamounts with the subduction margin will significantly affect the morpho-structural evolution of the frontal wedge and in turn influence sediment pathways.

1.3 TECTONIC SETTING

New Zealand straddles the plate boundary between the Pacific and Australian Plates (Figure 1.1). Much of the Upper Cenozoic geological development of the North Island is fundamentally related to the oblique subduction of the Pacific plate beneath the continental lithosphere of the Australian plate, forming what is known as the Taupo-Hikurangi arc-trench system. This system includes both the Hikurangi Trench off the east coast of the North Island, as well as the Taupo Volcanic Zone. The Pacific Plate is being subducted westwards beneath

the Australian plate at a rate of c. 50 mm/yr (De Mets et al., 1990) at an angle nearly perpendicular to the plate boundary. Offshore of the North Island, a 150 km wide emergent accretionary wedge has formed and is being progressively uplifted to form the ranges east of the Taupo Volcanic Zone (Figure 1.1). This region also incorporates the dextral North Island Shear Belt. This shear belt accommodates a lateral component of the plate motion with dextral strike-slip (Lewis, 1980; Beanland et al., 1998) and also net rotation of the eastern North Island (e.g. Wallace et al., 2004; Wallace and Beavan, 2006; Wallace et al., 2008). To the south subduction becomes increasingly oblique, and abruptly ceases to the south of a line from about Cheviot to Westport in northern South Island, as the anomalously thick oceanic crust of the Hikurangi Plateau changes to continental crust on the Pacific Plate (Walcott, 1978; Lewis and Pettinga, 1993; Barnes et al., 1998) (Figure 1.1). This leads into the Alpine Fault (Freund, 1971; Campbell, 1973; Wellman, 1979; Bibby et al., 1980; Chanier and Ferrière, 1991; Berryman et al., 1992), a major intracontinental dextral transform fault that runs through most of the South Island before linking to the east-facing subduction zone of the Australian Plate beneath the Pacific Plate, beginning in offshore Fiordland with the formation of the Puysegur Trench (Christoffel and Van der Linden, 1972; Davey and Smith, 1983; Barnes et al., 1998; Lamarche et al., 1998; Melhuish et al., 1999) (Figure 1.1).

1.4 HIKURANGI SUBDUCTION ZONE

The Hikurangi subduction zone (or Hikurangi margin) is a southward continuation of the Tonga-Kermadec subduction system (Figure 1.1). Outboard of the Hikurangi Trench the subducting plate incorporates the Hikurangi Plateau, a section of anomalously thick Mesozoic age oceanic crust (10-15 kms) comprised of an accumulation of seamount ridges, lava flows and Cretaceous sedimentary basins (Davy and Wood, 1994). To the west of the Hikurangi Trench, where the Pacific Plate is subducting beneath the Australian Plate, a very wide frontal accretionary wedge (prism) has developed in response to, and records, several phases of deformation and off-scraping of sediment (Lewis, 1980; Chanier and Ferrière, 1991; Lewis and Pettinga, 1993; Collot et al., 1996; Barnes et al., 1998; Barnes et al., 2002) (Figure 1.1).

The main structures of a subduction zone, such as are present in the Hikurangi margin, are faults in the outer wall of the trench (in the subducting Pacific Plate); a frontal wedge in the inner wall (the overriding Australian Plate); and trench morphology (affected by the angle at which the oceanic plate is subducting and asperities being subducted) (Aubouin, 1989).

Deformation in the overriding plate is dominantly controlled by the subduction of the oceanic plate and will reflect the rates of subduction, the angle at which the subducting plate is converging with the overriding plate, the amount of slip between plates, volume of sediments being underplated and presence or absence of seamounts (Nicol and Beavan, 2003). The central sector of the Hikurangi margin is classified as a convergent compressive margin (Aubouin, 1989) as the moderate subduction rate (45 mm/yr) and the high sedimentation rate from both transport of South Island material from the Hikurangi Channel and material from the Waipaoa catchment have formed a significant accretionary frontal wedge (Lewis and Pettinga, 1993). In contrast, the northern sector can perhaps be classified as a convergent erosional margin (Aubouin, 1989) due to sediment starvation in the region and high rates of erosion.

The Hikurangi margin is unique from other accretionary wedge-forming subduction margins due to the combination of the increased thickness of the subducting oceanic plate (Davy and Wood, 1994; Wood and Davy, 1994), the oblique nature of convergence (Collot et al., 1996) and the vast thickness of Quaternary trench fill sediments (>2-3 km) (Carter et al., 2002).

1.5 THE POVERTY INDENTATION

The study area for this research encompasses a feature known as the Poverty Indentation (Figure 1.2). This is a large (70 km in length) canyon system and associated large (4000 km^2) re-entrant in the Hikurangi Margin located just north of the boundary between the central sector and the northern sector. Locally, the study area highlights the differences between the characteristics of those two sectors, expressed as a well-developed accretionary wedge and gentler slopes in the southern half contrasting with steep slopes and numerous failures to the north of the canyon system.

High quality bathymetric and backscatter images of the Poverty Indentation submarine re-entrant across the northern part of the Hikurangi margin (subduction zone) were obtained by scientists from the National Institute of Water and Atmospheric Research (NIWA) (Lewis, 2001) using a SIMRAD EM300 multibeam swath-mapping system, hull-mounted on NIWA's research vessel Tangaroa. The entire accretionary slope of the re-entrant was mapped, at depths ranging from ~100 to 3500 metres. The level of seafloor morphologic resolution is comparable with some of the most detailed Digital Elevation Maps (DEM) onshore. Images

are available with spatial resolution down to 2 m, with an average of 25 m spatial resolution, potentially facilitating some extraordinarily detailed submarine landform analyses. The origin of the slope re-entrant is inferred to be related to multiple seamount impacts, and these collisions have initiated numerous large-scale gravitational collapse structures, multiple debris flow and avalanche deposits, which range in down-slope length from a few hundred metres to more than 40 km. At some places, head-scarp cracks in the slopes indicate incipient collapse. The Poverty Indentation has been simultaneously eroded by canyon systems that exhibit many of the features of incised river systems onshore, as well as capture and slump dams. A new canyon system, the route of which is partly controlled by avalanches, is developing north of the main canyon system. On the lower slope, a thrust-faulted accretionary wedge is developing, and slumping seaward of a bulge indicates collapse in the wake of a recently subducted, small seamount.

The detailed digital swath images are complemented by the availability of excellent high-quality processed multi-channel seismic reflection data, single channel high-resolution 3.5 kHz seismic reflection data, as well as core samples. These combined are supporting a study of the complex interactions of tectonic deformation with slope sedimentary processes and slope submarine geomorphic evolution at a convergent margin.

1.6 SEAMOUNT SUBDUCTION ALONG CONVERGENT MARGINS

The morpho-structural evolution, structural geometries and styles of deformation characteristic of active convergent margins are now recognised to be significantly influenced by the extent to which sediment is being underplated, and the subduction of seamounts and other asperities (e.g. ridges, guyots and plateaus) is taking place. Where seamounts are subducted the degree and geometry of deformation experienced by the margin depends on the dimensions and orientation of the asperity, the structure, dip and convergence rate of the oceanic plate, and the geology and tectonic regime of the overriding plate (Dominguez et al., 1998a; Dominguez et al., 1998b; Dominguez et al., 2000) (e.g. Figure 1.3). Early research on seamount subduction in the Mariana and Izu-Bonin trenches identified that seamounts and ridges larger than 100 km diameter may be able to interrupt normal subduction processes and cause uplift along the margin (Fryer and Smoot, 1985). Seamounts less than 40 km diameter were observed to have the same or greater degree of fracturing as the seafloor surrounding

them, suggesting that seamounts must be at least 40 km diameter or greater to have an influence on larger scale subduction margin dynamics. Despite the significant fracturing in small seamounts, it was thought that all seamounts are subducted at least substantially intact (e.g. Fryer and Smoot, 1985; Dominguez et al., 2000) and may have significant effects on material transfer, fluid expulsion and tectonic erosion (Dominguez et al., 2000) (Figure 1.4). The fluid pressure along the basal (plate) décollement may be modified by subduction and underplating of relatively undeformed, water-laden sediments and the associated fluid expulsion along faults in the over-riding wedge. Consequently, significant variations in the effective basal friction and local mechanical coupling between the two plates could be expected around the subducting seamount (Dominguez et al., 2000).

Both tectonic erosion and accretion on subduction margins may be determined by the subducting oceanic plate, despite frontal tectonic erosion being more frequently documented in conventional surveys. Tectonic erosion is mostly due to the relaxation and collapse of the margin slope in the wake of a subducting asperity (Lallemand et al., 1990). During subduction, the lower (outboard) margin slope topography will reflect the underlying oceanic plate topography, even if the irregularities are small amplitude fault scarps. This implies that even the smallest asperity will have some impact on the slope expression. In marine surveys the frontal wedge is observed to thicken directly inboard and above the leading slope of the seamount (or other asperity). Collapse will occur in the wake of the subducting asperity, over the trailing slope of the seamount (Lallemand et al., 1990). Transverse (strike-slip and oblique-slip) faulting in the lower slope resulting from the direct collision of the seamount appears to be a common occurance in many margins subject to seamount subduction (i.e. Japan, Costa Rica, Solomon Islands, Java, Tonga-Kermadec, New Hebrides/Vanuatu, Philipines, Peru). Eventual underplating or subcrustal accretion of tectonic slices of the seamount to the over-riding plate is thought to be highly likely (Maruyama and Liou, 1989; Lallemand et al., 1990; Park et al., 2002).

Subduction of seamounts in Japan and Java (Konishi, 1989; Lallemand et al., 1989; Yamazaki and Okamura, 1989; Masson et al., 1990) have been observed to produce significant disruption to margin accretion with resulting uplift, however, there are some key differences noted with respect to the geometry and degree of disruption between each margin setting. Research along the Japan Trench has revealed a possible link between the subduction of seamounts and the long-term seismic and tsunamic regime (Zhao et al., 1997). It has been proposed that subducted seamounts may act as strong asperities, causing rupture by stick-slip

mechanism, and that the size of a seamount controls the maximum size of seamount-induced earthquakes (Cloos, 1992; Estabrook et al., 1994). This has been illustrated to some extent in the Japan trench as, taking into account the sizes of the seamounts colliding along this margin, expected earthquake magnitudes are limited to M 7.0 – 7.5 in the southern sector of the NE segment of the trench, based on records from 830 – 1995 AD (Zhao et al., 1997).

1.7 MARGIN COLLAPSE AS A RESULT OF SEAMOUNT SUBDUCTION

Convergent margins are highly unstable as the active forearc slopes are maintained at a critical taper angle, resulting in a dominance of catastrophic slope failure (Torelli et al., 1997). These types of failures along subduction margins, while relatively numerous, are generally not of the large scale observed on oceanic volcanoes and passive margins (Garcia and Hull, 1994; Moore et al., 1994; Clague and Moore, 2002), despite the instability of convergent margins.

Many large submarine landslides are thought to have failed as rotational slumps which involve the 'slow or intermittent, downslope movement of largely intact, back-tilting blocks on glide planes as much as 10 km below the seabed' (Moore et al., 1994). Large catastrophic slope failures also occur as 'disaggregated debris avalanches', with blocks up to many kilometres across and run-out distances of many tens to more than a hundred kilometres (Bugge et al., 1987; Barnes and Lewis, 1991; Garcia and Hull, 1994; Moore et al., 1994; Lewis, 1997; Torelli et al., 1997; Gardner et al., 1999; Collot et al., 2001; Clague and Moore, 2002; Locat and Lee, 2002a; von Huene et al., 2004). Other types of failures occur as smaller, thinner, more disaggregated sediment slurries and contain fewer, rafted blocks. These are known as debris flows and will travel faster and further than the debris avalanches. The latter may, however, incorporate water and mud to transform into turbidity currents, thus able to travel over a thousand kilometres away from source (Garcia and Hull, 1994). Failure for many submarine slopes along convergent margins can be associated with excess pore pressure in the sedimentary successions, maintained by gas, often in the form of unstable clathrates (e.g. Bugge et al., 1987). Rapid sediment overloading or tectonic stresses can also be causes of slope failure.

Unlike the frequent smaller collapse features observed along the likes of the California continental margin and other convergent margins (e.g. Torelli et al., 1997; Gardner et al.,

1999; Orange, 1999; Yun et al., 1999), large-scale collapse appears to be a common occurrence along the Hikurangi margin. These large-scale collapse features are suggested to have formed by a variety of mechanisms including underplating of trench fill, seamount subduction, seismic activity, pore pressures, gas bubble formation and sediment loading on steep slopes (Barnes and Lewis, 1991; Lewis, 1997; Lewis, 1998; Chanier et al., 1999; Collot et al., 2001; Lewis et al., 2004; Pettinga, 2004). Seamount subduction appears to be the dominant mechanism for the largest collapse features, as illustrated in the Ruatoria indentation to the north of the Poverty Indentation (Collot et al., 2001; Lewis et al., 2004) (Figure 1.5), unlike the dominance of gas, seismic and sedimentation rate-determined collapse observed on some other continental margins (i.e. Moore et al., 1994; Torelli et al., 1997; Gardner et al., 1999).

The giant Ruatoria debris avalanche cuts across the Hikurangi margin directly offshore from East Cape and just north of this project field area (Lewis et al., 1998; Collot et al., 2001; Lewis et al., 2004) (Figure 1.5). To produce a submarine failure of this magnitude, collapse is likely to have required the influence of an outside process or feature that disrupts the 'normal/expected' subduction margin processes (Robertson and Karamata, 1994; Dominguez et al., 1998b). Failure in the Ruatoria region is possibly synchronous with major extensional collapse in the upper slope, marked by a smaller indentation. It is suggested that the main collapse was triggered in response to progressive seamount collision into the slope as it was subducted beneath the Australian Plate around 2.0-0.16 Ma. The seamount cut an oblique groove in the slope as it subducted, causing instability in a triangle-shaped region in the oversteepened margin front. This eventually collapsed as the blocky avalanche deposit now observed radiating out of the main scalloped indentation (Lewis et al., 1998; Collot et al., 2001) (Figure 1.5). Volume calculations on the amount of material that should have originated out of the indentation, suggest that 600 km^3 of material is missing from the avalanche deposits. This may indicate either that erosion can not be the primary mechanism by which indentations are created with material displaced landward by thrusting and folding ahead of an asperity (Masson et al., 1990), or subduction of some of the deposits since collapse and resulting in internal compression of the margin. This may also help explain why features of this size are not often observed along convergent margins, and also perhaps the origin of olistostromes (a bed or layer of olistoliths – waterlain block of pebble to boulder-sized grains that differs greatly in its petrography, composition or texture from the surrounding rocks) in fold belts (Collot et al., 2001). Doming hills onshore with coastal

terraces that are experiencing uplift rates of 2.6 m/ka suggest that the seamount responsible for the Ruatoria indentation and debris avalanche now lies some 10 km west of East Cape (Lewis et al., 1998; Lewis et al., 2004).

1.8 SUBMARINE CANYON DEVELOPMENT

Submarine canyons, gullies and other seafloor valleys provide important conduits for sediment across continental margins all over the globe (e.g. Soh et al., 1990; Hagen et al., 1994; Hagen et al., 1996; Lewis and Barnes, 1999; Lastras et al., 2007; Arzola et al., 2008; Kuehl et al., 2008). Their location and morphology are controlled by a number of factors including structural fabric, regional tectonic processes, sea-level variations and sediment supply (Soh and Tokuyama, 2002). Many canyons are restricted to the upper slope but some manage to extend all the way to the base of the lower slope and incise significantly into the continental shelf. These extensive canyon systems are important sediment conduits, intersecting the along-shelf sediment transport pathways and significantly contributing to dispersal of terrigenous sediment by gravity-driven turbidites to the margin structural trench depocentres (e.g. Lewis and Barnes, 1999). During low-stands, the continental shelf depocentres can be directly bypassed.

Significant sediment conduits on the Hikurangi margin from the continental shelf edge to trench floor include the extensive Cook Strait Canyon at the southern end of the margin (Mountjoy et al., 2009; Mountjoy, 2009), the smaller Pahaua Canyon, offshore Wairarapa (Mountjoy et al., 2009), the Poverty Canyon (Lewis, 2001; Pedley et al., 2010), and to a lesser extent, the Ruatoria debris avalanche, offshore East Cape (e.g. Lewis et al., 2004) (Figure 1.6). The distribution of these canyons along the continental slope means that the Poverty Canyon system, a 70 km long incision directly down the axis of the Poverty Indentation, represents the only significant sediment transport pathway to directly reach the Hikurangi Trough for nearly 300 km north along the margin (Lewis et al., 1998). Directly south of the Poverty Canyon, the large 200 km wide accretionary wedge prevents sediment from transferring directly to the trough from the continental shelf, due to thrust fault-propagated anticlinal ridges acting as baffles (e.g. Barnes et al., 2009). The Hikurangi margin also contains the Madden Canyon (Figure 1.6), a shelf to mid-slope incision that appears to be constrained by the active thrust faulted anticlines of the accretionary wedge, preventing it

from reaching the trench floor (Lewis and Pettinga, 1993; Mountjoy et al., 2009; Mountjoy, 2009).

This project investigates the important link between the creation of the indentation as a result of seamount impact and subduction, and the subsequent formation of the canyon as a significant sediment pathway.

References

Arzola, R.G., Wynn, R.B., Lastras, G., Masson, D.G. and Weaver, P.P.E., 2008. Sedimentary fetaures and processes in the Nazare and Setubal submarine canyons, west Iberian margin. Marine Geology, 250: 64-88.

Aubouin, J., 1989. Some aspects of the tectonics of subduction zones. Tectonophysics, 160(1-4): 1-3, 7-21.

Barnes, P.M. and Lewis, K., 1991. Sheet slides and rotational failures on a covergent margin: the Kidnappers Slide, New Zealand. Sedimentology, 38: 205-221.

Barnes, P.M., Mercier de Lepinay, B., Collot, J.-Y., Delteil, J. and Audru, J.-C., 1998. Strain partitioning in the transition area between oblique subduction and continental collision, Hikurangi Margin, New Zealand. Tectonics, 17(4): 534-557.

Barnes, P.M., Nicol, A. and Harrison, T., 2002. Late Cenozoic evolution and earthquake potential of an active listric thrust complex above the Hikurangi subduction zone, New Zealand. GSA Bulletin, 114(11): 1379-1405.

Barnes, P.M., Lamarche, G., Bialas, J., Henrys, S., Pecher, I.A., Netzeband, G., Greinert, J., Mountjoy, J.J., Pedley, K.L. and Crutchley, G., 2009. Tectonic and Geological Framework for Gas Hydrates and Cold Seeps on the Hikurangi Subduction Margin, New Zealand. Marine Geology, in press.

Beanland, S., Melhuish, A., Nicol, A., Ravens, J.M. and Anonymous, 1998. Structure and deformational history of the inner forearc region, Hikurangi subduction margin, New Zealand. New Zealand Journal of Geology and Geophysics, 41(4): 325-342.

Berryman, K.R., Beanland, S., Cooper, A.F., Cutten, H.N., Norris, R.J., Wood, P.R., Buckman, R.C. and Hancock, P.L., 1992. The Alpine Fault, New Zealand; variation in Quaternary structural style and geomorphic expression. Annales Tectonicae, 6, Suppl.: 126-163.

Bibby, H.M., Haines, A.J., Walcott, R.I. and Anonymous, 1980. Structure and kinematics of the Pacific/Indian plate boundary zone through New Zealand.

Bugge, T., Befring, S., Belderson, R.H., Eidvin, T., Jansen, E., Kenyon, N.H., Holtedahl, H. and Sejrup, H.P., 1987. A giant three-stage submarine slide off Norway. Geo-Marine Letters, 7(4): 191-198.

Campbell, J.K., 1973. Displacement data from the Alpine Fault at Lake Rotoiti and its relevance to glacial chronology and the tempo of tectonism, Abstracts from the IXth INQUA Congress, Christchurch, New Zealand, pp. 57-58.

Carter, L., Manighetti, B., Elliot, M., Trustrum, N. and Gomez, B., 2002. Source, sea level and circulation effects on the sediment flux to the deep ocean over the past 15 ka off eastern New Zealand. Global and Planetary Change, 33(3-4): 339-355.

Chanier, F. and Ferrière, J., 1991. From a passive to an active margin; tectonic and sedimentary processes linked to the birth of an accretionary prism (Hikurangi Margin, New Zealand). Bulletin de la Societe Geologique de France, 162(4): 649-660.

Chanier, F., Ferrière, J., Angelier, J. and Anonymous, 1999. Relations between large scale rotations and tectonic deformations in an active margin setting; Hikurangi subduction margin (New Zealand). Memoires Geosciences-Montpellier, 14: 253-257.

Christoffel, D.A. and Van der Linden, W.J.M., 1972. Macquarie Ridge-New Zealand Alpine Fault transition. Antarctic Research Series, 19: 235-242.

Clague, D.A. and Moore, J.G., 2002. The proximal part of the giant submarine Wailau Landslide, Molokai, Hawaii. Journal of Volcanology and Geothermal Research, 113(1-2): 259-287.

Cloos, M., 1992. Thrust-type subduction-zone earthquakes and seamount asperities; a physical model for seismic rupture. Geology, 20(7): 601-604.

Collot, J.-Y., Delteil, J., Lewis, K.B., Davy, B., Lamarche, G., Audru, J.-C., Barnes, P., Chanier, F., Chaumillon, E., Lallemand, S.E., Mercier de Lepinay, B., Orpin, A., Pelletier, B., Sosson, M., Toussaint, B. and Uruski, C., 1996. From oblique subduction to intra-continental transpression; structures of the southern Kermadec-Hikurangi margin from multibeam bathymetry, side-scan sonar and seismic reflection. Marine Geophysical Researches, 18(2-4): 357-381.

Collot, J.-Y., Lewis, K., Lamarche, G. and Lallemand, S., 2001. The giant Ruatoria debris avalanche on the northern Hikurangi margin, New Zealand; results of oblique seamount subduction. Journal of Geophysical Research, B, Solid Earth and Planets, 106(9): 19,271-19,297.

Davey, E.J. and Smith, E.G.C., 1983. The tectonic setting of the Fiordland region, South-West New Zealand. Geophysical Journal of the Royal Astronomical Society, 72(1): 23-38.

Davy, B. and Wood, R., 1994. Gravity and magnetic modelling of the Hikurangi Plateau. Marine Geology, 118(1-2): 139-151.

De Mets, C., Gordon, R.G., Argus, D.F. and Stein, S., 1990. Current plate motions. Geophysical Journal International, 101: 425-478.

Dominguez, S., Lallemand, S., Malavieille, J. and Schnurle, P., 1998a. Oblique subduction of the Gagua Ridge beneath the Ryukyu accretionary wedge system: Insights from marine observations and sandbox experiments. Marine Geophysical Researches, 20: 383-402.

Dominguez, S., Lallemand, S.E., Malavieille, J. and von Huene, R., 1998b. Upper plate deformation associated with seamount subduction. Tectonophysics, 293(3-4): 207-224.

Dominguez, S., Malavieille, J. and Lallemand, S., 2000. Deformation of accretionary wedges in response to seamount subduction - insights from sandbox experiments. Tectonics, 19(1): 182-196.

Dubois, J., Deplus, C., Diament, M., Daniel, J. and Collot, J.-Y., 1988. Subduction of the Bougainville seamount (Vanuatu): mechanical and geodynamic implications. Tectonophysics, 149(1-2): 111-119.

Estabrook, C.H., Jacob, K.H. and Sykes, L.R., 1994. Body wave and surface wave analysis of large and great earthquakes along the eastern Aleutian Arc, 1923-1993; implications for future events. Journal of Geophysical Research, B, Solid Earth and Planets, 99(6): 11,643-11,662.

Freund, R., 1971. The Hope Fault: a strike-slip fault in New Zealand. Bulletin of the New Zealand Geological Survey, 86, 49 pp.

Fryer, P. and Smoot, N.C., 1985. Processes of seamount subduction in the Mariana and Izu-Bonin trenches. Marine Geology, 64(1-2): 77-90.

Garcia, M.O. and Hull, D.M., 1994. Turbidites from giant Hawaiian landslides; results from Ocean Drilling Program Site 842. Geology, 22(2): 159-162.

Gardner, J.V., Prior, D.B. and Field, M.E., 1999. Humboldt Slide; a large shear-dominated retrogressive slope failure. Marine Geology, 154(1-4): 323-338.

Greene, H.G., Maher, N.M. and Paull, C.K., 2002. Physiography of the Monterey Bay National Marine Sanctuary and implications about continental margin development. Marine Geology, 181(1-3): 55-82.

Hagen, R.A., Bergersen, D.D., Moberly, R. and Coulbourn, W.T., 1994. Morphology of a large meandering submarine canyon system on the Peru-Chile forearc. Marine Geology, 119: 7-38.

Hagen, R.A., Vergara, H. and Naar, D.F., 1996. Morphology of San Antonio submarine canyon on the central Chile forearc. Marine Geology, 129: 197-205.

Haq, B., Karner, G.D. and Morris, J.D., 2004. NSF MARGINS Program Science Plans 2004, Lamont-Doherty Earth Observatory of Columbia University, New York.

Hühnerbach, V., Masson, D.G., Bohrmann, G., Bull, J.M. and Weinrebe, W., 2005. Deformation and submarine landsliding caused by seamount subduction beneath the Coasta Rica continental margin - new insights from high-resolution sidescan sonar data. In: D.M. Hodgson and S.S. Flint (Editors), Submarine Slope Systems: Processes and Products. Geological Society, Special Publications, London, pp. 195-205.

Konishi, K., 1989. Limestone of the Daiichi Kashima Seamount and the fate of a subducting guyot: fact and speculation from the Kaiko "Nautile" dives. Tectonophysics, 160(1-4): 249-265.

Kuehl, S., Miller, A.J., Kniskern, T.A., Gerber, T. and Pratson, L., 2008. Sediment trapping and bypassing in active continental margin settings: New insights from MARGINS Source-to-Sink studies. Geological Society of America Abstracts with Programs, 40(6): 319.

Lallemand, S. and Le Pichon, X., 1987. Coloumb wedge model applied to the subduction of seamounts in the Japan Trench. Geology, 15: 1065-1069.

Lallemand, S., Culotta, R. and Von Huene, R., 1989. Subduction of the Daiichi Kashima Seamount in the Japan Trench. Tectonophysics, 160(1-4): 231-233.

Lallemand, S., Collot, J.-Y., Pelletier, B., Rangin, C. and Cadet, J.-P., 1990. Impact of oceanic asperities on the tectogenesis of modern convergent margins. Oceanologica Acta, Special 10: 56-69.

Lamarche, G., Lebrun, J.F., Collot, J.Y. and Anonymous, 1998. Tectonics at a transform-subduction relay zone, the Puysegur area, south of New Zealand. Annales Geophysicae (1988), 16, Suppl. 1: 47.

Lastras, G., Canals, M., Urgeles, R., Amblas, D., Ivanov, M., Droz, L., Dennielou, B., Fabres, J., Schoolmeester, T., Akhmetzhanov, A., Orange, D.L. and Garcia-Garcia, A., 2007. A walk down the Cap de Creus canyon, Northwestern Mediterranean Sea: Recent processes inferred from morphology and sediment bedforms. Marine Geology, 246(2-4): 176-192.

Lewis, K., Collot, J.-Y. and Lallemand, S., 1998. The dammed Hikurangi Trough: a channel-fed trench blocked by subducting seamounts and their wake avalanches (New Zealand-France GeodyNZ Project). Basin Research, 10(4): 441-468.

Lewis, K.B., 1980. Quaternary sedimentation on the Hikurangi oblique-subduction and transform margin, New Zealand. Special Publication of the International Association of Sedimentologists(4): 171-189.

Lewis, K.B. and Pettinga, J.R., 1993. The emerging, imbricate frontal wedge of the Hikurangi Margin. Sedimentary Basins of the World, 2: 225-250.
Lewis, K.B., 1997. The succession of seamount impacts and giant avalanches on the Hikurangi margin. In: D.N.B. Skinner (Editor), Geological Society of New Zealand 1997 annual conference; programme and abstracts Geological Society of New Zealand Lower Hutt pp. 99.
Lewis, K.B., 1998. Kaikoura Canyon; recurrent failure in a nearshore canyon-head and catastrophic input to a deep-ocean channel system. Geological Society of New Zealand Miscellaneous Publication, 101A: 147.
Lewis, K.B. and Barnes, P.M., 1999. Kaikoura Canyon, New Zealand: active conduit from near-shore sediment zones to trench-axis channel. Marine Geology, 162(1): 39-69.
Lewis, K.B., 2001. Voyage Report TAN0106, National Institution of Water and Atmospheric Research, Wellington, New Zealand.
Lewis, K.B., Lallemand, S. and Carter, L., 2004. Collapse in a Quaternary shelf basin off East Cape, New Zealand: evidence for passage of a subducted seamount inboard of the Ruatoria giant avalanche. New Zealand Journal of Geology and Geophysics, 47: 415-429.
Locat, J. and Lee, H.J., 2002a. Submarine landslides: Advances and challenges. Canadian Geotechnical Journal, 39(1): 193-213.
Maruyama, S. and Liou, J.G., 1989. Possible depth limit for underplating by a seamount. Tectonophysics, 160(1-4): 327-337.
Masson, D.G., Parson, L.M., Milsom, J., Nichols, G., Sikumbang, N., Dwiyanto, B. and Kallagher, H., 1990. Subduction of seamounts at the Java Trench: a view with long-range sidescan sonar. Tectonophysics, 185(1-2): 51-65.
Melhuish, A., Sutherland, R., Davey, F.J. and Lamarche, G., 1999. Crustal structure and neotectonics of the Puysegur oblique subduction zone, New Zealand. Tectonophysics, 313(4): 335-362.
Moore, J.G., Normark, W.R. and Holcomb, R.T., 1994. Giant Hawaiian landslides. Annual Review of Earth and Planetary Sciences, 22: 119-144.
Mountjoy, J.J., Barnes, P.M. and Pettinga, J.R., 2009. Morphostructure and evolution of submarine canyons across an active margin: Cook Strait sector of the Hikurangi Margin, New Zealand. Marine Geology, 260(1-4): 45-68.
Mountjoy, J.J., 2009. Submarine canyon evolution: Quantifying geomorphic processes on New Zealand's active continental margin. PhD Thesis, University of Canterbury.
Nicol, A. and Beavan, J., 2003. Shortening of an overriding plate and its implications for slip on a subduction thrust, central Hikurangi Margin, New Zealand. Tectonics, 22(6): 1070.
Orange, D.L., 1999. Tectonics, sedimentation, and erosion in Northern California; submarine geomorphology and sediment preservation potential as a result of three competing processes. Marine Geology, 154(1-4): 369-382.
Park, J.-O., Tsuru, T., Takahashi, N., Hori, T., Kodaira, S., Nakanishi, A., Miura, S. and Kaneda, Y., 2002. A deep strong reflector in the Nankai accretionary wedge from multichannel seismic data: Implications for underplating and interseismic shear stress release. Journal of Geophysical Research, 107(B4).
Pedley, K.L., Barnes, P.M., Pettinga, J.R. and Lewis, K., 2010. Seafloor structural geomorphic evolution of the accretionary frontal wedge in response to seamount subduction, Poverty Indentation, New Zealand. Marine Geology, 270(1-4): 119-138.
Pettinga, J.R., 2004. Three-stage massive gravitational collapse of the emergent imbricate frontal wedge, Hikurangi Subduction Zone, New Zealand. New Zealand Journal of Geology and Geophysics, 47: 399-414.

Robertson, A.H.F. and Karamata, S., 1994. The role of subduction-accretion processes in the tectonic evolution of the Mesozoic Tethys in Serbia. Tectonophysics, 234(1-2): 73-94.
Robertson, A.H.F., 1998. Tectonic significance of the Eratosthenes Seamount: a continental fragment in the process of collision with a subduction zone in the eastern Mediterranean (Ocean Drilling Program Leg 160). Tectonophysics, 298(1-3): 63-82.
Soh, W., Tokuyama, H., Fujioka, K., Kato, S. and Taira, A., 1990. Morphology and development of a deep-sea meandering canyon (Boso Canyon) on an active plate margin, Sagami Trough, Japan. Marine Geology, 91: 227-241.
Soh, W. and Tokuyama, H., 2002. Rejuvenation of submarine canyon associated with ridge subduction, Tenryu Canyon, off Tokai, central Japan. Marine Geology, 187: 203-220.
Torelli, L., Sartori, R. and Zitellini, N., 1997. The giant chaotic body in the Atlantic Ocean off Gibraltar; new results from a deep seismic reflection survey. Marine and Petroleum Geology, 14(2): 125-138.
von Huene, R., Ranero, C.R. and Watts, P., 2004. Tsunamigenic slope failure along the Middle America Trench in two tectonic settings. Marine Geology, 203(3-4): 303-317.
Walcott, R.I., 1978. Present tectonics and late Cenozoic evolution of New Zealand. Geophysical Journal of the Royal Astronomical Society, 52: 137-164.
Wallace, L., Beavan, J., McCaffrey, R. and Darby, D.J., 2004. Subduction zone coupling and tectonic block rotations in the North Island, New Zealand. Journal of Geophysical Research, 109.
Wallace, L. and Beavan, J., 2006. A large slow slip event on the central Hikurangi subduction interface beneath the Manawatu region, North Island, New Zealand. Geophysical Research Letters, 33(11).
Wallace, L., Ellis, S. and Mann, P., 2008. Tectonic block rotation, arc curvature, and back-arc rifting: Insights into these processes in the Mediterranean and the western Pacific. IOP Conf. Series: Earth and Environmental Science, 2.
Wellman, H.W., 1979. An uplift map of the South Island of New Zealand and a model for the origin of the Southern Alps. In: R.I. Walcott and M.M. Cresswell (Editors), Origin of the Southern Alps. Bulletin of the Royal Society of New Zealand, pp. 13-20.
Wood, R. and Davy, B., 1994. The Hikurangi Plateau. Marine Geology, 118(1-2): 153-173.
Yamazaki, T. and Okamura, Y., 1989. Subducting seamounts and deformation of overriding forearc wedges around Japan. Tectonophysics, 160(1-4): 207-217.
Yun, J.W., Orange, D.L. and Field, M.E., 1999. Subsurface gas offshore of northern California and its link to submarine geomorphology. Marine Geology, 154(1-4): 357-368.
Zhao, D., Matsuzawa, T. and Hasegawa, A., 1997. Morphology of the subducting slab boundary in the northeastern Japan arc. Physics of The Earth and Planetary Interiors, 102(1-2): 89-104.

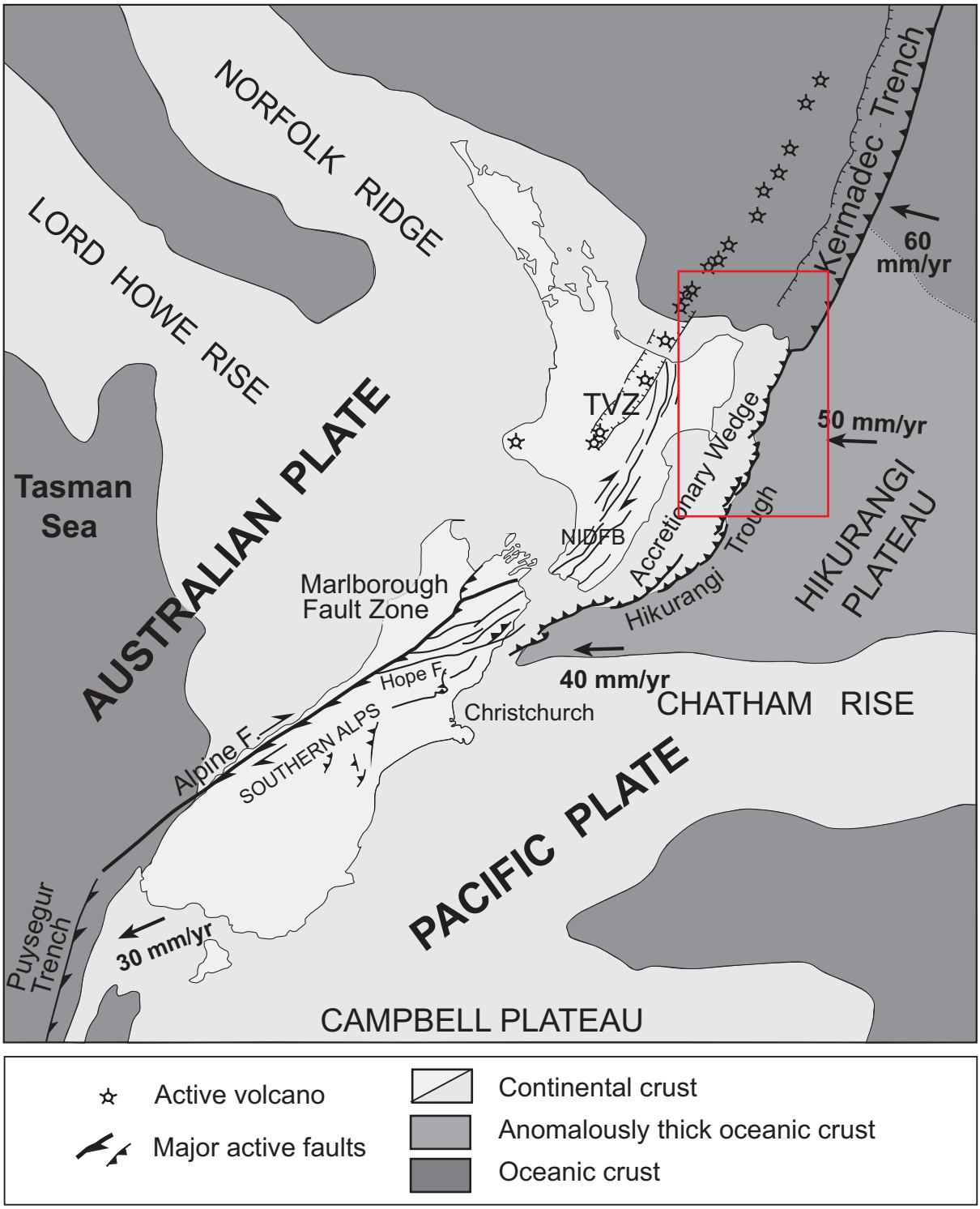

Figure 1.1 Map of the main structural features of the New Zealand associated with the obliquely convergent Australia-Pacific plate boundary zone. (F) = fault. Red box indicates location of Figure 1.2. Figure modified after Lewis & Pettinga, 2004.

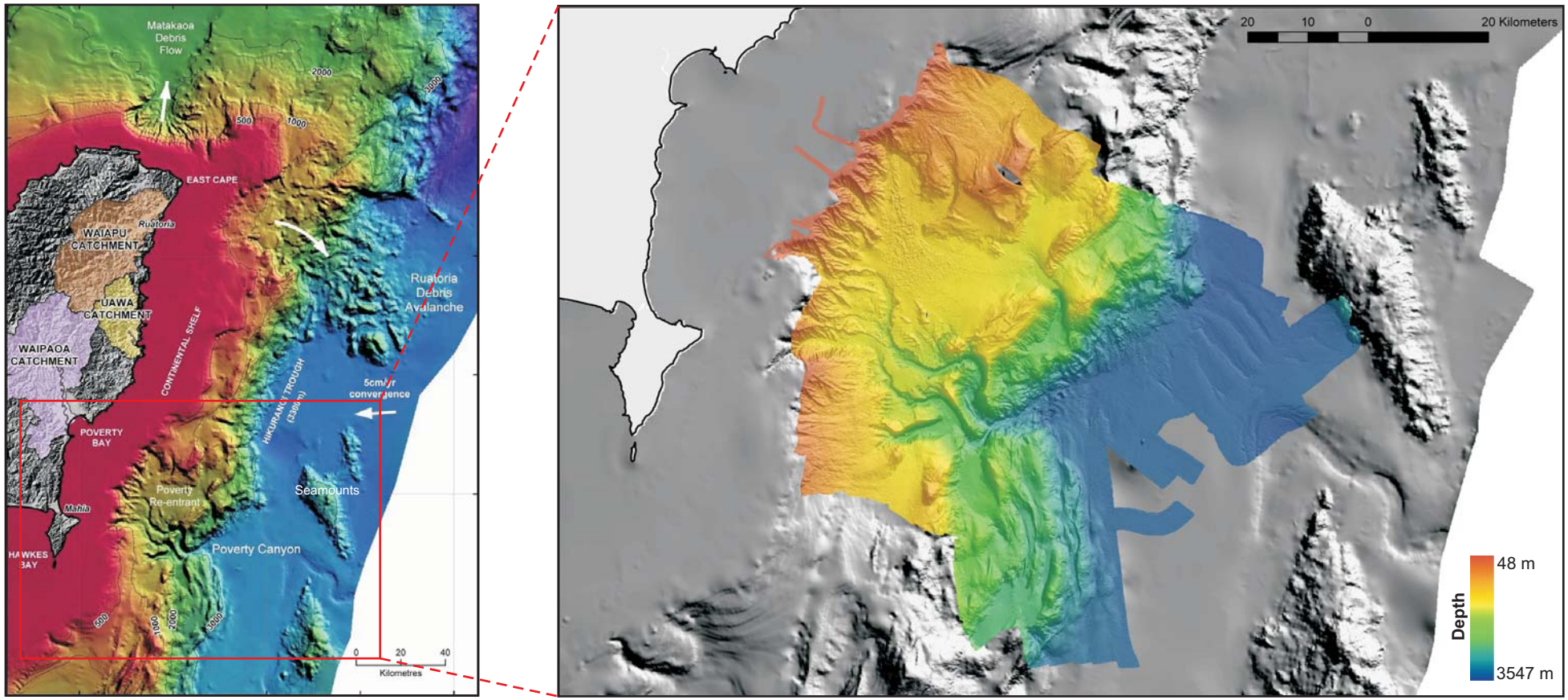

Figure 1.2 A: The Hikurangi margin offshore the East Coast of the North Island. Waipaoa River catchment shaded in pink. Diagram supplied by NIWA. B: The Poverty Indentation with swath bathymetry coverage used for this project.

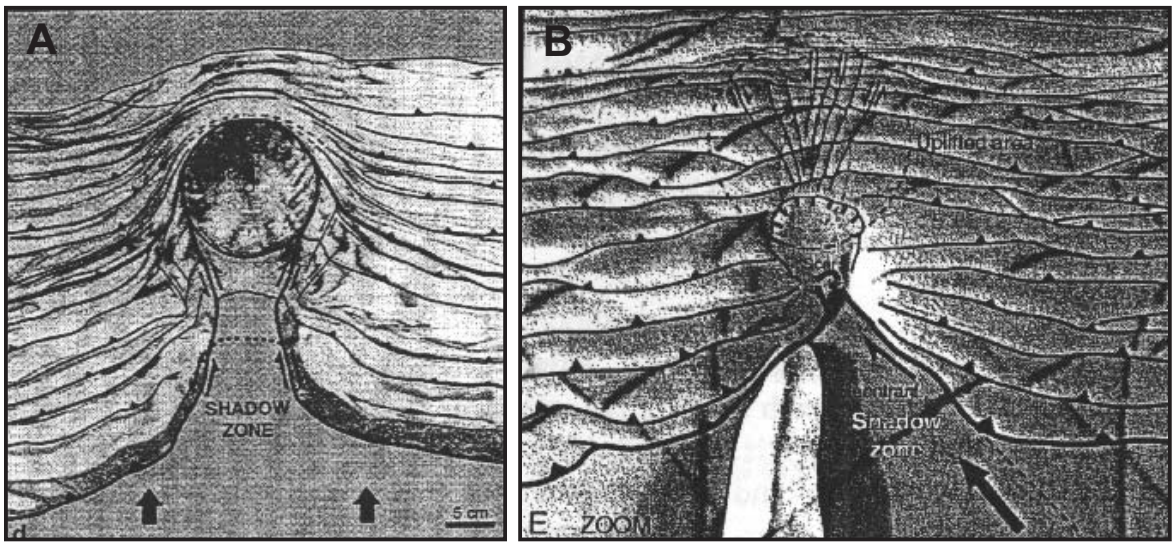

Figure 1.3 Planar photos and interpretations of sandbox experiments undertaken by Dominguez et al. (1998) & (2000), highlighting the different responses of the accretionary wedge to variations in convergence direction and geometry of the seamount.

A: Orthogonal subduction of a conical seamount.

B: Oblique subduction of a ridge or elongated seamount.

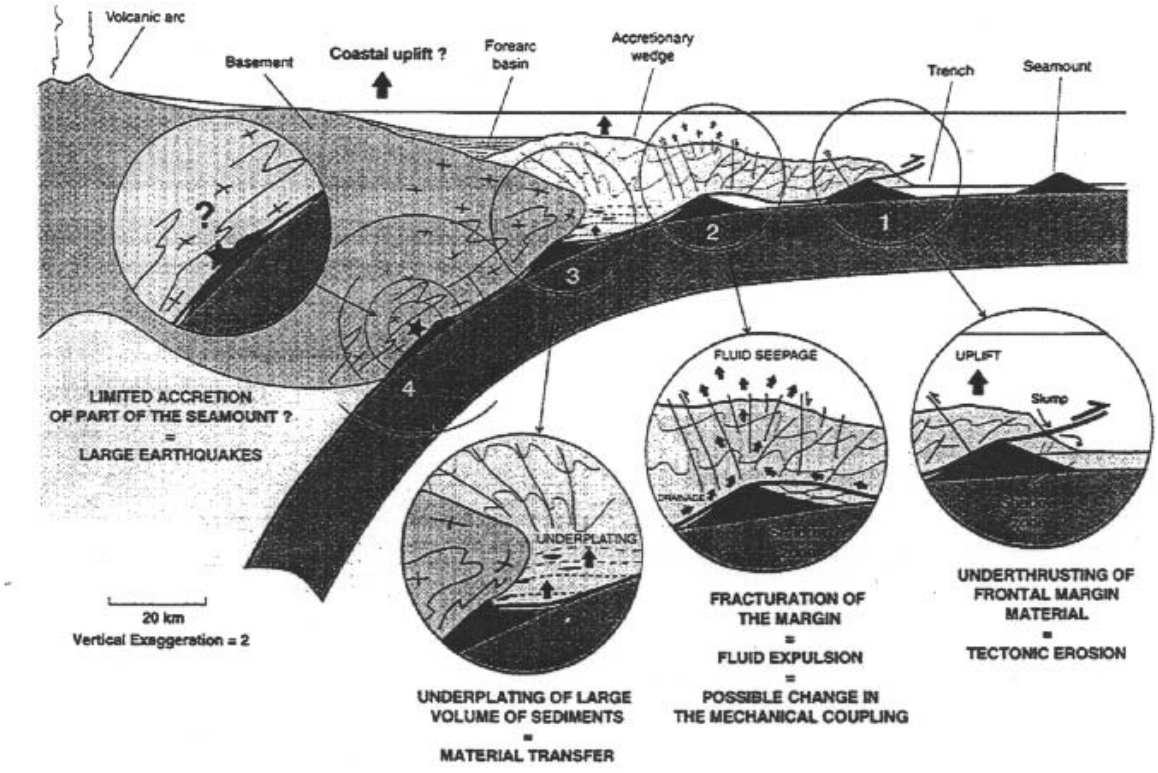

Figure 1.4 Schematic cross section illustrating material transfers inside the accretionary wedge induced by seamount subduction, with the seamount left largely intact until it is well beneath the backstop (Dominguez et al. 2000).

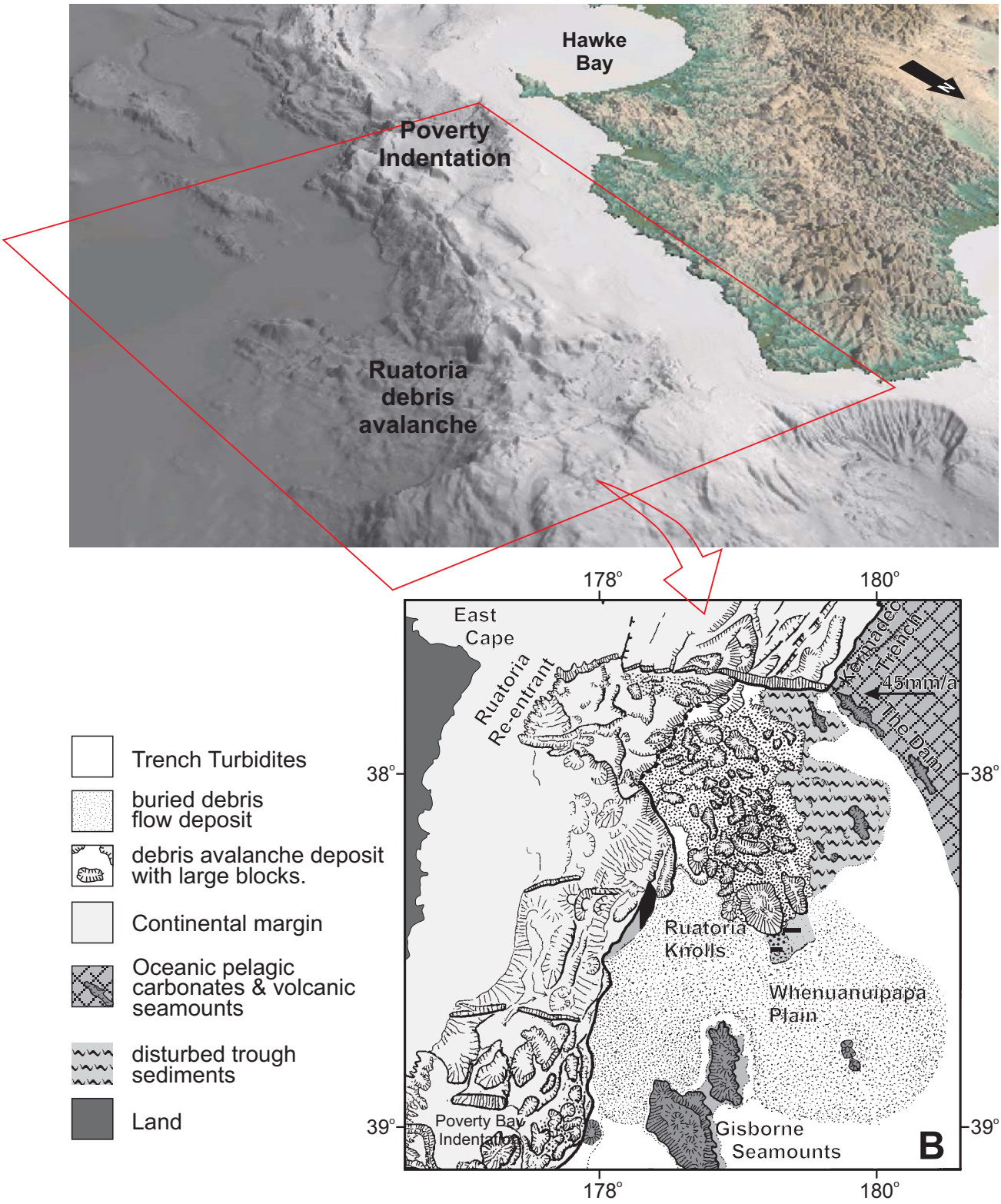

Figure 1.5 A: Oblique view of the East Coast North Island showing the location of the Ruatoria debris avalanche in relation to the Poverty Indentation. View is facing approximately southwest. DEM generated by J. Mountjoy (UoC, NIWA).

B: Interpretation of the Ruatoria debris avalanche based on seismic profiles and bathymetry (modified from Lewis et al. 1998).

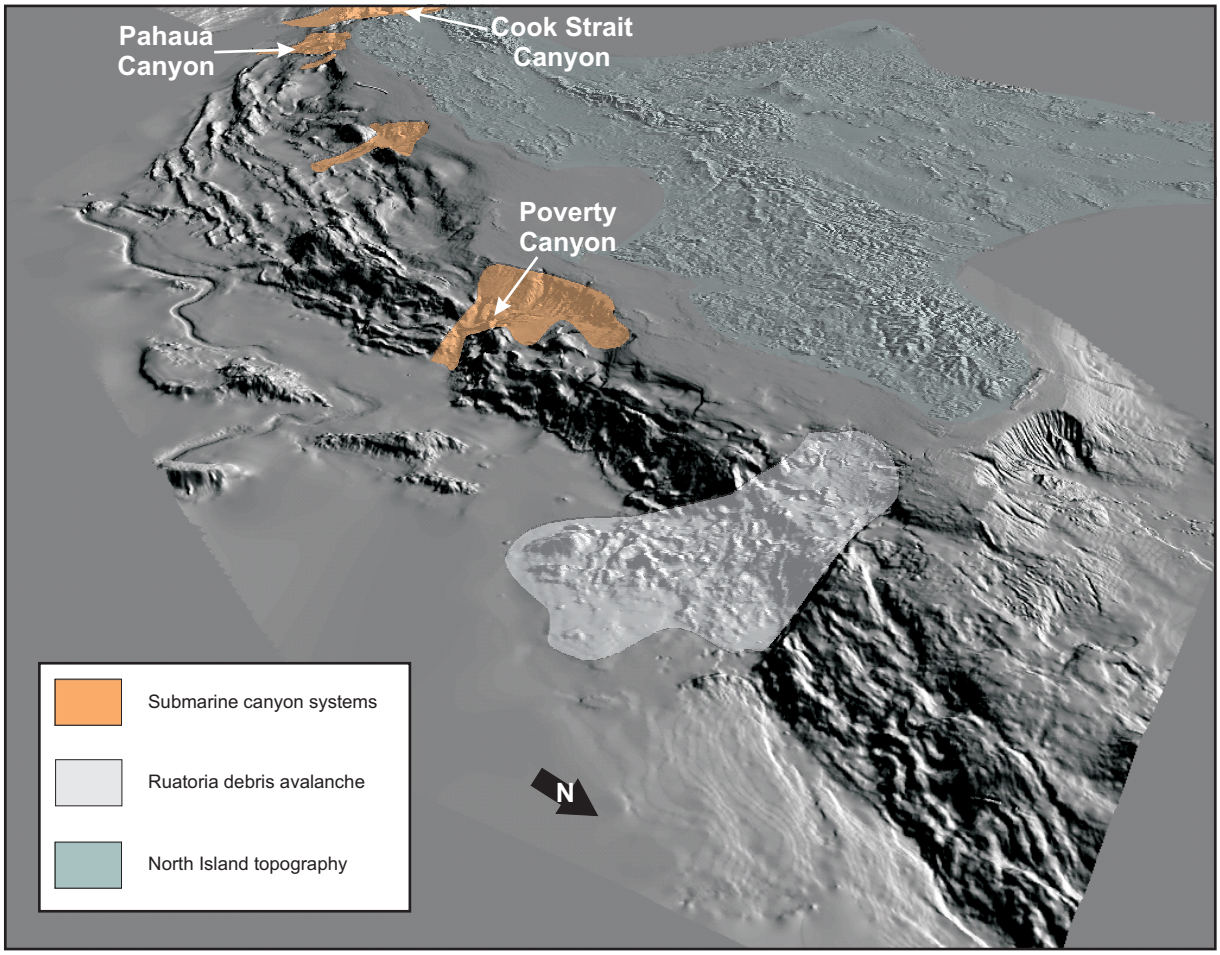

Figure 1.6 Significant sediment conduits from the continental shelf to trench floor on the Hikurangi margin, offshore North Island - The Cook Strait Canyon, the Pahaua Canyon and the Poverty Canyon. DEM processed by J. Mountjoy (NIWA).

CHAPTER 2: METHODS AND DATA ACQUISITION

2.1 INTRODUCTION

The data set for this project consists of over 4000 km^2 of the rugged continental slope encompassing the Poverty Bay Indentation mapped with high quality bathymetry at a resolution comparable to the most detailed Digital Elevation Maps (DEM) onshore. The detailed digital swath images are complemented by the availability of excellent high-quality processed multi-channel seismic reflection data as well as core, rock and dredge samples.

2.2 MULITBEAM SWATH BATHYMETRY

Swath bathymetry mapping utilises sonar waves to build up a high-resolution image of seafloor bathymetry by measuring the travel time and arrival angle of echoes from the seafloor. The use of swath bathymetry for viewing the morphology of the seafloor is a relatively new area of technology and has increasing importance in marine and earth sciences. There are two main techniques of swath bathymetry in use today – Multibeam and Sidescan (Sidescan sonar was not used for this project so it will not be addressed). A Multibeam swath bathymetry system generates many acoustic beams from a hull-mounted location at different vertical angles in an array extending to both sides of the ship's track. This spread allows measurement of multiple depths within a wide swath either side of the ship (Figure 2.1). It allows intricate and detailed mapping of the sea floor, revealing in detail seafloor morphologic features with accurate scale and depth control. Each beam determines the travel time to the seafloor in a specific direction, independent of the others. As the ship moves forward, a complete swath of the seafloor is mapped with detail dependant on the number of beams used (increase in beam no. = increase in detail) (Blackinton, 1991). For a more detailed review of swath bathymetry techniques readers are referred to de Moustier (1988) and Blackinton (1991).

The four main factors affecting the measurements derived from swath bathymetry are system design, acoustic noise, transducer attitude and sound speed structure (Blackinton, 1991). With multibeam systems, as the seafloor depth increases it also becomes more difficult to resolve

short wavelength targets from the surface. This is a result of the increasing width of the projected beam footprint, the increase in inter-beam spacing, and the lack of a uniform sounding density due to ship/platform movement on the sea surface. Sidescan sonar towed behind a ship at depth can resolve these issues, however, this requires much slower speeds and may require additional acoustic positioning systems (Hughes Clarke et al., 1998). The advantage of using swath bathymetry in deep water is that it can cover a much greater area in one pass than in shallow water where the width of the beam is much smaller.

Interpretation of swath bathymetry data relies on proper system measurements and calibration, and understanding of the limitations and artifacts produced by data collection and processing. These artifacts and problems can include: roll misalignment, pitch, yaw and heave of the ship, tides, refraction, achieving seafloor ensonification with adequate coverage and beam energy, significant gaps between swath passes, rough/steep slope resulting in masking of features through shadows and interference patterns from overlapping swath paths.

2.2.1 Multibeam bathymetry in New Zealand

Up until the 1930's mapping of the ocean floor around New Zealand consisted of a few lead line soundings from a ship. This was accomplished by measuring depths at a single point using a line with a lead sinker attached to the end. This was very time consuming as the ship had to stop to take each measurement, sinker positions were obtained from the stars and mariners needed to be experienced in determining when the sinker had reached the seafloor. During World War II, echo-sounders were able to be used to produce lines of closely-spaced soundings from directly beneath ships but areas mapped in this were very limited with most deep water regions still only mapped by depth soundings spaced far apart (Lewis, 1994). Swath mapping has only been in use around New Zealand since around the early 1990's (Lewis, 1994). Global positioning of the data is now available linked with Global Positioning Satellite (GPS) coordinates, while computer involvement has meant that raw data is able to be viewed in real time, adding the acquisition process, with the final processed data viewed as a colour image and able to be explored in three dimensions.

2.2.2 Multibeam bathymetry in the Poverty Indentation

Multibeam swath bathymetry data collected for this project (Figure 2.1) is the first of a new generation of mapping with high resolution and high level of detail, rivalling the terrain elevation data produced on land (e.g. McKean and Roering, 2004). Although some specific

locality maps onshore have extremely high resolution (down to 1 m), most are around 30 m resolution only. While much research has been done with swath bathymetry along the Californian Margin (Goff et al., 1999; Lee et al., 1999; Orange, 1999; Rogers et al., 1999; Yun et al., 1999; Nelson et al., 2000a; Spinelli and Field, 2001; Anima et al., 2002; Eittreim et al., 2002; Greene et al., 2002; Orange et al., 2002; Wong and Eittreim, 2002; Lee et al., 2002b), the Java Margin (Fryer and Smoot, 1985; Masson et al., 1990; Huang et al., 2000) and the Japan Margin (Konishi, 1989; Lallemand et al., 1989; Zhao et al., 1997), New Zealand swath mapping has only really taken off since around the turn of the century and is rapidly becoming one of the main tools in helping understand submarine tectonic and geomorphic processes. Few researchers have used extensive swath bathymetry around the Hikurangi Margin (Collot et al., 1996a; Lewis et al., 2004), with many only using it to help illustrate seismic data in one or two diagrams (Barnes et al., 2002; Barnes and Nicol, 2004) rather than for extensive geomorphic analyses. The data presented here brings a higher level of detail to a restricted region of the Hikurangi Margin, providing imaging and therefore analysis of far more detailed geomorphology than previously obtained by wider margin surveys.

High quality bathymetric and backscatter images of the Poverty Indentation were obtained by the National Institute of Water and Atmospheric Research (NIWA) in 2001 using a SIMRAD EM300 multibeam swath-mapping system mounted on the hull of the RV Tangaroa. Over 4000 km^2 of rugged submarine slope topography was mapped, encompassing the entire accretionary slope of the indentation, at depths ranging from 100 to 3500 metres (Figure 2.1). Some limitations or artifacts affecting this interpretation of this particular data include interference patterns from overlapping swath tracks (see Figure 2.1) and a few small areas (circled in white, Figure 2.1) where data is missing or was not collected. Resolution of this grid at 25 m was chosen as the optimal resolution for imaging the deeper section of the study area with maximum resolution lower than at shallow depths, where spatial resolution is available down to 4 m (Figure 2.1). Topographic contours are closely spaced and textures (i.e. mud, rock, landslide debris, sedimentary structures, faulting, lava flows) are all precisely defined and may be further analysed using backscatter data from the swath files. This high resolution mapping has allowed extensive and enhanced reinterpretation of this section of the Hikurangi margin with implications for onshore geology, modern and ancient plate boundary systems, allowing investigation into the entire source to sink fluvial systems, and allowing

extensive research into the variety of processes occurring at this convergent compressive margin, not previously attempted with such detail in the offshore setting.

In 2007 NIWA revisited the Poverty Indentation and obtained an additional swath map imaging the shelf edge and Tuaheni slides complex to the north of the Paritu Basin (Figure 2.1 section imaged in grey).

The digital elevation models (DEM) generated from this data are presented and interpreted using ESRI ArcGIS software version 9.0 using a combination of spatial and 3D Analyst surface models including:

- Contour - generates depth contours at specified regular intervals.
- Slope - generates model of the DEM surface slope inclination in degrees or percentage.
- Aspect - generates model of slope facing direction in an azimuth (bearing) from 0^o to 360^o (N).
- Hillshade - generates shaded relief illumination model of the DEM surface, lit from a specified azimuth at a specified altitude.

In particular, numerous Hillshade models at varying vertical exaggeration, illumination azimuth and altitude were generated and compared to significantly aid structural geomorphic analyses and confirm the reproducibility of individual features. Comparisons and adjustments of the observed seafloor features with features interpreted in seismic sections were also done to provide a more accurate interpretation of specifically structural features in both sets of data.

2.3 MULTI-CHANNEL SEISMIC

Analyses can be significantly enhanced by incorporating data from seismic reflection surveys. The gathering of seismic reflection data enables depth profiling and insights into the sub-surface geology, sedimentary packages and structures compared to surface geomorphology obtained from swath bathymetry surveys. The two are often collected in conjunction and complement each other to build a three dimensional view of a study area.

The obtaining of seismic reflection data relies primarily on the abrupt vertical changes in physical properties between layers of rock. In essence, sound waves are bounced off the

interfaces between the various rock layers, measuring the two-way-time (TWT) to that layer by the time it takes for a pulse of sound to travel from the ship, reflect off the sea floor and sub-seafloor interfaces and return to the receiving system. In reality, this technique is more difficult and complicated when dealing with rock interfaces:

1) the signal received after reflection at significant depth is very weak;

2) vertical and horizontal resolution is limited by frequencies in seismic energy, firstly by source content, and secondly by attenuation of higher frequencies as energy propagates through the geology. Higher frequencies result in higher resolution but will not propagate to greater depths, therefore the source frequency must be designed for the target depth and resolution required, with a trade-off between the two;

3) repeated reflections between layers cause a signal to bounce back and forth many times resulting in *multiples* which can obscure other reflectors. The most significant of these is usually the strong water bottom multiples, where energy is bouncing between the sea floor and the sea surface. Good processing can remove this interference, but many seismic sections are left unprocessed, or unable to be processed, such that no reliable interpretation is possible below the first seabed multiple;

4) the velocity of sound varies both laterally and vertically in the Earth so that the two-way-time of the acoustic energy is more difficult to convert into depths. Obtaining velocity information from a survey for depth conversion is also dependent on the length of the streamer;

and 5) problems arise with non-vertical acoustic paths caused by structural dips at depth and survey geometries.

These problems have been addressed and repeated over the preceeding 6-7 decades to try and obtain the most accurate seismic cross-sections. Digital seismic data processing techniques have been developed to try and minimise these effects. For a more comprehensive review of the well established seismic reflection theory and practice, and for a fuller treatment of this topic, readers are referred to Brown & Fisher (1980), McQuillin et al. (1984) and Badley (1985).

For marine surveys a variety of acoustic energy sources are used to generate seismic waves: air guns, the Helmholtz resonator, electrical-impulse generators, and water guns. Towed

behind the sound source, as part of the recording cable, are pressure-sensitive receivers called *hydrophones*. These read the signals of sound (as acoustic pulses) when they are reflected from the seafloor or rock interfaces. The cable containing the hydrophones, generally referred to as a *streamer*, can be many kilometres in length. One *channel*, a single receiver, is often the summation of input from a group of closely-spaced hydrophones. A cable with one channel collects single-channel seismic reflection data (SCS); these data provide excellent images of shallow-level stratigraphy but do not record seismic velocities. Multi-channel seismic reflection data (MCS) uses multiple channels along one streamer and is able to image structures and provide velocity information (Miles, 2000; Pecher and Holbrook, 2000). MCS can also be used with multiple streamers for creating 3-dimensional seismic surveys.

A single-channel seismic system consists of a sound source system, typically a boomer, sparker or air gun and a towed single-channel hydrophone array to collect the returned seismic signals. It has low frequency energy in the range of 400-10,000 Hz, for deep penetration through coarse materials, and provides excellent high frequency resolution for determining the depth of sub-bottom horizons. SCS has achieved 30 m penetration in tills and over 100 m penetration in post-glacial marine sediments using the boomer system. The multi-channel system (MCS) includes a hydrophone containing 24, 48 or 96 channels and a digital seismograph for recording the seafloor returns to each channel. Typically used for deeper or difficult shallow exploration, the multi-channel data must be digitally processed and seismic sections generated. This seismic technique is more accurate for shallow surface depths but slower to obtain and process than single-channel (Barnes, 1993).

2.3.1 Multi-channel seismic on the Hikurangi Margin

Significant multi-channel seismic use on the Hikurangi Margin has really only developed during the last two decades. Up until 1985, the hydrocarbon exploration companies were the only organizations using multi-channel seismic systems, and the data obtained was not readily available to research scientists or the public sector. Prior to 1990 the only multi-channel seismic profiling for purely scientific purposes in New Zealand was conducted across the Hikurangi margin offshore from Hawke Bay (Pettinga et al., 1984). The acquisition of a modern multi-channel seismic system by NIWA in the mid-1990's consisting of a 48 channel streamer, has provided the capability to process seismic signals into a readable cross-section in real-time. This development in seismic acquisition has significantly opened up the opportunities to detailed scientific seismic research across the margin.

2.3.2 Multi-channel seismic across the Poverty Indentation

In early 2006, the Ministry of Economic Development (MED) released very high quality multi-channel seismic sections to the public from their latest hydrocarbon exploration of East Coast North Island. For this research we use the MED seismic lines covering the Poverty Bay region, on the continental shelf and bordering the study area to complement the seismic data collected by NIWA and their collaborators.

Multi-channel seismic data is used from a number of voyages covering the northern sector of the Hikurangi Margin (Figure 2.2), specifically, reprocessed Mobil Exploration seismic data from 1972, the joint NIWA and French GeodyNZ expedition in 1993 (Lewis, 1994), NIWA voyage TAN0106 (low fold) in 2001 on the RV TANGAROA (Lewis, 2001) and the Ministry of Economic Development CM05/05CM exploration block in 2005 (hi-fold, deep penetration industry) on the MV PACIFIC TITAN (Funnell and Benchilla, 2005; Maslan, 2005; Multiwave, 2005) (Figure 2.3). All surveys are presented using The Kingdom Suite (TKS) seismic interpretation software. The multi-channel seismic profiles gathered for this research project are among the highest quality data sets available at the present time with the most recent technology and available budget. This has allowed analyses of the Poverty Bay section of the Hikurangi margin to a level not yet achieved in this region by researchers.

2.3.3 GeodyNZ & Mobil

Reprocessed 3-fold Mobil Exploration seismic data (1972), and GeodyNZ RV L'ATALANTE 1993 3-fold profiles (Lewis, 1994; Collot et al., 1996b; Lewis et al., 1997). These are historical low quality seismic surveys, used in this project to support the TAN0106 and CM05 data. The GeodyNZ data is of particular use as strike profiles across the Poverty Indentation, and for correlating dated horizon picks up north into the region in the trench-fill sequence (see Chapter 6).

2.3.4 TAN0106

RV TANGAROA 2001 (TAN0106) 6-fold profiles (Lewis, 2001). The source for the TAN0106 survey is a 45/105 ci GI gun with a shot spacing of 25.0 m and receiver spacing of 12.5 m. Sample rate and record length are 1 ms and 8 s respectively. These seismic profiles were collected in conjunction with the multibeam bathymetry, and form the majority of the seismic information for the indentation itself. These low-fold profiles that cover the middle

and lower part of the indentation, where we focus much of our work, were acquired with short seismic streamers and provide poor seismic velocity information, hampering our ability to produce quality depth sections across the outer part of the frontal wedge. We therefore present time-sections for these data throughout this project, with the exception of Chapter 6. For a discussion on velocities and comparisons with depth converted horizons around the Poverty Indentation, readers are referred to (Barker et al., 2009; Bell et al., 2009).

2.3.5 CM05

MV PACIFIC TITAN 2005 (CM05/05CM) seismic data is high fold (960-channel), deep penetration to 12 s two-way-travel time (TWT) profiles acquired by Ministry of Economic Development Ltd. (MED) (Funnell and Benchilla, 2005; Maslan, 2005; Multiwave, 2005; Barker et al., 2009). Recording parameters for the CM05/05CM survey include a Bolt (1500 & 1900 Long Life) airgun source with shot spacing of 37.5 m and receiver spacing of 12.5 m. Sample rate and record length are 2000 ms and 8000/12000 ms respectively. These seismic profiles, although very high quality, do not extend very far into the Poverty Indentation (being concentrated along the continental slope edge), and only have two profiles that extend down across the frontal wedge and into the Hikurangi Trough (CM05-01 and -04). Both of these sections lie just outside the indentation and can be used to extrapolate velocity profiles for the low-fold TAN0106 data.

2.4 CORES AND SEAFLOOR SAMPLES

The Poverty Shelf directly inboard of the Poverty Indentation has a number of core and dredge samples (Figure 2.4) particularly on the Lachlan Ridge to the south of the indentation and has been studied in reasonable detail (Foster and Carter, 1997; Barnes et al., 2002; Orpin et al., 2003; Orpin, 2004; Alexander et al., 2006c; Alexander et al., 2006b; Alexander et al., 2006a; Gerber et al., 2006; Orpin et al., 2006; Walsh et al., 2006a; Walsh et al., 2006b; Alexander et al., 2007; Walsh et al., 2007). The Hawke Bay-1 well in central Hawke Bay also provides good stratigraphic control on the continental shelf and ties in directly with MED seismic line CM05-01 (Figure 2.5). This has been used to provide ages of horizons present in the upper clinoform sequence across the shelf edge in CM05-23, relevant to Chapters 3 and 6. Stratigraphic control via sediment samples obtained within the Poverty Indentation is currently very limited due to costs and high water depths. For further detail and discussions

on the stratigraphy of the Poverty continental shelf region please refer to Foster & Carter (1997), Barnes et al. (2002), Orpin (2004), and Orpin et al. (2006).

2.4.1 Hawke Bay-1 Well

The Hawke Bay-1 was drilled in 1976 (BP Shell Aquitaine and Todd Petroleum Development Ltd, 1976) to a depth of 2,372 metres (Figure 2.5). The following paragraph is a summary of this well and its limitations and is compiled here from Nicol and Uruski (2005) and the original BP well report (1976):

The Hawke Bay-1 well drilled an apparent Neogene succession through to the middle Miocene before passing abruptly into rocks of Middle Oliocene age. Gas was encountered in the Oligocene succession but the gas flow in the well was not tested as the drill string became permanently lodged in expanding clays. Two unsuccessful side-tracks were attempted, but ultimately the bottom 500 metres of the well were abandoned and log suites were run from 1828 metres to the surface. Seismic ties are therefore reliable only to this point and the seismic locations of deeper units, particularly the Middle Miocene and Oligocene, must be inferred. The absence of the Late Oligocene and Early Miocene section in the well is attributed to erosion or non-deposition across a growing anticline (BP Shell Aquitaine and Todd Petroleum Development Ltd, 1976; Nicol and Uruski, 2005). The Middle Miocene succession is thin and consists of sandstones and limestone. Overlying Late Miocene strata are predominantly mudstones and siltstones. The Late Neogene succession is represented by discontinuous moderate to low amplitude reflectors with poor continuity although general trends are clearly visible. The possible reasons for this may be: the presence of small faults that can not be easily resolved by seismic, considerable remnant multiple energy and/or the presence of gas. All three features are observed in the late Neogene interval (Nicol and Uruski, 2005).

Seismic line CM05-01 from the MED voyage in 2005 directly intersects the Hawke Bay-1 well (Figure 2.5) enabling correlation of some deep level stratigraphic horizons along the continental shelf and upper slope around the CM05 grid, intersecting with Mobil-176 and the TAN0106 seismic survey. The unconformity (labelled in green) at the top of the succession is correlated to CM05-01 from research undertaken by Paquet (2007; 2009) and Barnes et al. (2002) and is equivalent to Unconformity 5, developed between c. 0.43 Ma-0.41 Ma (Paquet, 2007). The next major unconformity labelled in yellow corresponds to Unconformity 12 at the

base of a Castlecliffian and Haweran sequence (New Zealand stratigraphic stages). This unconformity has been dated at an age of c. 1.07 Ma and represents the top of the Pliocene (Paquet, 2007).

It is difficult to trace these top horizons along the continental shelf due to the presence of the actively propagating Lachlan Ridge (Barnes et al., 2002) but the base of the clinoform sequence is consistent with Unconformity 12 (from Paquet, 2007) at the top of the Pliocene and imaged in line CM05-46. Below this sequence, the faulted units correlate more easily with the Miocene (and older) ages of the Hawke Bay - 1 well (BP Shell Aquitaine and Todd Petroleum Development Ltd, 1976). This is also consistent with dredge samples obtained from the northern Ritchie Ridge at the eastern end of line CM05-19 (Barnes et al., 2009).

2.4.2 Core, dredge and rock samples

Samples used for this project come from a variety of stations from multiple voyages around the Poverty region from 1956 - 2001 (refer to Figure 2.4). Cores, dredge and rock samples reveal generally lime-rich muds interbedded with graded volcanic tephras, pumiceous layers, sandy muds, volcanic glass and some limestones (Table 2.1). Holocene activity is dominant on the continental shelf and in the mid-slope basins and debris flows of the indentation (Paritu Basin and Lower Paritu Basin). Early and Middle Miocene sequences outcrop at the head of the Poverty Canyon and continental shelf break, and in the head scarp of the Riwha Scar on the northern deformation front (Table 2.1, refer also to Figures 2.1 and 2.4). Previous work on the Poverty continental shelf and shelf edge/upper slope (Foster and Carter, 1997; Carter, 2000; Lewis, 2001; Barnes et al., 2002; Orpin et al., 2003; Orpin, 2004; Ricketts and Nelson, 2004; Kuehl et al., 2006; Orpin et al., 2006; Walsh et al., 2006b; Walsh et al., 2007; Kuehl et al., 2008) highlight the presence of a large (area = 980 km^2, volume = 17.9 km^3) sediment depocentre on the shelf directly outboard of the Waipaoa River and Poverty Bay, and with a smaller (area = 140 km^2, volume = ~3 km^3) depocentre situated on the shelf edge at the head of the Poverty Gullies (Orpin et al., 2006). Sediment is channelled through to this smaller depocentre through a gap between the topographic expressions of the structurally active Lachlan and Ariel Ridges (Foster and Carter, 1997; Barnes et al., 2002; Orpin et al., 2006). It is thought that during low stand sea levels, these depocentres are bypassed, with sediment transported directly down the Poverty Canyon. Currently, the high stand situation appears to be one of infilling in the canyon heads and a largely inactive system (Walsh et al., 2007).

In February 2005, the RV KILO MOANA (Honolulu, HI) conducted box dredge sampling (Figure 2.6) of the Poverty shelf and upper slope targeting the head zones of the Poverty Gullies and the Poverty Canyon as part of ongoing studies with the MARGINS Source-to-Sink initiative (see Alexander et al., 2006c; Alexander et al., 2006a; Walsh et al., 2006a; Walsh et al., 2006b; Walsh et al., 2007). In 2007, when the RV TANGAROA underwent the voyage around the Poverty Indentation and Poverty continental shelf and collected the swath bathymetry of the Tuaheni slide complex region to the north, we applied for further sediment samples to be taken at various key locations around the indentation. Unfortunately because of bad weather, time constraint, significant water depths and costs, these samples were unable to be gathered.

Despite the limited range of sediment samples for the Poverty re-entrant slope, these samples are useful as insights into the age ranges of some of the main features of the indentation and have been used in this project to support the observations and interpretations of the high-quality swath bathymetry and multi-channel seismic data.

References

Alexander, C., Walsh, J.P., Sumners, B., Orpin, A. and Kuehl, S., 2006a. Continental slope sediment delivery and storage on an active margin: The Waipaoa Margin example. Eos Trans. AGU, 87(52): Fall Meeting Abstracts.

Alexander, C., Walsh, J.P., Orpin, A., Sumners, B., Kuehl, S., Pratson, L., Gerber, T. and Carter, L., 2006b. Tectonic influences on sedimentary processes and submarine landscape evolution: the Waipaoa River, New Zealand example. Geophysical Research Abstracts, 8: European Geosciences Union 2006.

Alexander, C., Walsh, J.P., Orpin, A., Sumners, B. and Kuehl, S., 2006c. Modern sedimentation on the Continental Slope seaward of the Waiapaoa River, New Zealand. Eos Trans. AGU, 87(36): Ocean Sciences Meeting Abstracts.

Alexander, C., Walsh, J.P. and Orpin, A., 2007. Modern sediment dispersal and accumulation on the Waipaoa outer continental margin. Marine Geology, xxxx.

Anima, R.J., Eittreim, S.L., Edwards, B.D. and Stevenson, A.J., 2002. Nearshore morphology and late Quaternary geologic framework of the northern Monterey Bay Marine Sanctuary, California. Marine Geology, 181(1-3): 35-54.

Badley, M.E., 1985. Practical Seismic Interpretation. International Human Resourses Development Corporation, Boston, MA.

Barker, D.H., Sutherland, R., Henrys, S. and Bannister, S.C., 2009. Geometry of the Hikurangi subduction thrust and upper plate, North Island, New Zealand. Geochemistry, Geophysics, Geosystems, 10(2).

Barnes, P.M., 1993. Structural styles and sedimentation at the southern termination of the Hikurangi Subduction Zone, offshore North Canterbury, New Zealand. Ph.D Thesis, University of Canterbury, Christchurch, 211 pp.

Barnes, P.M., Nicol, A. and Harrison, T., 2002. Late Cenozoic evolution and earthquake potential of an active listric thrust complex above the Hikurangi subduction zone, New Zealand. GSA Bulletin, 114(11): 1379-1405.

Barnes, P.M. and Nicol, A., 2004. Formation of an active thrust triangle zone associated with structural inversion in a subduction setting, eastern New Zealand. Tectonics, 23(TC1015).

Barnes, P.M., Lamarche, G., Bialas, J., Henrys, S., Pecher, I.A., Netzeband, G., Greinert, J., Mountjoy, J.J., Pedley, K.L. and Crutchley, G., 2009. Tectonic and Geological Framework for Gas Hydrates and Cold Seeps on the Hikurangi Subduction Margin, New Zealand. Marine Geology, in press.

Bell, R.E., Sutherland, R., Barker, D.H., Henrys, S., Bannister, S.C., Wallace, L. and Beaven, R.J., 2009. Seismic reflection character of the Hikurangi subduction interface, New Zealand, in the region of repeated Gisborne slow slip events. Geophysical Journal International, submitted.

Blackinton, J.G., 1991. Bathymetric resolution, precision and accuracy considerations for swath bathymetry mapping sonar systems, Oceans Technologies and Opportunities in the Pacific for the 90's'. Proceeding. OCEANS '91. IEEE, pp. 550-557.

BP Shell Aquitaine and Todd Petroleum Development Ltd, 1976. Well completion report Hawke Bay-1. 667, New Zealand Ministry of Commerce.

Brown, J., L.F. and Fisher, W.L., 1980. Seismic Stratigraphic Interpretation and Petroleum Exploration. Continuing Education Course Note Series #16, 16. AAPG Department of Education, Austin, Texas.

Carter, L., 2000. Voyage Report TAN0005, Report lodged in the National Institute of Water and Atmosphereic Research Library, Wellington, New Zealand.

Collot, J.-Y., Delteil, J., Lewis, K.B., Davy, B., Lamarche, G., Audru, J.-C., Barnes, P., Chanier, F., Chaumillon, E., Lallemand, S.E., Mercier de Lepinay, B., Orpin, A., Pelletier, B., Sosson, M., Toussaint, B. and Uruski, C., 1996a. From oblique subduction to intra-continental transpression; structures of the southern Kermadec-Hikurangi margin from multibeam bathymetry, side-scan sonar and seismic reflection. Marine Geophysical Researches, 18(2-4): 357-381.

Collot, J.-Y., Davy, B., Lamarche, G. and Anonymous, 1996b. Forearc structures and tectonic regimes at the oblique collision zone between the Hikurangi Plateau and the southern Kermadec arc. Eos, Transactions, American Geophysical Union, 77(22): 121.

de Moustier, C., 1988. State of the art in swath bathymetry survey systems. International Hydrographic Review, 65(2).

Eittreim, S.L., Anima, R.J. and Stevenson, A.J., 2002. Seafloor geology of the Monterey Bay area continental shelf. Marine Geology, 181(1-3): 3-34.

Foster, G. and Carter, L., 1997. Mud sedimentation on the continental shelf at an accretionary margin; Poverty Bay, New Zealand. New Zealand Journal of Geology and Geophysics, 40(2): 157-173.

Fryer, P. and Smoot, N.C., 1985. Processes of seamount subduction in the Mariana and Izu-Bonin trenches. Marine Geology, 64(1-2): 77-90.

Funnell, R. and Benchilla, L., 2005. 1D Basin Models in the East coast Basin, New Zealand. Report 3183, Ministry of Economic Development.

Gerber, T., Pratson, L., Kuehl, S., Gerald, L., Walsh, J.P. and Alexander, C., 2006. Late Pleistocene and Holocene Seismic Stratigraphy of an active Forearc Basin, Waipaoa Continental Shelf, New Zealand. Eos Trans. AGU, 87(36): Ocean Sci. Meet. Suppl. Abstract.

Goff, J.A., Orange, D.L., Mayer, L.A. and Hughes-Clarke, J.E., 1999. Detailed investigation of continental shelf morphology using a high-resolution swath sonar survey; the Eel margin, northern California. Marine Geology, 154(1-4): 255-269.

Greene, H.G., Maher, N.M. and Paull, C.K., 2002. Physiography of the Monterey Bay National Marine Sanctuary and implications about continental margin development. Marine Geology, 181(1-3): 55-82.

Huang, C.-Y., Yuan, P.B., Lin, C.-W., Wang, T.K. and Chang, C.-P., 2000. Geodynamic processes of Taiwan arc-continent collision and comparison with analogs in Timor, Papua New Guinea, Urals and Corsica. Tectonophysics, 325(1-2): 1-21.

Hughes Clarke, J.E., Gardner, J.V., Torresan, M. and Mayer, L.A., 1998. The limits of spatial resolution achievable using a 30kHz multibeam sonar: model predictions and field results. IEEE Oceans Proceedings, 3: 1823-1827.

Konishi, K., 1989. Limestone of the Daiichi Kashima Seamount and the fate of a subducting guyot: fact and speculation from the Kaiko "Nautile" dives. Tectonophysics, 160(1-4): 249-265.

Kuehl, S., Pratson, L. and Addington, L., 2006. Contrasting shelf sediment dispersal off small mountainous rivers: The Waipaoa and Waiapu Rivers, NZ. Eos Trans. AGU, 87(36): Ocean Sciences Meeting Abstracts.

Kuehl, S., Miller, A.J., Kniskern, T.A., Gerber, T. and Pratson, L., 2008. Sediment trapping and bypassing in active continental margin settings: New insights from MARGINS Source-to-Sink studies. Geological Society of America Abstracts with Programs, 40(6): 319.

Lallemand, S., Culotta, R. and Von Huene, R., 1989. Subduction of the Daiichi Kashima Seamount in the Japan Trench. Tectonophysics, 160(1-4): 231-233.

Lee, H., Locat, J., Dartnell, P., Israel, K. and Florence Wong, 1999. Regional variability of slope stability: application to the Eel margin, California. Marine Geology, 154(1-4): 305-321.

Lee, S.E., Talling, P.J., Ernst, G.G.J. and Hogg, A.J., 2002b. Occurrence and origin of submarine plunge pools at the base of the U. S. continental slope. Marine Geology, 185(3-4): 363-377.

Lewis, K.B., 1994. Mapping a muddy swath. NZ Science Monthly, 5(9): 6-9.

Lewis, K.B., Collot, J.-Y., Davy, B., Delteil, J., Lallemand, S. and Uruski, C., 1997. GeodyNZ Team 1997:North Hikurangi GeodyNZ swath maps: depths, texture and geological interpretation, NIWA Chart Miscellaneous Series 72. National Institute of Water and Atmospheric Research Ltd, Wellington.

Lewis, K.B., 2001. Voyage Report TAN0106, National Institution of Water and Atmospheric Research, Wellington, New Zealand.

Lewis, K.B., Lallemand, S. and Carter, L., 2004. Collapse in a Quaternary shelf basin off East Cape, New Zealand: evidence for passage of a subducted seamount inboard of the Ruatoria giant avalanche. New Zealand Journal of Geology and Geophysics, 47: 415-429.

Maslan, G., 2005. Fast track seismic processing of selected data from the 05CM survey offshore East Coast, New Zealand. Report 3182, Ministry of Economic Development.

Masson, D.G., Parson, L.M., Milsom, J., Nichols, G., Sikumbang, N., Dwiyanto, B. and Kallagher, H., 1990. Subduction of seamounts at the Java Trench: a view with long-range sidescan sonar. Tectonophysics, 185(1-2): 51-65.

McKean, J. and Roering, J., 2004. Objective landslide detection and surface morphology mapping using high-resolution airborne laser altimetry. Geomorphology, 57(3-4): 331-351.

McQuillin, R., Bacon, M. and Barclay, W., 1984. An Introduction to Seismic Interpretation: Reflection Seiemics in Petroleum Exploration. Gulf Publishing Company, Houston, Texas.

Miles, P.R., 2000. Geophysical sensing and hydrate. In: M.D. Max (Editor), Natural Gas Hydrate in Oceanic and Permafrost Environments. Kluwer Academic Publishers, Netherlands, pp. 261-274.

Multiwave, 2005. 05CM 2D Seismic survey, offshore East Coast - North Island. Report 3136, Ministry of Economic Development.

Nelson, C.H., Goldfinger, C. and Anonymous, 2000a. Variation of modern turbidite systems along the subduction zone margin of Cascadia Basin; implications for turbidite reservoir modeling. Annual Meeting Expanded Abstracts - American Association of Petroleum Geologists, 2000: 105.

Nicol, A. and Uruski, C., 2005. Structural Interpretation and Cross Section Balancing, East Coast Basin, New Zealand. Unpublished Petroleum Report PR3184, Ministry of Economic Development New Zealand.

Orange, D.L., 1999. Tectonics, sedimentation, and erosion in Northern California; submarine geomorphology and sediment preservation potential as a result of three competing processes. Marine Geology, 154(1-4): 369-382.

Orange, D.L., Yun, J., Maher, N., Barry, J. and Greene, G., 2002. Tracking California seafloor seeps with bathymetry, backscatter and ROVs. Continental Shelf Research, 22(16): 2273-2290.

Orpin, A., Carter, L., Lewis, K., Kuehl, S. and Alexander, C., 2003. Quantifying deposition from the very muddy Waipaoa River on the Poverty shelf and margin re-entrant, New Zealand. EGS - AGU - EUG Joint Assembly, Abstract 4871.

Orpin, A., 2004. Holocene sediment deposition on the Poverty-slope margin by the muddy Waipaoa River, East Coast New Zealand. Marine Geology, 209(1-4): 69-90.

Orpin, A., Alexander, C., Carter, L., Kuehl, S. and Walsh, J.P., 2006. Temporal and spatial complexity in post-glacial sedimentation on the tectonically active, Poverty Bay continental margin of New Zealand. Continental Shelf Research, 26(17-18): 2205-2224.

Paquet, F., 2007. Morphostructural evolution of active margin basins: the example of the Hawke Bay forearc basin, New Zealand. Ph.D. Thesis, University of Canterbury, Christchurch, 263 pp.

Paquet, F., Proust, J.-N., Barnes, P.M. and Pettinga, J.R., 2009. Inner-Forearc Sequence Architecture in Response to Climatic and Tectonic Forcing Since 150 ka: Hawke's Bay, New Zealand. Journal of Sedimentary Research, 79(3): 97-124.

Pecher, I.A. and Holbrook, W.S., 2000. Seismic methods for detecting and quantifying marine methane hydrate/free gas reservoirs. In: M.D. Max (Editor), Natural Gas Hydrate in Oceanic and Permafrost Environments. Kluwer Academic Publishers, Netherlands, pp. 275-294.

Pettinga, J., Lewis, K., Hampton, M.A. and Davey, F.J., 1984. Preliminary interpretations of near-surface multi-channel seismic data, across the obliquely convergent Hikurangi margin; offshore eastern North Island. Geological Society of New Zealand Miscellaneous Publication, 31A.

Ricketts, B.R. and Nelson, C.S., 2004. Early Pliocene landward submarine slumping, Lachlan Basin, Hawke Bay, New Zealand. New Zealand Journal of Geology and Geophysics, 47: 431-435.

Rogers, J.N., Kelley, J.T., Belknap, D.F., Beard-Tisdale, K., Agouris, P. and Anonymous, 1999. Study of pockmark evolution using seafloor imaging, Belfast Bay, Maine. Abstracts with Programs - Geological Society of America, 31(2): 64.

Spinelli, G.A. and Field, M.E., 2001. Evolution of continental slope gullies on the Northern California margin. Journal of Sedimentary Research, 71(2): 237-245.

Walsh, J.P., Sumners, B., Alexander, C., Orpin, A., Gerber, T. and Pratson, L., 2006a. Late Quaternary Morphological Changes of the Waipaoa River Outer Shelf and Upper Slope, New Zealand. Eos Trans. AGU, 87(52): Fall Meet. Suppl. Abstract.

Walsh, J.P., Sumners, B., Alexander, C., Orpin, A., Gerber, T., Pratson, L. and Kuehl, S., 2006b. Variations in Depositional Signals across the Shelf-Slope Transition on the Waipaoa River Margin, New Zealand. Eos Trans. AGU, 87(36): Ocean Sci. Meet. Suppl. Abstracts.

Walsh, J.P., Alexander, C., Gerber, T., Orpin, A. and Sumners, B., 2007. Demise of a submarine canyon? Evidence for highstand infilling on the Waipaoa River continental margin, New Zealand. Geophysical Research Letters, 34.

Wong, F.L. and Eittreim, S.L., 2002. Continental shelf GIS for the Monterey Bay National Marine Sanctuary. Marine Geology, 181(1-3): 317-321.

Yun, J.W., Orange, D.L. and Field, M.E., 1999. Subsurface gas offshore of northern California and its link to submarine geomorphology. Marine Geology, 154(1-4): 357-368.

Zhao, D., Matsuzawa, T. and Hasegawa, A., 1997. Morphology of the subducting slab boundary in the northeastern Japan arc. Physics of The Earth and Planetary Interiors, 102(1-2): 89-104.

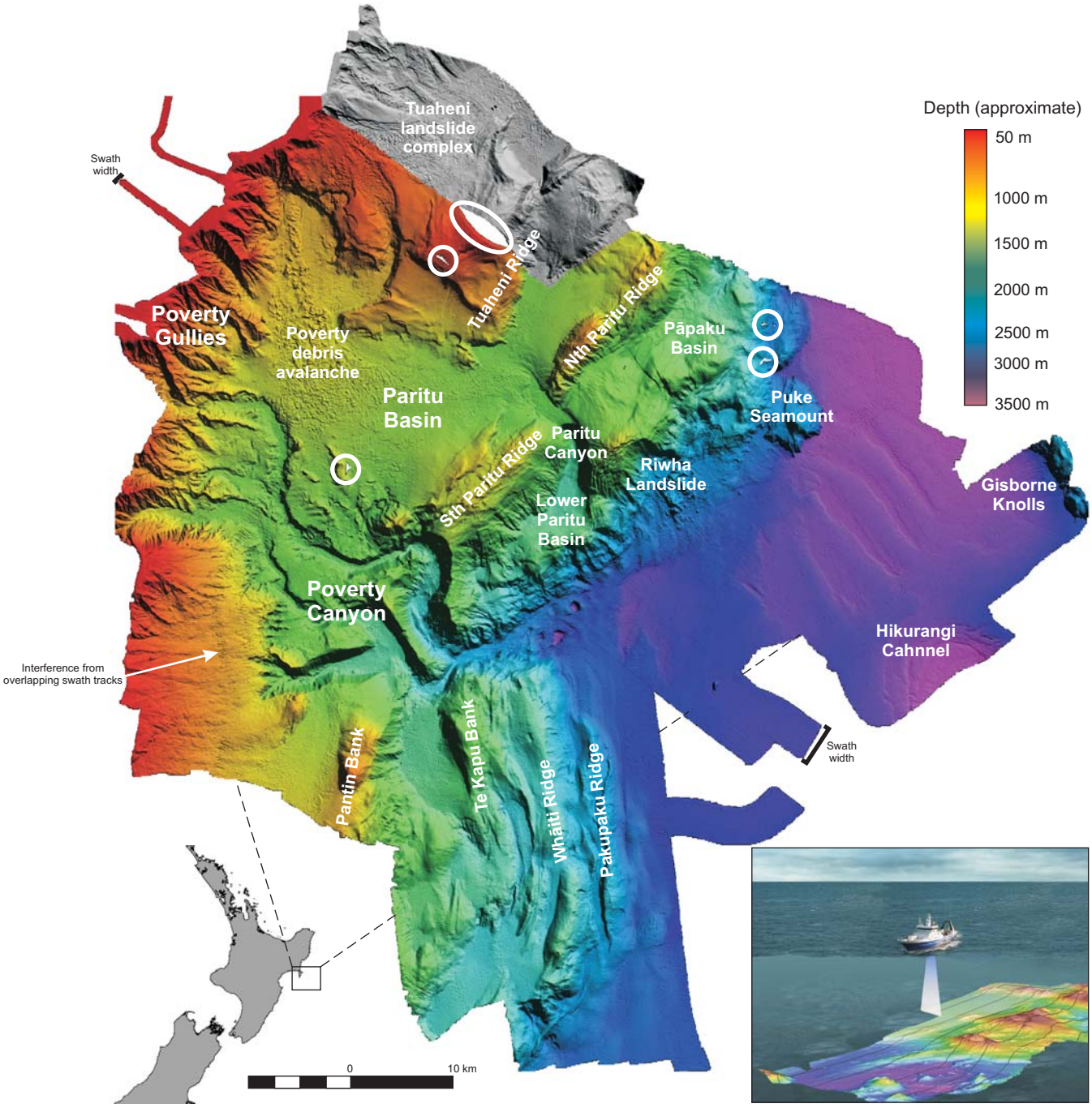

Figure 2.1 Obliquely illuminated Digital Elevation Model (DEM) of the Poverty Indentation produced by the EM300 swath mapping systemfrom the RV Tangaroa (see insert) in 2001. The red area covers the edge of the continental shelf offshore Poverty Bay, Mahia Peninsula and northern Hawke Bay. Dark blue to purple covers the trench fill sequence in the 3,300 m deep Hikurangi Trough. Area shaded in grey was collected more recently in 2007. Feature names used and/or generated for this project are labelled in white. Data artifacts labelled include interference patterns produced by overlapping swath tracks, missing data (circled in white) and variation in swath width (and therefore upper limit of resolution) due to water depth.

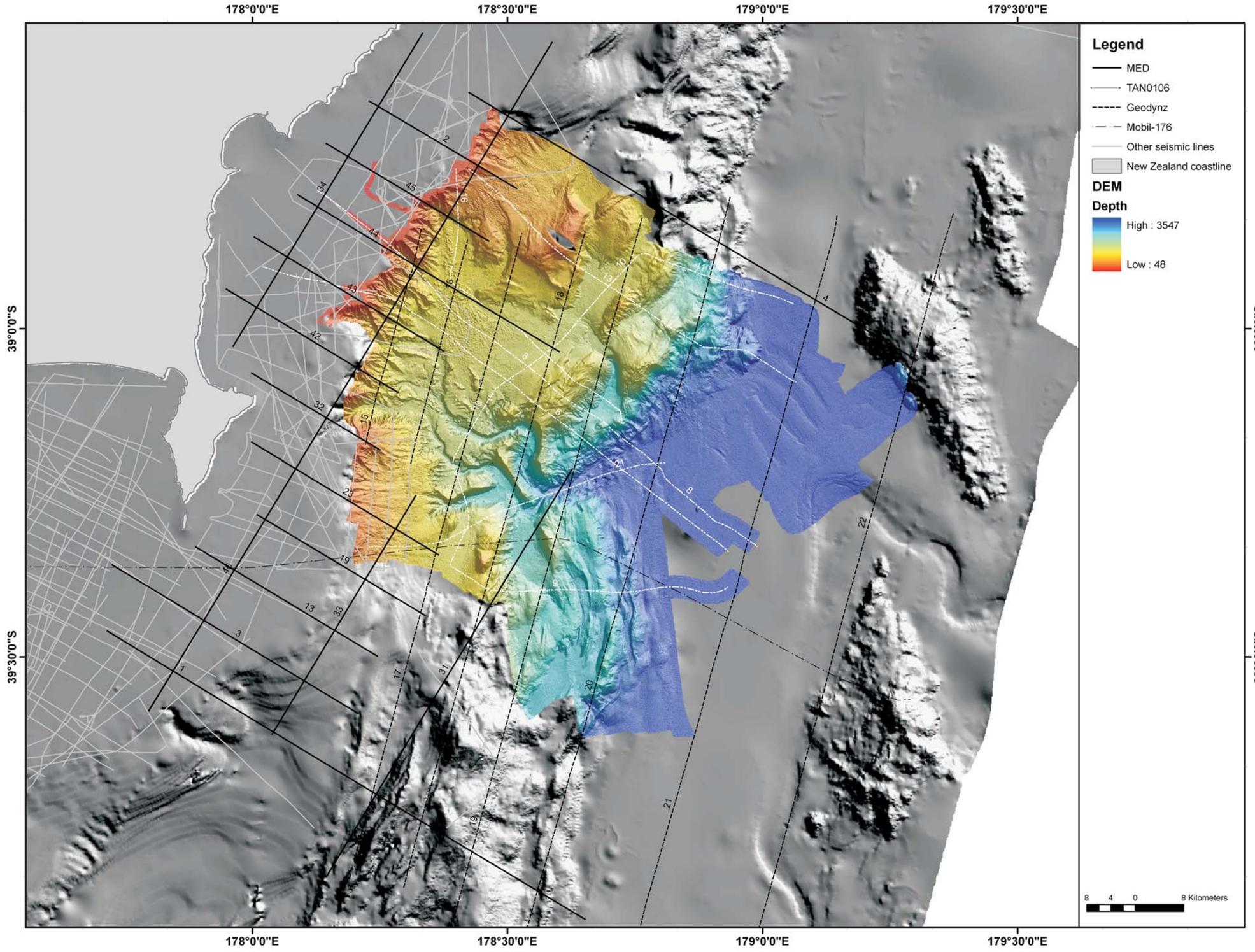

Figure 2.2 Seismic profiles available across the Poverty Indentation. Numbers beside each seismic line indicate the line number. Other regional seismic lines (indicated in grey) are not used in this project. MED in legend refers to the CM05/05CM survey.

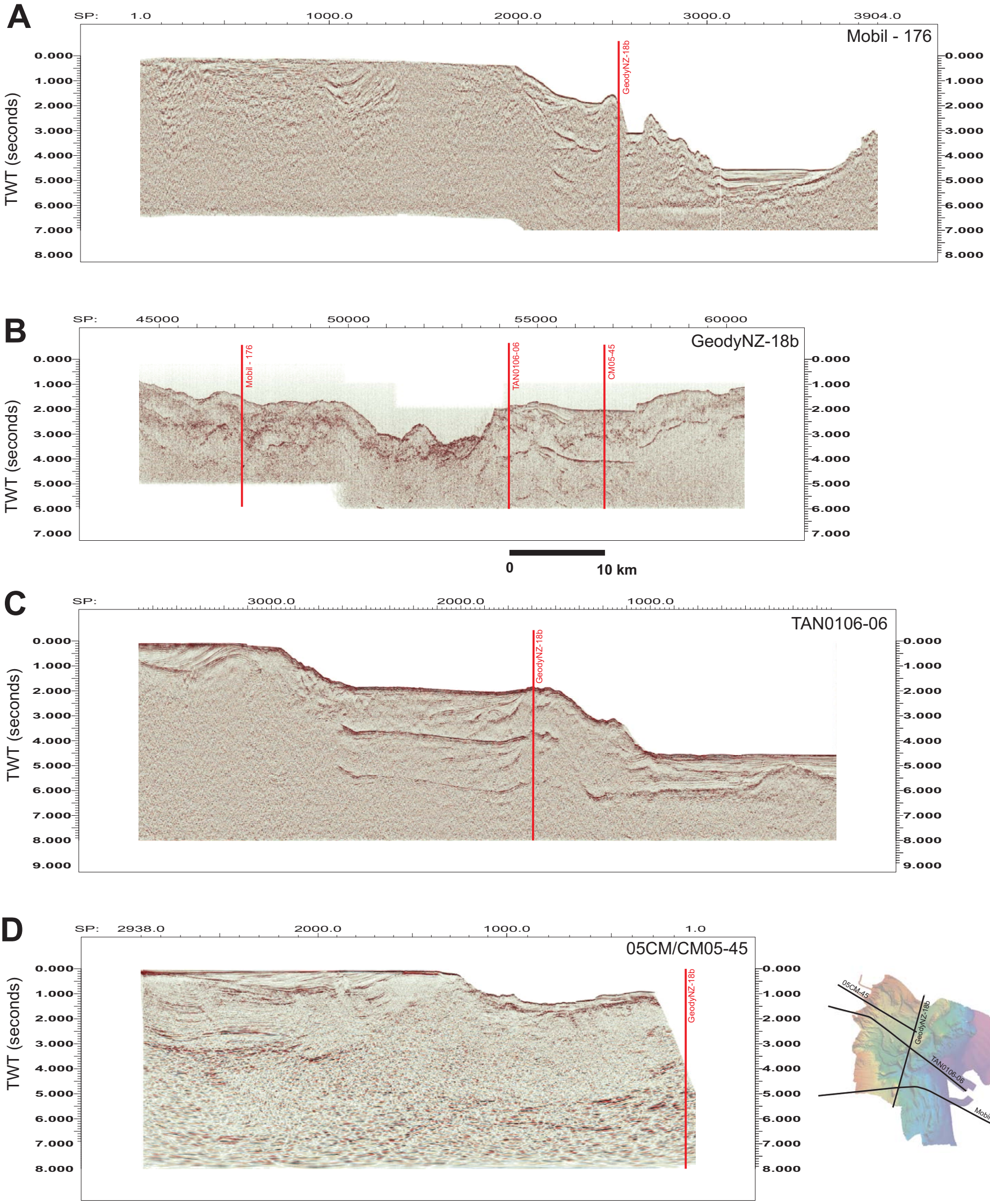

Figure 2.3 Examples of multi-channel seismic profiles used in this project. Vertical exaggeration is x 5. Red lines indicate tie points. SP = shotpoint number

A: Mobil (Line 176)

B: GeodyNZ (Line 18b)

C: TAN0106 (Line 06)

D: 05CM/CM05 (Line 45)

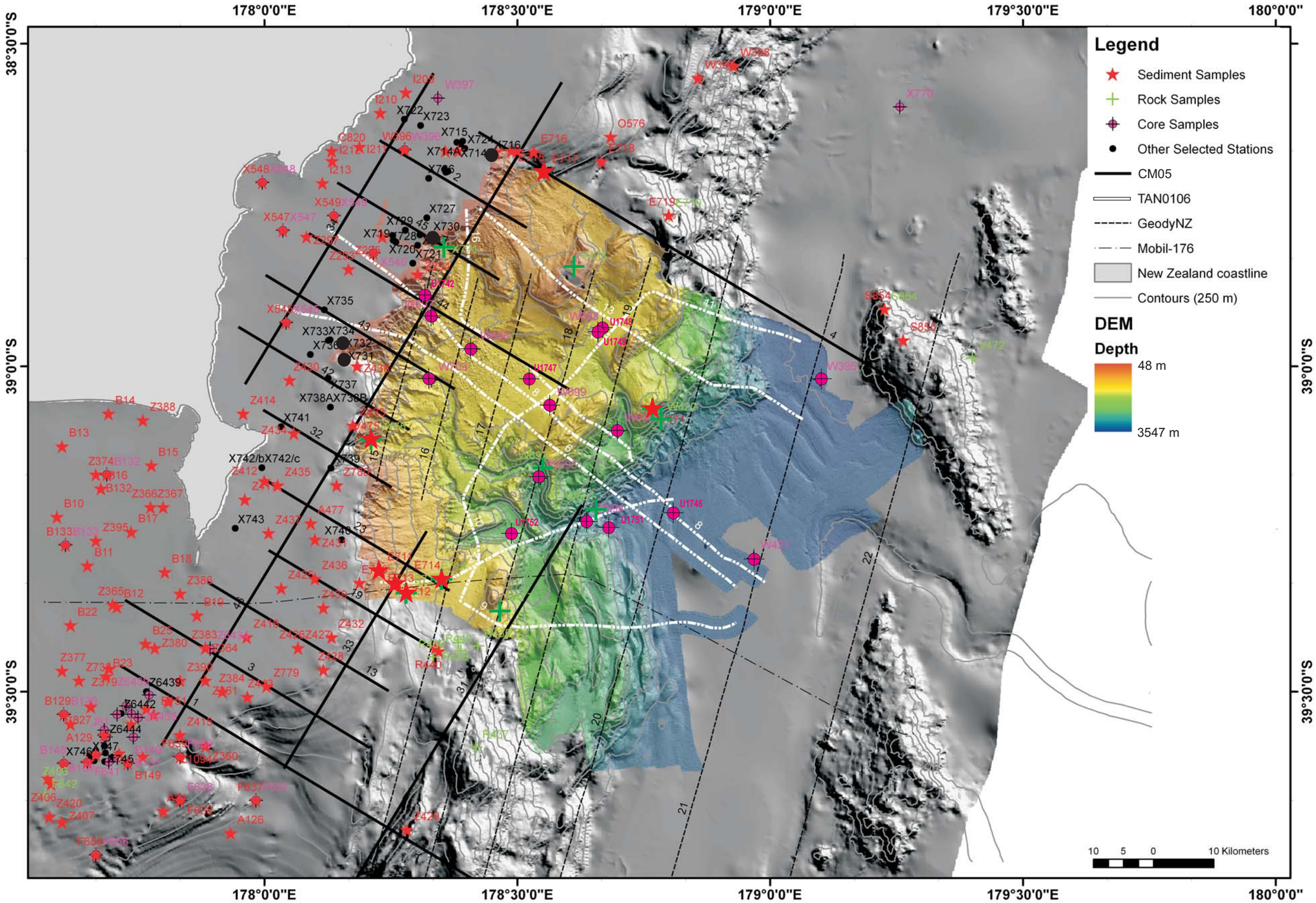

Figure 2.4 Core, dredge and rock samples in the region of the Poverty Indentation with accompanying seismic profiles. Sample stations specific to the indentation are enlarged.

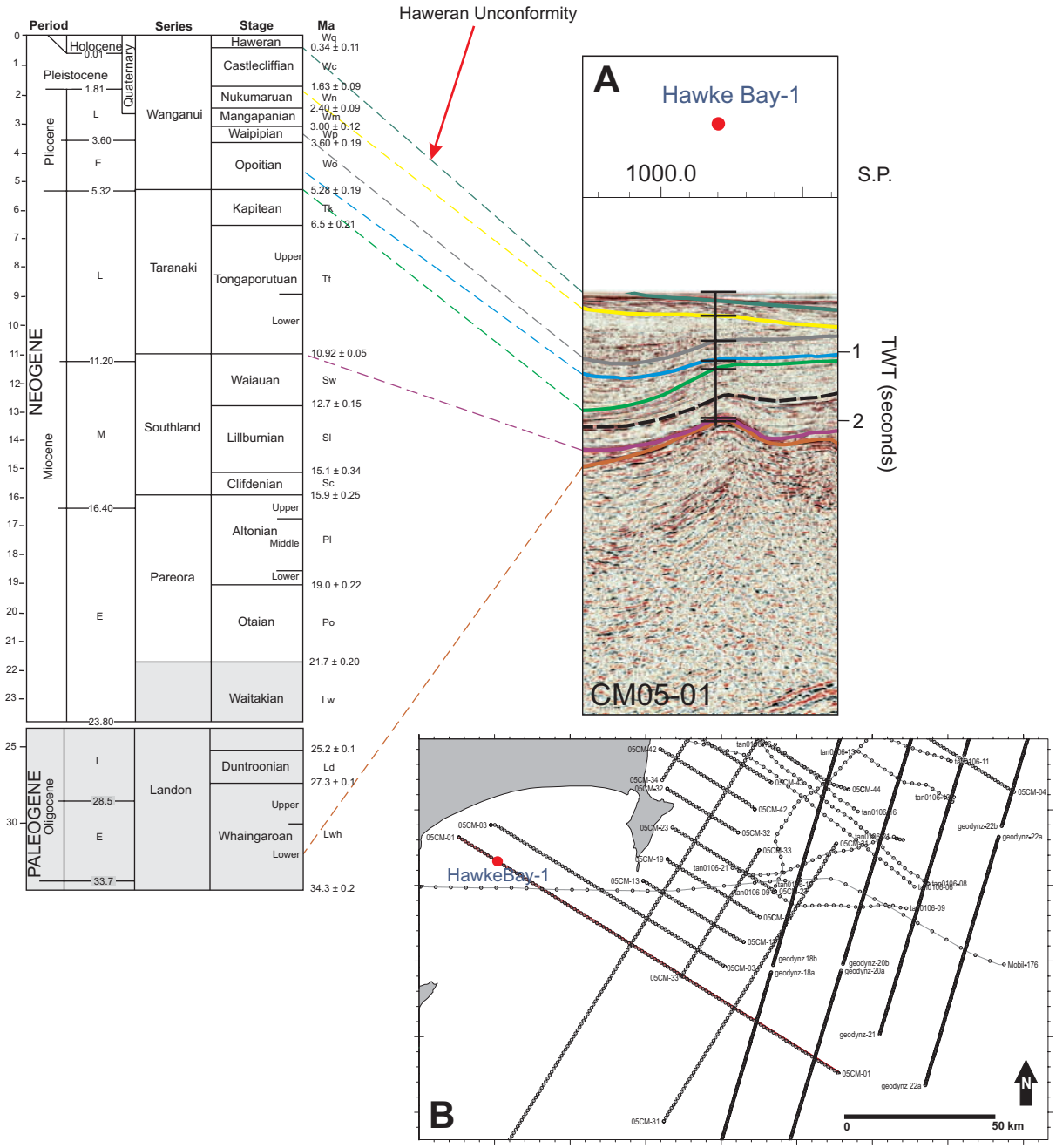

Figure 2.5 A: Summary of the seismic stratigraphy from well Hawke Bay - 1 (BP Shell Aquitaine and Todd Petroleum Development Ltd, 1976. Well completion report Hawke Bay-1. 667, New Zealand Ministry of Commerce). Haweran Unconformity extrapolated from Paquet (2007) and Barnes et al. (2004). Unknown aged unconformity indicated in black dashed line.

B: Location of the Hawke Bay - 1 well intersecting seismic line CM05-01. Grey shaded region represents the onshore North Island.

NZ Stage diagram after Cooper, R.A., (2004) New Zealand Geological Timescale 2004/2 wallchart. Institute of Geological and Nuclear Sciences information series 64.

Sample	Cruise ID	Date	Type	Sample Interval (cm)	Location	Water Depth (m)	Age (purple = nanofossils) (blue = foramanifera) (green = pollen) (red = tephra chronology)	Approximate Age (Ma)	Sediment Sources
E711	563	1967	Sediment		Clinoform sequence				
E712	563	1967	Sediment		Clinoform sequence				
E713	563	1967	Sediment		Clinoform sequence				
E713	563	1967	Rock		Clinoform sequence				
E714	563	1967	Sediment		Base of clinoform sequence				
E714	563	1967	Rock		Base of clinoform sequence				
E717	563	1967	Sediment		Tuaheni Landslides				
U1742	TAN0005	2000	Piston core	base (170)	Upper slope	477	Late Holocene	<0.005	Mud to sandy mud
U1746	TAN0005	2000	Piston core	base (300)	Hikurangi Trough	3405	Not determined		Mud to sandy mud with sandy volcanics and pumiceous layers
U1747	TAN0005	2000	Piston core	base (120)	Lower Paritu Basin	1463	Holocene		Mud to sandy mud
U1748	TAN0005	2000	Piston core	base (50)	Lower Paritu Basin	1461	Holocene		Mud to sandy mud. Sandy volcanics
U1749	TAN0005	2000	Piston core	base (200)	Lower Paritu Basin	1470	Holocene	0.0056	Mud to sandy mud. Graded tephra, pumiceous layers and volcanics
U1751	TAN0005	2000	Pilot core	base	Axis of Poverty Canyon mouth	3367	Upper Castlecliffian to upper Haweran	<0.5	Fast deposition to deep sea. Interglacial deposit
U1752	TAN0005	2000	Piston core	base (150)	Southern branch of Poverty canyon	2264	Late Holocene	<0.005	Mud to sandy mud with graded tephra and pumiceous layers
V471	3017	1994	Dredge		Headscarp of Riwha Scar	1500	Middle Opoitian to upper Haweran. Possibly middle or upper Opoitian	4	Medium grey compact mudstone. Deposited from subdued water at upper bathyl depths
V473	3017	1994	Rock		Tuaheni Ridge	365-800	Not determined		Deposited at a fast rate from agitated water at ?shelfal depths. Pale grey hard massive fine-grained limemud
V475	3017	1994	Dredge		Head of Poverty Canyon	700-1200	Upper Otaian to lower Clifdenian, probably lower to middle Altonian	19-16	Grey calcareous claystone. Deposited at medium fast rate from subduced water at lower bathyl depths
V477	3017	1994	Rock		Pantin Bank/Nth Ritchie Ridge	800-1400	Upper Castlecliffian to middle Haweran	0.9-0.2	Medium grey soft massive chalk. Deposited at a slow rate from quiet water at lower shelfal or upper bathyl depths
W395	3021	1994	Core		Trench fill				
W421	3021	1994	Core		Trench fill				
W422	3021	1994	Rock		Riwha Scar	1900-2600	Middle Altonian to upper Lillburnian	17-13	Medium grey compact massive mudstone. Deposited at fast rate from quiet water at lower shelfal or upper bathyl depths
W691	TAN0106	2001	Dredge/rock		First accretionary ridge at bottom of Poverty Indentation	2750-3214	Upper Nukumaruan - lower Haweran (early to mid Pleistocene)	1.8 - 0.2	Shallow hard-ground and a late Eocene-Oligocene limestone. Deep-sea deposition, significant volcanic glass
W692	TAN0106	2001	Dredge/rock	large block	Northern wall of Poverty Canyon	1572-2176	Lower Castlecliffian (early Pleistocene)	1.4	Not listed
W692	TAN0106	2001					Castlecliffian to Haweran (Pleistocene)	1.6 - 0.3	No benthics, significant volcanic glass
W693	TAN0106	2001	Piston core	base (60)	Axis of Poverty Canyon	2404	Middle Haweran (Late Pleistocene)	0.15	Shallow hard-ground
W694	TAN0106	2001	Pilot core	14-16	Axis of Poverty Canyon	3121	Middle Castlecliffian (lower Pleistocene)	1.2	Shallow hard-ground
W695	TAN0106	2001	Piston core	base (250)	Lower slope basin	2384	Holocene	0.0035	Mud to sandy mud with volcanics, graded tepha and pumiceous layers
W696	TAN0106	2001	Piston core	base (225)	Mid-slope Paritu Trough debris flow	1303	Holocene	0.0035	Mud to sandy mud with graded tephra
W697	TAN0106	2001	Multicore		Poverty upper slope	1198	late Holocene	0.002	Upper slope base of feeder canyon
W698	TAN0106	2001	Multicore		Mid-slope basin	1469	late Holocene	0.0027	Mid-slope depositional flank
W699	TAN0106	2001	Multicore		End of Poverty debris flows	1428	late Holocene	0.003	Mid-slope depositional basin
W703	TAN0106	2001	Piston core	32-34	Axis of upper slope Poverty Canyon	1455	Upper Altonian to lower Lillburnian (topmost lower Miocene to middle mid Miocene)	16 - 14	Excellent Pleistocene contaminant. Fairly fast deposition to deep-sea. Mud to sandy mud with indurated/stiff layers
X716		1998			Poverty shelf				
X730		1998	Dredge/rock		Poverty shelf	92	Lower Waiauan to top Opoitian - most likely Waiauan (middle Miocene)	12	Hard medium grey fine-grained limestone
X731		1998	Dredge		Head of Poverty Canyon/shelf break	217	Not determined		Bored mudstone
X732		1998	Dredge		Poverty Shelf	79	Upper Castlecliffian to lower Haweran (middle Pleistocene)	0.3	Very soft medium grey calcareous clay. Deposited at a moderate rate from subdued water at middle shelfal to upper bathyl depths
X771	3057	1999	Dredge		Gisborne continental shelf	700	Middle Altonian to topmost Liburnian (lower Miocene to middle Miocene)	18 - 13	Hard grey cm-bedded mildy calcareous mudstone. Pyrite bearing biogenic lime volcanic mud.

Table 2.1 Core, dredge and rock samples in the Poverty Indentation. Ages have been identified by nanofossils and foraminifera (Anthony R Edwards, Stratigraphic Solutions Ltd), palynology (Graeme J Wilson, GNS Science) and tephra chronology (Phil Shane, Uniservices, University of Auckland). Samples lacking information (blank boxes) were unable to be obtained from archives.

Figure 2.6 Collecting box dredge samples from the Poverty shelf and upper slope on the RV KILO MOANA (Honolulu, HI), February 2005.

CHAPTER 3: SEAFLOOR STRUCTURAL GEOMORPHIC EVOLUTION OF THE ACCRETIONARY FRONTAL WEDGE IN RESPONSE TO SEAMOUNT SUBDUCTION, POVERTY INDENTATION, NEW ZEALAND

Abstract

High quality swath bathymetry and seismic reflection data reveal that the steep forearc slope along the northern sector of the obliquely convergent Hikurangi subduction zone is characteristic of non-accretionary and tectonically eroding continental margins, with reduced sediment supply in the trench relative to further south, and the presence of subducting seamount relief on the Hikurangi Plateau. These seamounts influence the subduction process and the structurally-driven geomorphic development of the over-riding margin of the Australian Plate frontal wedge.

The origin of the Poverty Indentation, on the inboard trench-slope, is attributed to multiple seamount impacts over the last c. 1 Myr period, accompanied by canyon incision, thrust fault propagation into the trench fill, and numerous large-scale gravitational collapse structures with multiple debris flow and avalanche deposits ranging in down-slope length from a few hundred metres to more than 40 km. The indentation is directly offshore of the Waipaoa River which is currently estimated to have a high sediment yield into the marine system. The Poverty Canyon stretches 70 km from the continental shelf edge directly offshore from the Waipaoa to the trench floor, incising into the axis of the indentation. The sediment delivered to the margin from the Waipaoa catchment and elsewhere during sea-level high-stands, including the Holocene, has remained largely trapped in a large depocentre on the Poverty shelf, while during low-stand cycles, sediment bypassed the shelf to develop a prograding clinoform sequence out onto the upper slope. The formation of the indentation and the development of the upper branches of the Poverty Canyon system has led to the progressive removal of a substantial part of this prograding wedge by mass movements and gully incision. Sediment has also accumulated in the head of the Poverty Canyon and episodic mass flows contribute significantly to continued modification of the indentation by driving canyon incision and triggering instability in the adjacent slopes.

Prograding clinoforms lying seaward of active faults beneath the shelf, and overlying a buried inactive thrust system beneath the upper slope, reveal a history of deformation accompanied by the creation of accommodation space. The middle to lower Poverty Canyon represents a structural transition zone within the indentation coincident with the indentation axis. The lower to mid-slope south of the canyon conforms more closely to a classic accretionary slope deformation style with a series of east-facing thrust-propagated asymmetric anticlines, separated by early-stage slope basins. North of the canyon system, seamount impact has resulted in frontal tectonic erosion associated with the development of an over-steepened lower to mid-slope margin, fault reactivation and structural inversion and over-printing.

3.1 INTRODUCTION

Sedimentary sequences accumulating at continental margins may provide records of paleo-climates, sea-level change, tectonics/deformation, geomorphic evolution and anthropogenic effects (e.g. Orange, 1999; Carter et al., 2002; Greene et al., 2002). Subduction zones associated with thick trench fill sequences and high sediment flux rates along continental margins commonly form wide and voluminous accretionary wedges in response to the interaction of the subducting plate with the over-riding plate (e.g. Dickinson and Seely, 1977; Dickinson and Seely, 1979).

Seamount subduction plays a significant role in the morpho-structural evolution of convergent margins (e.g. Fryer and Smoot, 1985; Lallemand and Le Pichon, 1987; Dubois et al., 1988; Konishi, 1989; Lallemand et al., 1989; Maruyama and Liou, 1989; Yamazaki and Okamura, 1989; Masson et al., 1990; Dominguez et al., 1998b; Mann et al., 1998; Robertson, 1998; Dominguez et al., 2000; Hühnerbach et al., 2005). Many studies have primarily focused on the localized effects of these collisions, such as inhibiting or modifying frontal accretion and producing re-entrants (e.g. Dominguez et al., 1998b; Hühnerbach et al., 2005), rather than their contribution to the temporal and spatial aspects of the evolution of the forearc slope as a whole.

In recent years, the acquisition of high quality SIMRAD EM300 multibeam bathymetry and deep-penetration multi-channel seismic data (Lewis, 2001; Multiwave, 2005) across the northern Hikurangi Margin is providing new insights into the off-shelf sediment transport, dispersal and storage system, seamount subduction effects on the margin, and the structural

and morphological evolution of the frontal wedge. We focus here on the Poverty Indentation (Figure 3.1), a large ~4000km^2 structural re-entrant containing the Poverty Canyon system, located directly outboard of the Waipaoa River in Poverty Bay. This indentation was inferred to have possibly resulted from the effect of seamount subduction on the margin (Lewis and Pettinga, 1993; Wood and Davy, 1994; Collot et al., 1996a; Collot et al., 1996b; Lewis, 1997; Lewis et al., 1998; Collot et al., 2001; Lewis et al., 2004).

The Poverty shelf and slope on the northern sector of the Hikurangi Margin is recognized as the "sink" for recent Waipaoa River and along shelf sediment (Haq et al., 2004). Our study of the Poverty Indentation and Poverty Canyon provides the basic structural framework for the marine section of the Waipaoa Source-to-Sink system. In this study we demonstrate that it is not a closed sedimentary system over time scales of 10^5-10^7 years. The primary role of the system is one of conveying, distributing and temporary storage of sediment from the continental shelf to the trench floor. The morphology of the margin, the ongoing deformation accompanying seamount subduction, and associated mass wasting are important factors affecting the accumulation, dispersal and redeposition of shelf sediments.

We present here a morpho-structural evolutionary model for the Poverty Indentation and address the role that the evolving indentation has played in influencing the sediment pathways from the continental shelf to the trench floor. The key objectives of this paper are: (i) to determine the role of subducting seamount topography in shaping the large-scale morphology of the present re-entrant in the Hikurangi Margin; (ii) to investigate the evolution and deformation of the Poverty Indentation slope basins and their sediment fill inboard of the deformation front; (iii) to document the role of Poverty Canyon in conveying sediment from the continental shelf to the trench floor; and (iv) to identify seabed processes involved in sediment entrapment and flux across the margin slope at a variety of timescales.

3.2 HIKURANGI MARGIN

The Hikurangi Margin (Figures 3.1A and 3.1B) became an active subduction margin ~25 Myr ago and is now represented by a significant deformation zone 50 to 200 km wide, stretching from the offshore Hikurangi Trough (structural trench), to the eastern side of the extensional arc system of the Taupo Volcanic Zone (TVZ) (e.g. Walcott, 1978; Lewis, 1980; Lewis and Pettinga, 1993). Outboard of the axis of the Hikurangi Trough lies the Hikurangi Plateau, a

Mesozoic age Large Igneous Province (c.15 km thick) (Davy and Wood, 1994; Davy et al., 2008). The plateau is draped by an Upper Cretaceous – Cenozoic succession thought to be comprised partly of terrestrial-derived sediments (Davy et al., 2008). The upper part is a turbidite succession derived from the Hikurangi Channel that funnels density currents from the south along the axis of the Hikurangi Trough (Lewis and Pantin, 2002). Inboard of the Hikurangi Trough, west of where the Pacific Plate is subducting beneath the Australian Plate, the subduction-driven contractional deformation forms a composite frontal wedge (Lewis and Pettinga, 1993; Barnes et al., 2009). This can be divided into a lower slope accretionary wedge formed of accreted trench-fill sediments, and a mid to upper slope section of similarly thrust Mesozoic and Early Cenozoic New Zealand continental platform units predating the local inception of the subduction. Late Cenozoic sediments cover most of the shelf and frontal wedge slope (Pantin, 1966; Pantin and Gibb, 1968; Foster and Carter, 1997; Orpin, 2004; Alexander et al., 2006a; Alexander et al., 2006c; Walsh et al., 2007; Alexander et al., 2009) and south of Poverty Bay are deposited preferentially in actively forming slope basins (e.g. Lewis, 1980). In the central sector of the margin, the contractional deformation is accompanied by the episodic trench-ward propagation of the deformation front, leading to a widening of the lower accretionary slope, associated with the incorporation of off-scraped trench-fill sediments (Lewis, 1980; Lewis and Pettinga, 1993; Collot et al., 1996a; Barnes and Mercier de Lepinay, 1997; Barnes et al., 1998; Barnes et al., 2009). The pre-subduction upper part of the frontal wedge is emergent, forming the coastal ranges and basins of the East Coast. The forearc backstop comprises Mesozoic greywacke units of the North Island Dextral Fault Belt (NIDFB) (Walcott, 1987; Beanland and Haines, 1998) (Figures 3.1A and 3.1B).

The Hikurangi Margin has been subdivided into three sectors along its length based on tectonic processes and deformation styles (Figure 3.1A) (Lewis and Pettinga, 1993). The central sector of the margin is characterised by a moderate relative convergence rate of ~43 mm/yr (Wallace et al., 2004) and a high sedimentation rate in the adjacent trough. A significant accretionary wedge has developed from the accretion of South Island derived trench-fill sediments, longitudinally-fed northward along the Hikurangi Channel and Trough, combined with sediment derived from the North Island across the margin slope. Slope basins (often stretching up to 50 km in length, parallel to the trench) trap sediment on the frontal wedge. In contrast, the northern sector can be classified as an erosional convergent margin, characterised by an over-steepened frontal slope, subducting seamounts, frontal tectonic erosion, and extensive regions of gravitational collapse within the inboard trench slope

(Collot et al., 1996b; Barker et al., 2009). The tectonic and geomorphic transition between presently wide accretionary wedge in the central part of the margin, and subducting seamounts in northern part of the margin has recently been located south of the Rock Garden bank off southern Hawke Bay (Figure 3.1A) (Barnes et al., 2009).

Kinematic modelling indicates that relative rates of convergence between the northern Hikurangi Margin and the Pacific Plate decrease southwards from ~ 60 mm/yr off East Cape to 45 mm/yr off southern Hawke Bay (Wallace et al., 2004; Wallace et al., 2008) (Figure 3.1A). The northern convergence vector is faster than the Pacific – Australia relative plate motion rate and is more orthogonal to the margin (c.f. Beavan et al., 2002), because of the combined effects of plate convergence, backarc extension, and large scale crustal rotation of the east coast of North Island. The northern margin includes two margin-scale re-entrants , the Poverty and Ruatoria indentations, accompanied by large-scale gravitational collapse and structural deformation of the frontal wedge, which have previously been attributed to the effects of impacting seamounts (e.g. Lewis and Pettinga, 1993; Collot et al., 1996a; Collot et al., 1996b; Lewis, 1997; Lewis et al., 1998; Collot et al., 2001; Lewis et al., 2004). Evidence of multiple seamount subduction at various stages of evolution, a high sediment supply and moderate sediment thickness in the Hikurangi Trough, make the Hikurangi Margin an excellent candidate to observe the range of structural and geomorphic features associated with seamount subduction processes, accretion, and canyon development.

3.2.1 *The Poverty Indentation*

The Poverty Indentation extends from the trench floor virtually to the shelf edge across the entire forearc slope. Based on the overall geometry of the indentation, the presence of multiple seamounts on the Hikurangi Plateau directly outboard from the margin, and evidence of tectonic erosion along the frontal slope, it is inferred to be directly related to one or more large seamount impacts (Lewis and Pettinga, 1993; Collot et al., 1996a; Collot et al., 1996b; Lewis et al., 1998). Subducting seamounts have been well imaged in seismic data from the margin off Hawke Bay, south of the indentation (Barnes et al., 2009). The axis of the indentation is defined by the branched Poverty Canyon (Arron and Lewis, 1992) system (Figures 3.1C and 3.2). South of the Poverty Canyon mouth, the lower slope ridges have been dragged inwards creating a distinctive arcuate frontal accretionary wedge oriented 165/345^{o} in the north off southern Mahia Peninsula, and swinging to 030/210^{o} towards the south, off Hawke Bay. North of the canyon, the frontal wedge has an average width of 50-60 km, while

to the south it widens progressively to ~ 85 km off Hawke Bay and more than 100 km in the central (Wairarapa) sector of the margin (Figures 3.1 and 3.2). A 10 km right step in the deformation front at 39° 10'S (Figure 2) results from seamount subduction beneath the lower slope off Hawke Bay (Barnes et al., 2009).

The shelf and slope are significantly influenced by sediment input from the Waipaoa River, and the Poverty Indentation is recognised as a significant pathway and temporary sink for sediment transported from the continental shelf to the Hikurangi Trough (e.g. Foster and Carter, 1997; Haq et al., 2004; Orpin, 2004; Alexander et al., 2006c). Historically, the Waipaoa River has one of the highest discharges of suspended sediment load in New Zealand (~15 Mt $year^{-1}$), despite its relatively small catchment of 2205 km^2 (Griffiths and Glasby, 1985; Hicks et al., 2000). This voluminous sediment supply has had a significant influence on the Quaternary evolution of the adjacent shelf and Poverty Canyon system (Figures 3.1C and 3.2). On the shelf a large structurally controlled depocentre for sediment has captured significant volumes of sediment during high-stand sea levels, with some in-filling of the canyon head (Walsh et al., 2007). Conversely, during low-stand sea levels, sediment is thought to largely bypass the shelf and enter the Poverty Gullies and Canyon, creating turbidites and mass debris flows; small lower slope basins located between thrust-propagated anticlines represent transient and permanent depocentres for sediment delivered to the continental slope (Foster and Carter, 1997; Orpin, 2004; Alexander et al., 2006a; Alexander et al., 2006b; Alexander et al., 2006c; Walsh et al., 2007; Mountjoy, 2009).

3.3 DATA & METHODS

High quality 30 kHz multibeam bathymetric data of the Poverty Indentation were obtained by the National Institute of Water & Atmospheric Research (NIWA) in 2001 (survey TAN0106) using a SIMRAD EM300 multibeam system on RV TANGAROA. Over 4000 km^2 of submarine seafloor was mapped, encompassing the entire indentation, at depths ranging from 50 to 3500 metres (Figures 3.1C and 3.2). The data have been processed to 10m and 25m grid digital elevation models (DEMs). Additional areas were surveyed during 2006 (TAN0616) and 2008 (TAN0808 and TAN0810), extending bathymetric data in the northern area of the indentation (see also Mountjoy et al., 2009b).

Multi-channel seismic reflection data used in this study include: 1) reprocessed 3-fold Mobil Exploration seismic data (1972); 2) GeodyNZ RV L'ATALANTE 1993 3-fold profiles (Collot et al., 1996a; Lewis et al., 1997); 3) RV TANGAROA 2001 (TAN0106) 6-fold (45/105 ci GI gun source) profiles; and 4) high fold (960-channel), deep penetration to 12 s two-way-travel time (TWT), Bolt (1500 & 1900 Long Life) airgun source profiles acquired by Ministry of Economic Development Ltd. (MED) on the MV PACIFIC TITAN in 2005 (CM05/05CM) (Funnell and Benchilla, 2005; Maslan, 2005; Multiwave, 2005; Barker et al., 2009). The low-fold profiles that cover the middle and lower part of the indentation, where we focus much of our work, were acquired with short seismic streamers and provide poor seismic velocity information, hampering our ability to produce quality depth sections across the outer part of the frontal wedge. We therefore present time-sections for these data. For comparisons with depth-sections around the Poverty Indentation, readers are referred to (Barker et al., 2009; Bell et al., 2009).

3.4 HIKURANGI TROUGH

The incoming Pacific Plate east of the Poverty Indentation comprises the Hikurangi Plateau and sediment fill in the Hikurangi Trough (structural trench) (Figures 3.1 and 3.2). Sediment generated or remobilised from the Poverty Indentation or derived directly from the Poverty Canyon, are either deposited into a significant trench floor depocentre proximal to the toe of slope, or are conveyed away from the margin, along the Hikurangi Channel (Lewis and Pantin, 2002) (Figure 3.2). The Hikurangi Channel is deflected here out to the northeast across the Hikurangi Plateau, away from the margin (Lewis, 1994) (Figure 1A).

A key feature on the Hikurangi Plateau is the presence of numerous Mesozoic (Wood and Davy, 1994) seamounts. Some seamounts are now at the deformation front, while others are still approaching as a result of plate convergence. On the northern margin of the indentation, the small (>6 x 8 km, 600 m high) Puke Seamount (Note: New feature names introduced in this paper are underlined) is in the process of being subducted (see Figures 3.1C and 3.2). Larger seamounts, including the most proximal of the Gisborne Knolls, lies within 20 km from the deformation front, and is 1500 m high (Figure 3.1). Multi-channel seismic profiles of the trough in the vicinity of these seamounts reveal substantial basement relief (~200->1000m) buried beneath the overlying sediments (Figure 3.3).

Directly covering the Pacific Plate basement (Figure 3.3A) is a horizontal succession of volcaniclastic sediments interpreted to be of Mesozoic age and a condensed Paleogene sequence (Wood and Davy, 1994; Davy et al., 2008; Barnes et al., 2009). This is in turn covered by a ~1.0 second TWT (~1 km thickness) succession of hemipelagic and trench-fill sediments with buried paleo-channels (Figure 3.3B(i)) and large paleo-sediment waves (Figures 3.3A(i) and 3.3B(i)). The paleo-channels are on a scale comparable to the modern day Hikurangi Channel, and may record previous locations of the channel. These are also imaged in GeodyNZ-21 and previously attributed to a linkage of the Poverty Canyon to the Hikurangi Channel (Lewis et al., 1998). The sedimentary succession onlaps onto seamount flanks and progressively overtops them (Figure 3.3A(i) and (ii)). A basal volcaniclastic apron also surrounds and onlaps onto the seamount flanks (Figure 3.3A(ii)).

A chaotic, reflection free reflector package up to 0.25 seconds TWT (~300 m thickness) is also interpreted in seismic profiles as a voluminous buried debris flow deposit (Figure 3.3A) (Figure 3.3A(i) and (ii)), which in along trough seismic profiles (i.e. GeodyNZ-21 and 14) is observed to thicken northward from the study area. This large debris flow unit has been interpreted as the southern-most extent of the Ruatoria debris avalanche deposit (Lewis, 1997; Collot et al., 2001). The seismic data reveal no similar scale buried debris avalanche deposit originating from the Poverty Bay Indentation itself. Other reflection-free layers occur on the flanks of seamounts and are interpreted as debris units locally derived from the steep seamounts (Figure 3.3A(ii)).

Large-scale sediment waves (spaced approximately 5 km apart) are also a significant feature of the seafloor between the present-day Hikurangi Channel and the deformation front (Figure 3.2). Immediately downstream from the Poverty Canyon mouth, large (1-1.5 km) scour holes are also detected in the swath bathymetry data (Figure 3.2). The scour holes vary in depth, with one reaching 100-120 m. We infer that the scour holes may be related to the occurrence of turbidity currents down the Poverty Canyon due to their location at the mouth of the canyon (bathymetry ~3300 m). The canyon mouth is notable for the lack of development of a sediment fan on the trench floor.

3.5 MORPHOLOGY OF THE POVERTY INDENTATION

The Poverty Indentation covers an area over 4000 km^2 stretching across the entire continental slope (Figure 3.1). The Poverty Canyon system covers an area of ~600 km^2 and is up to 70 km long, up to 40 km across at the rim and up to 2.1 km wide in the channel axis, with axial gradients of up to 12° (Figure 3.4). It is sinuous, with the head of the canyon separated into three branches. The two northern branches originate from a series of gullies incised into the continental shelf edge and upper slope. A third branch originates from the base of an upper slope clinoform sequence (Figure 3.2) to the south. Extensive arcuate erosional head-scarps extend northward along the western edge of the middle channel (Figure 2), and incise into the clinoform sequence (Figure 3.2). The canyon passes through the south-western edge of the Paritu Basin. Here slumps from the canyon walls are common in the upper reaches, as the canyon incises into the basin fill (Figure 3.2). There are a number of nick-points observed in the canyon floor, particularly where the canyon incises through the mid-slope ridge complexes (South Paritu Ridge and Pantin Bank) and immediately "upstream" from the slope toe deformation front (Figure 3.4).

The lower slope frontal wedge of the Poverty Indentation shows lateral variation north and south of the Poverty Canyon. Deformation on the northern frontal wedge directly inboard of the subducting Puke Seamount is overprinted on the sea floor with extensive zones of gravitational collapse and/or regions of normal faulting (Figure 3.5A). Anticlinal ridges are asymmetric, with the steeper southeast-facing forelimb slopes of 14-40^o, and are dominated by the numerous landslides scars. The structural backlimbs are characterised by slopes ranging from 2-29^o (generally <11^o). Landslide scars are rare on these backlimb slopes (Figures 3.5 and 3.6). South-facing landslide scars are also concentrated in the zone immediately north of the canyon mouth. The significant Riwhā Landslide and scar (2 x 4 km with slope angles of up to 45^o) on the deformation front on the edge of the Lower Paritu Basin, has a debris run-out of nearly 9 km and has previously been inferred to have resulted from a small seamount impact (Figure 3.7) (Lewis, 1997). Blocks in the debris flow from this landslide are up to 3 km in length.

South of the Poverty Canyon, plate convergence has produced a well developed accretionary wedge of off-scraped trench sediments characterised by a series of east-facing thrust-propagated asymmetric anticlinal ridges (Figure 3.8). The wedge consists of three main frontal anticlines, Te Kapu Bank, Whāiti Ridge and Pakupaku Ridge, and a series of smaller

ridges. Bathymetric elevation is much more gentle over this accretionary wedge, than along the toe of the slope north of the canyon. Numerous submarine slide scars are observed in the bathymetry, but these have less relief compared to scars on the north side of the Poverty Canyon. These slides are mostly concentrated on the fault-bounded, east-facing forelimbs where the slopes are over-steepened (up to 40^{o}) (Figure 3.8A).

The mid-slope North and South Paritu ridges are separated from the deformation front and lower slope by two, 10 km-long slope basins, the Pāpaku Basin in the north and the Lower Paritu Basin in the south (Figures 3.1C, 3.2 and 3.5). The Pāpaku Basin is a wide (5 - 8 km), moderately sloping (<17^{o} averaging ~5^{o}) depression east of North Paritu Ridge. This depression is situated in a complex structural setting, with growing thrust-propagated anticlines developing underneath, gravitational collapse at the outboard and southern edges, and faulting orthogonal to the margin front developing in the zone directly inboard of the Puke Seamount. Sediment is restricted mostly to veneers on anticline cored slopes without the development of significant syn-kinematic basin fill.

In its upper reaches Paritu Canyon is choked with sediment. Two nick-points represent significant escarpment steps (~400 m and <200 m) on the canyon floor (Figure 3.4). The lower reaches of the canyon, leading to the Lower Paritu Basin is evacuated of sediment fill (Figure 3.6A). Canyon wall morphology indicates it has previously been filled with sediment which is now being progressively scoured out. Sediment transport through this canyon from the main, upper/mid-slope Paritu Basin has resulted in thick (~500 m) triangular sediment wedge in the Lower Paritu Basin.

The Paritu Basin covers an area of nearly 500 km^{2}. Landslides and an extensive gully system originate from immediately below the shelf edge at the head of the basin and erode into the upper slope (Figure 3.9). The Poverty Debris Avalanche (Mountjoy et al., 2009b) is comprised of a series of extensive debris flows originating from the shelf break and gully region, cutting obliquely across Paritu Basin (Figure 3.9). The youngest flows have been emplaced southward over 30 km and into the upper and mid-reaches of the Poverty Canyon, covering ~200 km^{2} of Paritu Basin floor. The head zones of these flows are accompanied by large escarpments up to 520 m high, with slope angles of up to 40^{o}. The debris flows have multiple sediment lobes fanning out across the lower half of the Paritu Basin, indicating multiple failure events associated within the debris flow complex. North of the Paritu Basin, the southern part of Tuaheni Ridge partially traps and deflects components of the Tuaheni

Landslide Complex. These have been interpreted by Mountjoy et al. (2009a) as submarine earthflows (Figure 3.9). Some of the slide mass is being conveyed to the south into the Paritu Basin via the Tuaheni Canyon, or by spilling over a ~300 m high escarpment at the head of the Poverty debris flows. The bulk of the sediment is deflected to the north and around the Tuaheni Ridge where there is a structural gap, allowing some of the mass flows to find their way down into the lower reaches of the Paritu Basin, just above the Paritu Canyon (Figure 3.9). Further debris flows are derived from continued modification of the gully systems and remobilisation of sediment around the upper slope.

The shelf-slope break is marked by the Poverty Gullies, a spectacular, morphologically complex escarpment up to 1000 m in height, with seafloor slope angles ranging from 8^{o} in the head zones to 30-48^{o} on the steepest slopes (Figure 3.2). To the north, the headscarps of the Tuaheni Landslides may indicate initial processes responsible for gully development with mass movement encroaching into the shelf break clinoforms (Mountjoy et al., 2009b). The central section of the Poverty Gullies is characterised by a well developed escarpment with a progressive decrease in seafloor slope angles and widening and lengthening of the gullies southward to the southern branch of the upper Poverty Canyon. To the south of the Poverty Canyon, slopes are formed on a largely depositional prograding wedge. Shallow gullies (2-10 m) dominate on the 6.5 km wide upper slope with relatively superficial mass movements affecting the prograding clinoform sequence, characterised by the gentle base slope angle of ~5^{o} (Figures 3.2 and 3.10).

3.6 TECTONIC STRUCTURE

Active tectonic deformation is partitioned spatially across the indentation, with high activity in the mid-lower slope frontal wedge (this study), and beneath the shelf (Barnes et al., 2002; Gerber et al., 2006; Mountjoy, 2009). The active faults commonly produce large thrust-cored anticlines. The upper slope of the indentation is currently largely inactive, with substantial thrusting of Miocene age now buried beneath upper slope clinoforms and basin sediments (Figure 3.10). Lateral variations in structure across the active frontal wedge can be divided into three distinct regions (Figure 3.2) - i) narrow (~8 km wide) accretionary wedge north of Puke Seamount, ii) erosional and cross-cutting complex deformation with an absence of accretionary processes between Puke Seamount and Poverty Canyon, and iii) well-developed (>30 km wide) accretionary wedge south of the Poverty Canyon.

3.6.1 Active Frontal Accretionary Wedge

North of the Poverty Canyon, the zone defining the deformation front is narrow (~4.5 km) and very steep (up to 45^{o}), widening to over 8 km near Puke Seamount (Figure 3.2). The deformation front has continued activity post emplacement of the Riwhā landslide, with incipient thrusts forming across the debris (Figure 3.7). The lower slope above the deformation front is steep and eroded, with few well-developed thrust propagated anticlines (Figures 3.5 and 3.6). North of the subducting Puke Seamount, the growth of anticlinal ridges (i.e. Puke Ridge, Fig. 3.3A) and slope basins between the ridges, is more representative of evolving thrust-driven accretionary wedge style geometry, widening up to 6 km (Figure 3.5). The frontal wedge contains numerous thrust splays propagating up from the subduction décollement (Figures 3.5 and 3.6). These thrusts break out on the trenchward-facing slopes of the structural ridges, accompanied by a multitude of hanging-wall and footwall imbricate splays, leading to a stepped deformation front (Figure 3.6). Whilst the major structures are imaged in the seismic sections, many linear slope inflections, interpreted as imbricate thrust traces, are visible in the high-resolution EM300 bathymetry. Backthrusts are commonly observed throughout the lower slope and deformation front north of the canyon. In the north sector of the frontal slope, these backthrusts increase in frequency as the deformation front widens and the lower sector of the accretionary wedge becomes structurally more evolved (Figure 3.5). In the core of the South Paritu Ridge, and inboard of the Puke Seamount there is significant complexity in the deforming frontal wedge (Figures 3.5 and 3.6). This may be attributed to a number of factors including seamount subduction and loading by both basin-fill and anticlinal growth, resulting in reactivation and cross-cutting of pre-existing structures.

South of the Poverty Canyon, the accretionary wedge is dominated by a series of major thrusts propagating directly from the subduction décollement with backthrusts common in the folded hanging-wall sequences (Figure 3.8) (see also Barnes et al., 2009; their Figure 11). Imbricate splays are common in the near-surface and are reflected in detailed seabed morphology. Evolving proto-thrusts and associated incipient thrust propagated anticlines are developing in the trench-fill sequence immediately outboard of the principal deformation front (Figure 3.8). Seismic reflection profiles of the lower slope reveal the frontal thrusts are progressively incorporating the trench fill sequence. Key marker horizons and seismic reflector packages can be traced from the Hikurangi Trough sequence into the lower slope deformation zone with some confidence across the first 3-4 thrusts propagating up from the décollement (Figure 3.8B). Immediately seaward of the principal deformation thrust, we

recognise incipient proto-thrusts and growing anticlines. This zone is on the verge of being incorporated into the toe of slope by the propagating deformation front, and is characteristic of frontal accretion (Figure 3.8B). A subducted sequence of Hikurangi Plateau sediments is interpreted to underlie the frontal part of the thrust wedge, overlaying and occupying relief space created by normal faults in the subducting Pacific Plate.

Slope basins on the southern accretionary wedge are narrow and elongate (1-2 km x 7-25 km) and well imaged in seismic sections. They contain no more than 0.2 s TWT (~200 m) of sediment, indicating that they are young and highly active. They commonly have thrusts propagating underneath them and into their sedimentary fill (Figure 3.8B). As the basins and depocentres evolve, thrusting becomes progressively concentrated into narrow, preferred zones of deformation. Seismic profiles show a complex history of sediment fill in basins, with progressive tilting and incorporation of basin-fill into the inboard margins of the structural ridges as foot-wall thrusts develop and propagate. This is an evolutionary sequence very similar to that described by Lewis & Pettinga (1993). Some more evolved slope basins with thicker sedimentary successions are located higher up the slope and are highly deformed, with progressive structural incorporation into the accretionary wedge (Figure 3.8B).

Internal seismic reflector packages are chaotic and incoherent beneath the Pantin Bank (Figure 3.8B). This is consistent with observations beneath Ritchie Ridge further south (see Barnes et al., 2009), and interpreted as a transition from frontally accreted trench-fill to an imbricated foundation of Cretaceous and Paleogene rocks (Lewis and Pettinga, 1993; Barnes et al., 2009).

3.6.2 *Tectonically inactive upper slope and mid-slope Paritu Basin*

The mid to upper slope region of the Poverty Indentation appears to be have been largely inactive since the Late Miocene. Previously thrust deformed Cretaceous-Paleogene foundation rocks (Barnes et al., 2009) and Miocene sediments are covered by basin fill of >1000 m thickness in the Paritu Basin (Figure 3.6B). The basin fill includes a number of large (up to 0.5 s TWT thick), seismically chaotic debris flow deposits originating from the shelf-break, interbedded with continuous reflector sequences. Active thrust faulting within this basin is restricted to the eastern margin of the basin, where hanging-wall imbricate thrusts are propagating to the seafloor on the backlimb of the North and South Paritu Ridges. Presently active thrusts within the upper slope have produced, and are restricted to the Tuaheni Ridge, north of the Paritu Basin (Figure 3.2). The prograding shelf edge – upper slope clinoform

sequence covers the Miocene structures south of the Poverty Canyon to a depth of ~ 1 s TWT (> 1 km) (Figure 3.10). Key marker horizons within this sequence extrapolated from further south along the margin, suggest the sequence has developed over ~1 Myrs (BP Shell Aquitaine and Todd Petroleum Development Ltd, 1976; Barnes et al., 2002; Paquet, 2007; Paquet et al., 2009). Post-Pliocene (blue horizon, c.1.1 Ma) tectonic activity during the development of this sequence is minimal, with activity ceasing by approximately the base of the Haweran (green horizon, c. 0.4 Ma) beneath the present shelf break, and earlier beneath the slope (Figure 3.10). The clinoform sequence east of Mahia Peninsula is intact and has not been directly affected by incision and development of the Poverty Canyon system.

3.6.3 Active Shortening beneath the Continental Shelf

While our study does not specifically address the active deformation occurring beneath the continental shelf, it is clear from previous studies that active deformation inboard of the Poverty Indentation occurs on several significant thrust faults (Mountjoy, 2009), particularly beneath Lachlan and Ariel banks (Lewis, 1973; Foster and Carter, 1997; Barnes et al., 2002) (see Figure 1C). Two sediment depocenters lie on the mid-shelf and thin seaward against the Lachlan and Ariel Anticlines (Gerber et al., 2006). These anticlines are structurally offset, creating a gap connecting the mid-shelf with a third major depocenter seaward of the Lachlan Anticline (Gerber et al., 2006) and situated directly at the head of the Poverty Canyon (Walsh et al., 2007). Positive inversion structures are common in the lower sequence beneath the shelf (Mountjoy and Barnes, pers comm. 2009). In Hawke Bay, similar structures are normal faults reactivated as thrusts during the Plio-Pliestocene (Barnes and Nicol, 2004). Previous geological (Barnes et al., 2002; Nicol et al., 2007) and geodetic (Wallace and Beavan, 2006) estimates of shortening rates across onshore and shelf structures have shown current activity of typically ~5 mm/yr.

3.7 DISCUSSION

The frontal wedge along the Poverty sector of the Hikurangi margin reveals significant lateral variations in structure and geomorphology that can be related to subduction and sedimentary processes. In the following sections we discuss how spatial and temporal variations in tectonic faulting, frontal accretion, seamount subduction, and tectonic erosion each play a significant

role in the evolution of the Poverty Indentation, as well as how they influence the development of a major canyon and other sediment pathways from shelf to trench floor.

3.7.1 *Competing accretionary tectonics and tectonic erosion responding to multistage seamount subduction*

Our structural observations together with published data indicate that active deformation across the Poverty sector of the Hikurangi margin is partitioned between the shelf and mid-lower slope regions, with Pleistocene-Recent inactivity characteristic of the mid-upper slope. The vast majority (perhaps 90%) of the total ~50 mm/yr regional convergence between the coast and the deformation front (Wallace et al., 2004; Wallace et al., 2008) must be occurring within the frontal accretionary wedge beneath the mid-lower slope, across the up-dip extent of the interplate thrust, due to the inactivity in the upper slope and mid-slope regions of the indentation. In addition to contractional strain being concentrated within the frontal wedge, significant lateral variations in the structure of the wedge occur along this sector of the margin. In order to understand the geodynamic evolution of the margin, the following primary observations that we and others have made must be accounted for:

(1) There is substantial basement relief (up to several km) on the subducting Hikurangi Plateau, and about 1 km of trench-fill sedimentary cover currently in the adjacent Hikurangi Trough (Figures 3.1 and 3.3);

(2) There is a substantial re-entrant, of about 15 km depth, into the line of the deformation front at the mouth of Poverty Canyon, and a significant change in strike of the frontal structures, with numerous thrust faults bending into the re-entrant apex (Figure 3.2);

(3) A classical frontal accretionary wedge, about 27 km in width, is well developed south of Poverty Canyon, between Pantin Bank and the deformation front (Figure 3.8) (Barnes et al., 2009). Relatively coherent reflection stratigraphy of the Hikurangi Trough can be confidently traced into the accretionary wedge. Behind the accretionary wedge lies a deformed foundation of Cretaceous, Paleogene, and Miocene rocks (Figure 3.10). There is minimal sediment subduction (< 10%) currently occurring beneath the frontal accretionary wedge, but up to 1 km of subducting sediments underlies the inner part of the margin landward of Pantin Bank (Figure 3.10) (see also Barker et al., 2009; Bell et al., 2009);

(4) Immediately north of Poverty Canyon the lower margin is significantly oversteepened, and characterised by fewer imbricate thrust ridges than to the south, complex structural overprinting including thrust reactivation and faulting orthogonal to the deformation front, large-scale gravitation collapse, debris avalanches, and an absence of coherent accreted reflection stratigraphy;

(5) One or more seamount highs on the subducting Pacific Plate currently underlie Rock Garden, Ritchie Bank, Pantin Bank, and South and North Paritu ridges (Figures 3.5, 3.6 and 3.8) (see also Barker et al., 2009; Barnes et al., 2009; Bell et al., 2009, where overall relief is 2-4 km);

(6) The subducting Puke Seamount is presently colliding with the deformation front north of Poverty Canyon;

(7) The landward incision of Poverty Canyon in the axis of the indentation has excavated a substantial part of a laterally extensive succession of shelf-edge to upper slope clinoforms of Pleistocene age.

These observations collectively support previous interpretations that the Poverty Indentation results from a multistage evolution of seamount subduction, associated with a high convergence rate, and moderate trench-fill sediment thickness (Collot et al., 1996a; Collot et al., 1996b; Lewis, 1997). Many of the above structural, geomorphic, and compositional features of the frontal wedge correlate well with similar features developed in sandbox models of seamount subduction (Figure 11) (Malavieille, 1984; Malavieille et al., 1991; Lallemand et al., 1992; Kukowski et al., 1994; Dominguez et al., 1998a; Dominguez et al., 1998b; Gutscher et al., 1998; Dominguez et al., 2000). These experiments show that when very significant positive relief (e.g., seamount or ridge) on the subducting plate impacts and then subducts beneath the frontal wedge, it commonly induces a characteristic series of deformations and geomorphic changes. Depending on the scale of the subducting relief and the thickness of trench-fill sediment, it may lead to significant indentation and removal of part of the wedge as a result of deformation of the wedge and/or localised tectonic erosion. Focused thrusting and conjugate normal or strike-slip faults oblique to the margin may develop inboard of the leading slope of the seamount where the basal décollement is deflected upwards. The upward deflection of the interplate thrust may create a large shadow zone in the wake of the seamount as it subducts, evacuating the former upper plate sediments, behind the seamount's trailing slope (Dominguez et al., 2000).

The new seismic reflection data reveals the subducted seamounts beneath Pantin Bank and the North and South Paritu ridges. Above the seamounts these ridges reveal complex thrust fault reactivation, with many imbricate splays developed in both footwall and hanging wall sequences of the major structures (Figure 3.6). We infer that this out-of-sequence thrusting has resulted from a localised change in the wedge taper. Sandbox experiments have shown that accretionary wedges thicken and contract when the forward propagation of the basal décollement ceases or is perturbed (Lallemand et al., 1992). This wedge thickening leads to a local taper change, with reactivation of pre-existing thrusts and retreat of the frontal segment. The passage of the subducting seamounts beneath the Paritu ridges have also left an array of normal-separation faults superimposed orthogonally on thrusts beneath the Papaku Basin (Figure 3.5) (cf. Figures 3.11B and 3.11D), and an oversteepened deformation front now undergoing deep seated collapse (Figure 3.7).

The new multibeam bathymetric and seismic data also clearly reveal the structural responses to incipient subduction of Puke Seamount. Puke Seamount results in a localised impact on the margin with a directly inboard set of oblique faults developing orthogonal to the deformation front (Figure 3.11F). The deformation front itself is responding to the increased compressional stress by propagation of a closely-spaced series of thrusts in the zone of increased contraction between the Puke Seamount and the frontal wedge. Similar observations were made at Rock Garden and Bennett Knoll, near the deformation front farther south (Figure 3.1A) (Barnes et al., 2009).

None of the subducted seamounts beneath Pantin Bank and the North and South Paritu ridges, nor the subducting Puke Seamount, appear responsible for the margin scale indentation in the frontal wedge. The overall geometry and geomorphology of the indentation mirrors the geometry accompanying the structure observed in sandbox models after a very large seamount has passed completely through the deformation front and is no longer exposed on the slope (Figures 3.11A to 3.11D) (e.g. Lewis et al., 1998). This inferred subduction event must have preceded the arrival and subduction of the Pantin Bank and Paritu ridges seamounts. The impact produced a relatively linear margin immediately north of the canyon mouth with respect to the more arcuate shape of the accretionary wedge immediate to the south. The margin-wide subsidence and tectonic erosion in the wake of the subducted seamount extended well up into the Paritu Basin region, and facilitated the initiation and incision of the Poverty Canyon system. The original form of the wake indentation (e.g., Figures 3.11A and 3.11D) has since been highly modified by development and incision of

Poverty Canyon as a major shelf to trough sedimentary pathway. It has also been significantly modified by subsequent tectonic deformation in the frontal wedge, including accretionary tectonics and the younger seamount subduction events.

These observations indicate that the tectonic evolution of the Poverty margin relates closely to at least three stages of seamount subduction (Figure 3.12). The geometries of these seamounts is expected to be comparable to other major seamounts on the Hikurangi Plateau (i.e. Gisborne Knolls) as a NW-SE trending extended feature, rather than a symmetrical cone. This would also imply a more abrupt episode of uplift and subsidence accompanying each impact than with a conical seamount (e.g. Dominguez et al., 1998b). The relative sizes of the subducting asperities had markedly different effects on the margin. The oldest recognisable seamount impact must have been produced by a seamount of very substantial relief, at least the scale of Gisborne Knolls (Figure 3.1C), and possibly comparable to that subducted beneath the Ruatoria re-entrant to the north (Figure 1A) (Collot et al., 2001; Lewis et al., 2004). The seamount was unable to subduct beneath the margin without significant indentation and removal of a substantial part of the frontal wedge by tectonic erosion. We infer the seamount collided with the margin at least 1 Myr ago (e.g., Figure 3.12B), and perhaps 2 Myr (Lewis et al., 1998), based on current convergence rates and allowing time for the seamount to fully subduct beneath the present coast. There is no evidence of the subducted seamount beneath the present shelf in the high-quality, deep penetration seismic data (e.g., Figure 3.10) (Barker et al., 2009; Bell et al., 2009).

The second stage of seamount subduction includes those asperities currently beneath Pantin Bank and the Paritu ridges. Like the larger seamounts subducted beneath Rock Garden and Ritchie Ridge further south (Barnes et al., 2009; Barker et al., 2009), their relatively reduced oceanic relief compared to the earlier Poverty seamount enabled subduction beneath the already indented frontal wedge, causing uplift and complex faulting above and in front of the seamounts, but not margin scale indentation. Because these features now lie about 25 km into the margin, we infer they collided with the deformation front about 0.5 Myr ago (Figure 3.12C), assuming there has not been substantial change to the width of the frontal wedge during that time. The final stage of seamount subduction involves the incipient subduction processes associated with Puke Seamount (Figure 3.12D). The Poverty Indentation thus appears to represent an evolved stage of subducting seamount deformation, and also the effects of multiple seamount impacts over time in the same region of frontal wedge (Collot et al., 2001; Lewis et al., 2004).

Many of the observed structural and geomorphic features also correlate well with other sediment-rich convergent margins where seamount subduction is prevalent (i.e. Masson et al., 1990; Moore et al., 1990; Bangs et al., 2005; Moore et al., 2009). The general structural style of the deformation front is very similar at the Nankai margin with proto-thrusts, out-of-sequence thrust activity and megasplay faults, although there appears to be a higher degree of trough sediment subducted at Nankai (e.g. Park et al., 1999; Moore et al., 2009). In Sumatra, landward convergence is common and an increase in plate dip at the deformation front differs from both the Nankai and Hikurangi margins. The Sumatra margin is undergoing oblique convergence, with a pronounced backstop structure arising from slip partitioning (e.g. Moore and Curray, 1980; Malod et al., 1995; Kopp et al., 2001). Seamount subduction along all of these margins results in localised wedge uplift and subduction of sediment around the seamount (e.g. Yamazaki and Okamura, 1989; Masson et al., 1990; Park et al., 1999; Park et al., 2003). Oversteepening and erosion of the frontal wedge slope occurs at the earliest stages of seamount subduction at both the Sumatra and Hikurangi margins, but only at latter stages of subduction along the Nankai margin. The Costa Rican margin is also affected by multiple seamount impacts but is dominated by tectonic erosion with rapid convergence and limited sediment input (e.g. von Huene et al., 2004; Hühnerbach et al., 2005; Sak et al., 2009). Seamount subduction effects on the Costa Rican margin are similar to those experienced on sediment-rich margins, producing significant re-entrant scars and collapse following uplift and subduction into the margin front. However, these scarring effects appear to be more pronounced at the Costa Rican margin (Hühnerbach et al., 2005) due to the small accretionary wedge and the conical geometry of the seamounts (i.e. compared to the more elongate seamounts present at Hikurangi and Nankai). At all margins, the seamounts are stronger and less deformable than the inner accretionary wedge lithology and are therefore not offscraped onto inner trench slopes, remaining relatively intact during subduction, until possible underplating well under the margin (e.g. Moore and Curray, 1980; Hühnerbach et al., 2005; Sak et al., 2009).

The growth and propagation of thrust ridges in the Poverty Indentation appears to be highly influenced by the subduction evolution, and fall into two distinct types of anticlinal development processes. Classical accretionary wedge processes dominate for the deformation front south of Poverty Canyon. The thrusts appear to be propagating forward into the trench fill but remain widely active across the frontal accretionary wedge. The sequence of anticlines produced by these processes contrast with the mid-slope ridge geometries of the North and

South Paritu ridges, and Pantin Bank. The en echelon structure of these mid-slope ridge complexes may indicate segmentation of thrust splays, at a depth of about 5 km, responding to subduction of seamounts beneath them (Figure 3.13). Their complex structural evolution reflects the progressive re-establishment of contractional deformation in the wake of the first major seamount subduction event recognisable, and to increased wedge taper in response to over-steepening of the deformation front north of the canyon. As the slope basins re-establish and evolve, thrusting is progressively concentrated into narrow, preferred zones. Propagating structures now active at the deformation front are in the process of re-establishing a smoother deformation front geometry across the indentation, but they are competing with incision of the lower canyon.

3.7.2 Tectonic controls on canyon development

Tectonic control on development of canyon features within the Poverty Indentation consist of: i) first order subsidence and drainage development in the wake of the very large earliest seamount impact recognised, and ii) local modification and steering of the canyon(s) between the major mid-slope thrust ridges (e.g. Mountjoy et al., 2009a).

The Poverty Canyon has developed initially by incision into the axis of a major margin indentation. Continued tectonic modification and development is concentrated primarily in the mid- lower reaches of the canyon as a response to activity on the mid-slope ridges and deformation front. The knick points observed in gradient profiles (see Figure 3.4) coincide with thrust structures propagating across the channel floor, particularly associated with thrust fault activity around the mid-slope ridge anticlines. The smaller Paritu Canyon appears to be a significantly later feature, independent of seamount impact and controlled by active ridge growth between the structurally segmented North and South Paritu Ridges (Figure 3.13). Future seamount impacts (i.e. Gisborne Knolls) may have significant influence on these important sediment pathways via uplift development of frontal wedge and mid-slope anticlines, depending on the scale of impact damage to the frontal wedge, and the canyons' ability to keep pace with deformation through antecedence (e.g. Mountjoy et al., 2009a).

Unloading by removal of sediment across both the Poverty and Paritu Canyons may be modifying the local structures (e.g. Tribaldi, 1998; Eusden et al., 2000; Howard et al., 2005). Sediment removal by the Poverty Canyon, and the associated decrease in load across the subduction faults in the frontal wedge, may be contributing to the observed discontinuity along the deformation front. Excavation by the Paritu Canyon may be modifying the fault

mechanics through the Paritu Ridge Complex, reinforcing separation into discrete anticlinal structures.

3.7.3 Development of a major shelf to trench sedimentary conduit over 10^5-10^7 yrs

Development of the Poverty Canyon system, with gullying and landsliding, has been instrumental in the retreat and widening of the upper margin re-entrant and catchment, leading to large-scale excavation of the shelf-edge and upper slope low-stand sediment wedge. This wedge is well developed along the margin to the north and south of the re-entrant, as a ~1 Ma prograding clinoform sequence, in response to very high sediment flux onto the margin during glacio-eustatic low-stands. The wedge excavation reflects the growth of the Poverty Canyon and gully system, which initiated as a response to impact of the early Poverty indentation seamount, and developed contemporaneously with fluctuating glacio-eustatic sediment flux to the upper slope. The re-entrant scar created by the passing of one or more seamounts provided a corridor for sediment from the continental shelf to the trench floor, relative to the surrounding clinoform sequence along the margin (Figure 3.12). Incision of the canyon has shortened the path to the trench floor, which has resulted in the relatively steep gradient. The canyon is presently largely evacuated of sediment in the lower region, with active sediment infill progressively increasing into the head zones (Alexander et al., 2006a; Alexander et al., 2006c; Walsh et al., 2007; Alexander et al., 2009). The extrapolated age of the clinoform wedge constrains the timing of canyon incision and gully development; as the 1 Ma clinoforms are incised, the canyon must be younger. For the seamount to have been subducted west of Mahia Peninsula, as it appears to be, the ~1 Ma timing suggests the canyon developed to its full extent significantly later than the impact event (see Figure 3.12C), possibly triggered by the high sediment flux during the low-stand clinoform progradation. Incision of the base-level within the middle branch of the Poverty Canyon has driven incision in the southern branch up into the base of the clinoform sequence (e.g. Mountjoy et al., 2009a).

Landslides and debris flows are numerous in the region and can be classed as of two types: aerially-extensive and local. Locally-derived landslides are attributed to over-steepening thrust-bound anticlinal slopes and remain local to their source. Aerially-extensive debris flows cover large areas of basin fill and are sourced from the shelf-break. In terms of sediment transport potential, aerially-extensive debris flows are expected to be very important as major contributors in terms of sediment flux from the continental shelf across the frontal slope to the trench depocentre. The repetitiveness of these events, as evidenced in seismic section (see

Figure 3.6), also suggests either a strong link to the fluctuating glacio-eustatic influence on sediment flux onto the upper slope, link to seismic activity, or a combination of both. Volumetrically, local landslides would not be expected to greatly contribute to sediment flux, as they do not transport sediment far from source, and often involve older sediment exposed in anticlines.

The Poverty Indentation is of significant importance as a major shelf to trench sedimentary conduit for the wider Hikurangi margin, not only sediment derived from the local Waipaoa system. It contains the only full shelf to trench canyon system along the margin north of the Cook Strait Canyon system (Mountjoy et al., 2009a), so is an effective route for sediment to bypass the numerous slope basins associated with the accretionary wedge. The canyon has been a major supplier of sediment to the trough, and perhaps the distal Hikurangi Channel system over a timeframe of 10^5-10^7 years. .

3.8 CONCLUSIONS

Our study of the Poverty Indentation and Poverty Canyon provides the basic structural framework for the marine section of the Waipaoa Source-to-Sink system. The Poverty Indentation in the Hikurangi margin offshore Gisborne has evolved and been modified by numerous active margin processes. We infer that several subducting seamounts have significantly influenced the structural evolution and submarine geomorphology of the margin, and relate to the generation of large-scale gravitational collapse features and significant modification of the across-slope sediment transport system.

Evidence points to at least three main seamount subduction events within the Poverty Indentation, each with different margin responses:

i) older substantial seamount impact that drove the first-order perturbation in the margin, since approximately ~1-2 Ma

ii) subducted seamount(s) now beneath Pantin and Paritu Ridge complexes, initially impacting on the margin approximately ~0.5 Ma, and

iii) incipient seamount subduction of the Puke Seamount at the current deformation front.

Margin tectonic activity is partitioned into three main regions from continental shelf to trench floor. Activity is concentrated in the frontal wedge, with inactivity in the mid-upper slope and activity restricted to a few key structures on the continental shelf. Activity along the frontal wedge appears to account for much (perhaps 90%, ie. ~ 45 mm/yr) of the regional convergence at the up dip end of the interplate thrust, and shows lateral variation from north to south. Accretion is developing north of Puke Seamount, erosion and over-steepening dominant north of the Poverty Canyon in the axis of the indentation, and a well-developed accretionary wedge is developing south of Poverty Canyon. Ongoing modification of the Indentation appears to be driven by: i) continued smaller seamount impacts at the deformation front, and currently subducting beneath the mid-lower slope, ii) low and high sea-level stands accompanied by variations on sediment flux from the continental shelf, iii) over-steepening of the deformation front and mass movement, particularly from the shelf edge and upper slope.

Development of the Poverty Canyon system and excavation of a margin-wide prograding clinoform sequence into the first-order re-entrant following initial seamount impact has provided a major conduit for sediment from the continental shelf directly to trench floor. We infer development of the margin-wide clinoform sequence over the last ~1 Myrs. Development of the Poverty Canyon is inferred to be as follows:

i) initial incision into the axis of the indentation following indentation-forming seamount impact ~1 Ma

ii) incipient canyon eroding into the clinoform sequence ~1 - 0.5 Ma, and

iii) full-scale development of a three branched canyon system and extensive erosion of the local clinoform sequence by gullying and landsliding

The morphology of the margin, the ongoing deformation accompanying seamount subduction, and associated mass wasting are important factors affecting the accumulation, dispersal and redeposition of shelf sediments.

References

Alexander, C., Walsh, J.P. and Orpin, A., 2009. Modern sediment dispersal and accumulation on the Waipaoa outer continental margin. Marine Geology, This issue.

Alexander, C., Walsh, J.P., Orpin, A., Sumners, B. and Kuehl, S., 2006a. Modern sedimentation on the Continental Slope seaward of the Waiapaoa River, New Zealand. Eos Trans. AGU, 87(36): Ocean Sciences Meeting Abstracts.

Alexander, C. et al., 2006b. Tectonic influences on sedimentary processes and submarine landscape evolution: the Waipaoa River, New Zealand example. Geophysical Research Abstracts, 8: European Geosciences Union 2006.

Alexander, C., Walsh, J.P., Sumners, B., Orpin, A. and Kuehl, S., 2006c. Continental slope sediment delivery and storage on an active margin: The Waipaoa Margin example. Eos Trans. AGU, 87(52): Fall Meeting Abstracts.

Arron, E.S. and Lewis, K., 1992. Mahia Bathymetry. In: N.Z.O. Institute (Editor), Coastal Chart Series. Department of Scientific and Industrial Research.

Bangs, N.L. et al., 2005. The 3-D architecture of the Nankai trough accretionary wedge and the development of the seismogenic zone. Margins Newsletter, 14: 1-5.

Barker, D.H., Sutherland, R., Henrys, S. and Bannister, S.C., 2009. Geometry of the Hikurangi subduction thrust and upper plate, North Island, New Zealand. Geochemistry, Geophysics, Geosystems, 10(2).

Barnes, P.M. et al., 2009. Tectonic and Geological Framework for Gas Hydrates and Cold Seeps on the Hikurangi Subduction Margin, New Zealand. Marine Geology, in press.

Barnes, P.M. and Mercier de Lepinay, B., 1997. Rates and mechanics of rapid frontal accretion along the very obliquely convergent southern Hikurangi margin, New Zealand. Journal of Geophysical Research, 102(B11): 24,931-24,952.

Barnes, P.M., Mercier de Lepinay, B., Collot, J.-Y., Delteil, J. and Audru, J.-C., 1998. Strain partitioning in the transition area between oblique subduction and continental collision, Hikurangi Margin, New Zealand. Tectonics, 17(4): 534-557.

Barnes, P.M. and Nicol, A., 2004. Formation of an active thrust triangle zone associated with structural inversion in a subduction setting, eastern New Zealand. Tectonics, 23(TC1015).

Barnes, P.M., Nicol, A. and Harrison, T., 2002. Late Cenozoic evolution and earthquake potential of an active listric thrust complex above the Hikurangi subduction zone, New Zealand. GSA Bulletin, 114(11): 1379-1405.

Beanland, S. and Haines, J., 1998. The kinematics of active deformation in the North Island, New Zealand, determined from geological strain rates. New Zealand Journal of Geology and Geophysics, 41: 311-323.

Beavan, J., Tregoning, P., Bevis, M., Kato, T. and Meertens, C.M., 2002. Motion and rigidity of the Pacific Palte and implications for plate boundary deformation. Journal of Geophysical Research, 107(B10).

Bell, R.E. et al., 2009. Seismic reflection character of the Hikurangi subduction interface, New Zealand, in the region of repeated Gisborne slow slip events. Geophysical Journal International, submitted.

BP Shell Aquitaine and Todd Petroleum Development Ltd, 1976. Well completion report Hawke Bay-1. 667, New Zealand Ministry of Commerce.

Carter, L., Manighetti, B., Elliot, M., Trustrum, N. and Gomez, B., 2002. Source, sea level and circulation effects on the sediment flux to the deep ocean over the past 15 ka off eastern New Zealand. Global and Planetary Change, 33(3-4): 339-355.

Collot, J.-Y., Davy, B., Lamarche, G. and Anonymous, 1996a. Forearc structures and tectonic regimes at the oblique collision zone between the Hikurangi Plateau and the southern Kermadec arc. Eos, Transactions, American Geophysical Union, 77(22): 121.

Collot, J.-Y. et al., 1996b. From oblique subduction to intra-continental transpression; structures of the southern Kermadec-Hikurangi margin from multibeam bathymetry,

side-scan sonar and seismic reflection. Marine Geophysical Researches, 18(2-4): 357-381.
Collot, J.-Y., Lewis, K., Lamarche, G. and Lallemand, S., 2001. The giant Ruatoria debris avalanche on the northern Hikurangi margin, New Zealand; results of oblique seamount subduction. Journal of Geophysical Research, B, Solid Earth and Planets, 106(9): 19,271-19,297.
Davy, B., Hoernle, K. and Werner, R., 2008. Hikurangi Plateau: Crustal structure, rifted formation, and Gondwana subduction history. 9.
Davy, B. and Wood, R., 1994. Gravity and magnetic modelling of the Hikurangi Plateau. Marine Geology, 118(1-2): 139-151.
Dickinson, W.R. and Seely, D.R., 1977. Stratigraphy and structure of compressional continental margins. AAPG Bulletin, 61(5): 781.
Dickinson, W.R. and Seely, D.R., 1979. Structure and stratigraphy of forearc regions. AAPG Bulletin, 63(1): 2-31.
Dominguez, S., Lallemand, S., Malavieille, J. and Schnurle, P., 1998a. Oblique subduction of the Gagua Ridge beneath the Ryukyu accretionary wedge system: Insights from marine observations and sandbox experiments. Marine Geophysical Researches, 20: 383-402.
Dominguez, S., Lallemand, S.E., Malavieille, J. and von Huene, R., 1998b. Upper plate deformation associated with seamount subduction. Tectonophysics, 293(3-4): 207-224.
Dominguez, S., Malavieille, J. and Lallemand, S., 2000. Deformation of accretionary wedges in response to seamount subduction - insights from sandbox experiments. Tectonics, 19(1): 182-196.
Dubois, J., Deplus, C., Diament, M., Daniel, J. and Collot, J.-Y., 1988. Subduction of the Bougainville seamount (Vanuatu): mechanical and geodynamic implications. Tectonophysics, 149(1-2): 111-119.
Eusden, J.D., Pettinga, J.R. and Campbell, J.K., 2000. Structural evolution and landscape development of a collapsed transpressive duplex on the Hope Fault, North Canterbury, New Zealand. New Zealand Journal of Geology and Geophysics, 43: 391-404.
Foster, G. and Carter, L., 1997. Mud sedimentation on the continental shelf at an accretionary margin; Poverty Bay, New Zealand. New Zealand Journal of Geology and Geophysics, 40(2): 157-173.
Fryer, P. and Smoot, N.C., 1985. Processes of seamount subduction in the Mariana and Izu-Bonin trenches. Marine Geology, 64(1-2): 77-90.
Funnell, R. and Benchilla, L., 2005. 1D Basin Models in the East coast Basin, New Zealand. Report 3183, Ministry of Economic Development.
Gerber, T. et al., 2006. Late Pleistocene and Holocene Seismic Stratigraphy of an active Forearc Basin, Waipaoa Continental Shelf, New Zealand. Eos Trans. AGU, 87(36): Ocean Sci. Meet. Suppl. Abstract.
Greene, H.G., Maher, N.M. and Paull, C.K., 2002. Physiography of the Monterey Bay National Marine Sanctuary and implications about continental margin development. Marine Geology, 181(1-3): 55-82.
Griffiths, G.A. and Glasby, G.P., 1985. Input of river-derived sediment to the New Zealand continental shelf, 1: Mass. Estuarine, Coastal and Shelf Science, 21: 773-787.
Gutscher, M.-A., Kukowski, N., Malavieille, J. and Lallemand, S., 1998. Material transfer in accretionary wedges from analysis of a systematic series of analog experiments. Journal of Structural Geology, 20(4): 407-416.
Haq, B., Karner, G.D. and Morris, J.D., 2004. NSF MARGINS Program Science Plans 2004, Lamont-Doherty Earth Observatory of Columbia University, New York.

Hicks, D.M., Gomez, B. and Trustrum, N.A., 2000. Erosion thresholds and suspended sediment yields, Waipaoa River basin, New Zealand. Water Resources Research, 36(4): 1129-1142.

Howard, M., Nicol, A., Campbell, J.K. and Pettinga, J.R., 2005. Holocene paleoearthquakes on the strike-slip Porters Pass Fault, Canterbury, New Zealand. New Zealand Journal of Geology and Geophysics, 48: 59-74.

Hühnerbach, V., Masson, D.G., Bohrmann, G., Bull, J.M. and Weinrebe, W., 2005. Deformation and submarine landsliding caused by seamount subduction beneath the Coasta Rica continental margin - new insights from high-resolution sidescan sonar data. In: D.M. Hodgson and S.S. Flint (Editors), Submarine Slope Systems: Processes and Products. Geological Society, Special Publications, London, pp. 195-205.

Konishi, K., 1989. Limestone of the Daiichi Kashima Seamount and the fate of a subducting guyot: fact and speculation from the Kaiko "Nautile" dives. Tectonophysics, 160(1-4): 249-265.

Kopp, H., Flueh, E.R., Klaeschen, D., Bialas, J. and Reichert, C., 2001. Crustal structure of the central Sunda margin at the onset of oblique subduction. Geophysical Journal International, 147: 449-474.

Kukowski, N., Huene, R., Malavieille, J. and Lallemand, S.E., 1994. Sediment accretion against a buttress beneath the Peruvian continental margin at 12Â° S as simulated with sandbox modeling. International Journal of Earth Sciences, 83(4): 822-831.

Lallemand, S., Culotta, R. and Von Huene, R., 1989. Subduction of the Daiichi Kashima Seamount in the Japan Trench. Tectonophysics, 160(1-4): 231-233.

Lallemand, S. and Le Pichon, X., 1987. Coloumb wedge model applied to the subduction of seamounts in the Japan Trench. Geology, 15: 1065-1069.

Lallemand, S., Malavieille, J. and Calassou, S., 1992. Effects of oceanic ridge subduction on accretionary wedges: experimental modelling and marine observations. Tectonics, 11(6): 1301-1313.

Lewis, K., Collot, J.-Y. and Lallemand, S., 1998. The dammed Hikurangi Trough: a channel-fed trench blocked by subducting seamounts and their wake avalanches (New Zealand-France GeodyNZ Project). Basin Research, 10(4): 441-468.

Lewis, K.B., 1973. Erosion and deposition on a tilting continental shelf during Quaternary oscillations of sea level. New Zealand Journal of Geology and Geophysics, 16: 281-301.

Lewis, K.B., 1980. Quaternary sedimentation on the Hikurangi oblique-subduction and transform margin, New Zealand. Special Publication of the International Association of Sedimentologists(4): 171-189.

Lewis, K.B., 1994. Mapping a muddy swath. NZ Science Monthly, 5(9): 6-9.

Lewis, K.B., 1997. The succession of seamount impacts and giant avalanches on the Hikurangi margin. In: D.N.B. Skinner (Editor), Geological Society of New Zealand 1997 annual conference; programme and abstracts Geological Society of New Zealand Lower Hutt pp. 99.

Lewis, K.B., 2001. Voyage Report TAN0106, National Institution of Water and Atmospheric Research, Wellington, New Zealand.

Lewis, K.B. et al., 1997. GeodyNZ Team 1997:North Hikurangi GeodyNZ swath maps: depths, texture and geological interpretation, NIWA Chart Miscellaneous Series 72. National Institute of Water and Atmospheric Research Ltd, Wellington.

Lewis, K.B., Lallemand, S. and Carter, L., 2004. Collapse in a Quaternary shelf basin off East Cape, New Zealand: evidence for passage of a subducted seamount inboard of the Ruatoria giant avalanche. New Zealand Journal of Geology and Geophysics, 47: 415-429.

Lewis, K.B. and Pantin, H.M., 2002. Channel-axis, overbank and drift sediment waves in the southern Hikurangi Trough, New Zealand. Marine Geology, 192(1-3): 123-151.
Lewis, K.B. and Pettinga, J.R., 1993. The emerging, imbricate frontal wedge of the Hikurangi Margin. Sedimentary Basins of the World, 2: 225-250.
Malavieille, J., 1984. Modelisation experimentale des chevauchements imbriques: Application aux chaines de montagnes. Bulletin de la Societe Geologique de France, 7: 129-138.
Malavieille, J., Larroque, C., Lallemand, S. and Stephan, J.-F., 1991. Experimental modelling of accretionary wedges. Terra Nova Abstracts, 3: 367.
Malod, J.A., Karta, K., Beslier, M.O. and Zen Jr, M.T., 1995. From normal to oblique subduction: Tectonic relationships between Java and Sumatra. Journal of Southeast Asian Earth Sciences, 12(1/2): 85-93.
Mann, P., Taylor, F.W., Lagoe, M.B., Quarles, A. and Burr, G., 1998. Accelerating late Quaternary uplift of the New Georgia Island Group (Solomon island arc) in response to subduction of the recently active Woodlark spreading center and Coleman seamount. Tectonophysics, 295(3-4): 259-306.
Maruyama, S. and Liou, J.G., 1989. Possible depth limit for underplating by a seamount. Tectonophysics, 160(1-4): 327-337.
Maslan, G., 2005. Fast track seismic processing of selected data from the 05CM survey offshore East Coast, New Zealand. Report 3182, Ministry of Economic Development.
Masson, D.G. et al., 1990. Subduction of seamounts at the Java Trench: a view with long-range sidescan sonar. Tectonophysics, 185(1-2): 51-65.
Moore, G.F. and Curray, J.R., 1980. Structure of the Sunda Trench lower slope off Sumatra from multichannel seismic reflection data. Marine Geophysical Researches, 4: 319-340.
Moore, G.F. et al., 2009. Structural and seismic stratigraphic framework of the NanTroSEIZE Stage 1 transect. Proceedings of the Integrated Ocean Drilling Program, 314/315/316.
Moore, G.F. et al., 1990. Structure of the Nankai trough accretionary zone from multichannel seismic reflection data. Journal of Geophysical Research, 95(B6): 8753-8765.
Mountjoy, J.J., 2009. Submarine canyon evolution: Quantifying geomorphic processes on New Zealand's active continental margin. Submitted PhD Thesis, University of Canterbury.
Mountjoy, J.J., Barnes, P.M. and Pettinga, J.R., 2009a. Morphostructure and evolution of submarine canyons across an active margin: Cook Strait sector of the Hikurangi Margin, New Zealand. Marine Geology, 260(1-4): 45-68.
Mountjoy, J.J., McKean, J., Barnes, P.M. and Pettinga, J.R., 2009b. Terrestrial-style slow-moving earthflow kinematics in a submarine landslide complex. Marine Geology, submitted.
Multiwave, 2005. 05CM 2D Seismic survey, offshore East Coast - North Island. Report 3136, Ministry of Economic Development.
Nicol, A. et al., 2007. Tectonic evolution of the active Hikurangi subduction margin, New Zealand, since the Oligocene. Tectonics, 26(3).
Orange, D.L., 1999. Tectonics, sedimentation, and erosion in Northern California; submarine geomorphology and sediment preservation potential as a result of three competing processes. Marine Geology, 154(1-4): 369-382.
Orpin, A., 2004. Holocene sediment deposition on the Poverty-slope margin by the muddy Waipaoa River, East Coast New Zealand. Marine Geology, 209(1-4): 69-90.
Pantin, H.M., 1966. Sedimentation in Hawke Bay. New Zealand Oceanographic Institute memoir, 28, 70 pp.

Pantin, H.M. and Gibb, J.G., 1968. Mahia sediments, New Zealand Oceanographic Institute coastal series 1:200 000.
Paquet, F., 2007. Morphostructural evolution of active margin basins: the example of the Hawke Bay forearc basin, New Zealand. Ph.D. Thesis, University of Canterbury, Christchurch, 263 pp.
Paquet, F., Proust, J.-N., Barnes, P.M. and Pettinga, J.R., 2009. Inner-Forearc Sequence Architecture in Response to Climatic and Tectonic Forcing Since 150 ka: Hawke's Bay, New Zealand. Journal of Sedimentary Research, 79(3): 97-124.
Park, J.-O., Moore, G.F., Tsuru, T., Kodaira, S. and Kaneda, Y., 2003. A subducted oceanic ridge influencing the Nankai megathrust earthquake rupture. Earth and Planetary Science Letters, 217(1-2): 77-84.
Park, J.-O. et al., 1999. A subducting seamount beneath the Nankai accretionary prism off Shikoku, southwestern Japan. Geophysical Research Letters, 26(7): 931-934.
Robertson, A.H.F., 1998. Tectonic significance of the Eratosthenes Seamount: a continental fragment in the process of collision with a subduction zone in the eastern Mediterranean (Ocean Drilling Program Leg 160). Tectonophysics, 298(1-3): 63-82.
Sak, P.B., Fisher, D.M., Gardner, T.W., Marshall, J.S. and LaFemina, P.C., 2009. Rough crust subduction, forearc kinematics, and Quaternary uplift rates, Costa Rican segment of the Middle American Trench. GSA Bulletin, 121(7/8): 992-1012.
Tribaldi, A., 1998. Effects of topography on surface fault geometry and kinematics: examples from the Alps, Italy and Tien Shan, Kazakstan. Geomorphology, 24(2-3): 225-243.
von Huene, R., Ranero, C.R. and Watts, P., 2004. Tsunamigenic slope failure along the Middle America Trench in two tectonic settings. Marine Geology, 203(3-4): 303-317.
Walcott, R.I., 1978. Present tectonics and late Cenozoic evolution of New Zealand. Geophysical Journal of the Royal Astronomical Society, 52: 137-164.
Walcott, R.I., 1987. Geodetic Strain and the Deformational History of the North Island of New Zealand during the Late Cainozoic. Philosophical Transactions of the Royal Society of London. Series A, Mathematical and Physical Sciences, 321(1557): 163-181.
Wallace, L. and Beavan, J., 2006. A large slow slip event on the central Hikurangi subduction interface beneath the Manawatu region, North Island, New Zealand. Geophysical Research Letters, 33(11).
Wallace, L., Beavan, J., McCaffrey, R. and Darby, D.J., 2004. Subduction zone coupling and tectonic block rotations in the North Island, New Zealand. Journal of Geophysical Research, 109.
Wallace, L., Ellis, S. and Mann, P., 2008. Tectonic block rotation, arc curvature, and back-arc rifting: Insights into these processes in the Mediterranean and the western Pacific. IOP Conf. Series: Earth and Environmental Science, 2.
Walsh, J.P., Alexander, C., Gerber, T., Orpin, A. and Sumners, B., 2007. Demise of a submarine canyon? Evidence for highstand infilling on the Waipaoa River continental margin, New Zealand. Geophysical Research Letters, 34.
Wood, R. and Davy, B., 1994. The Hikurangi Plateau. Marine Geology, 118(1-2): 153-173.
Yamazaki, T. and Okamura, Y., 1989. Subducting seamounts and deformation of overriding forearc wedges around Japan. Tectonophysics, 160(1-4): 207-217.

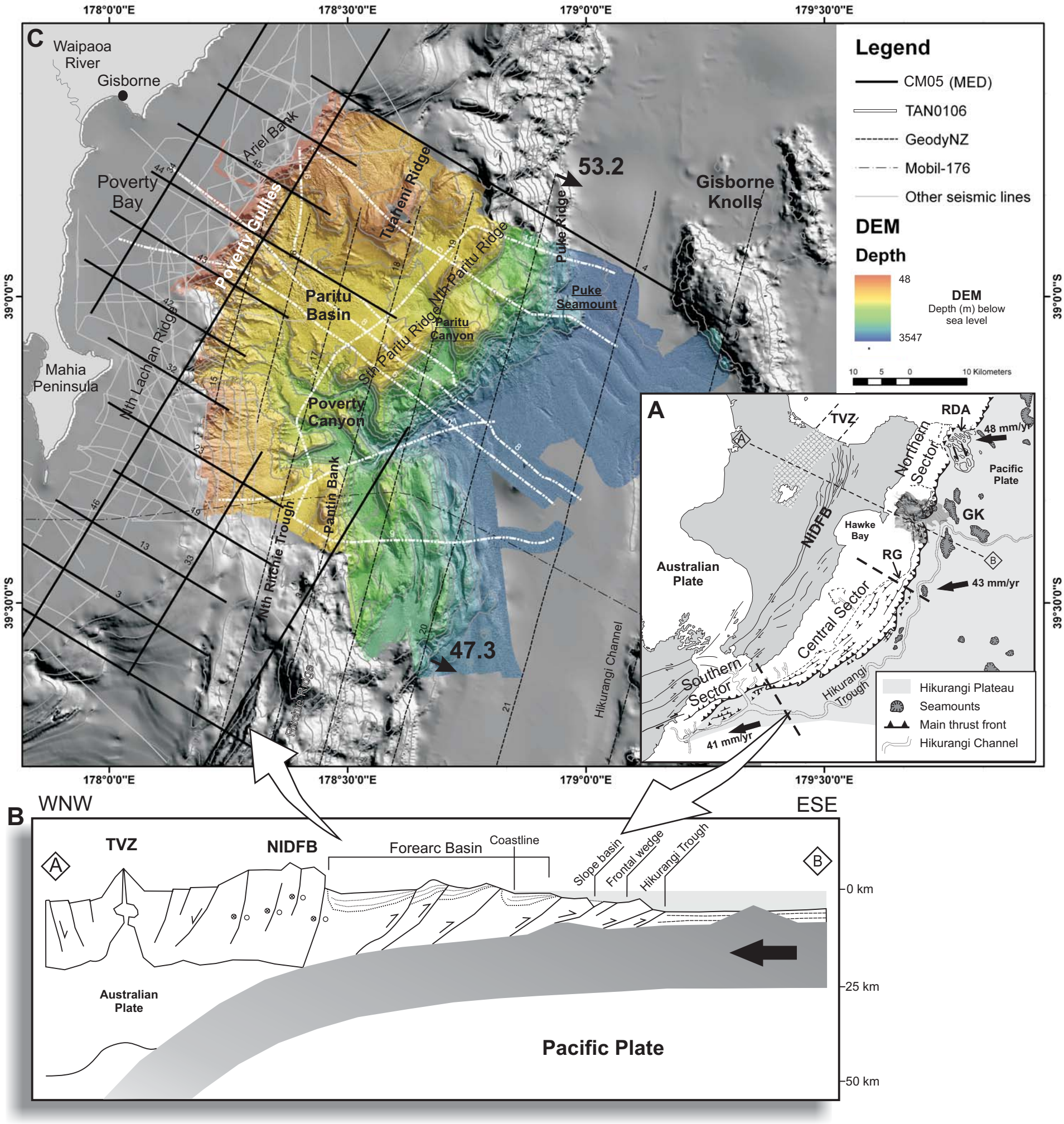

Figure 3.1 A: Location map of the Hikurangi Margin and the Poverty Indentation (Modified from Lewis et al. 2004), with the major seafloor geomorphic features labelled. The Hikurangi Margin is divided up into Southern, Central and Northern Sectors. The Poverty Bay Indentation is located north of the transition from the Central to the Northern Sector, located at the southern end of the Rock Garden (labelled RG) (see Barnes et al. 2009). Plate motion vectors (relative to a fixed Australian Plate) are indicated by the heavy black arrows (from Beavan et al. 2002). Line A-B represents the approximate location for the representative cross-section detailed in Figure 1B. GK = Gisborne Knolls, RDA = Ruatoria Debris Avalanche, NIDFB = North Island Dextral Fault Belt. TVZ = Taupo Volcanic Zone, with subduction related volcanics and back arc extension (after Walcott, 1978; Lewis, 1980; Cole & Lewis, 1981; Beanland et al., 1998).

B: Schematic cross-section A-B, not to scale, through the northern Hikurangi Margin showing the relationship between the subducting Pacific Plate and the large-scale deformation features observed in the over-riding Australian Plate. NIDFB = North Island Dextral Fault Belt, TVZ = Taupo Volcanic Zone.

C: Swath bathymetry generated digital elevation model (DEM) and seismic lines for the Poverty Indentation offshore from Poverty Bay, North Island, New Zealand. Bold black numbers indicate modelled convergence rates (mm/yr) and vectors between the Hikurangi Margin and the Pacific Plate (Wallace at al., 2004). Names of significant morphological features within and around the Poverty Bay Indentation are shown, with names introduced in this paper underlined. Bathymetry contours = 250m. Grey area is a background hillshade from archived SIMRAD EM12 Dual multibeam data acquired by RV L'ATALANTE, and coastal echo-soundings.

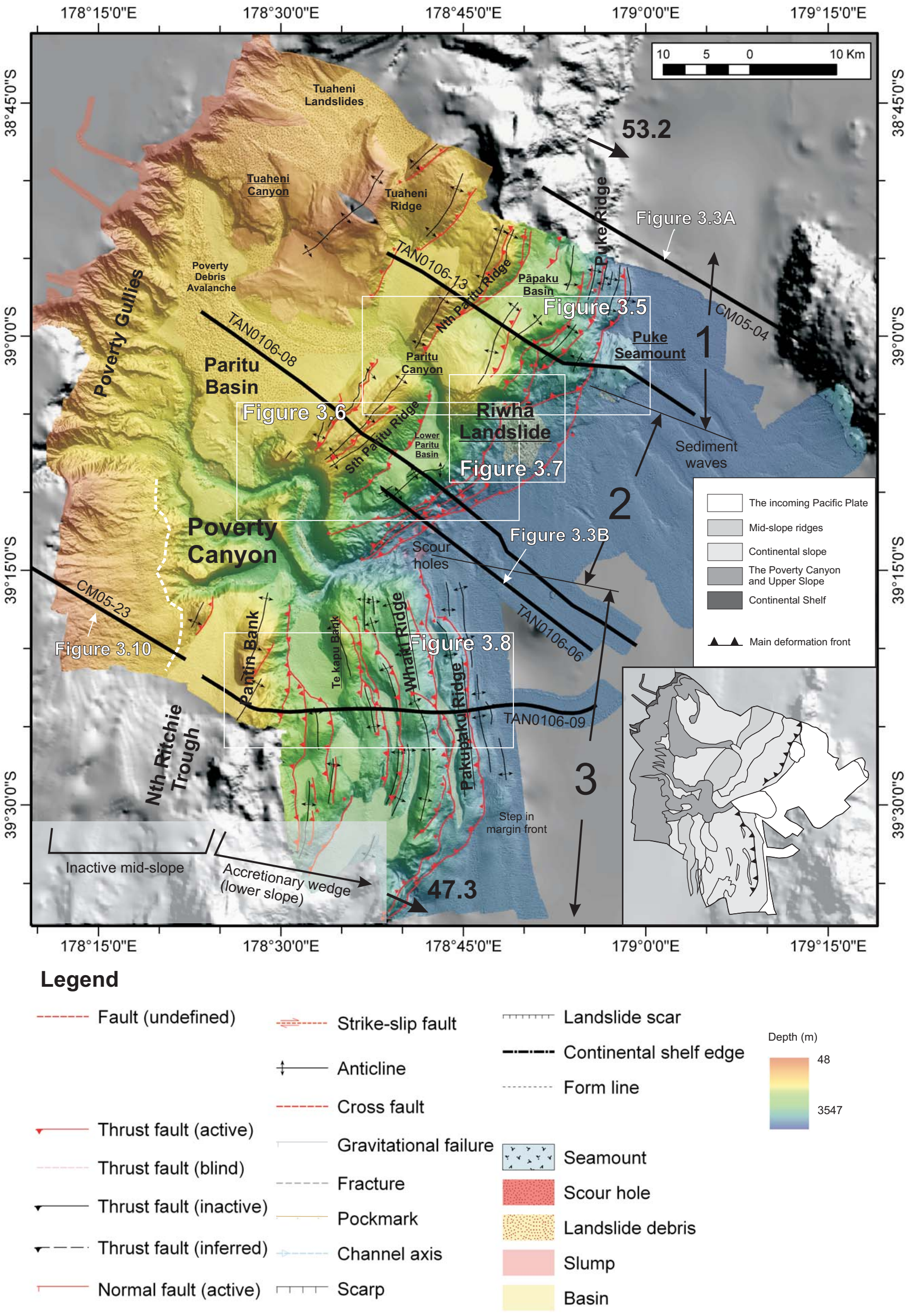

Legend

Figure 3.2 DEM map showing synoptic structural geomorphology of the Poverty Indentation with locations of Figures 3.5, 3.6, 3.7 and 3.8 indicated (boxed). Seismic profiles used in Figures 3.3, 3.5, 3.6, 3.8 and 3.10 are also indicated by bold black lines. The approximate position of the downslope edge of a shelf edge-upper slope clinoform sequence is marked by a bold white dashed line. The margin front is divided into three divisions (labelled in black corresponding numbers): (1) Puke Seamount and north, (2) canyon mouth to Puke Seamount, (3) accretionary wedge south of canyon mouth. Grey area is a background hillshade from archived SIMRAD EM12 Dual multibeam data acquired by RV L'ATALANTE, and coastal echo-soundings. Inset shows simplified key for distinct morphological regions within the indentation. Relative convergence rates and vectors are indicated in bold as in Figure 3.1C (from Wallace et al. 2004). Refer to this figure for symbol key used for structural and geomorphic features in subsequent figures.

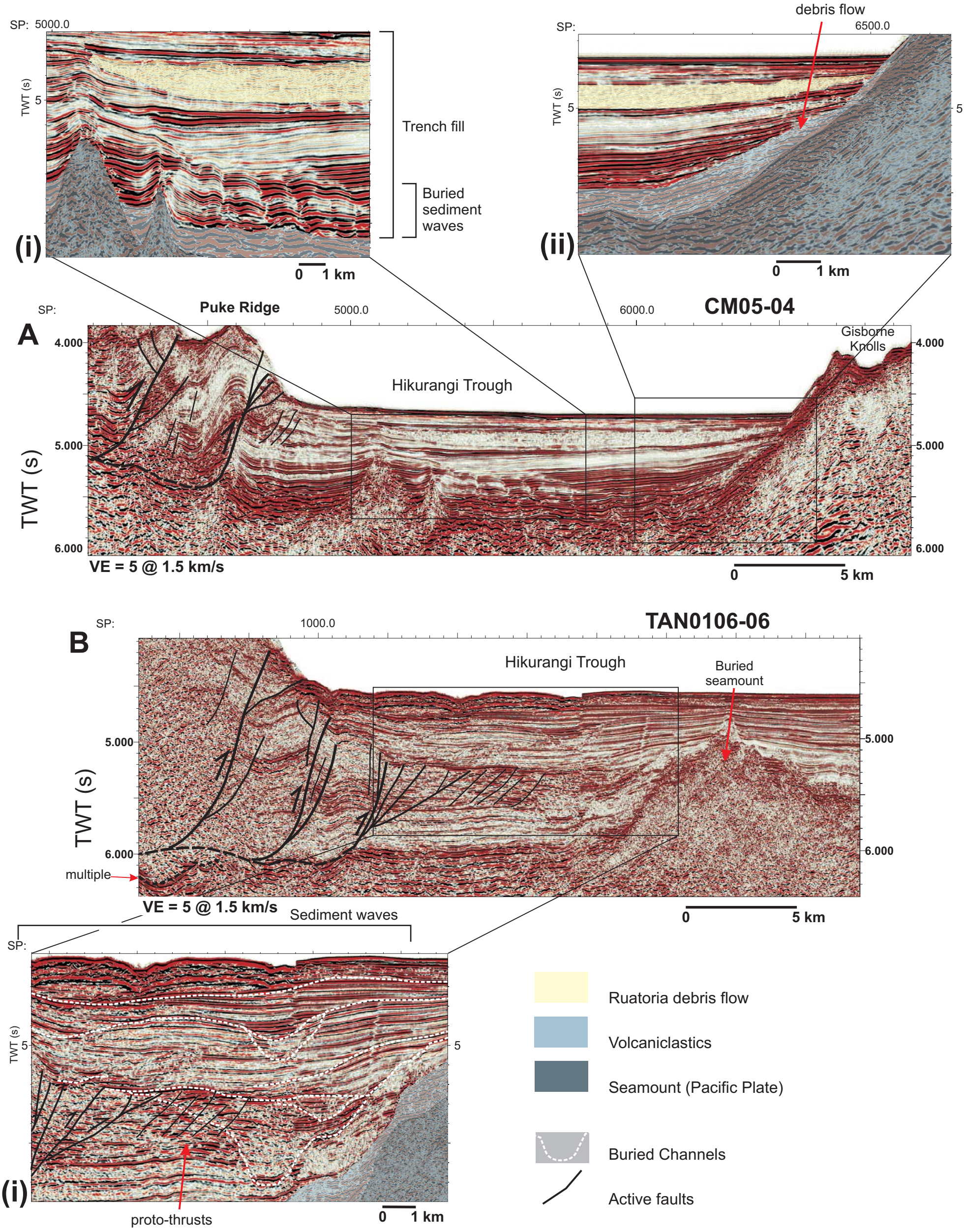

Figure 3.3 Two seismic reflection profiles across the Hikurangi Trough showing the deformation front and incoming seamounts. SP = shot point number along seismic line. TWT = two-way-time in seconds. VE = vertical exaggeration. For locations of seismic lines, refer to Figure 3.2.

A: Seismic profile line CM05-04 imaging the deformation front and Puke Ridge, the trench-fill sequence with deposits from the Ruatoria debris flow, buried sediment waves, volcaniclastic sequence and the Gisborne Knolls Seamount. (i) Detail of the buried sediment waves, Ruatoria debris flow and two small buried seamounts. (ii) Onlap of the trench-fill sequence on to the flanks of the Gisborne Knolls and volcaniclastic sequence. Locally derived debris flows are inferred on the lower flanks of the seamount.

B: Seismic profile line TAN0106-06 imaging the deformation front and trench-fill sequence outboard of South Paritu Ridge. (i) Detail showing undulating surface formed by sediment waves, paleo-channels, and proto-thrusts propagated out into the trench-fill sequence.

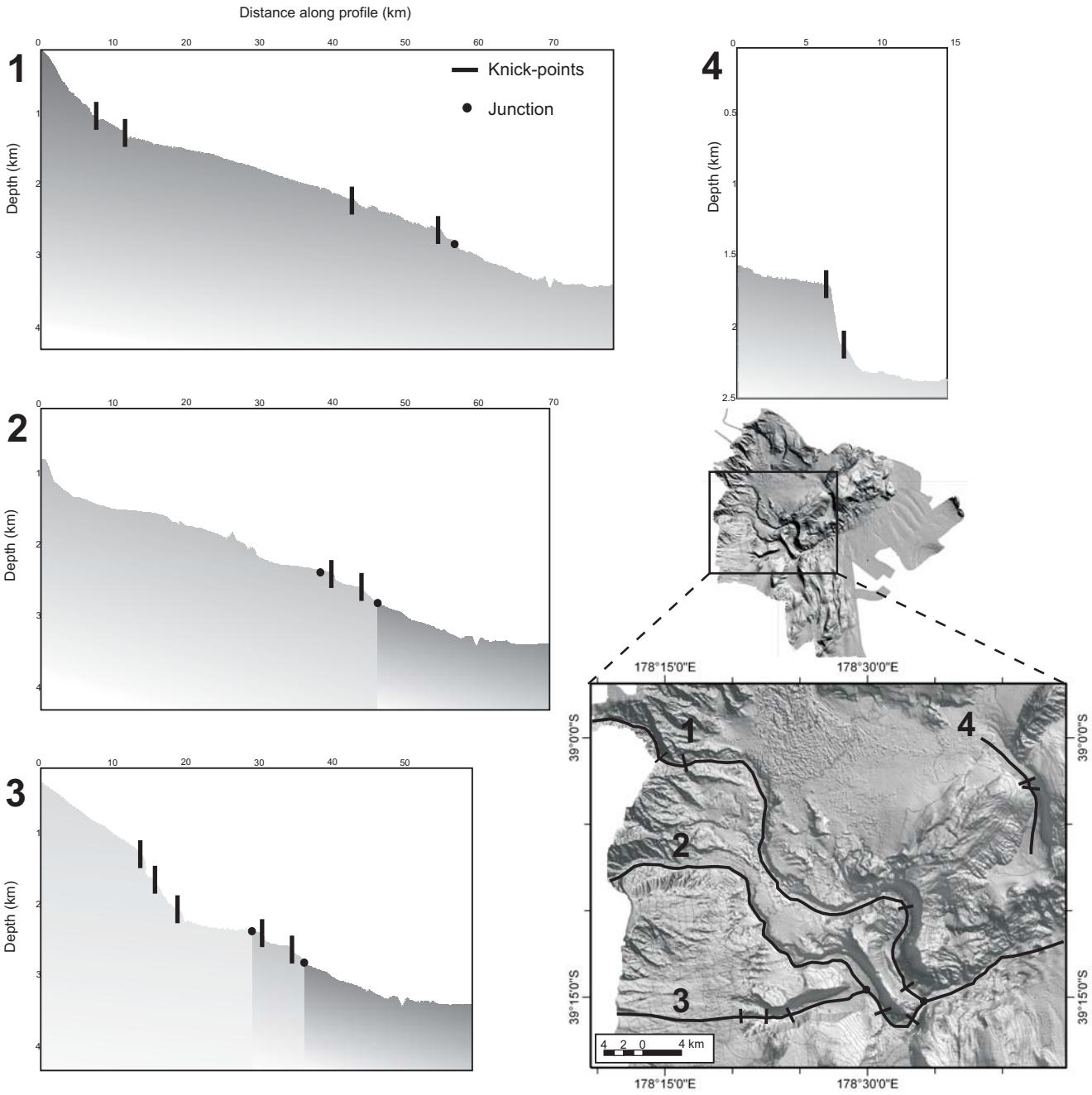

Figure 3.4 Gradient profiles of the (1) north, (2) middle and (3) south branches of the Poverty Canyon, and (4) Paritu Canyon. Location of branches shown on map insert. VE = 10.

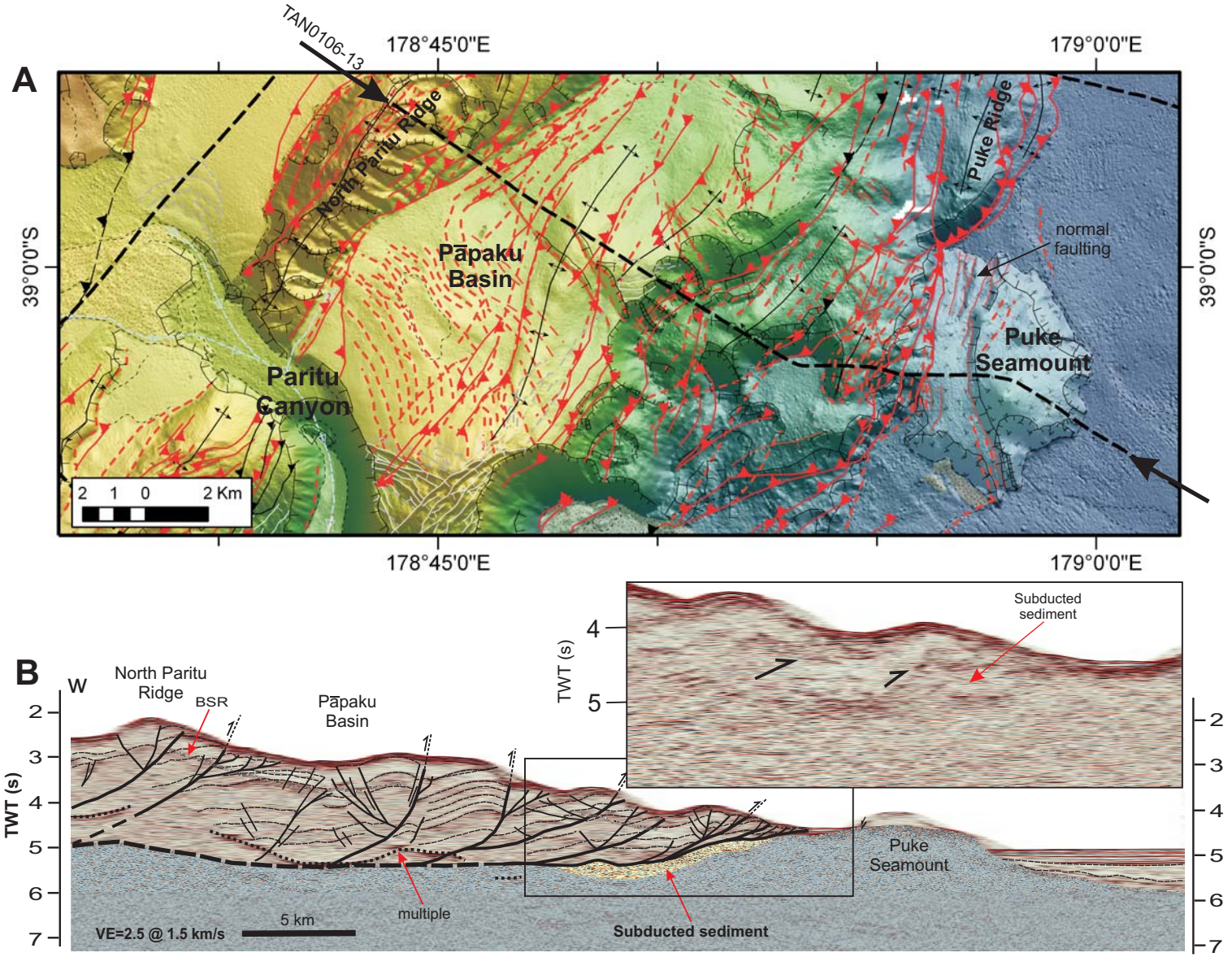

Figure 3.5 Structure north of the Poverty Canyon. Complexity in the deforming frontal wedge is concentrated in a zone directly inboard of the Puke Seamount. For symbol key refer to Figure 3.2.

A: Structural geomorphic detail of region crossed by seismic line TAN0106-13 as indicated by black arrows.

B: Interpreted seismic profile line TAN0106-13. TWT = two-way-time in seconds. Inset shows detail of deformation front without interpretation.

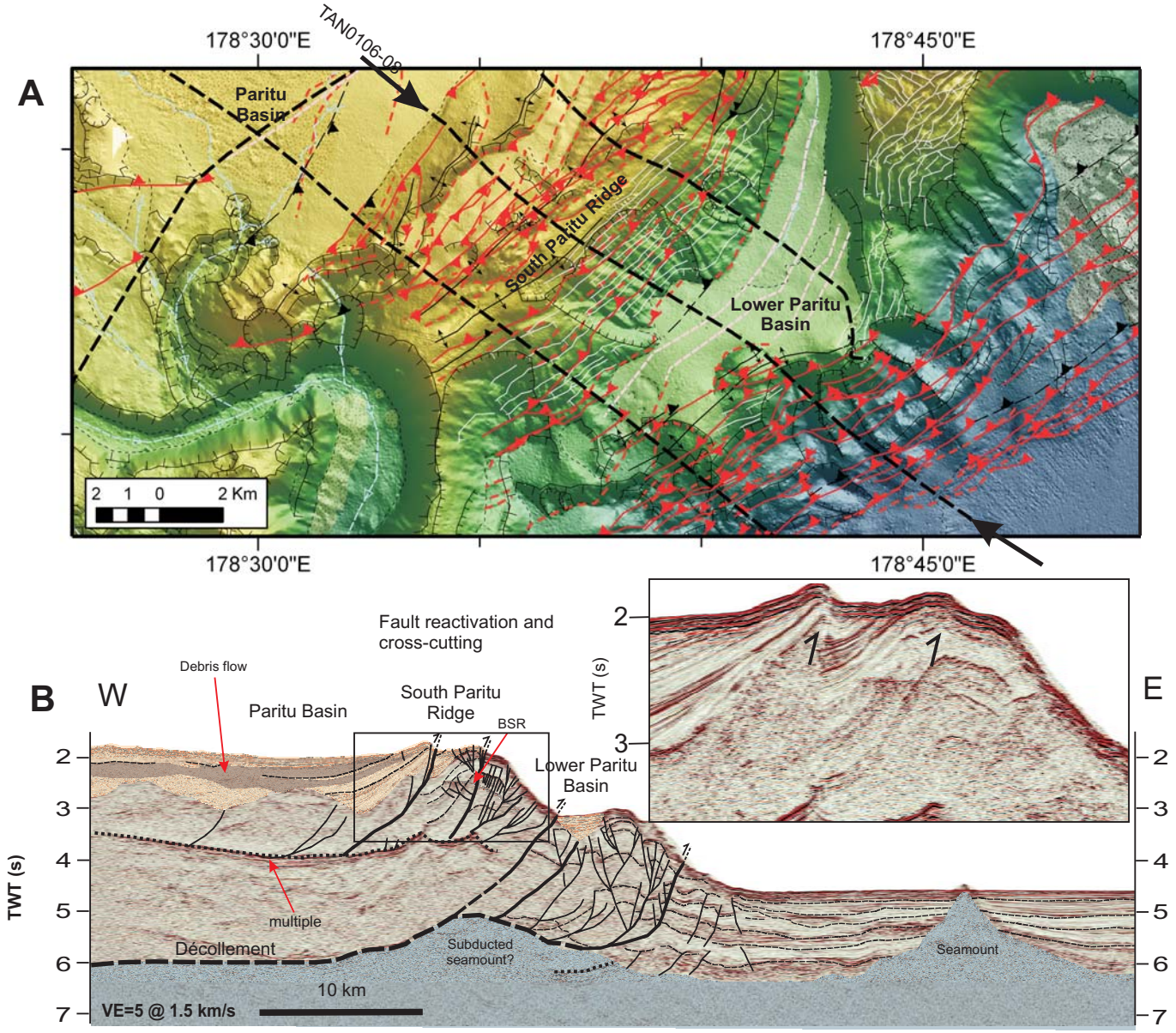

Figure 3.6 Structure north of the Poverty Canyon. Complexity in the deforming frontal wedge is concentrated in the core of the South Paritu Ridge. For symbol key refer to Figure 3.2.

A: Structural geomorphic detail of region intersected by seismic line TAN0106-08 as indicated by black arrows.

B: Seismic profile line TAN0106-08. TWT = two-way-time in seconds. BSR = Bottom simulating reflector. See insert for enlarged seismic detail of the deformation front without interpretation.

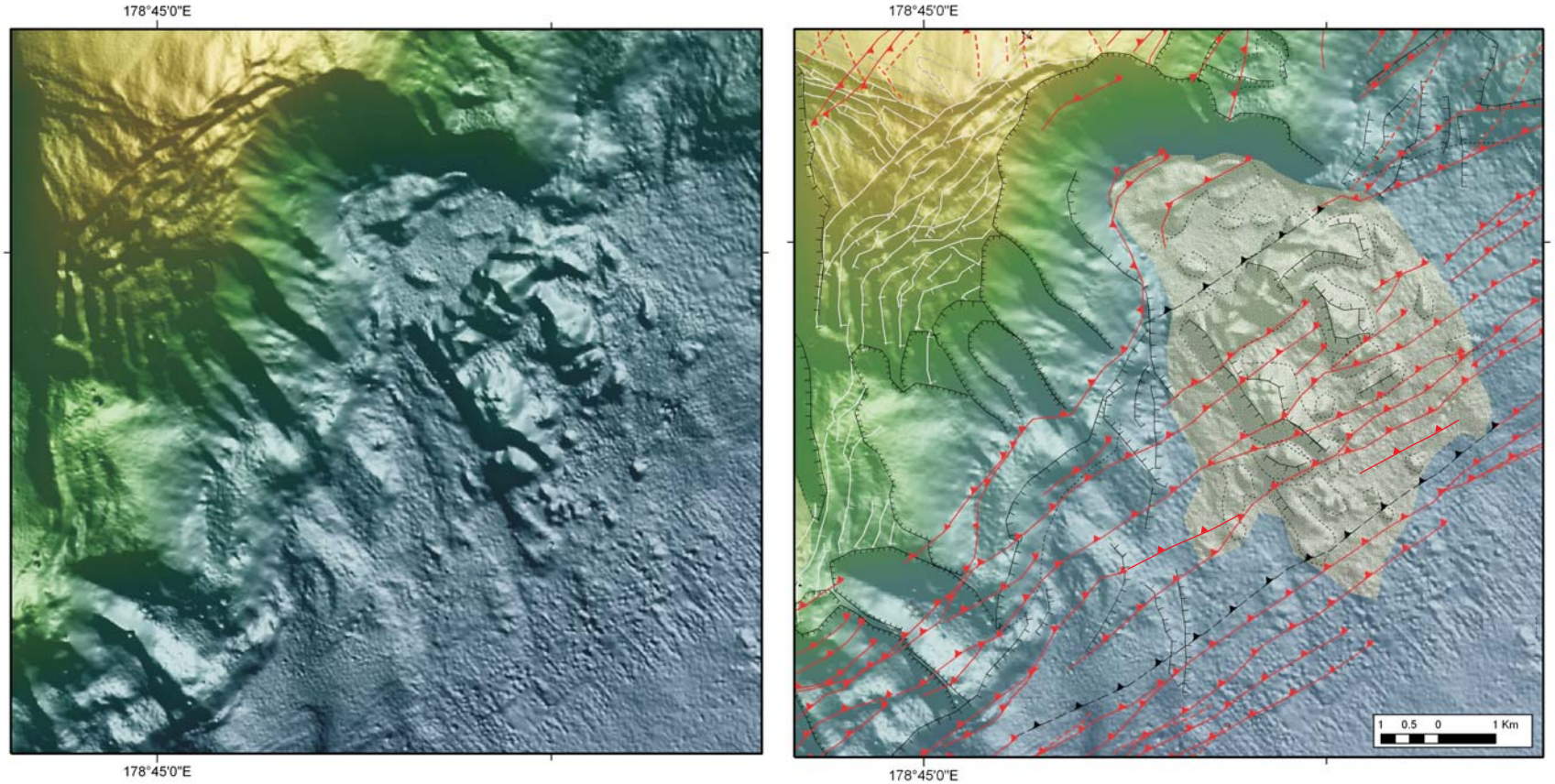

Figure 3.7 The Riwhā Scar on the northern deformation front. See Figure 3.2 for key to symbols. DEM illuminated from 045° at 45°. Bathymetry contours = 100m. VE = x5.

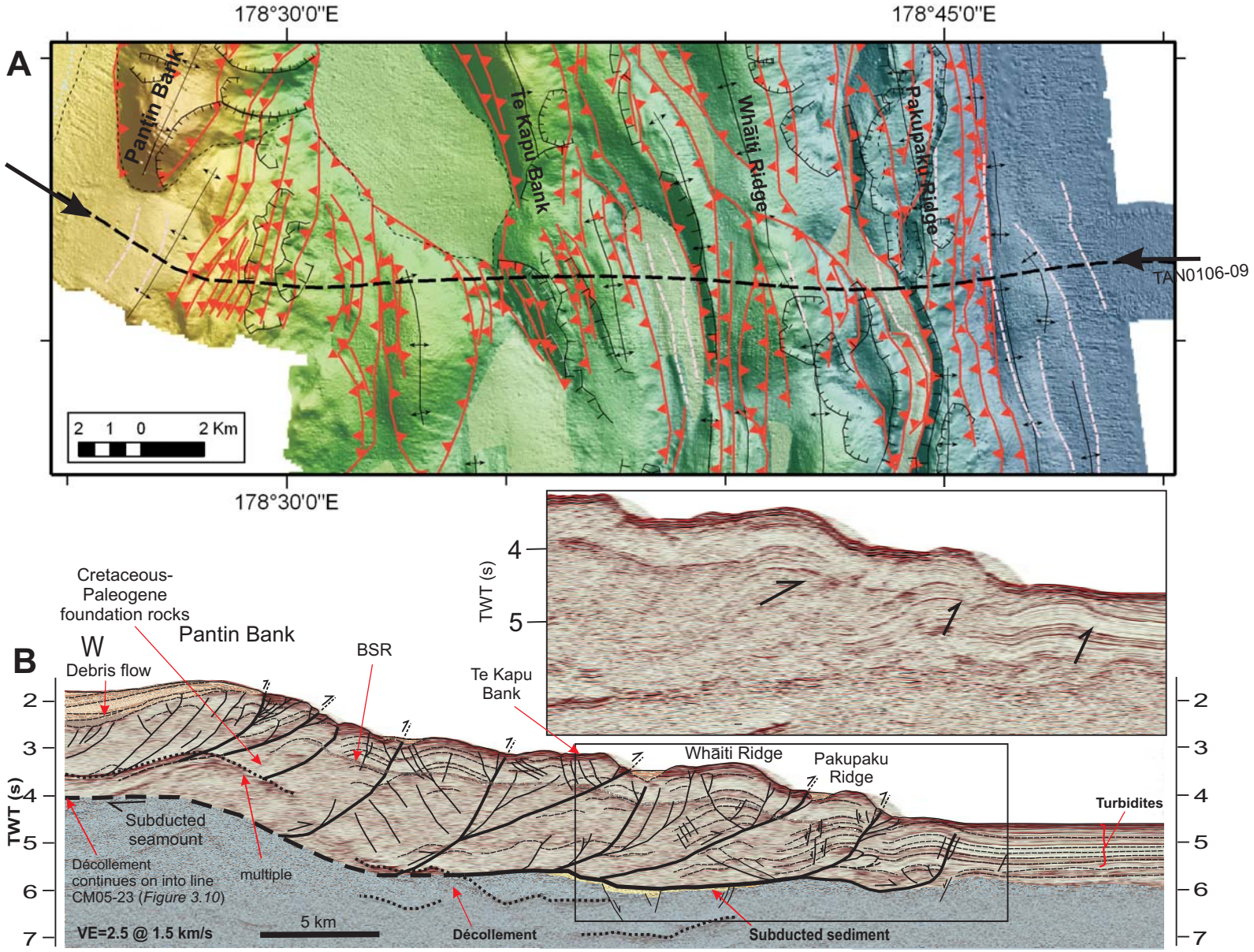

Figure 3.8 Structure south of the Poverty Canyon. For key refer to Figure 3.2.

A: Structural geomorphic detail of region crossed by seismic line TAN0106-09 as indicated by black arrows.

B: Seismic profile line TAN0106-09. TWT = two-way-time in seconds. BSR = Bottom simulating reflector. See insert for enlarged seismic detail of the deformation front without interpretation.

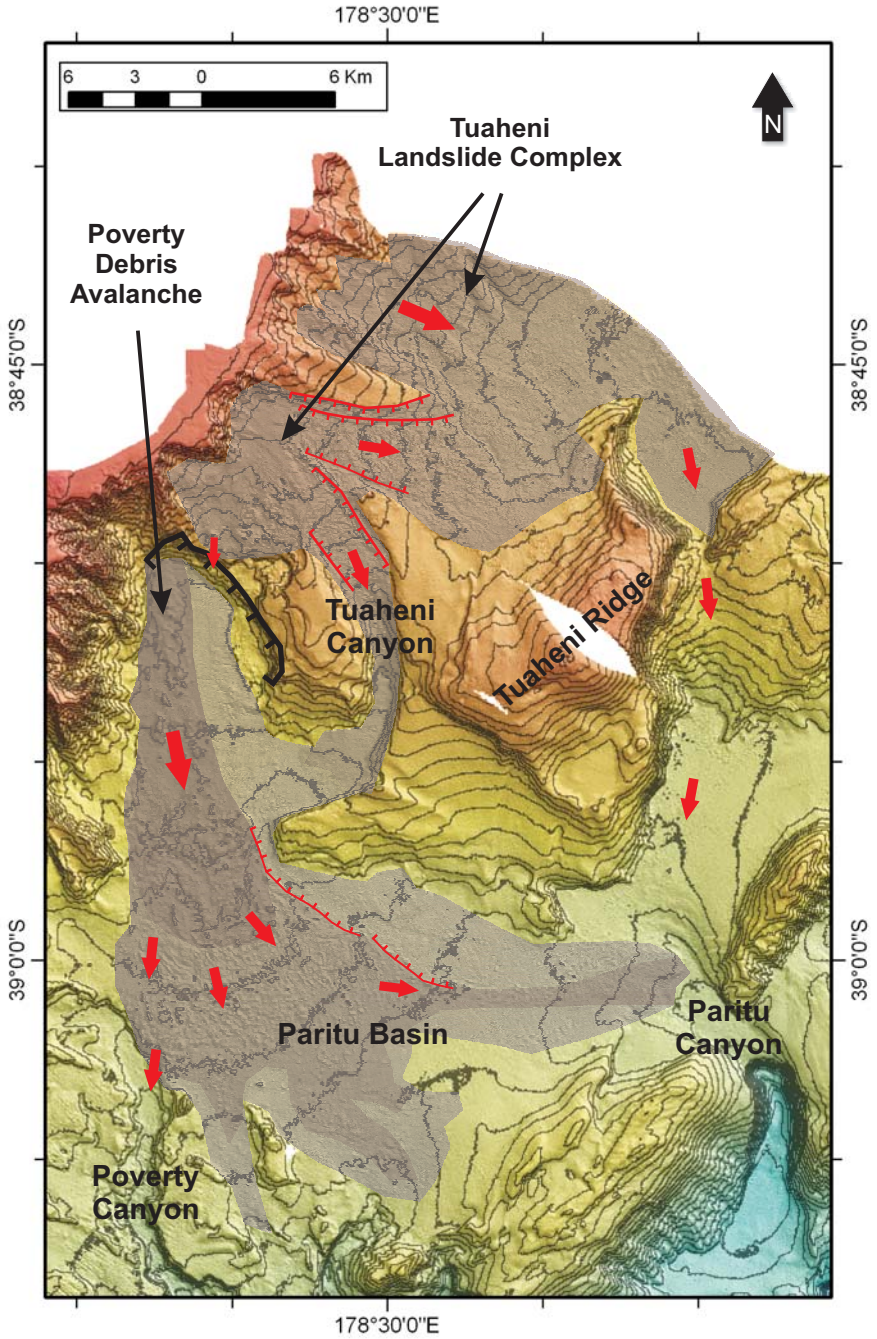

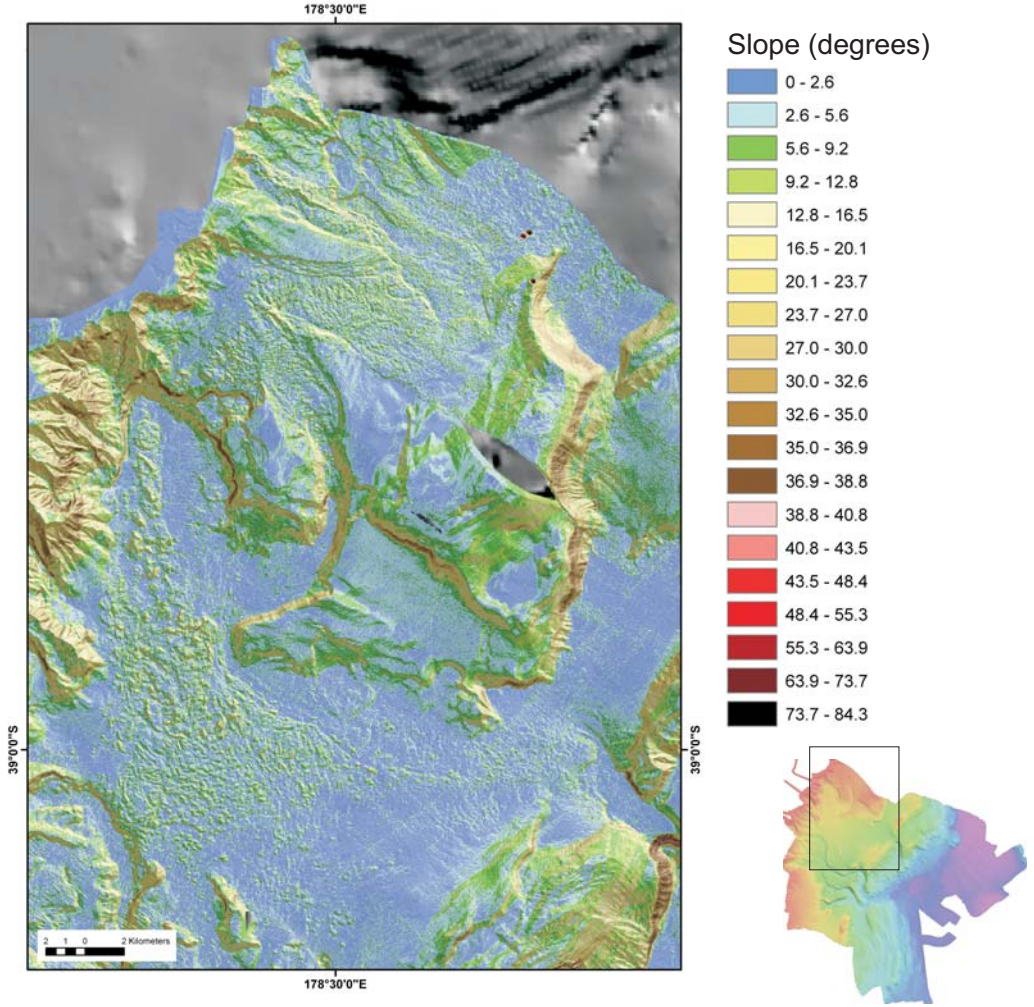

Figure 3.9 A: The Poverty Debris Avalanche and Tuaheni Landslide Complex.

B: Slope map of the upper slope debris flows and slides. DEM is obliquely illuminated from 040° with a vertical exaggeration of x5.

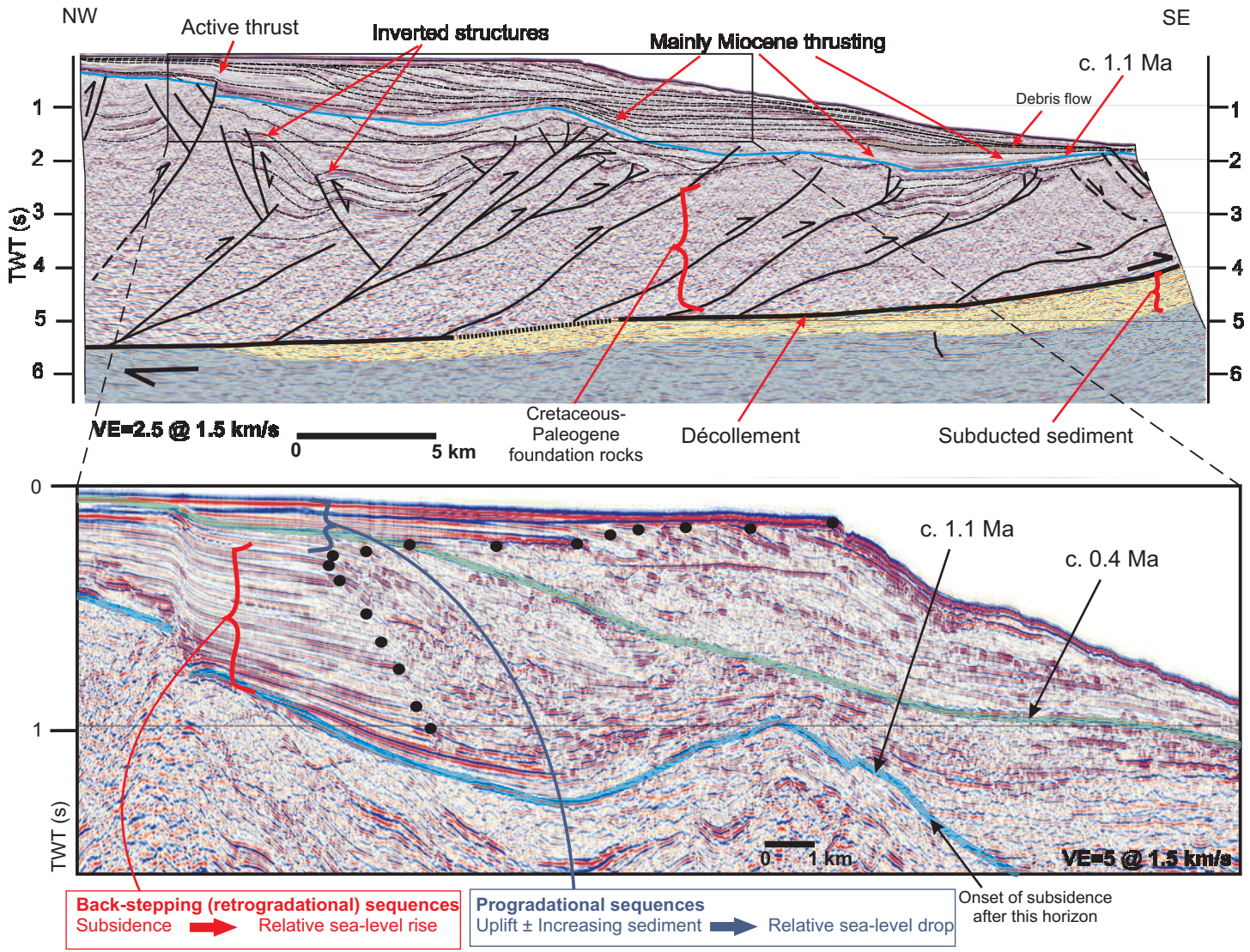

Figure 3.10 Prograding clinoform sequence across the shelf edge/upper slope at the south margin of the Poverty Indentation as imaged in seismic line CM05-23. Cretaceous-Paleogene foundation rocks (Barnes et al., 2009). Horizons labelled in green (c. 0.4 Ma) and blue (c.1.1 Ma) are extrapolated from BP Shell Aquitaine and Todd Petroleum Development Ltd, 1976, Barnes et al., 2002, Proust and Chanier, 2004, Paquet, 2007, and Barnes et al., (in press). Black bullets indicate locations of shelf edge at time of deposition.

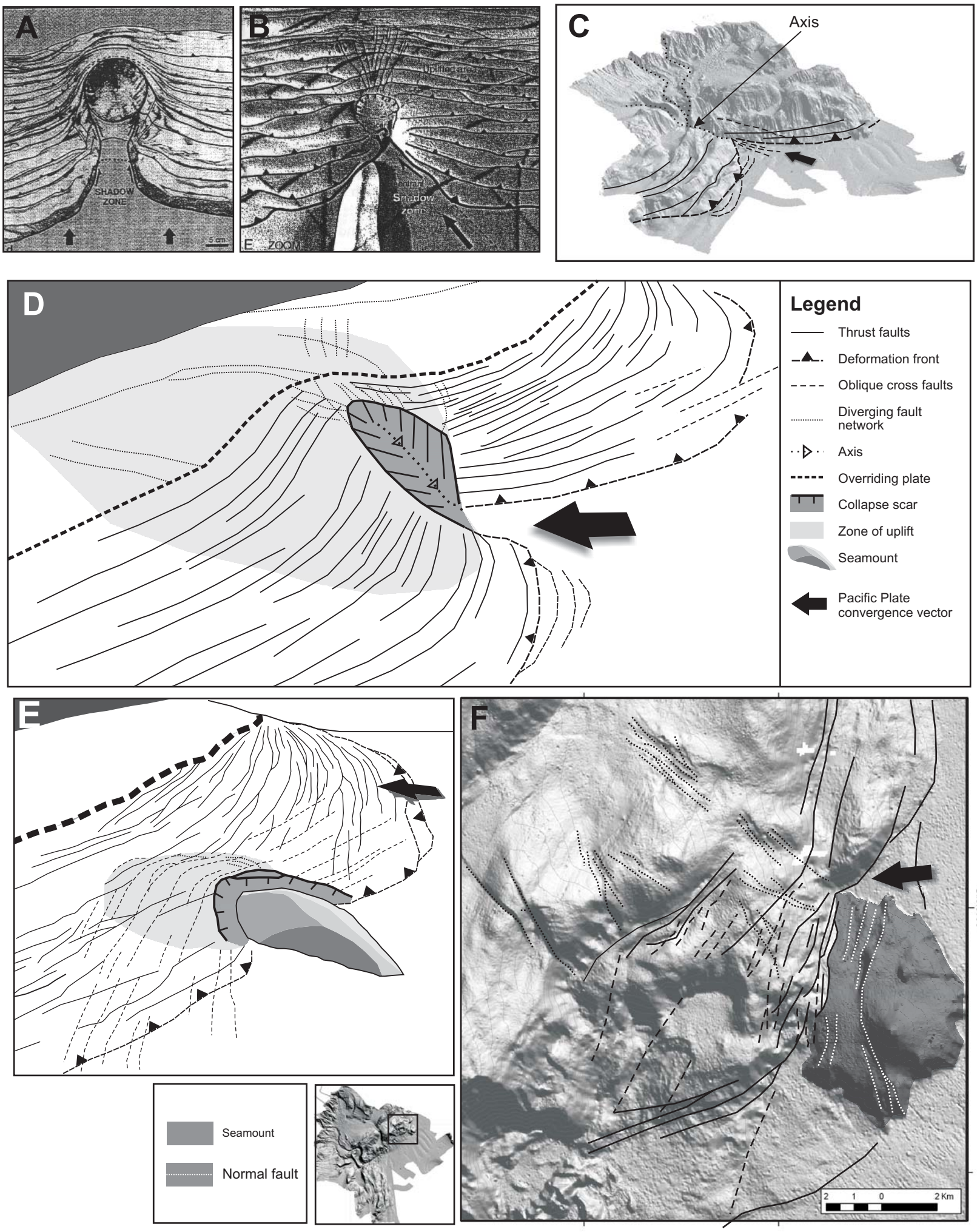

Figure 3.11 Planar photos and interpretations of sandbox experiments undertaken by Dominguez et al. (1998) & (2000), highlighting the different responses of the accretionary wedge to variations in convergence direction and geometry of the seamount.

A: Orthogonal subduction of a conical seamount.

B: Oblique subduction of a ridge or elongated seamount.

Response of the Poverty Indentation to seamount impact and subduction as illustrated by sandbox models and observed features within the indentation. Sandbox models represent seamount subduction under oblique convergence. Convergence on the Poverty section of the Hikurangi margin is currently near orthogonal (see Figure 3.1C) (Wallace et al., 2004, 2008).

C: Oblique DEM of the Poverty Indentation, highlighting key features that correlate with sandbox models and response to an indentation-forming seamount impact event.

D: Sandbox model and structural interpretation of the creation of an indentation accompanying elongate seamount subduction under oblique convergence.

E: Sandbox model interpretation of initial seamount impact with the deformation front.

F: Structural geomorphic interpretation of the Puke Seamount impact and effects on the deformation front and frontal wedge. For key to features and location of region within Poverty Indentation please refer to insert left and D legend.

Sandbox models are interpreted after University of Montpellier experiment NZ3 (Lewis et al. 2004; Chapter 7, this thesis).

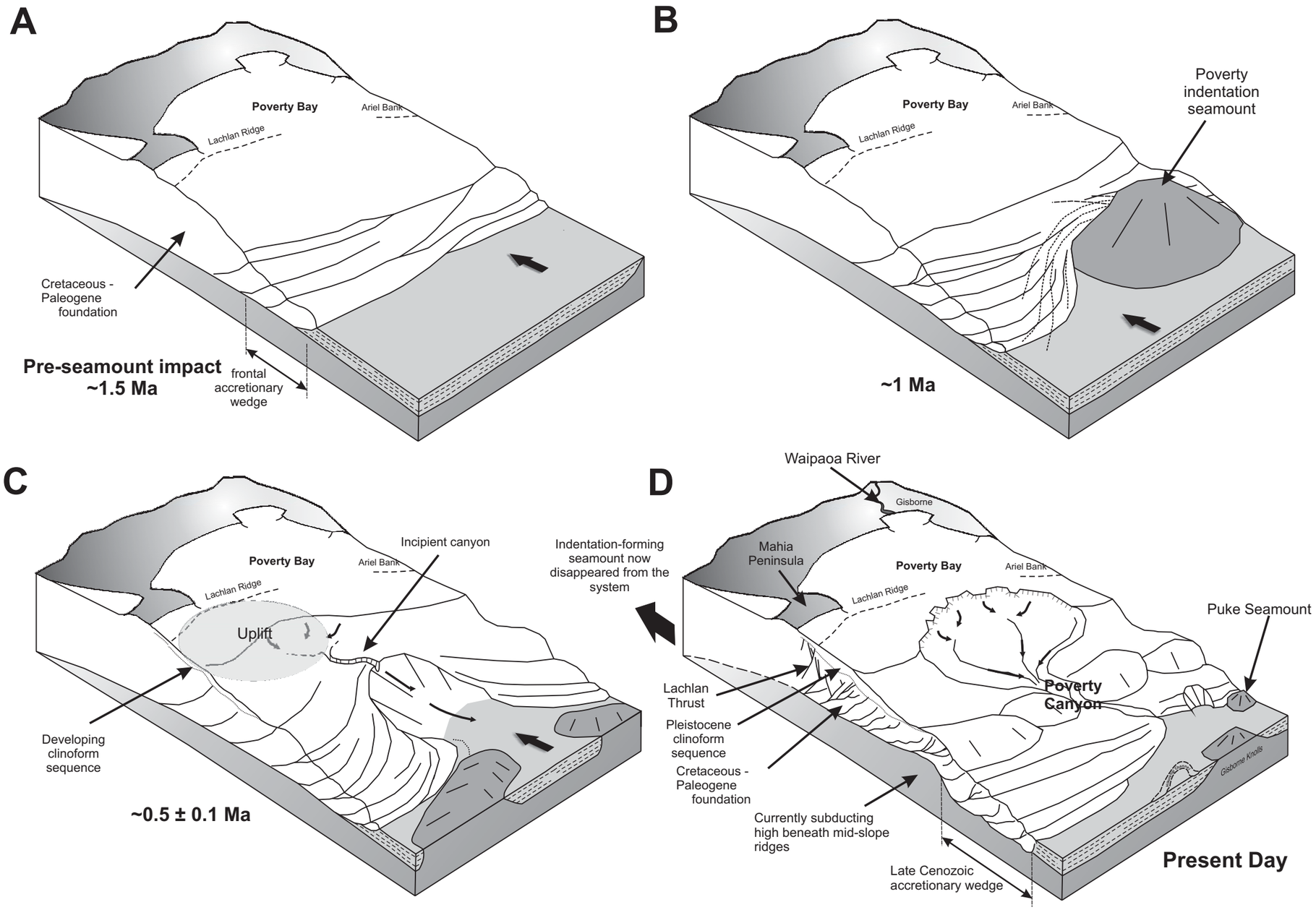

Figure 3.12 Schematic sequential evolutionary model of seamount subduction and the development of the Poverty Indentation based on the progressive encroachment, collision, and subduction of seamounts into the northern Hikurangi Margin. The present day shoreline and currently active shelf faults are for reference only and not to scale. The response of the frontal wedge of the over-riding Australian Plate is illustrated with the key effects on the margin being:

A: The pre-collision Hikurangi margin offshore Poverty Bay.

B: Impact of large indentation-forming seamount between approximately 1-2 My ago.

C: Re-adjustment of the deformation front and development of anticlinal ridges; development of the Poverty Canyon incising into the axis of the indentation; gully formation and mass movement processes into the upper slope clinoform sequence, and accompanying slope basin development. Initiation of 2nd stage seamount subduction at ~0.5 My ago.

D: The Poverty Indentation present day. Ongoing processes appear to be driven by: i) continued smaller seamount impacts at the deformation front, and current subduction beneath the mid-lower slope, ii) low and high sea-level stands accompanied by variations of sediment flux from the continental shelf, iii) over-steepening of the deformation front and mass movement, particularly from the shelf edge and upper slope.

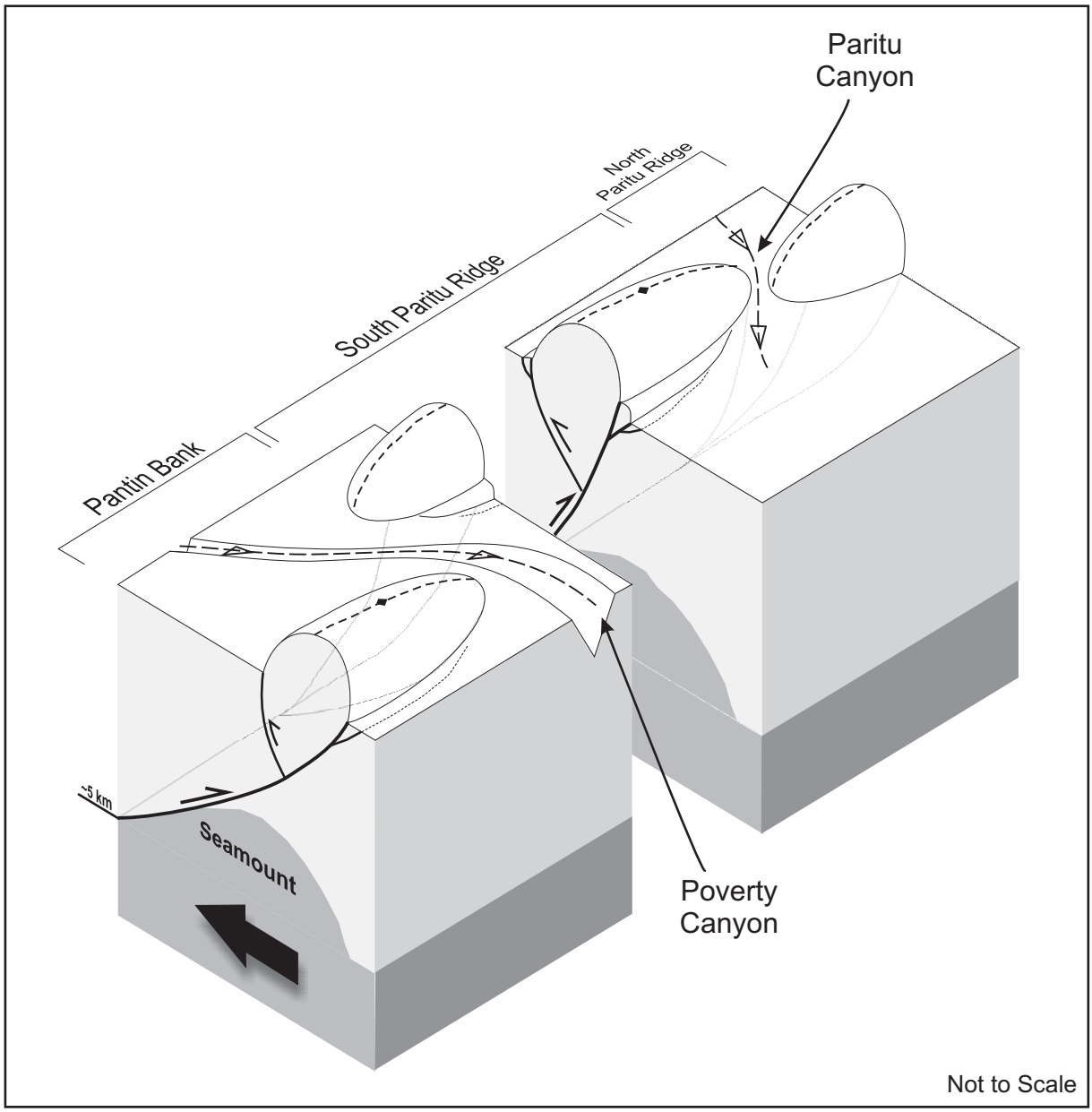

Figure 3.13 Schematic 3D block diagram oblique view of a simplified Pantin Bank and the Paritu Ridge complex in the Poverty Indentation, showing the possible seamount subduction-driven segmentation geometry and propagation of fault planes to the surface producing the anticlinal thrust bounded ridges.

CHAPTER 4: SEDIMENTARY PROCESSES & GEOMORPHOLOGY

4.1 INTRODUCTION

The Poverty Indentation (Figures 4.1A and B) is a large margin re-entrant covering an area of just over 4000 km^2 and encompassing the continental slope from the edge of the continental shelf (~100 m water depth) to the trench floor (~3500 m water depth) of the Hikurangi margin, offshore East Coast, North Island, New Zealand. The axis of the re-entrant is defined by the branched Poverty Canyon system (Figures 4.1A and B) stretching 70 km from the continental shelf edge to the trench floor and incising up to 950 m into the sediments and bedrock. The northern sector of the re-entrant has a frontal slope with an average width of 50-60 km, while the southern sector accretionary wedge widens progressively southward from the indentation to more than 100 km off Hawke Bay (Figure 4.1A).

The high quality bathymetric data obtained for this study have enabled a very detailed study into the sea floor morphology of the Poverty Indentation, comparable to onshore geomorphic analyses and emerging international literature on marine seafloor morphology. We present here an investigation into the overall indentation morphology and geomorphic features, with insights into landslide and erosional features, ridges and basins, and the Poverty Canyon system morphology and sediment processes.

4.1.1 Sedimentary transport across the Hikurangi margin

The Hikurangi Margin (Figures 4.1A) became an active subduction margin ~25 Myr ago and is now represented by a significant deformation zone 50 to 200 km wide, stretching from the offshore Hikurangi Trough (structural trench), to the eastern side of the extensional arc system of the Taupo Volcanic Zone (TVZ) (e.g. Walcott, 1978; Lewis, 1980; Lewis and Pettinga, 1993). The Hikurangi Margin has been subdivided into three sectors along its length based on tectonic processes and deformation styles (Lewis and Pettinga, 1993) with the Poverty Indentation located just north of the transition between the central and northern sectors. The central sector of the margin , offshore Wairarapa, is characterised by a moderate relative convergence rate of ~43 mm/yr (Wallace et al., 2004) and a high sedimentation rate in

the adjacent trough (> 3 km thick compared to <600 m in the northern margin, offshore East Cape (Lewis, 1980)). A significant accretionary wedge has developed from the accretion of South Island derived trench-fill sediments, longitudinally-fed northward along the Hikurangi Channel and Trough, combined with sediment derived from the North Island across the margin slope. Slope basins, often stretching up to 50 km in length and parallel to the trench, trap sediment on the frontal wedge. In contrast, the northern sector can be classified as an erosional convergent margin, characterised by an over-steepened frontal slope, subducting seamounts, frontal tectonic erosion, and extensive regions of gravitational collapse within the inboard trench slope (Collot et al., 1996; Barker et al., 2009). The tectonic and geomorphic transition between the presently wide accretionary wedge in the central part of the margin, and subducting seamounts in northern part of the margin has recently been located south of the Rock Garden bank off southern Hawke Bay (Barnes et al., 2009).

Typical of high-sediment yield rivers with mountainous small catchments globally, the muddy fluvial systems that drain the steep and unstable terrain of the Raukumara Ranges on the northern East Coast have deposited thick postglacial sequences on the adjacent continental shelf (e.g. Orpin, 2004). Sediments along the length of the Hikurangi margin continental shelf are largely terrigenous and derived directly from the east coast of the North Island. These sediments are dominated by mud, reflecting the highly erodable soft rock Tertiary strata on the East Coast, active tectonism, meterological extremes, and more recent effects of historical land clearance with subsequent increases in erosion rates (Foster and Carter, 1997). Continental slope sediments also include off-scraped sediment from the Pacific Plate largely sourced from the South Island. Sediment transport across the continental shelf and slope is affected by a number of processes, including: 1) eustatic sea level, 2) the Tasman Inflow and the Subtropical Front (e.g. Carter et al., 1996; Foster and Carter, 1997; Carter et al., 2002; Carter et al., 2004; Orpin et al., 2008), and 3) tectonic regime.

4.1.2 The role of submarine canyon systems as sediment conduits

Submarine canyons, gullies and other seafloor valleys provide important conduits for sediment across continental margins worldwide (e.g. Soh et al., 1990; Hagen et al., 1994; Hagen et al., 1996; Lewis and Barnes, 1999; Lastras et al., 2007; Arzola et al., 2008; Kuehl et al., 2008). Their location and morphology are controlled by a number of factors including structural fabric, regional tectonic processes, sea-level variations and sediment supply (Soh and Tokuyama, 2002). Many canyons are restricted to the upper slope but some evolve to

extend all the way to the base of the lower slope and incise significantly into the continental shelf. These extensive canyon systems are important sediment conduits, intersecting the current-driven along-shelf sediment transport pathways and significantly contributing to dispersal of terrigenous sediment by gravity-driven turbidites to the margin structural trench depocentres (e.g. Lewis and Barnes, 1999). During low-stands, the continental shelf depocentres can be directly bypassed (e.g. Foster and Carter, 1997; Orpin, 2004; Alexander et al., 2006b; Alexander et al., 2006c; Alexander et al., 2006a; Walsh et al., 2007).

Significant sediment conduits on the Hikurangi margin from the North Island continental shelf edge to trench floor include the extensive Cook Strait Canyon at the southern end of the margin (Mountjoy et al., 2009a; Mountjoy, 2009), the smaller Pahaua Canyon, offshore Wairarapa (Mountjoy et al., 2009a), the Poverty Canyon (Lewis, 2001; Mountjoy, 2009; Pedley et al., 2010), and to a lesser extent, the Ruatoria debris avalanche, offshore East Cape (e.g. Lewis et al., 2004). The Hikurangi margin also contains the Madden Canyon, a shelf to mid-slope incision that appears to be constrained by the active thrust faulted anticlines of the accretionary wedge, preventing it from reaching the trench floor (Lewis and Pettinga, 1993; Mountjoy et al., 2009a; Mountjoy, 2009). The distribution of these canyons along the continental slope means that the Poverty Canyon system (Figures 4.1B and 4.1C), a 70 km long incision directly down the axis of the Poverty Indentation, represents the only significant sediment transport pathway to directly reach the trough for nearly 300 km along the margin (Lewis et al., 1998).

Previous work on the Poverty continental shelf and shelf edge/upper slope (Foster and Carter, 1997; Carter, 2000; Lewis, 2001; Barnes et al., 2002; Orpin et al., 2003; Orpin, 2004; Ricketts and Nelson, 2004; Kuehl et al., 2006; Orpin et al., 2006; Walsh et al., 2006; Walsh et al., 2007; Kuehl et al., 2008) highlight the presence of a large (area = 980 km^2, volume = 17.9 km^3) sediment depocentre on the shelf directly outboard of the Waipaoa River and Poverty Bay, and with a smaller (area = 140 km^2, volume = ~3 km^3) depocentre situated on the shelf edge at the head of the Poverty Gullies (Orpin et al., 2006). Sediment is channelled through to this smaller depocentre through a gap between the topographic expressions of the structurally active Lachlan and Ariel Ridges (Foster and Carter, 1997; Barnes et al., 2002; Orpin et al., 2006). It is thought that during low-stand sea levels, these depocentres are bypassed, with sediment transported directly down the Poverty Canyon. Currently, the high-stand situation

appears to be one of infilling in the canyon heads and a largely inactive system (Walsh et al., 2007).

4.2 METHODS

High quality 30 kHz multibeam bathymetric data and backscatter images of the Poverty Indentation were obtained by the National Institute of Water & Atmospheric Research (NIWA) in 2001 (survey TAN0106) using a SIMRAD EM300 multibeam system on RV TANGAROA (Lewis, 2001). Over 4000 km^2 of submarine seafloor was mapped, encompassing the entire indentation, at depths ranging from ~50 to >3500 metres (Figure 4.1B). The swath bathymetry data have been processed to 10m and 25m grid digital elevation models (DEMs) by NIWA staff. Additional areas were surveyed during 2006 (TAN0616) and 2008 (TAN0808 and TAN0810), extending swath bathymetry data in the northern area of the indentation (see also Mountjoy et al., 2009b). In this study the DEM data have been interpreted using ESRI ArcGIS software version 9.0.

4.3 INTERPRETATION OF BATHYMETRIC DATA

The Poverty Indentation is a distinctive morphological feature on the Hikurangi convergent margin. To qualitatively characterise morphology and investigate sedimentary pathways through this re-entrant, a number of graphic analyses were undertaken in ArcGIS. These include models of slope (in degrees), and aspect (direction) of slope and landslide features.

4.3.1 Slope model (refer to Figure 4.2)

The slope model function in ArcGIS generates a coloured image of the DEM where each colour represents a discrete range of slope angles in degrees (Figure 4.2). The dark brown colours on the slope model immediately highlight slopes of >34 degrees; these occur on the sides of the Poverty and Paritu Canyons and in major landslide scarps across the indentation (Figure 4.2). Anticlinal ridges across the lower slope are asymmetric, with the steeper southeast-facing forelimb slopes yellow through brown and pink at 14-40^o, and are dominated by the numerous landslides scars. The shallower structural backlimbs (inboard-facing) of these anticlines are characterised by blue, green and yellow coloured slopes ranging from 2-

29° (generally <11°). The significant Riwhā Landslide and scar shows slope angles of up to 45° (dark pink) in the deformation front, on the edge of the Lower Paritu Basin (Figure 4.2). South of the Poverty Canyon, numerous submarine slide scars are observed in the bathymetry, but these have less relief compared to scars on the north side of the canyon. These slides are mostly concentrated on the fault-bounded, east-facing forelimbs where the slopes are inferred to be over-steepened (up to 40°), causing the concentration of slope instability (Figure 4.2).

The rough surface expression of debris flow deposits across the Paritu Basin and northwest of the Tuaheni Ridge is highlighted in the slope model by a high density of spatially alternating colours from blue to yellow (Figure 4.2). The head zones of these flow deposits are accompanied by large escarpments, some up to 520 m high, with slope angles of up to 40° (pink colour).

The shelf-slope break itself is marked by the Poverty Gullies, a spectacular, morphologically complex escarpment up to 1000 m in height, with seafloor slope angles ranging from 8° in the head zones to 30-48° on the steepest slopes (Figure 4.2). The southern section of these gullies is not characterised by brown colouration, but is dominated by yellow and green, indicating that these are shallow gullies characterised by a base slope angle of ~5° (Figure 4.2).

Basins are clearly marked on the slope model by the mostly uniform blue colour (<5.6°), particularly the slope basins wedged between the anticlinal ridges across the accretionary wedge south of the Poverty Canyon (Figure 4.2). The Lower Paritu Basin at the base of the Paritu Canyon is also well defined by the blue colour in the slope model (Figure 4.2). The Pāpaku Basin is a wide (5 - 8 km), moderately sloping (<17° averaging ~5°) depression east of North Paritu Ridge (labelled on Figure 4.1).

4.3.2 Aspect model (refer to Figure 4.3)

The aspect model function in ArcGIS presents the direction (aspect) that slopes face in the DEM. Each slope-facing direction is represented by a different colour (Figure 4.3). Overall, the slope aspect model highlights the change to a SE facing margin north of the canyon from a directly E facing margin in the accretionary wedge (Figure 4.3). This is particularly evident in both the frontal section and upper slope – the upper slope faces due E but swings to dominantly SE facing where it transitions into the gullies at the top of the canyon. There is a clear switch to W and NW facing slopes in the mid and lower continental slope regions, assisting definition of locations and extents of the anticlinal structures (Figure 4.3).

The debris flows across the Paritu Basin and inboard of Tuaheni, evident by their alternating colour pattern in the slope model, are further highlighted in this aspect model as a pronounced stippled pattern due to changing slope directions of the individual blocks in the flow deposits (Figure 4.3).

4.3.3 Landslide scars and deposits

Landslide scars in the Poverty indentation are defined as erosional features with a head scarp and reasonably wide, smooth slope, when compared to gully features which are highly eroded, v-shaped, often with internal channels, and lacking in a head scarp. To model the landslide and gully features in the Poverty Indentation, each landslide and gully feature was manually digitised on to the DEM and given a distinct colour to show its facing-direction (aspect) (Figure 4.4). Many gravitational landslide scars are concentrated on the lower slope, directly inboard of the deformation front of the northern sector of the Poverty Indentation, with a large section appearing to be associated with the Riwhā Scar and debris avalanche, thought to be the result of a small seamount impact (Figure 4.4). Major landslide scars and debris on the upper slope originate from the shelf break and shelf-edge gullies. Landslide scars show preference for E-facing and S-facing slopes with some concentrations of landslide scars present on W-facing slopes on the back of anticlinal structures and eroding into the Poverty Canyon walls (Figure 4.4). N-facing landslide scars are associated mainly with the canyon system, and gully sides at the top of the continental slope (Figure 4.4).

4.3.4 Backscatter

The process of backscattering is the reflection of waves, particles or signals back to the direction they came from. It is a diffuse reflection, meaning that different substrate properties will either increase the scatter of the signals, providing a poor return signal, or have minimal scatter, allow the signal to return strongly to the origin. Seafloor backscatter strength can be described primarily as a function of grain size for sand and finer sediments, and that surface shape and roughness are an important consideration in understanding backscatter strength for coarser sediments (Kagesten, 2008). It appears that hard smooth surfaces, like boulders and bedrock, will often return much weaker backscatter signals than a fine gravel substrate. In fact, the backscatter signal of a hard sea floor surface with boulders might give the same signal as, and therefore not easily distinguished from, coarse sand (Kagesten, 2008).

Therefore, combining backscatter with bathymetry and available core samples provide a much more accurate interpretation of the substrate.

Backscatter data was collected in conjunction with the seafloor bathymetry data on the TAN0106 voyage in 2001 (Lewis, 2001) (Figure 4.5A). Backscatter image data of the Poverty Indentation reveals some regions of high (dark grey) and moderate (light grey) backscatter (Figure 4.5B). High backscatter typically corresponds to areas of gravel or debris flow deposits (e.g. Lewis and Barnes, 1999). Regions dominated by high backscatter, and therefore likely to contain gravel or debris flow deposits, within the Poverty Indentation include: The Poverty Gullies, the channel floors of the lower reaches of Poverty Canyon, in Paritu Canyon, and the Riwhā Landslide scar (Figure 4.5B). Moderate backscatter is characteristic in the lower Poverty Gullies, the Paritu debris flows across Paritu Basin, and across the Tuaheni Landslides. Moderate backscatter is also observed on the outboard (east) slope of the North Paritu Ridge and the middle reaches of Poverty Canyon (Figure 4.5B). In terms of sediment type, moderate backscatter is likely to indicate fine pebble gravel deposits (e.g. Lewis and Barnes, 1999).

4.4 INCISION PROCESSES

Erosion and incision processes in the Poverty Indentation can be divided into three main categories:

1) gullying and localised slope erosion
2) mass movement debris flows and slumps
3) canyon development

4.4.1 Poverty Gullies

The shelf-slope break is marked by the Poverty Gullies, a spectacular, morphologically complex escarpment up to 1000 m in height, with seafloor slope angles ranging from 8^{o} in the head zones to 30-48^{o} on the steepest slopes (Figure 4.6). The Poverty Gullies can be divided up into northern, central and southern zones, differentiated by the degree of erosion and subsequent average slope angles (Figure 4.6). In the northern zone, the head-scarps of the Tuaheni Landslides reflects what is inferred to be the initial processes responsible for gully development with mass movement encroaching into the shelf break clinoforms (Mountjoy et

al., 2009b). Slope angles in this zone are characterised by much steeper head-scarp slopes compared to the rapid shallowing out of the lower slopes (Figure 4.6). The central zone of the Poverty Gullies is characterised by a well developed escarpment with a progressive decrease in seafloor slope angles and widening and lengthening of the gullies southward to the southern branch of the upper Poverty Canyon (Figure 4.6). To the south of the Poverty Canyon, the southern zone is characterised by slopes formed on a largely (now relict) depositional prograding wedge. Shallow gullies (2-10 m) dominate on the 6.5 km wide upper slope with relatively superficial mass movements affecting the prograding clinoform sequence, characterised by the gentle base slope angle of ~5^{o} (Figure 4.6).

Sediment cores and samples from the Poverty Gullies (see Figure 2.4 and Table 2.1, Chapter 2) show the presence of Late Holocene sediments across the northern part of the central zone, between the head of the Poverty Canyon and the head zone region of the Poverty Debris Avalanche. This is likely to reflect post-glacial infilling of the gully head zones as discussed in Walsh et al. (2007). Sediment samples from sites across the Poverty Gullies show age ranges of 13-18 Ma and 12 Ma in the head zone region of the Poverty Debris Avalanche, 0.3 Ma in the Poverty shelf edge, just above the Poverty Gullies at the head of the northern branch of the Poverty Canyon, and 16-19 Ma in the gullies at the top of the middle branch of the Poverty Canyon. These ages are more likely to reflect past gully incision during low-stand.

Erosion on anticlinal limbs throughout the Poverty Indentation appears to be more concentrated on the outboard trench-facing slopes (e.g. Figure 4.7C). Anticlinal ridges are asymmetric, with the steeper southeast-facing forelimb (slopes of 14-40^{o}) dominated by the numerous landslides scars and gullying. Landslide scars and gullying are rare on backlimb slopes. Numerous submarine slide scars are observed in the bathymetry, south of the Poverty Canyon, but these have less relief compared to scars on the north side of Poverty Canyon. These slides are mostly concentrated on the fault-bounded, east-facing forelimbs where the slopes are steep (up to 40^{o}) (refer to Figure 4.2). The occurrence of numerous failures are indicative of limb over-steepening with respect to the geotechnical strength properties of sediments.

4.4.2 Mass movement features in the Poverty Indentation

Large-scale landslides in the Poverty Indentation originate from immediately below the shelf edge at the head of the Paritu Basin and erode into the upper slope (Figure 4.7A). The Poverty Debris Avalanche (Mountjoy et al., 2009b) is comprised of a series of extensive debris flows originating from the shelf break and gully region, cutting obliquely across Paritu Basin (Figure 4.7A). The youngest flows, by cross-cutting relationships, have been emplaced southward over 30 km and into the upper and mid-reaches of the Poverty Canyon, covering ~200 km^2 of Paritu Basin floor. The head zones of these flows are accompanied by large escarpments up to 520 m high, with slope angles of up to 40^o. The debris flows have multiple sediment lobes fanning out across the lower half of the Paritu Basin, indicating multiple failure events associated within the debris flow complex. Sediment samples taken from these flows provide a Holocene age for both the middle and terminus of the latest flows, and a Late Holocene age for sediment on the outboard edge of the Paritu Basin, directly below the avalanches (see Chapter 2, Figure 2.4 and Table 2.1 for details).

North of the Paritu Basin, the southern part of Tuaheni Ridge partially traps and deflects components of the Tuaheni Landslide Complex (from Mountjoy et al., 2009b). These have been interpreted by Mountjoy et al. (2009b) as submarine earthflows (Figure 4.7A). Some of the slide mass is being conveyed to the south into the Paritu Basin via the Tuaheni Canyon, or by spilling over a ~300 m high escarpment at the head of the Poverty debris flows. The bulk of the sediment is deflected to the north and around the Tuaheni Ridge where there is a structural gap, allowing some of the mass flows to find their way down into the lower reaches of the Paritu Basin, just above the Paritu Canyon (Figure 4.7A). Further debris flows are derived from continued modification of the gully systems and remobilisation of sediment around the upper slope.

The margin front in the slope section directly north of the Poverty Canyon mouth is highly eroded with many gullies and landslide scars (see Figure 4.8). The significant Riwhā Landslide and scar (2 x 4 km with slope angles of up to 45^o) on the deformation front at the edge of the Lower Paritu Basin (Figure 4.7B), has a debris run-out of nearly 9 km and has previously been inferred to have resulted from a small seamount impact (Lewis, 1997). Blocks in the debris flow from this landslide are up to 3 km in length. Rock and dredge samples obtained from the Riwhā Landslide headscarp date from the Early Pliocene (~4 Ma) to the Early to Middle Miocene (around 17-13 Ma) (see Table 2.1, Chapter 2). Inboard of the Riwha Scar, a series of prominent slump faults are evident in the headscarp, extending ~1 km

directly behind the head wall and extending in a widening zone nearly 7 km to the south west (Figure 4.7B).

Slump features are concentrated on slopes inferred to be affected by sediment movement eroding into the base of slope, particularly at the edge of the Paritu Basin, where sediment appears to be channelled into the edge of the Paritu Debris Avalanche and around the basal edge of the Tuaheni Ridge (Figure 4.7D). They are also concentrated off the Poverty Canyon walls, particularly in the middle reaches of the canyon branches as the canyon incises into basin fill (see Table 4.3).

4.4.3 Poverty Canyon

The central feature defining the axis of the Poverty Indentation is the Poverty Canyon (Figure 4.9). The canyon system covers an area of ~600 km^2 and its channel axis is up to 70 km long, up to 40 km wide at the rim, and up to 2.1 km wide in the axis (with axial gradients of up to 12° (see Chapter 3, Figure 3.4)). To help classify this feature, a series of transects were positioned intersecting the canyon branches, with spacing roughly equally along the axis of the canyon, but also taking into account major structural features that may affect canyon morphology. These transects are outlined in Tables 4.1, 4.2. The Poverty Canyon is separated into three branches, northern, middle and southern (Table 4.1). The northern and middle branches originate from a series of gullies incised into the continental shelf edge and upper slope. The southern branch originates from the base of an upper slope clinoform sequence extending to the south below the shelf-slope break. Extensive arcuate erosional head-scarps extend northward along the western edge of the middle channel, and incise into the clinoform sequence. The canyon passes through the south-western edge of the Paritu Basin. The entire canyon is sinuous, with Sinuosity Indexes (SI) of 1.04 to 1.45, where bedrock streams that flow directly downslope have a sinuosity index of 1, and meandering streams have a sinuosity index that is greater than 1. Sinuosity is measured on the incised meandering channel within the main canyon walls and is essentially made up of both the sinuosity of those meanders, but also of the outer canyon wall.

The northern and middle branches can be further divided up into upper, central and lower sections based on morphological criteria. To present the differences between these sections, we present the seven transects across the canyon (Figure 4.10, Table 4.2). The upper section (transects 1 & 2) is characterised by gully formation, high erosion, a narrow canyon floor and

a steep gradient, increasing back towards the shelf edge. Incision is high across transect 1 (780-950 m) but decreases significantly across transect 2 (250-400 m) as the gully morphology dominating this upper section of the canyon opens out into the mid-slope basin region of the Poverty Indentation. Canyon channel width also significantly changes between transect 1 and 2, widening from 468-702 m to 1108-1380 m. Sinuosity and canyon wall angle do not show significant changes, although sinuosity in the northern branch increases between transect 1 and 2 to 1.43, the most sinuous section of the entire Poverty Canyon (Table 4.2). There are two records of sinuosity in the Poverty Canyon system relating to two different sizes of flow. The outer walls of the canyon reflect large flow during low-stand cycles when sediments bypass the shelf and erode directly into the canyon (e.g. Foster and Carter, 1997; Orpin, 2004), while an internal meander channel incising into the wider canyon floor suggests flow associated with the current high-stand cycle and limited sediment supply (e.g. Walsh et al., 2007; Alexander et al., 2009). Sinuosity of both the outer canyon walls and the inner meander channel is similar. Calculations in Table 4.1 and Table 4.2 present sinuosity of the inner meander channel (representing the most recent canyon activity).

The middle section branches (transects 3 and 4) are wide (1246-2003 m) and shallowly incised (200-430 m) into the mid-slope Paritu Basin region across transect 3. Slumping from the canyon side walls is common across this section, as well as many side tributaries. Across transect 4, the channel width decreases significantly to 529-678 m with the channel morphology becoming more confined into the three main branches heading into the mid-slope ridge section of the Poverty Indentation (Table 4.2).

The lower section (transects 5, 6 and 7) is deeply incised (600-940 m) with a flat canyon floor, high sinuosity (up to 1.28) and steep canyon walls (32-45^{o}) (Table 4.2). The branches join into one channel between transects 6 and 7, with the channel widening significantly at the canyon mouth across transect 7 to well over 2 km.

There are a number of knick-points observed in the canyon floor, particularly where the canyon incises through the mid-slope ridge complexes (South Paritu Ridge and Pantin Bank) and immediately “up-stream” from the slope toe deformation front. This is evident in gradient profiles (see Chapter 3, Figure 3.4). The Poverty Canyon middle and southern branches appear to show lower gradients just before knickpoints on the up-stream limb and over the highest point of growth on Pantin Bank. Shallower gradients on the northern branch of the Poverty Canyon are harder to identify but seem to occur in the canyon floor incising through

the up-stream limb of the South Paritu Ridge. All three of these shallowing gradients occur between transects 4 and 5 and also between 5 and 6 on the middle and southern branches (Figure 4.10, Table 4.1).

Rock, dredge and core samples obtained from the Poverty Canyon are presented in Table 4.3 (see Chapter 2, Figure 2.4 and Table 2.1 for more details). Ages in the upper section range from approximately 14 to 19 Ma. The middle section is represented by two separate age ranges, <0.005 Ma in the intersection of the middle and southern branches, and 0.15 to 1.6 Ma in the northern branch (Table 4.3). At the mouth of the Poverty Canyon sample ages range from 0.2 to 1.8 Ma.

4.4.4 Paritu Canyon

The Paritu Canyon is a smaller canyon incising a structural gap between the mid-slope North and South Paritu Ridges, acting as a conduit for sediment to pass from the Paritu Basin, through the Lower Paritu Basin to the lower slope and Hikurangi Trough. In its upper reaches Paritu Canyon is choked with sediment, as interpreted from the surface roughness visible in the DEM (Figure 4.11). Two nick-points represent significant escarpment steps (~400 m and <200 m) on the canyon floor. The canyon stretches just over 12 km from initial incision into the Paritu Basin sediments, through the main channel escarpment at ~5 km and out to the Lower Paritu Basin (Figure 4.11). Above the escarpment, the canyon floor is wide (1700 m) and flat (0-3.5^{o}) with incision <150 m into the surrounding slope. Incision increases significantly in the lower reaches of the canyon up to a maximum of ~700 m (Figure 4.11). The lower reaches of the canyon, leading to the Lower Paritu Basin is evacuated of sediment fill. Canyon wall morphology indicates it has previously been filled with sediment which is now being progressively scoured out. Sediment transport through this canyon from the main, upper/mid-slope Paritu Basin has resulted in thick (~500 m) triangular sediment wedge in the Lower Paritu Basin. A piston core sediment sample obtained from the Lower Paritu Basin (see Chapter 2, Figure 2.4 and Table 2.1) gives a Holocene age.

4.5 DEVELOPMENT OF SEDIMENTARY PROCESSES ACROSS THE POVERTY INDENTATION

The Poverty Indentation is an important shelf to trench sedimentary conduit along the Hikurangi margin. It contains the only full shelf to trench canyon system along the margin slope north of the Cook Strait Canyon system (Mountjoy et al., 2009a), so is an effective route for sediment to bypass the numerous deformation front-parallel slope basins associated with the accretionary wedge. This has allowed the canyon to deliver sediment not only to the trough, but also into the distal Hikurangi Channel system, for at least several hundred thousand years and probably longer.

4.5.1. Development of slope erosion

Landslides and debris flows are numerous in the region and can be classed as one of two types: aerially-extensive and local. Locally-derived landslides are attributed to over-steepening thrust-bound anticlinal slopes and remain local to source. Aerially-extensive debris flows extend out over large areas of basin fill and are sourced from immediately below the shelf-break. In terms of sediment transport potential, aerially-extensive debris flows are expected to be very important as major contributors in terms of sediment flux from the continental shelf and upper slope across the frontal slope to the structural trench depocentre. The periodicity of these events, as evidenced in seismic sections TAN0106-06, -08 and -16, also indicates either: (i) a strong link to the fluctuating glacio-eustatic influence on sediment flux onto the upper slope; or (ii) cyclicity of seismic activity, or a combination of both. Volumetrically, local landslides would not be expected to greatly contribute to sediment flux, as they do not transport sediment far from source, and often involve older sediment structurally incorporated into anticlines. However, they are likely to occur with greater density along the margin and with far greater frequency than the larger aerially-extensive debris flows. The Holocene to Late Holocene sea floor surface ages of the Poverty Debris Avalanche suggest a correlation to post-glacial landslide activity with some sediment fines reaching the outer edge of the Paritu Basin more recently than the last major avalanche event.

The continental shelf edge sedimentary wedge is well developed along the margin to the north and south of the re-entrant, as a ~1 Ma prograding clinoform sequence, in response to very high sediment flux onto the margin during glacio-eustatic low-stands. The wedge excavation reflects the growth of the Poverty Canyon and gully system, initiated as a response to seamount impact and developing contemporaneously with fluctuating glacio-eustatic sediment flux to the upper slope. The re-entrant scar created by the impact and passage of one

or more seamounts provided a corridor for sediment from the continental shelf to the trench floor, relative to the surrounding clinoform sequence along the margin.

4.5.2. Development of the canyon systems

Development of the Poverty Canyon system and excavation of the margin-wide prograding clinoform sequence into the first-order re-entrant following initial seamount impact has provided a major conduit for sediment delivered to the continental shelf slope break directly to trench floor. We infer development of the margin-wide clinoform sequence over the last ~1 Myrs. A simplistic timeline of development of the Poverty Canyon with incision into the Poverty Indentation is inferred to be as follows:

i) initial incision into the axis of the indentation following indentation-forming seamount impact ~1 Ma

ii) incipient canyon eroding into the proto-clinoform sequence ~1 - 0.5 Ma, and

iii) full-scale development of a three branched canyon system and extensive erosion of the composite clinoform wedge sequence around the headwall of the re-entrant by gullying and landsliding

The upper sector of the indentation was subjected to erosion and mass movement progressively developing the crown area and head-wall. Then the clinoform sequences were deposited during low-stands (the most recent one during the Pleistocene last glacial maximum (LGM) around 20 ka), and repeatedly incised and reformed in response to both eustatic sea-level changes, as well as the progressive establishment of the branched upper canyon. Seismic data (lines CM05-04, -02, -45, -44, -43, -42, -32, -23, -19 and TAN0106-08, -06) reveal repeated episodes of sediment infilling and evacuation, reflecting especially the eustatic driver delivering large volumes of sediment into the crown region of the indentation.

Development of the Poverty Canyon system, with gullying and landsliding, has been instrumental in the retreat and widening of the upper margin re-entrant and catchment, leading to large-scale excavation of the shelf-edge and upper slope low-stand sediment wedge. Incision of the canyon has shortened the path to the trench floor, which has resulted in the relatively steep channel axial gradient. The canyon is largely evacuated of sediment in the lower region with sediment infill progressively increasing into the head zones (Alexander et al., 2006c; Alexander et al., 2006a; Walsh et al., 2007; Alexander et al., 2009). Our

extrapolated age (see Chapter 2, section 2.4) of the clinoform wedge constrains the timing of canyon incision and gully development to younger than 1 Ma with the canyon developing to its full extent significantly later than the indentation-forming seamount impact, possibly triggered by the high sediment flux during the low-stand clinoform progradation.

On the shelf a large structurally controlled depocentre for sediment has captured significant volumes of sediment during high-stand sea levels, with some in-filling of the canyon head (Walsh et al., 2007). Conversely, during low-stand sea levels, sediment is thought to largely bypass the shelf and enter the Poverty Gullies and Canyon, creating turbidites and mass debris flows; small lower slope basins located between thrust-propagated anticlines represent transient and permanent depocentres for sediment delivered to the continental slope (Foster and Carter, 1997; Orpin, 2004; Alexander et al., 2006b; Alexander et al., 2006c; Alexander et al., 2006a; Walsh et al., 2007; Mountjoy, 2009).

Sinuosity of sub-aerial rivers is often a result of shallowing of gradient in response to a growing anticline (Campbell and Yousif, 1985; Campbell et al., 2000). We can apply this to submarine canyon development by investigating the implications of gradient and sinuosity changes in the Poverty Canyon branches. As the SI values of the internal meander channel are comparable to the outer canyon walls, the SI values therefore also reflect the overall canyon sinuosity in response to the growth of the large anticlinal structures of the mid-slope ridge complexes. Highest sinuosity should occur on the up-stream limb side of an actively growing anticline (i.e. Campbell and Yousif, 1985; Campbell et al., 2000; Estrada, 2003) because the location of gradient shallowing is the greatest. In the Poverty Canyon, the section between transects 4 and 5 should therefore have the highest sinuosity and shallowest gradient as a response to growth on the South Paritu Ridge and Pantin Bank. While gradient profiles (see Chapter 3, Figure 3.4) do indeed show a shallowing of gradient on the up-stream limbs of the mid-slope ridge complexes across transects 4 to 5 (also including 5 to 6 in the middle and southern branches), sinuosity in these sections is not so easily correlated. In the northern branch, SI values of the internal meander channel is highest further downstream, between transects 5 and 6, and 6 and 7 (see Table 4.2). SI values in the middle and lower branch are also inconclusive. On the outer canyon walls, both the northern and middle branch channels deflect back south, away from the South Paritu Ridge on the downstream limb. This may be interpreted to be a relict channel response from when the seamount, currently beneath the mid-slope ridge complexes, was in the initial stages of entering the deformation front,

reflecting the unique and complex role that a moving anticline, one that is cored by a subducting seamount, may play on the development of such an incised canyon system. The role of antecedence (e.g. Campbell and Yousif, 1985; Campbell et al., 2000; Mountjoy et al., 2009a) in relation to these moving anticlines may also play an important part in the current morphology and sinuosity of the canyon, particularly the northern branch. This implies that a migrating structure and antecedence may result in a channel morphology that may not reflect the current structural location. Given that this tectonic environment is one of subduction with frequent seamount impacts, it is likely that the inboard/up-stream movement of these anticlines has affected the ability of the canyon to adjust its channel appropriately, particularly with the low sediment flow during high-stands.

It appears from the ages presented in Table 4.3 that incision and erosion into the shelf edge sediments is the dominant sedimentary process in the upper canyon reaches as part of the Poverty Gully system, which has yielded comparable age ranges across the head of the Poverty Indentation at around 18-13 Ma and 12 Ma (see Chapter 2, Table 2.1). Deposition, through not as dominant as erosion, appears to have been active in the middle and lower reaches of the canyon post-glacial at least as recent as the Late Holocene, with sediment reaching the mouth of the Poverty Canyon. Older Pleistocene sediment (0.3-1.6 Ma and 1.4 Ma) in the middle section of the northern branch is located where the canyon incises into the axis of the actively growing South Paritu Ridge anticline. Mid-Holocene ages have been determined for samples from the intersection of the middle and southern Poverty Canyon branches at around 5000 years BP. The southern branch feeds directly off the toe of the sediment wedge of the eroded clinoform sequence so there may be more recent transport and deposition of sediment down this section of the slope.

Tectonic controls on development of canyon features within the Poverty Indentation include: i) first-order subsidence and drainage development in the wake of the very large earliest seamount impact, and ii) local modification and progressive deflection of the canyon(s) between the major mid-slope thrust ridges (e.g. Campbell and Yousif, 1985; Campbell et al., 2000; Mountjoy et al., 2009a). The Poverty Canyon has developed initially by incision into the axis of a major margin indentation/re-entrant. Continued tectonic modification and development is concentrated primarily across the lower frontal slope in the lower reaches of the canyon. This is inferred as a response to tectonic growth of the mid-slope ridges and within the deformation front. Future seamount impacts (i.e. Gisborne Knolls) may have a

significant influence on these important sediment pathways via rapid uplift and structural development of the frontal wedge and mid-slope anticlines. The geomorphic response with respect to the canyon evolution will depend on the canyon ability to keep pace with deformation through antecedence.

The Paritu Canyon appears to be a feature formed much later than the larger Poverty Canyon, independent of seamount impact and controlled by active ridge growth between the structurally segmented North and South Paritu Ridges. The absence of structural load created by the Paritu Canyon is likely to be modifying the faults through the Paritu Ridge Complex, reinforcing separation into discrete anticlinal structures. With Holocene ages determined in a sediment core in the Lower Paritu Basin, sediment activity through this canyon appears to have been almost as recent as the main Poverty Canyon and is very likely connected to the most recent Paritu Debris Avalanche event (refer to Chapter 2, Figure 2.4 and Table 2.1). It appears from the morphology of the seafloor (e.g. Figures 4.2 and 4.11), that the more recent activity of channel incision into those debris flows around the northern edge of the Paritu Basin has also removed sediment from that basin and transported it through the Paritu Canyon.

4.6 CONCLUSIONS

The Poverty Indentation has a complex and interactive range of sedimentary and structural/tectonic processes. Its origins as a seamount impact-initiated margin indentation have enabled evolution of a significant sediment conduit from the North Island continental shelf to the structural trench floor and abyssal plain. It is, in fact, the only significant sediment transport pathway to directly reach the trough for nearly 300 km along the margin (Lewis et al., 1998).

Sedimentary processes within the Poverty Indentation can be divided into three main categories:

1) *gullying and localised slope erosion*

- concentrated in the Poverty Gullies extending across the upper slope beneath the shelf/slope break, and on anticlinal slopes throughout the indentation, particularly on the outboard limbs.

2) *mass movement debris flows and slumps*

- debris flows concentrated in the upper slope originating from the shelf/slope break - Paritu debris avalanche and Tuaheni Landslide Complex. Slumps concentrated off canyon walls and also at the edges of basins where the toe of slope is undercut.

3) *canyon development*

- two canyon systems, the Poverty Canyon (extending from shelf edge to trench floor) and the Paritu Canyon (connecting the Paritu Basin with the Lower Paritu Basin through a structural gap in the mid-slope anticlinal ridge complex.

Canyon incision and re-entrant headwall retreat have lead to a complex sedimentary-erosional response cycle, driven by eustatic sea-level change in Pleistocene time and reflected by the development of a composite low-stand clinoform succession repeatedly incised and cannibalised leading to the development of a re-entrant headwall gully system and large-scale submarine slides and debris flows. Sediments (re)mobilised from the clinoform wedge have lead to canyon incision and sediment transfer across the margin slope to the structural trench.

Structural activity driven by subduction processes (including seamount subduction) has led to the development of a series of margin parallel anticlinal ridges and associated slope basins strongly reflected in the margin morphology. The progressive evolution of the narrow structural ridges has strongly influenced canyon evolution.

References

Alexander, C., Walsh, J.P., Sumners, B., Orpin, A. and Kuehl, S., 2006a. Continental slope sediment delivery and storage on an active margin: The Waipaoa Margin example. Eos Trans. AGU, 87(52): Fall Meeting Abstracts.

Alexander, C., Walsh, J.P., Orpin, A., Sumners, B., Kuehl, S., Pratson, L., Gerber, T. and Carter, L., 2006b. Tectonic influences on sedimentary processes and submarine landscape evolution: the Waipaoa River, New Zealand example. Geophysical Research Abstracts, 8: European Geosciences Union 2006.

Alexander, C., Walsh, J.P., Orpin, A., Sumners, B. and Kuehl, S., 2006c. Modern sedimentation on the Continental Slope seaward of the Waiapaoa River, New Zealand. Eos Trans. AGU, 87(36): Ocean Sciences Meeting Abstracts.

Alexander, C., Walsh, J.P. and Orpin, A., 2009. Modern sediment dispersal and accumulation on the Waipaoa outer continental margin. Marine Geology, *In press*.

Arzola, R.G., Wynn, R.B., Lastras, G., Masson, D.G. and Weaver, P.P.E., 2008. Sedimentary fetaures and processes in the Nazare and Setubal submarine canyons, west Iberian margin. Marine Geology, 250: 64-88.

Barker, D.H., Sutherland, R., Henrys, S. and Bannister, S.C., 2009. Geometry of the Hikurangi subduction thrust and upper plate, North Island, New Zealand. Geochemistry, Geophysics, Geosystems, 10(2).

Barnes, P.M., Nicol, A. and Harrison, T., 2002. Late Cenozoic evolution and earthquake potential of an active listric thrust complex above the Hikurangi subduction zone, New Zealand. GSA Bulletin, 114(11): 1379-1405.

Barnes, P.M., Lamarche, G., Bialas, J., Henrys, S., Pecher, I.A., Netzeband, G., Greinert, J., Mountjoy, J.J., Pedley, K.L. and Crutchley, G., 2009. Tectonic and Geological Framework for Gas Hydrates and Cold Seeps on the Hikurangi Subduction Margin, New Zealand. Marine Geology, in press.

Campbell, J.K. and Yousif, H.S., 1985. Tectonic geomorphology of the Lower Waipara Gorge, North Canterbury. Geological Society of New Zealand Miscellaneous Publication, 32(B): 53-69.

Campbell, J.K., Bennett, D. and Brand, R., 2000. Actively emergent, fault-related fold structures beneath the Canterbury Plains. 2000 New Zealand Petroleum Conference, Pre-Conference Fieldtrip Guide.

Carter, L., 2000. Voyage Report TAN0005, Report lodged in the National Institute of Water and Atmosphereic Research Library, Wellington, New Zealand.

Carter, L., Manighetti, B., Elliot, M., Trustrum, N. and Gomez, B., 2002. Source, sea level and circulation effects on the sediment flux to the deep ocean over the past 15 ka off eastern New Zealand. Global and Planetary Change, 33(3-4): 339-355.

Carter, R.M., Carter, L. and McCave, I.N., 1996. Current controlled sediment deposition from the shelf to the deep ocean: the Cenozoic evolution of circulation through the SW Pacific gateway. Geologische Rundschau, 85(3): 438-451.

Carter, R.M., McCave, I.N., Carter, L., Richter, C., Aita, Y., Buret, C., Di Stefano, A., Fenner, J., Fothergill, P., Gradstein, F., Hall, I.R., Handwerger, D., Harris, S.E., Hayward, B., Hu, S., Joseph, L., Khim, B.-K., Lee, Y.-D., Millwood, L.D., Rinna, J., Smith, G., Suzuki, A., Weedon, G.P., Wei, K.-Y., Wilson, G. and Winkler, A., 2004. Leg 181 synthesis; fronts, flows, drifts, volcanoes, and the evolution of the southwestern gateway to the Pacific Ocean, eastern New Zealand. Proceedings of the Ocean Drilling Program, Scientific Results (CD-ROM), 181: 112.

Collot, J.-Y., Delteil, J., Lewis, K.B., Davy, B., Lamarche, G., Audru, J.-C., Barnes, P., Chanier, F., Chaumillon, E., Lallemand, S.E., Mercier de Lepinay, B., Orpin, A., Pelletier, B., Sosson, M., Toussaint, B. and Uruski, C., 1996. From oblique subduction to intra-continental transpression; structures of the southern Kermadec-Hikurangi margin from multibeam bathymetry, side-scan sonar and seismic reflection. Marine Geophysical Researches, 18(2-4): 357-381.

Estrada, B.E., 2003. Seismic hazard associated with the Springbank Fault, North Canterbury plains. M.Sc. (Engineering Geology) Thesis, University of Canterbury, Christchurch, 193 pp.

Foster, G. and Carter, L., 1997. Mud sedimentation on the continental shelf at an accretionary margin; Poverty Bay, New Zealand. New Zealand Journal of Geology and Geophysics, 40(2): 157-173.

Hagen, R.A., Bergersen, D.D., Moberly, R. and Coulbourn, W.T., 1994. Morphology of a large meandering submarine canyon system on the Peru-Chile forearc. Marine Geology, 119: 7-38.

Hagen, R.A., Vergara, H. and Naar, D.F., 1996. Morphology of San Antonio submarine canyon on the central Chile forearc. Marine Geology, 129: 197-205.

Kagesten, G., 2008. Geological seafloor mapping with backscatter data from a multibeam echo sounder. MSc Thesis, Gothenburg University, Gothenburg, 30 pp.

Kuehl, S., Pratson, L. and Addington, L., 2006. Contrasting shelf sediment dispersal off small mountainous rivers: The Waipaoa and Waiapu Rivers, NZ. Eos Trans. AGU, 87(36): Ocean Sciences Meeting Abstracts.

Kuehl, S., Miller, A.J., Kniskern, T.A., Gerber, T. and Pratson, L., 2008. Sediment trapping and bypassing in active continental margin settings: New insights from MARGINS Source-to-Sink studies. Geological Society of America Abstracts with Programs, 40(6): 319.

Lastras, G., Canals, M., Urgeles, R., Amblas, D., Ivanov, M., Droz, L., Dennielou, B., Fabres, J., Schoolmeester, T., Akhmetzhanov, A., Orange, D.L. and Garcia-Garcia, A., 2007. A walk down the Cap de Creus canyon, Northwestern Mediterranean Sea: Recent processes inferred from morphology and sediment bedforms. Marine Geology, 246(2-4): 176-192.

Lewis, K., Collot, J.-Y. and Lallemand, S., 1998. The dammed Hikurangi Trough: a channel-fed trench blocked by subducting seamounts and their wake avalanches (New Zealand-France GeodyNZ Project). Basin Research, 10(4): 441-468.

Lewis, K.B., 1980. Quaternary sedimentation on the Hikurangi oblique-subduction and transform margin, New Zealand. Special Publication of the International Association of Sedimentologists(4): 171-189.

Lewis, K.B. and Pettinga, J.R., 1993. The emerging, imbricate frontal wedge of the Hikurangi Margin. Sedimentary Basins of the World, 2: 225-250.

Lewis, K.B., 1997. The succession of seamount impacts and giant avalanches on the Hikurangi margin. In: D.N.B. Skinner (Editor), Geological Society of New Zealand 1997 annual conference; programme and abstracts Geological Society of New Zealand Lower Hutt pp. 99.

Lewis, K.B. and Barnes, P.M., 1999. Kaikoura Canyon, New Zealand: active conduit from near-shore sediment zones to trench-axis channel. Marine Geology, 162(1): 39-69.

Lewis, K.B., 2001. Voyage Report TAN0106, National Institution of Water and Atmospheric Research, Wellington, New Zealand.

Lewis, K.B., Lallemand, S. and Carter, L., 2004. Collapse in a Quaternary shelf basin off East Cape, New Zealand: evidence for passage of a subducted seamount inboard of the Ruatoria giant avalanche. New Zealand Journal of Geology and Geophysics, 47: 415-429.

Mountjoy, J.J., Barnes, P.M. and Pettinga, J.R., 2009a. Morphostructure and evolution of submarine canyons across an active margin: Cook Strait sector of the Hikurangi Margin, New Zealand. Marine Geology, 260(1-4): 45-68.

Mountjoy, J.J., 2009. Submarine canyon evolution: Quantifying geomorphic processes on New Zealand's active continental margin. PhD Thesis, University of Canterbury.

Mountjoy, J.J., McKean, J., Barnes, P.M. and Pettinga, J.R., 2009b. Terrestrial-style slow-moving earthflow kinematics in a submarine landslide complex. Marine Geology, submitted.

Orpin, A., Carter, L., Lewis, K., Kuehl, S. and Alexander, C., 2003. Quantifying deposition from the very muddy Waipaoa River on the Poverty shelf and margin re-entrant, New Zealand. EGS - AGU - EUG Joint Assembly, Abstract 4871.

Orpin, A., 2004. Holocene sediment deposition on the Poverty-slope margin by the muddy Waipaoa River, East Coast New Zealand. Marine Geology, 209(1-4): 69-90.

Orpin, A., Alexander, C., Carter, L., Kuehl, S. and Walsh, J.P., 2006. Temporal and spatial complexity in post-glacial sedimentation on the tectonically active, Poverty Bay continental margin of New Zealand. Continental Shelf Research, 26(17-18): 2205-2224.

Orpin, A., Carter, L., Goh, A., Mackay, E., Pallentin, A., Verdier, A.-L., Chiswell, S. and Sutton, P., 2008. New Zealand's diverse seafloor sediments. NIWA Chart, Miscellaneous Series No.86.

Pedley, K.L., Barnes, P.M., Pettinga, J.R. and Lewis, K., 2010. Seafloor structural geomorphic evolution of the accretionary frontal wedge in response to seamount subduction, Poverty Indentation, New Zealand. Marine Geology, 270(1-4): 119-138.

Ricketts, B.R. and Nelson, C.S., 2004. Early Pliocene landward submarine slumping, Lachlan Basin, Hawke Bay, New Zealand. New Zealand Journal of Geology and Geophysics, 47: 431-435.

Soh, W., Tokuyama, H., Fujioka, K., Kato, S. and Taira, A., 1990. Morphology and development of a deep-sea meandering canyon (Boso Canyon) on an active plate margin, Sagami Trough, Japan. Marine Geology, 91: 227-241.

Soh, W. and Tokuyama, H., 2002. Rejuvenation of submarine canyon associated with ridge subduction, Tenryu Canyon, off Tokai, central Japan. Marine Geology, 187: 203-220.

Walcott, R.I., 1978. Present tectonics and late Cenozoic evolution of New Zealand. Geophysical Journal of the Royal Astronomical Society, 52: 137-164.

Wallace, L., Beavan, J., McCaffrey, R. and Darby, D.J., 2004. Subduction zone coupling and tectonic block rotations in the North Island, New Zealand. Journal of Geophysical Research, 109.

Walsh, J.P., Sumners, B., Alexander, C., Orpin, A., Gerber, T., Pratson, L. and Kuehl, S., 2006. Variations in Depositional Signals across the Shelf-Slope Transition on the Waipaoa River Margin, New Zealand. Eos Trans. AGU, 87(36): Ocean Sci. Meet. Suppl. Abstracts.

Walsh, J.P., Alexander, C., Gerber, T., Orpin, A. and Sumners, B., 2007. Demise of a submarine canyon? Evidence for highstand infilling on the Waipaoa River continental margin, New Zealand. Geophysical Research Letters, 34.

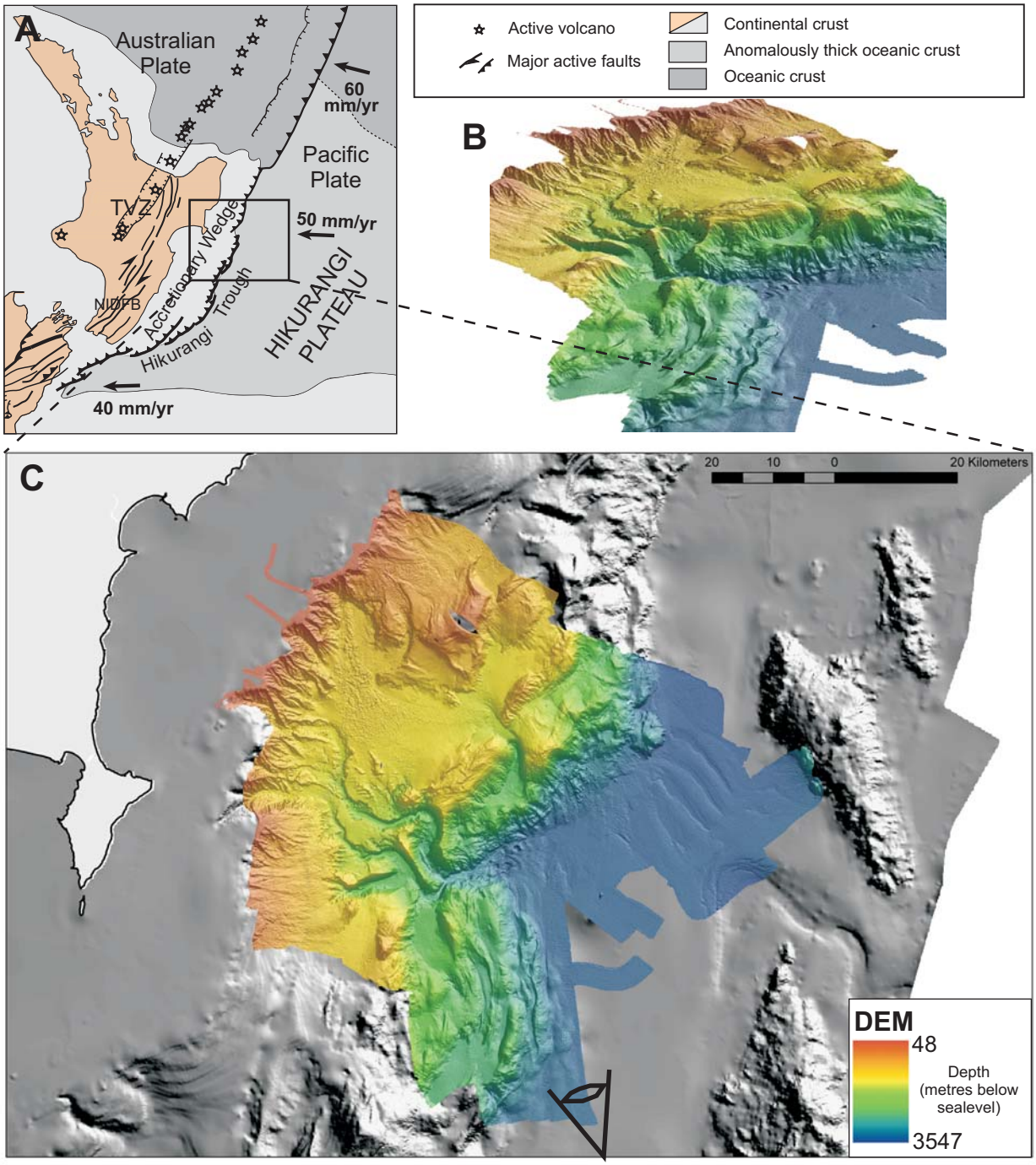

Figure 4.1 A: Location of the Poverty Bay Indentation on the Hikurangi margin, offshore North Island, New Zealand. Relative plate convergence vectors are marked with arrows. TVZ = Taupo Volcanic Zone. NIDFB = North Island Deformation Belt.

B: Oblique view of the Poverty Bay Indentation digital elevation model (DEM), vertical exaggeration (VE) = x5. View is from the southeast (eye symbol on C).

C: DEM (plan view) of the Poverty Bay Indentation. VE = x5.

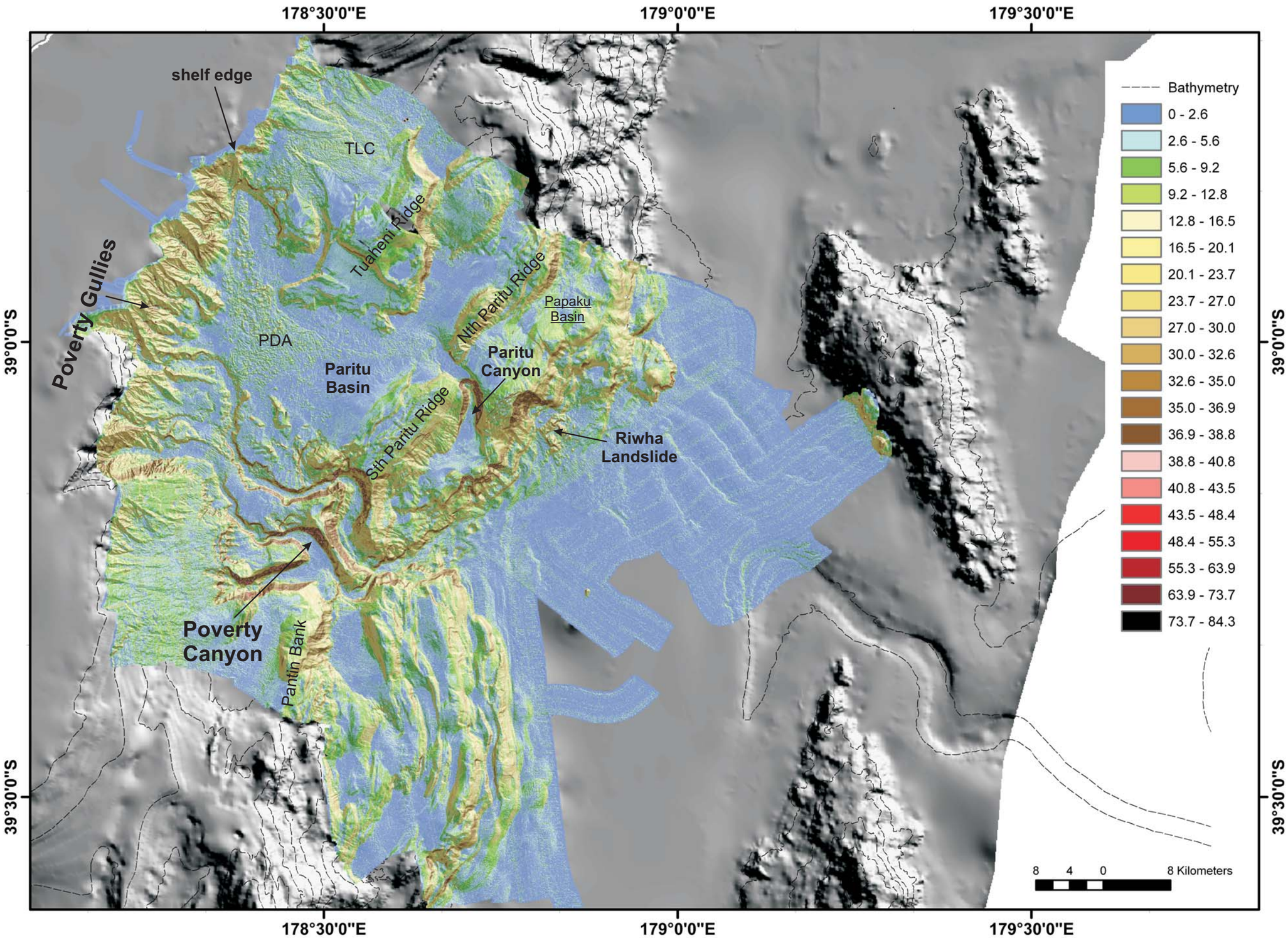

Figure 4.2 Shaded relief slope map (in degrees, referenced by colour coding scale) of the Poverty Indentation. Main morphological features discussed in this text are labelled. The two main regions of significant landsliding are the Poverty Debris Avalanche (PDA) and the Tuaheni Landslide Complex (TLC). Bathymetric contours outside the area covered by the slope map are at 250 m intervals.

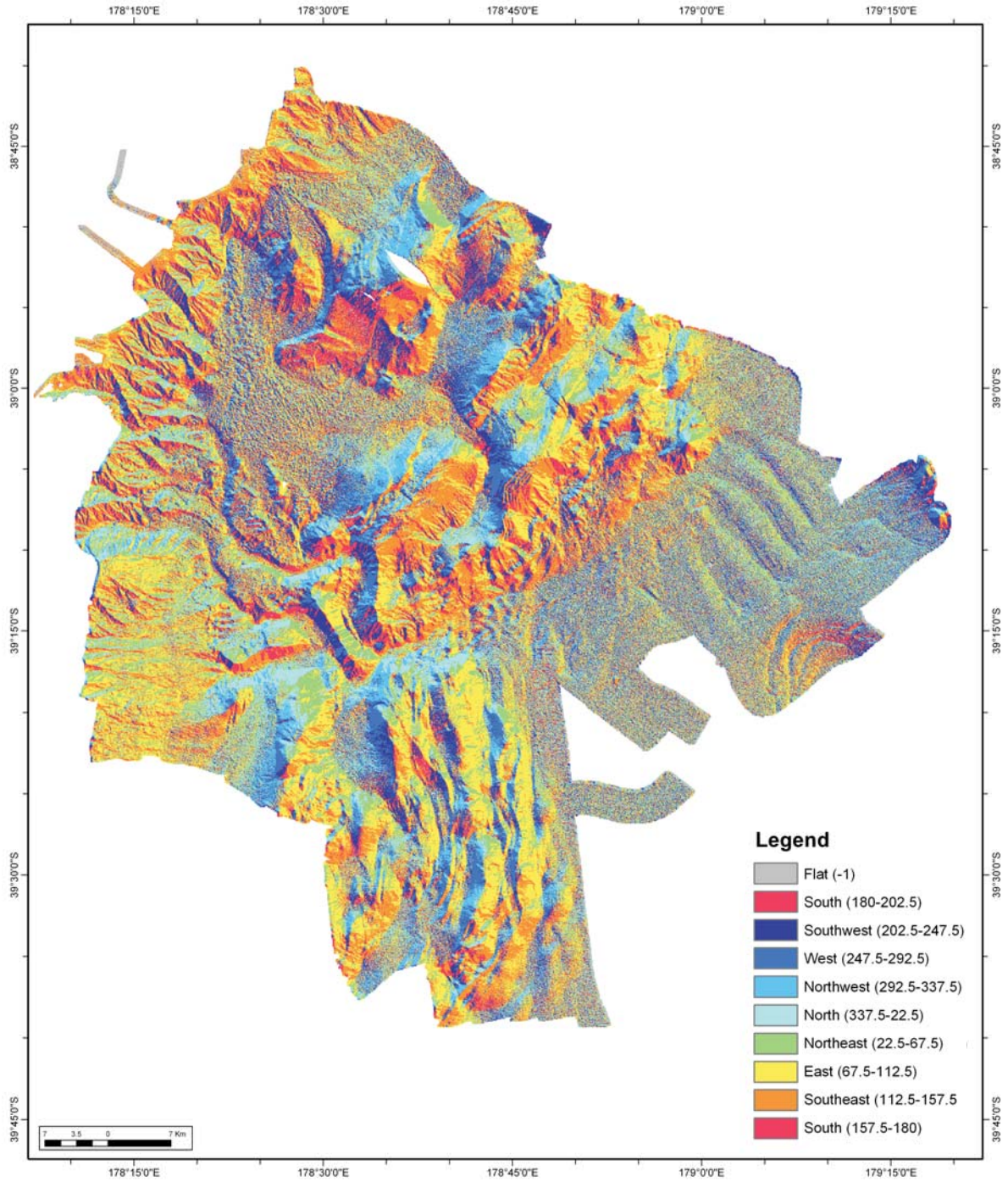

Figure 4.3 Slope aspect map of the Poverty Indentation. Aspect (direction of slope faces) in brackets are in degrees azimuth.

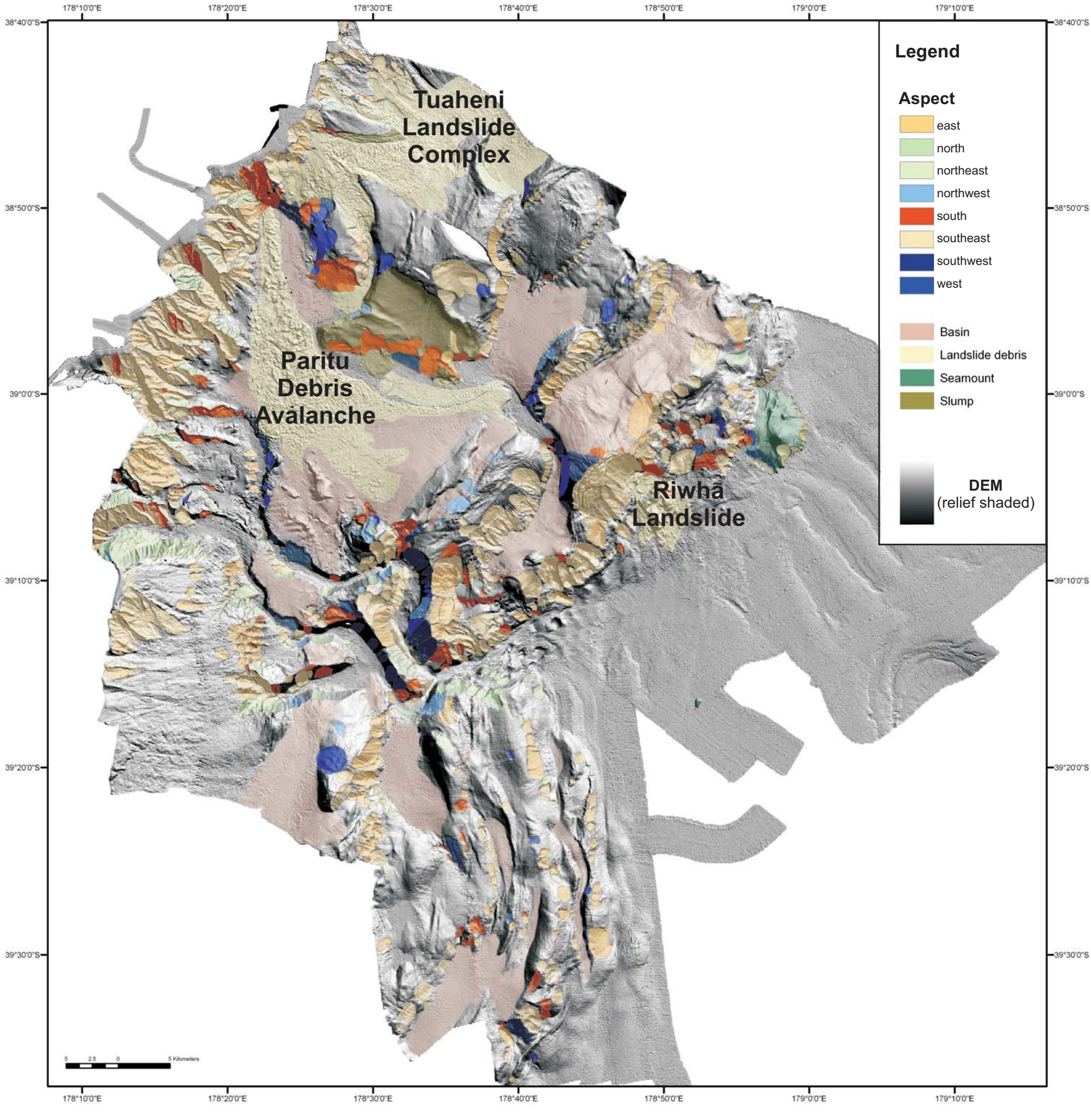

Figure 4.4 Map of landslide/erosional scars in the Poverty Indentation showing aspect orientation. Also shown are landslide deposits, basins, seamounts and mass movement slumps. DEM is illuminated at 45° from 045°, VE = x5.

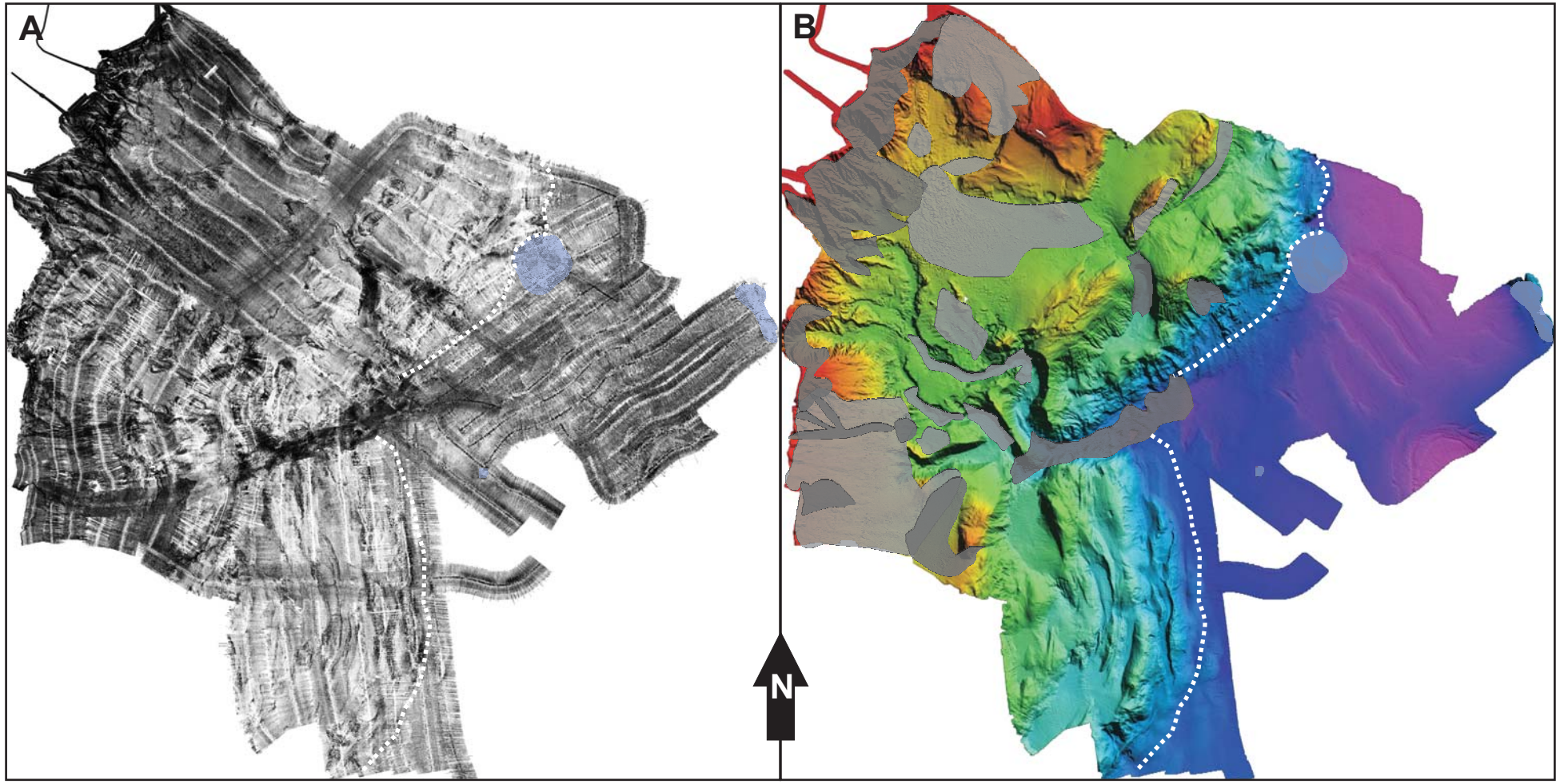

Figure 4.5 A: Backscatter image of the Poverty Indentation. High backscatter (black) most likely corresponds to areas of gravel or debris flow deposits. Low backscatter (white) most likely corresponds to fine muds and clays (e.g. Lewis and Barnes, 1999). Seamounts are highlighted in light blue, with the approximate position of the deformation front indicated by the dotted white line.

B: Regions of high (dark grey) and moderate (light grey) backscatter in the indentation. Seamounts are highlighted in light blue, with the approximate position of the deformation front indicated by the dotted white line. Background DEM is illuminated from 045° at 45° with VE = 5.

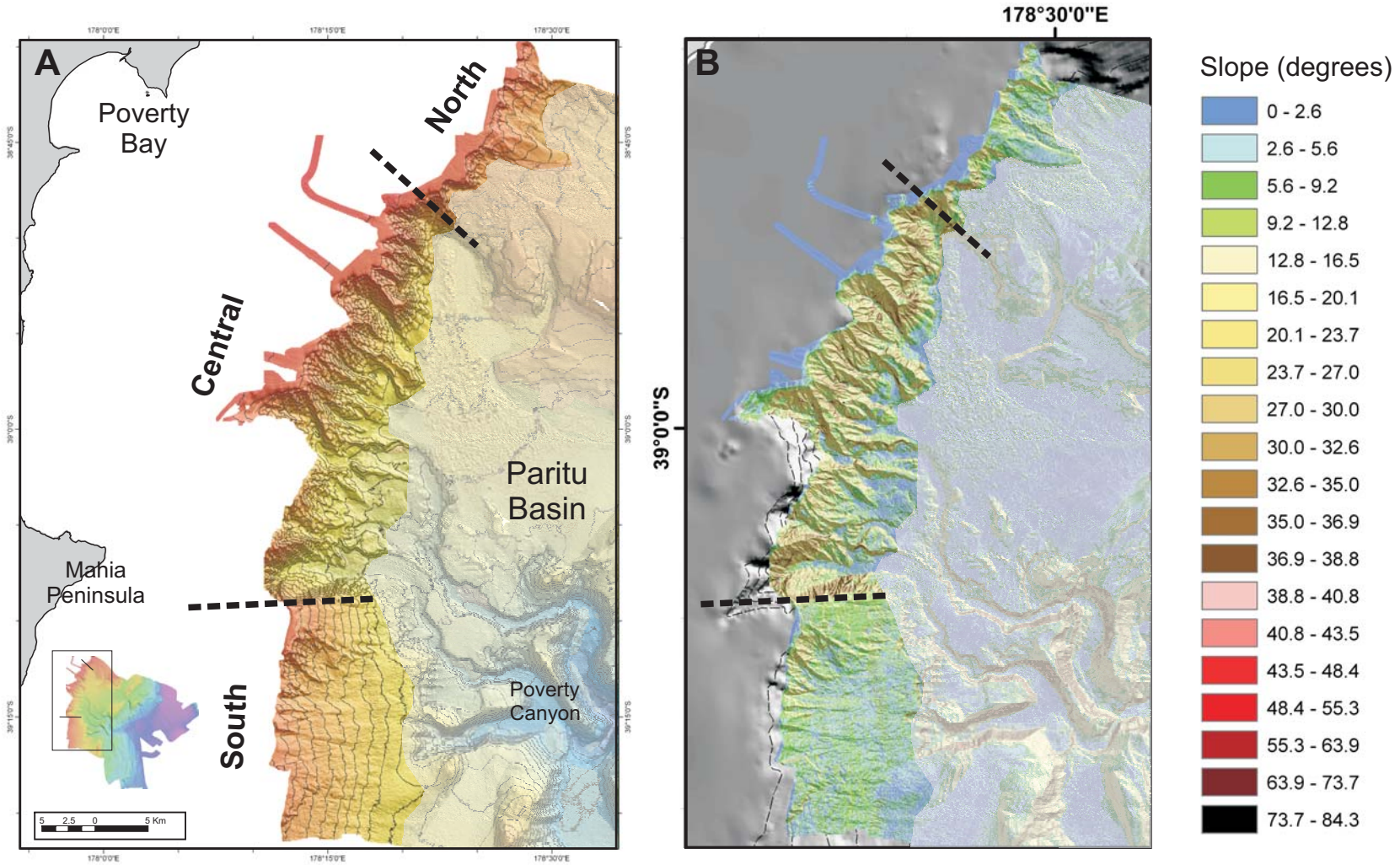

Figure 4.6 The Poverty Gullies, divided into southern, central and northern zones. Approximate transitions between each zone indicated by the dashed lines.

A: Location of the gullies at the shelf edge/upper slope transition into the Poverty Indentation. DEM is illuminated from 045° at 45°. VE = 5.

B: Slope model (in degrees) of the Poverty Gullies.

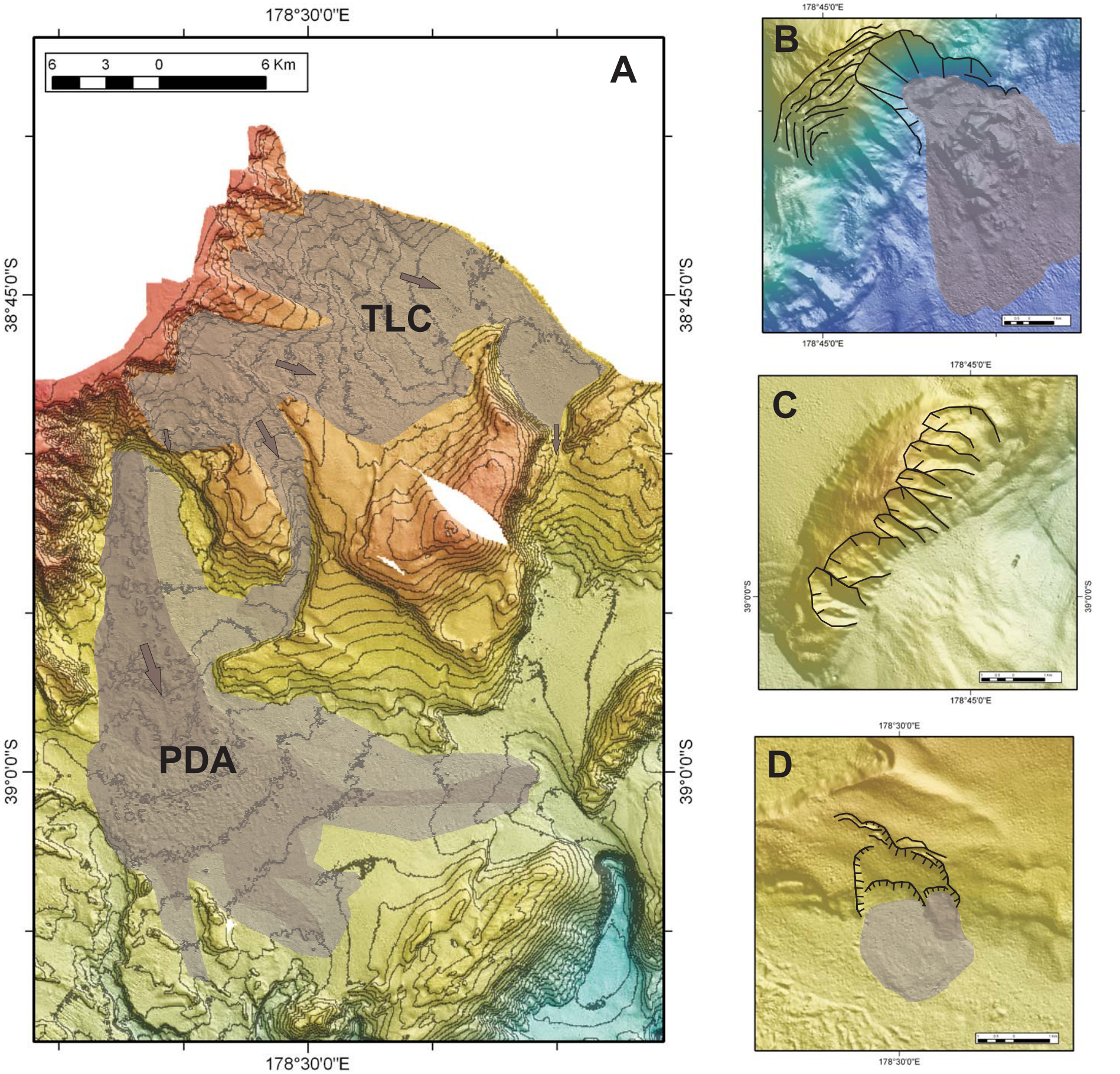

Figure 4.7 Mass movement and erosion features in the Poverty Indentation. DEM is illuminated from 045° at 45° and has a vertical exaggeration (VE) = x5. See insert right for locations within the Poverty Indentation. 3D oblique DEM view is from the south (eye symbol on location map), VE = x5.

A: Extent of the Poverty Debris Avalanche (PDA) and the Tuaheni Landslide Complex (TLC) in the upper and mid-slope basins.

B: The Riwhā Scar on the northern deformation front.

C: Landslide scars and erosional gullying into the southeastern flank of the North Paritu Ridge.

D: Slump on the northern edge of the Paritu Basin.

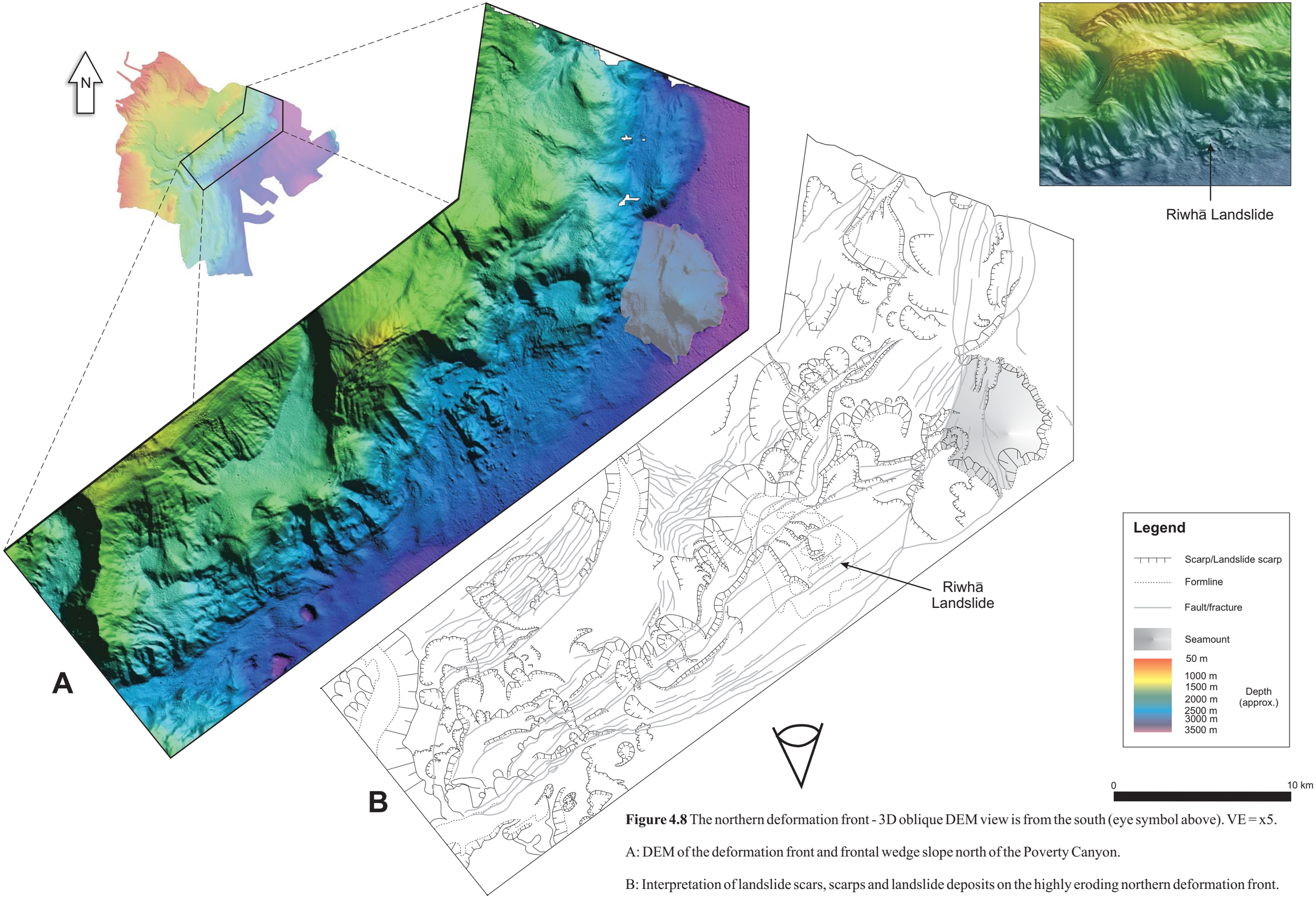

Figure 4.8 The northern deformation front - 3D oblique DEM view is from the south (eye symbol above). VE = x5.

A: DEM of the deformation front and frontal wedge slope north of the Poverty Canyon.

B: Interpretation of landslide scars, scarps and landslide deposits on the highly eroding northern deformation front.

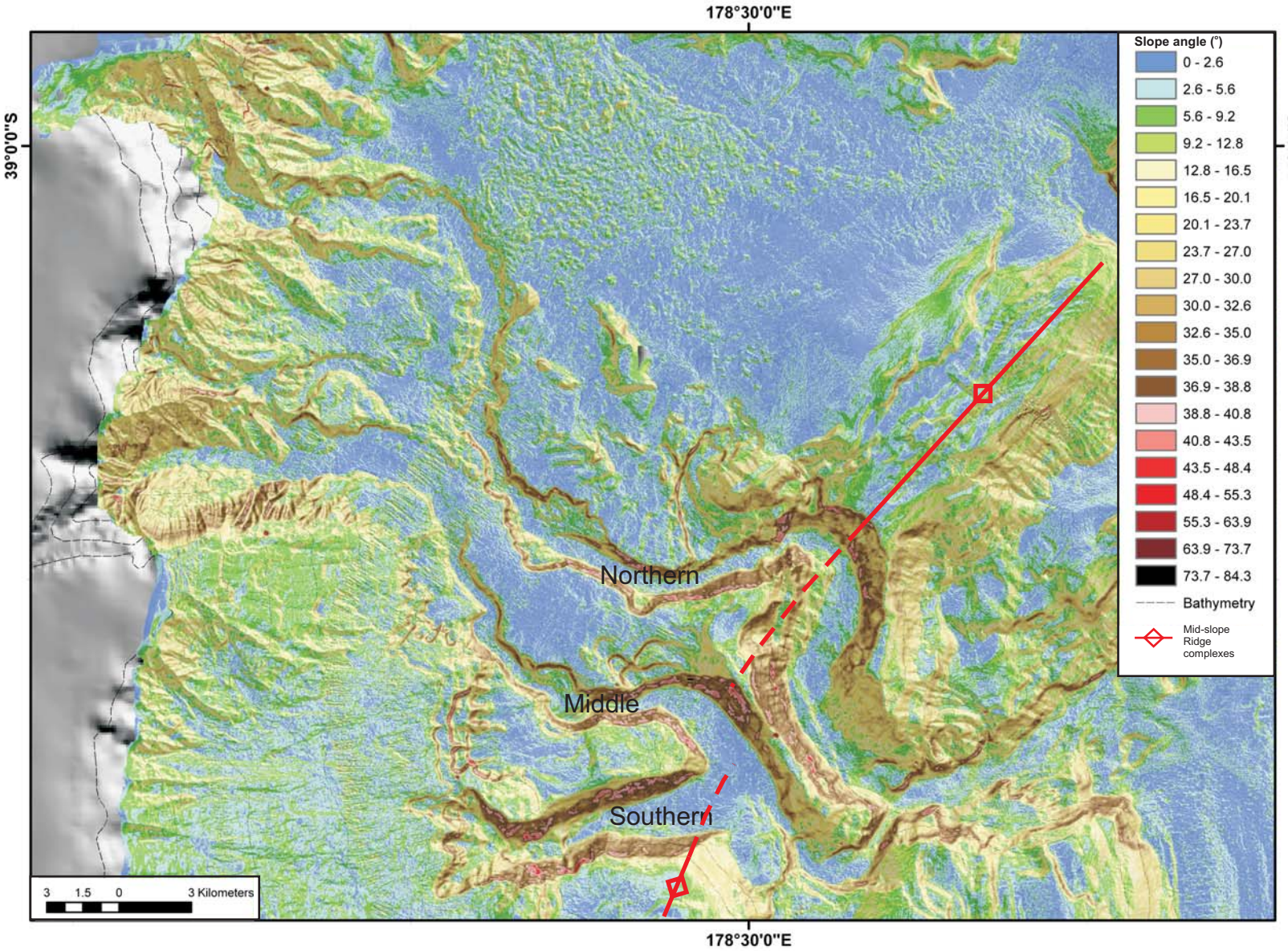

Figure 4.9 Slope map (in degrees) of the Poverty Canyon showing the region of maximum slope angles (therefore incision) of the canyon through the mid-slope ridge complexes (indicated in red). The three branches of the Poverty Canyon are northern, middle and southern as indicated. Bathymetric contours outside of the slope map are at 100 m.

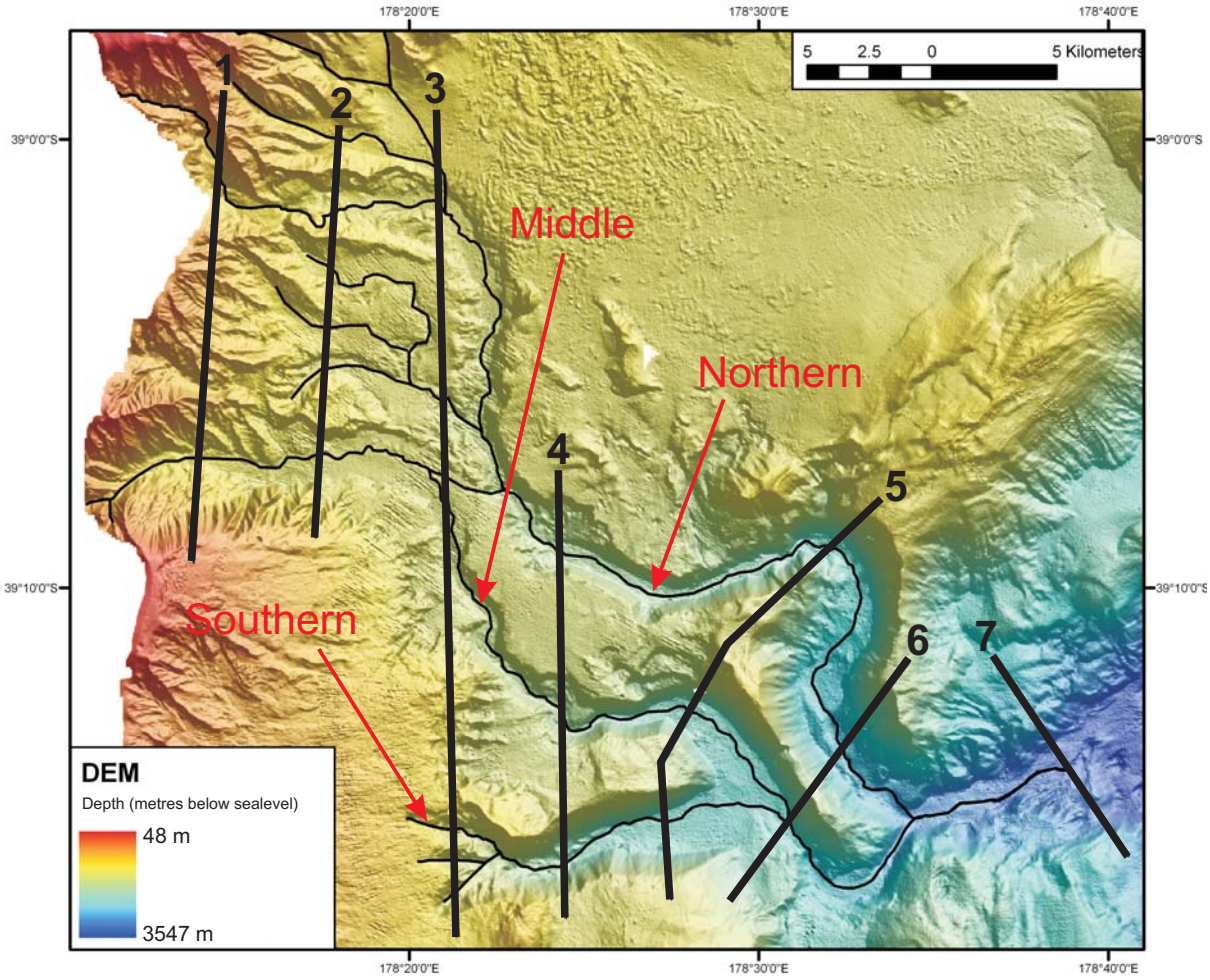

	Northern branch		Middle branch		Southern branch	
	Straight	Channel	Straight	Channel	Straight	Channel
1	4964.416	6017.874	4470.057	5187.303	-	-
2	4743.105	6783.705	4794.335	5189.723	-	-
3	4215.297	4534.794	5110.612	6661.551	1898.8	1972.573
4	14674.781	17190.913	10823.404	12179.093	4425.225	5191.21
5	10753.106	12057.221	5148.807	5952.188	4130.68	4683.691
6	8002.117	9915.789	5542.34	6443.708	4858.148	5439.328
7	9066.717	11219.797	11480.469	14733.421	11480.469	14733.421

	Straight	Channel	Sinuosity
Northern branch	46760.831	67720.1	1.45
Middle branch	40577.63	55723.2	1.37
Southern branch	26296.582	32020.2	1.22

Table 4.1 Sinuosity calculations for the Poverty Indentation. Lengths are in metres and are calculated from the preceeding transect to the listed one i.e. Length of 1 is the length from the origin at the head of the canyon to Transect 1 along the black line drawn in the canyon channel.

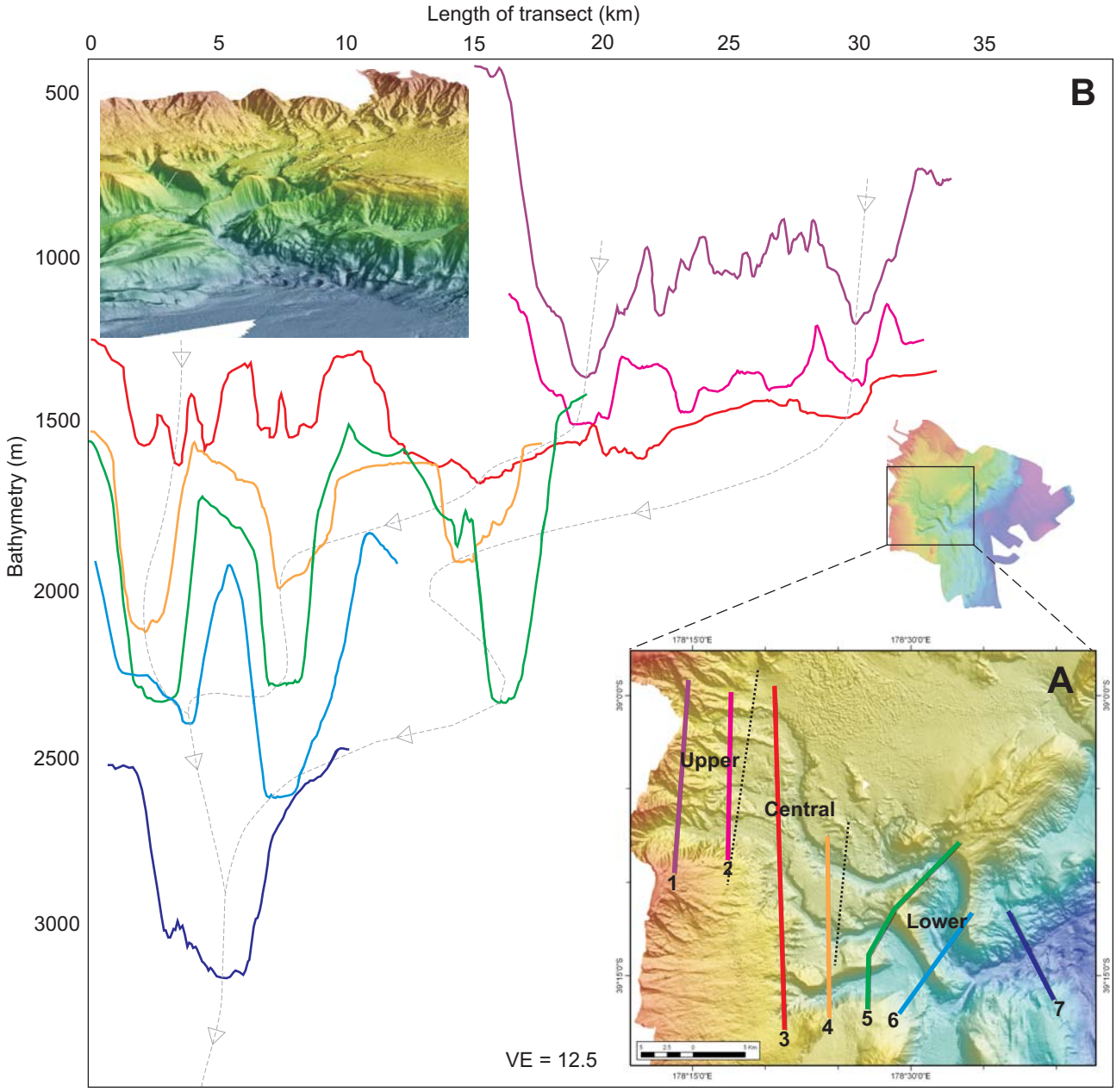

Figure 4.10 Poverty Canyon transects.

A: Location of cross section transects across the Poverty Canyon and divided into Upper, Central and Lower canyon. Numbers correspond to each profile detailed in Table 4.2. Transect locations are approximately orthogonal to canyon branch walls and spaced to be representative of the Upper, Central and Lower regions.

B: Bathymetry versus length of the transects and relative locations down the canyon. Dotted grey line represents the approximate location of each canyon channel axis. Accompanying image is a 3D oblique view digital elevation model (DEM) of the Poverty Canyon within the axis of the Poverty Indentation as viewed from the east, VE = x5.

A

	1	2	3	4	5	6	7	Total
Distance down canyon (km)	6.02	12.80	17.34	34.53	46.58	56.50	67.72	67.72
Channel incision (m)	780	250	200	400	940	810	620	
Channel width (m)	468	1108	1246	678	1060	1110	2145	
Sinuosity index (SI)	1.21	1.43	1.08	1.17	1.12	1.24	1.24	1.45
Wall angle (°)	35	32	32	40	45	32	35	
Description	Poverty Gullies	Base of gullies	Paritu Basin	Toe of basin	Sth Paritu Ridge	Leading edge of anticline	Deformation front	

B

	1	2	3	4	5	6	7	Total
Distance down canyon (km)	5.19	10.38	17.04	29.22	35.17	41.61	56.35	56.35
Channel incision (m)	950	400	430	480	900	600	620	
Channel width (m)	702	1380	2003	529	1375	482	2145	
Sinuosity index (SI)	1.16	1.08	1.30	1.13	1.16	1.16	1.28	1.39
Wall angle (°)	32	32	30	38	45	35	35	
Description	Poverty Gullies	Base of gullies	Toe of clinoforms	Toe of basin	Sth Paritu Ridge	Leading edge of anticline	Deformation front	

C

	1	2	3	4	5	6	7	Total
Distance down canyon (km)	-	-	1.97	7.16	11.85	17.29	32.02	32.02
Channel incision (m)	-	-	380	620	940	600	620	
Channel width (m)	-	-	365	1076	1772	482	2145	
Sinuosity index (SI)	-	-	1.04	1.17	1.13	1.12	1.28	1.22
Wall angle (°)	-	-	35	45	45	35	35	
Description			Clinoform sequence	Toe of clinoforms	Pantin Bank	Leading edge of anticline	Deformation front	

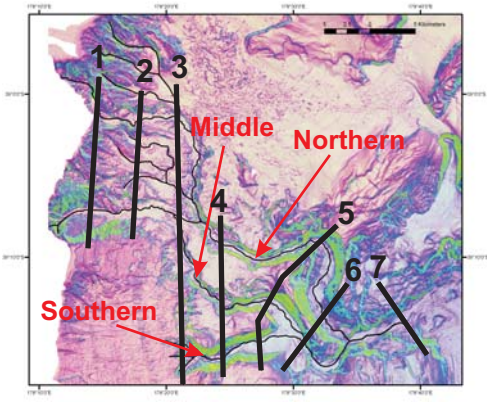

Table 4.2 Dimensional properties of the branches of the Poverty Canyon according to seven cross-sectional transects numbered 1 - 7. See insert for location (background slope map highlights the steepest slope region within the canyon in green). A: The northern branch. B: The middle branch. C: The southern branch. All measurements measured along the transect lines.

Sinuosity index (SI), where SI = length of channel axis/length of meander belt axis.

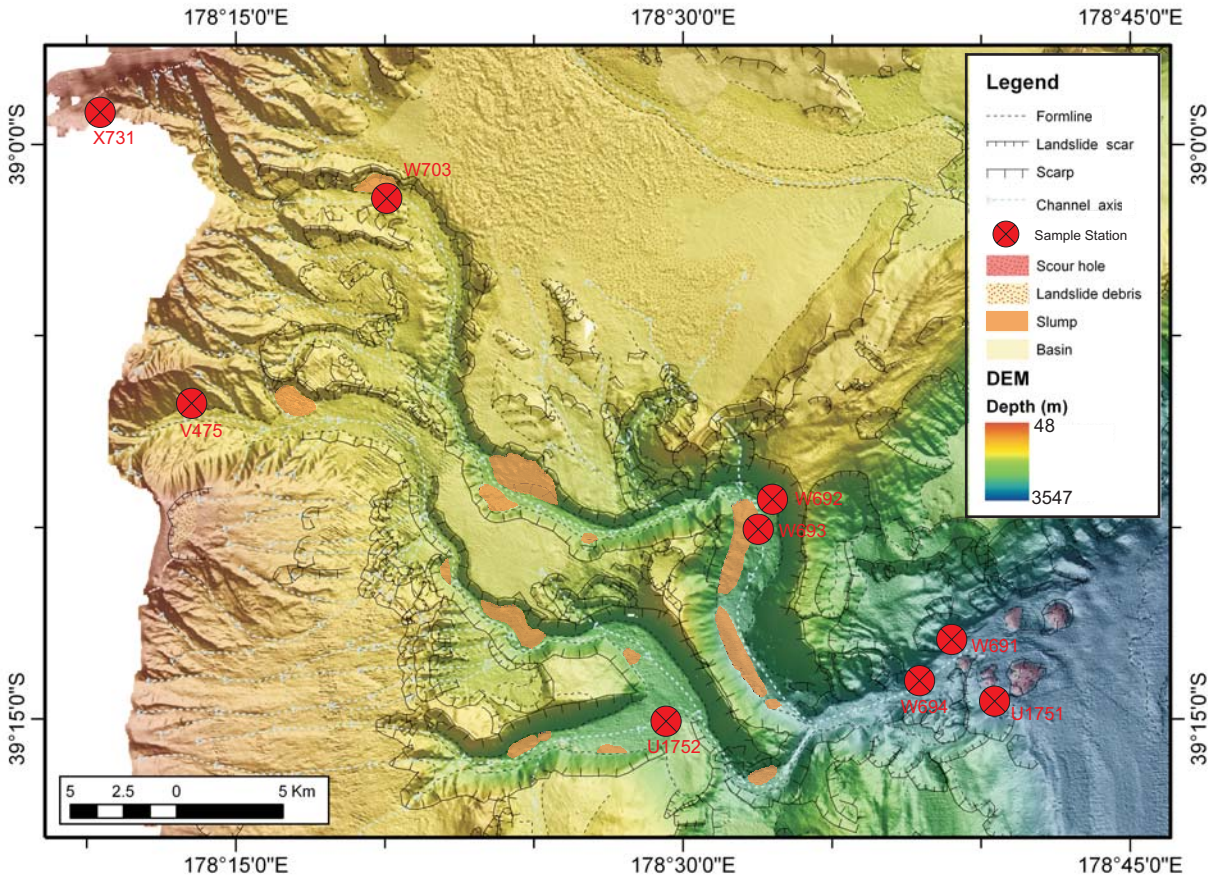

Location	Type	Approximate Age (Ma)
Head of Poverty Canyon, middle branch	V475 - dredge X731 - dredge	19-16 Not determined
Base of Poverty Gullies, northern branch	W703 - piston core	16-14
Middle Poverty Canyon, intersection of southern and middle branch, northern branch	U1752 - piston core W692 - dredge/rock W693 - piston core	<0.005 1.4, 1.6-0.3 0.15
Lower Poverty Canyon, canyon mouth	U1751 - pilot core W691 - dredge/rock W694 - pilot core	<0.5 1.8-0.2 1.2

Table 4.3 Rock, dredge and core sample stations in the Poverty Canyon. Please refer to Table 2.1, Chapter 2 for more detailed information.

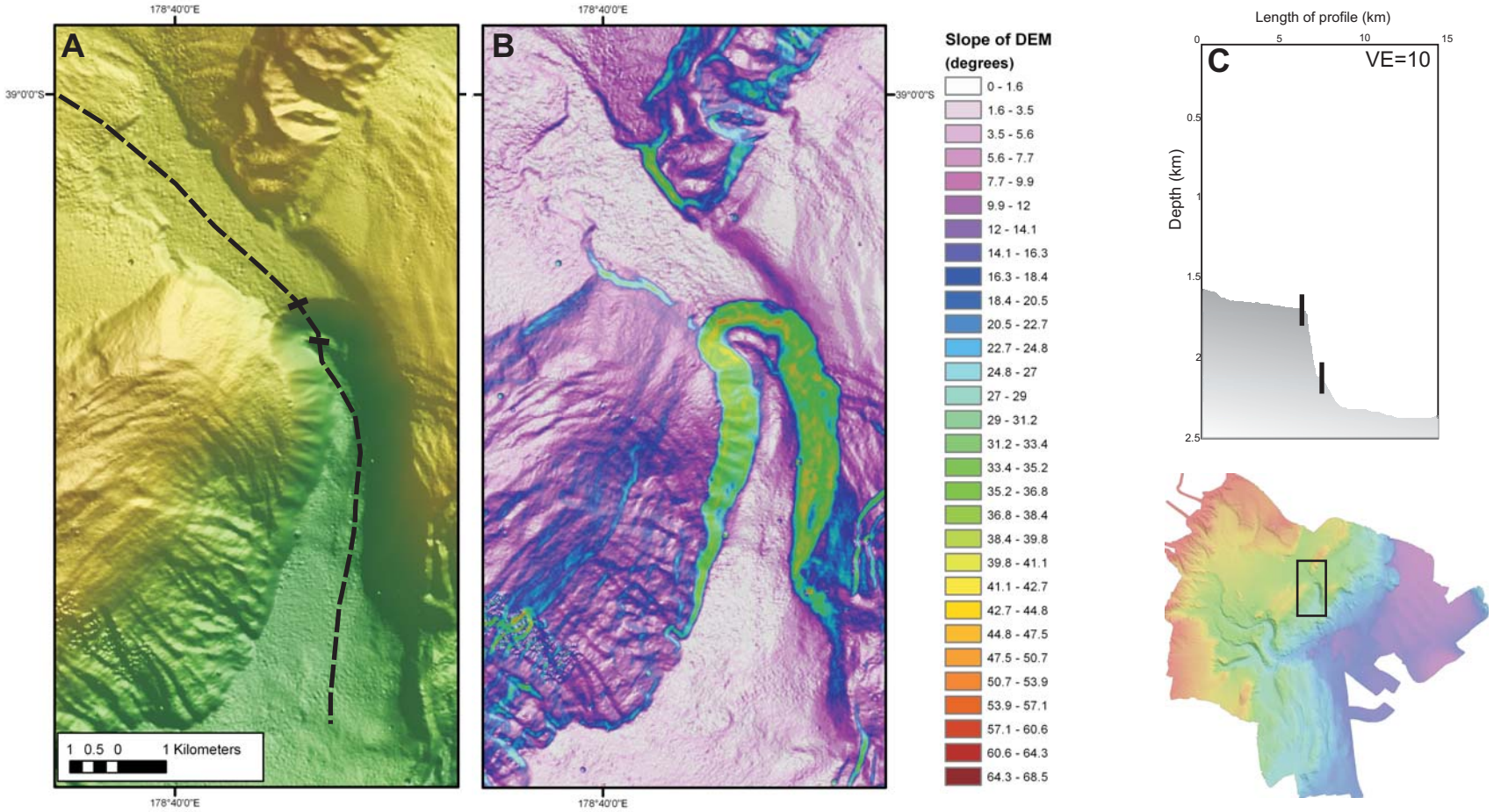

Figure 4.11 Morphology of the Paritu Canyon. Location of Paritu Canyon indicated by box on insert DEM of the Poverty Indentation (lower right).

A: DEM of the Paritu Canyon illuminated from 045° with VE = x5. Black dashed line represents location of gradient profile in C. Knickpoints indicated by black bars.

B: Slope map (degrees) of the Paritu Canyon.

C: Gradient profile of the Paritu Canyon. Knickpoints indicated by black bars. VE = x10.

CHAPTER 5: SEISMIC & STRUCTURAL GEOLOGY

5.1 INTRODUCTION

Combining high-quality seismic profiles with seafloor swath bathymetry enables a more detailed and accurate presentation of the links between subsurface structures and their morphological expressions. The following chapter is a presentation of some of the methods of interpretation used in this project as basis for developing the final overall structural geomorphic map of the Poverty Indentation and setting the groundwork for investigation and discussion into its formation and evolution.

The approach to interpreting the swath bathymetry and seismic data involved:

i) Manual annotation and interpretation of morphology, structures and sediment packages on high-quality paper print outs

ii) Application of various illumination angles and vertical exaggeration in ArcGIS 9.0 for the digital elevation model (DEM). Final presentation of all the DEM data is with relief illumination from bearing 045^{o} at a downwards angle of 45^{o}, and a vertical exaggeration of x5. These are standard presentation values consistent with other marine DEM images presented on the Hikurangi margin by other researchers, but is not the only combination of values investigated.

iii) Digital input of data using ArcGIS 9.0 and The Kingdom Suite software and manual comparison of the two data sets to facilitate accuracy and consistency of interpretations.

5.2 BLOCK DIAGRAMS

In the Poverty Indentation, a classical frontal accretionary wedge, about 27 km in width, is well developed south of Poverty Canyon, between Pantin Bank and the deformation front. This contrasts markedly to immediately north of Poverty Canyon where the lower margin is significantly over-steepened, and characterised by fewer imbricate thrust ridges than to the south, with complex structural overprinting including thrust reactivation and faulting orthogonal to the deformation front, large-scale gravitation collapse, debris avalanches, and

an absence of coherent accreted reflection stratigraphy. Further north again, where the Puke Seamount is currently impacting on the deformation front, the growth of anticlinal ridges and slope basins between the ridges, is more representative of evolving thrust-driven accretionary wedge style geometry, widening zone defining the deformation front from ~4.5 km to over 8 km.

Three 3D block diagrams were created across the deformation front of the Poverty Indentation to highlight the different structural styles of the frontal wedge, using seismic profiles and the corresponding seafloor swath bathymetry to the north of each profile trace. The seismic profiles used are: TAN0106-13, a section cutting through Puke Seamount and across the North Paritu Ridge; TAN0106-08, a section extending from just north of the Poverty Canyon, across the South Paritu Ridge and into the Paritu Basin; and TAN0106-09, a section south of the Poverty Canyon, extending across the accretionary wedge and Pantin Bank.

5.2.1 TAN0106-13

Seismic profile TAN0106-13 represents the most northern section of the Poverty Indentation deformation front and frontal wedge. As it intersects the Puke Seamount, it also provides the opportunity to investigate the subsurface structural response of the margin front to initial seamount impact and the first stages of subduction. Deformation on the northern frontal wedge directly inboard of the subducting Puke Seamount is overprinted on the sea floor with extensive zones of gravitational collapse and/or regions of normal faulting (Figure 5.1). Anticlinal ridges are asymmetric, with the steeper southeast-facing forelimb slopes dominated by the numerous landslides scars. The structural backlimbs are characterised by gentler gradients with landslide scars rare on these slopes. The mid-slope North Paritu Ridge is separated from the deformation front and lower slope by the Pāpaku Basin (Figure 5.1). This is a wide (5 - 8 km), moderately sloping depression east of North Paritu Ridge. The depression is situated in a complex structural setting, with growing thrust-propagated anticlines developing underneath, gravitational collapse at the outboard and southern edges, and faulting orthogonal to the margin front developing in the zone directly inboard of the Puke Seamount. Sediment is restricted mostly to veneers on anticline cored slopes without the development of significant syn-kinematic basin fill.

North of the subducting Puke Seamount, the growth of anticlinal ridges and slope basins between the ridges, is more representative of evolving thrust-driven accretionary wedge style

geometry. Backthrusts are commonly observed throughout the lower slope and deformation front. In the north sector of the frontal slope, these backthrusts increase in frequency as the deformation front widens and the lower sector of the accretionary wedge becomes structurally more evolved.

5.2.2 TAN0106-08

Further south and across the lower slope directly north of the Poverty Canyon, seismic line TAN0106-08 provides an important insight into the complex structures of the South Paritu Ridge and a collapsing frontal wedge (Figure 5.2). The lower slope above the deformation front is steep and eroded, with few well-developed thrust propagated anticlines. The frontal wedge contains numerous thrust splays propagating up from the subduction décollement. These thrusts break out on the trenchward-facing slopes of the structural ridges, accompanied by a multitude of hanging-wall and footwall imbricate splays, leading to a stepped deformation front. Whilst the major structures are imaged in the seismic sections, many linear slope inflections, interpreted as imbricate thrust traces and also as incipient collapse in the outboard limb of the South Paritu Ridge anticline, are visible in the high-resolution EM300 bathymetry (Figure 5.2, also refer to Figure 5.4). In the core of the South Paritu Ridge there is significant complexity in the deforming frontal wedge (Figure 5.2). This may be attributed to a number of factors including seamount subduction and loading by both basin-fill and anticlinal growth, resulting in reactivation and cross-cutting of pre-existing structures.

The mid-slope South Paritu Ridge is separated from the deformation front and lower slope by the 10 km-long Lower Paritu Basin. Sediment transport through the Paritu Canyon from the main, upper/mid-slope Paritu Basin has resulted in a thick (~500 m) triangular sediment wedge (Figure 5.2).

5.2.3 TAN0106-09

South of the Poverty Canyon, plate convergence has produced a well developed accretionary wedge of off-scraped trench sediments characterised by a series of east-facing thrust-propagated asymmetric anticlinal ridges. The accretionary wedge is dominated by a series of major thrusts propagating directly from the subduction décollement with backthrusts common in the folded hanging-wall sequences (Figure 5.3) (see also Barnes et al., 2009; their Figure 11). The wedge consists of three main frontal anticlines resulting from these thrusts, Te Kapu Bank, Whāiti Ridge and Pakupaku Ridge, and a series of smaller ridges (Figure 5.3).

Bathymetric elevation is much gentler over this accretionary wedge than along the toe of the slope north of the canyon. Numerous submarine slide scars are observed in the bathymetry, but these have less relief compared to scars on the north side of the Poverty Canyon. Imbricate splays are common in the near-surface and are reflected in the detailed seabed morphology. Evolving proto-thrusts and associated incipient thrust propagated anticlines are developing in the trench-fill sequence immediately outboard of the principal deformation front and progressively incorporating the trench fill sequence into the accretionary wedge (Figure 5.3). A subducted sequence of Hikurangi Plateau sediments is interpreted to underlie the frontal part of the thrust wedge, overlaying and occupying relief space created by normal faults in the subducting Pacific Plate (Figure 5.3).

Slope basins on the southern accretionary wedge are narrow and elongate and are well imaged in cross section. They commonly have thrusts propagating underneath them and into their sedimentary fill (Figure 5.3). There is a complex history of sediment fill in slope basins, with progressive tilting and incorporation of basin-fill into the inboard margins of the structural ridges as foot-wall thrusts develop and propagate. This is an evolutionary sequence very similar to that described by Lewis & Pettinga (1993). Some more evolved slope basins with thicker sedimentary successions are located higher up the slope and are highly deformed, with progressive structural incorporation into the accretionary wedge (Figure 5.3).

5.3 STRUCTURAL GEOMORPHIC MAP

Constructing an overall detailed structural geomorphological map of the Poverty Indentation has been an ongoing process as new interpretations, data and correlations come to light. Refer to Chapter 3, Figure 3.2 for feature nomenclature.

The Poverty Indentation covers an area over 4000 km^2 stretching across the entire continental slope (Figure 5.4). Active tectonic deformation is partitioned spatially across the indentation, with; (i) high activity in the mid-lower slope frontal wedge (this study), (ii) a largely inactive mid to upper slope, and (iii) some activity on major faults beneath the shelf (Barnes et al., 2002; Gerber et al., 2006; Mountjoy, 2009). Active faults in the Poverty Indentation commonly produce large thrust-cored anticlines. As highlighted by the block diagrams, lateral variations in structure across the active frontal wedge can be divided into three distinct regions - (i) narrow (~8 km wide) accretionary wedge north of Puke Seamount, (ii) erosional

and cross-cutting complex deformation with an absence of accretionary processes between Puke Seamount and Poverty Canyon, and (iii) well-developed (>30 km wide) accretionary wedge south of the Poverty Canyon.

The Poverty Indentation also contains some distinct structural features visible in seafloor morphology that are related to seamount subduction and in addition to the main structural regimes listed above:

i) Gravitational fractures in the headwall and a landslide seaward of a bulge indicating collapse in the wake of a recently subducted, small seamount along the northern deformation front at the Riwhā Landslide.
ii) Structures in the Poverty Canyon mouth almost at right angles to each other as a result of an initial indentation forming seamount impact.
iii) Complex cross-cutting of margin-parallel structures and degeneration of margin-normal structures inboard of the Puke Seamount.

Using the structural geomorphic map, the Poverty Indentation can also be simplified into five distinct domains, based on structural styles and major morphological features (Figure 5.5). The comparison of these sections highlights the different effects of seamount subduction on the evolution of the margin and the indentation and assists in organisation of interpretations and discussions. The domains are as follows (Figure 5.5):

1) The incoming Pacific Plate - includes sub-domains: The Hikurangi Trough and Plateau, Seamounts, Poverty Canyon mouth

2) North of the Canyon - includes sub-domains: Lower slope frontal wedge to deformation front, Lower slope basins and sediment fill, North and South Paritu Ridge Complex, Paritu Basin

*3) South of the Canyo*n - includes sub-domains: Lower slope accretionary wedge, Lower trench slope basins, Pantin Bank and Ritchie Trough, Prograding clinoform wedge

4) The Poverty Canyon and Upper Slope - includes sub-domains: Poverty Canyon, The Poverty debris avalanche and Tuaheni Landslide Complex, Poverty Gullies

5) Continental shelf

This domain approach has been used as a basis for organising classification of the morphology and structures presented and discussed in detail in Chapter 3.

References

Barnes, P.M., Nicol, A. and Harrison, T., 2002. Late Cenozoic evolution and earthquake potential of an active listric thrust complex above the Hikurangi subduction zone, New Zealand. GSA Bulletin, 114(11): 1379-1405.

Gerber, T., Pratson, L., Kuehl, S., Gerald, L., Walsh, J.P. and Alexander, C., 2006. Late Pleistocene and Holocene Seismic Stratigraphy of an active Forearc Basin, Waipaoa Continental Shelf, New Zealand. Eos Trans. AGU, 87(36): Ocean Sci. Meet. Suppl. Abstract.

Mountjoy, J.J., 2009. Submarine canyon evolution: Quantifying geomorphic processes on New Zealand's active continental margin. PhD Thesis, University of Canterbury.

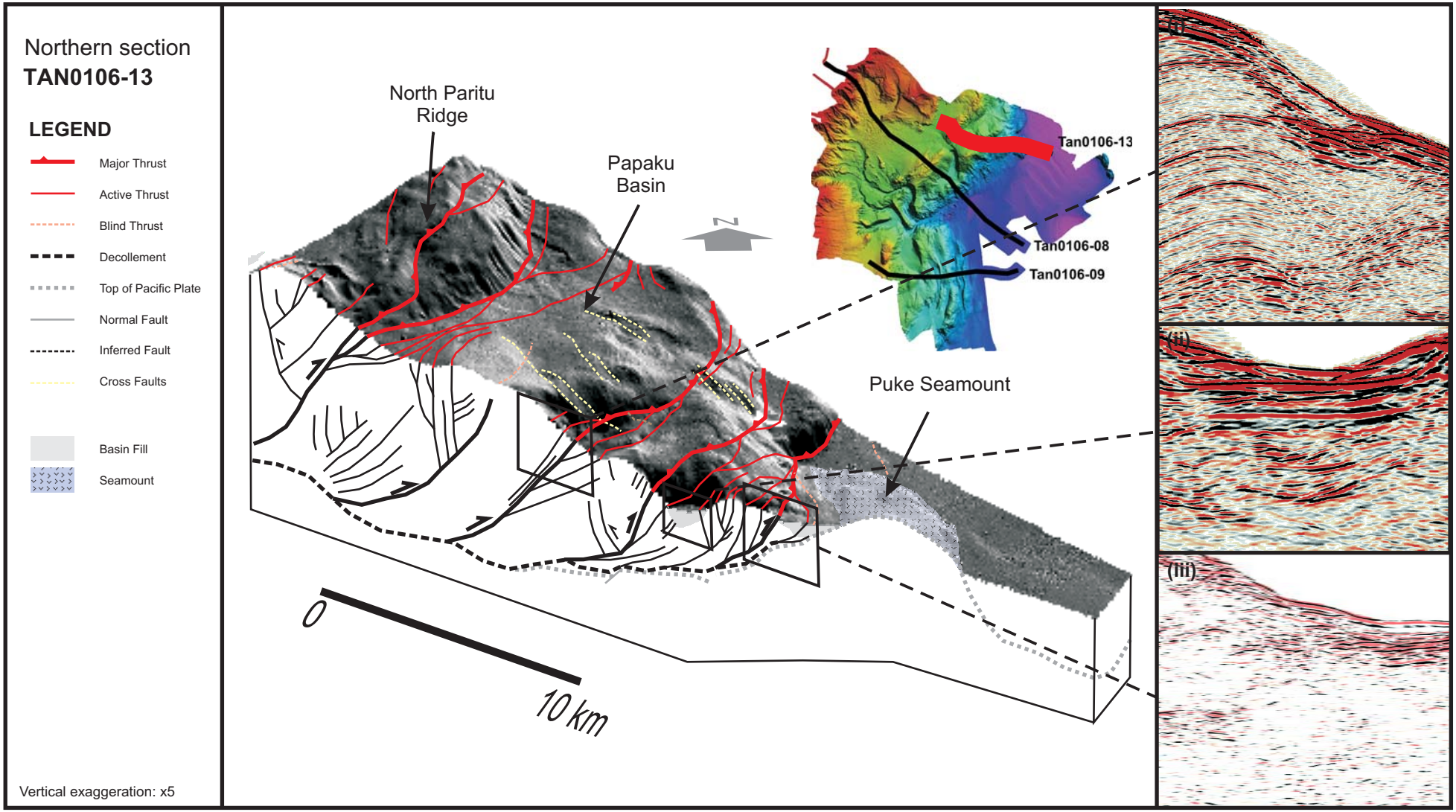

Figure 5.1 3D schematic block diagram of seismic profile TAN0106-13 combined with swath bathymetry DEM. DEM is illuminated from 045° at 45°, VE = x5. Uninterpreted seismic profile insets show detail of (i) wedge incorporated stratigraphy with propagating thrust faults on the outboard edge of Papaku Basin, (ii) mid-slope basin stratigraphy, and (iii) propagating thrust faults at the deformation front and inboard of the subducting Puke Seamount.

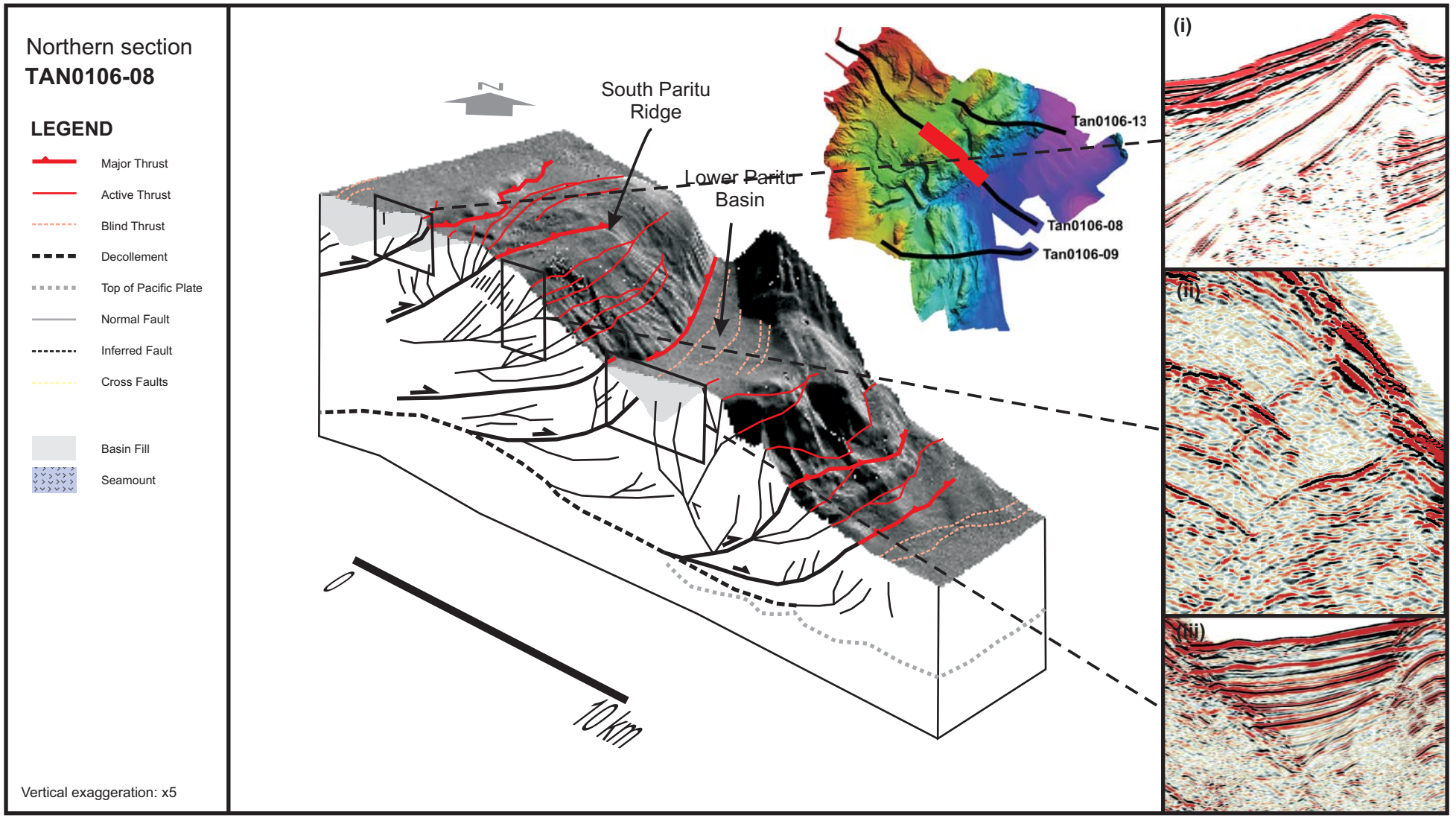

Figure 5.2 3D schematic block diagram of seismic profile TAN0106-08 combined with swath bathymetry DEM. DEM is illuminated from 045° at 45°, VE = x5. Uninterpreted sesimic profile inserts show detail of (i) a thrust-propagated anticline, (ii) propagation of thrusts through the outboard limb of the mid-slope South Paritu Ridge, and (iii) slope basin stratigraphy from the Lower Paritu Basin.

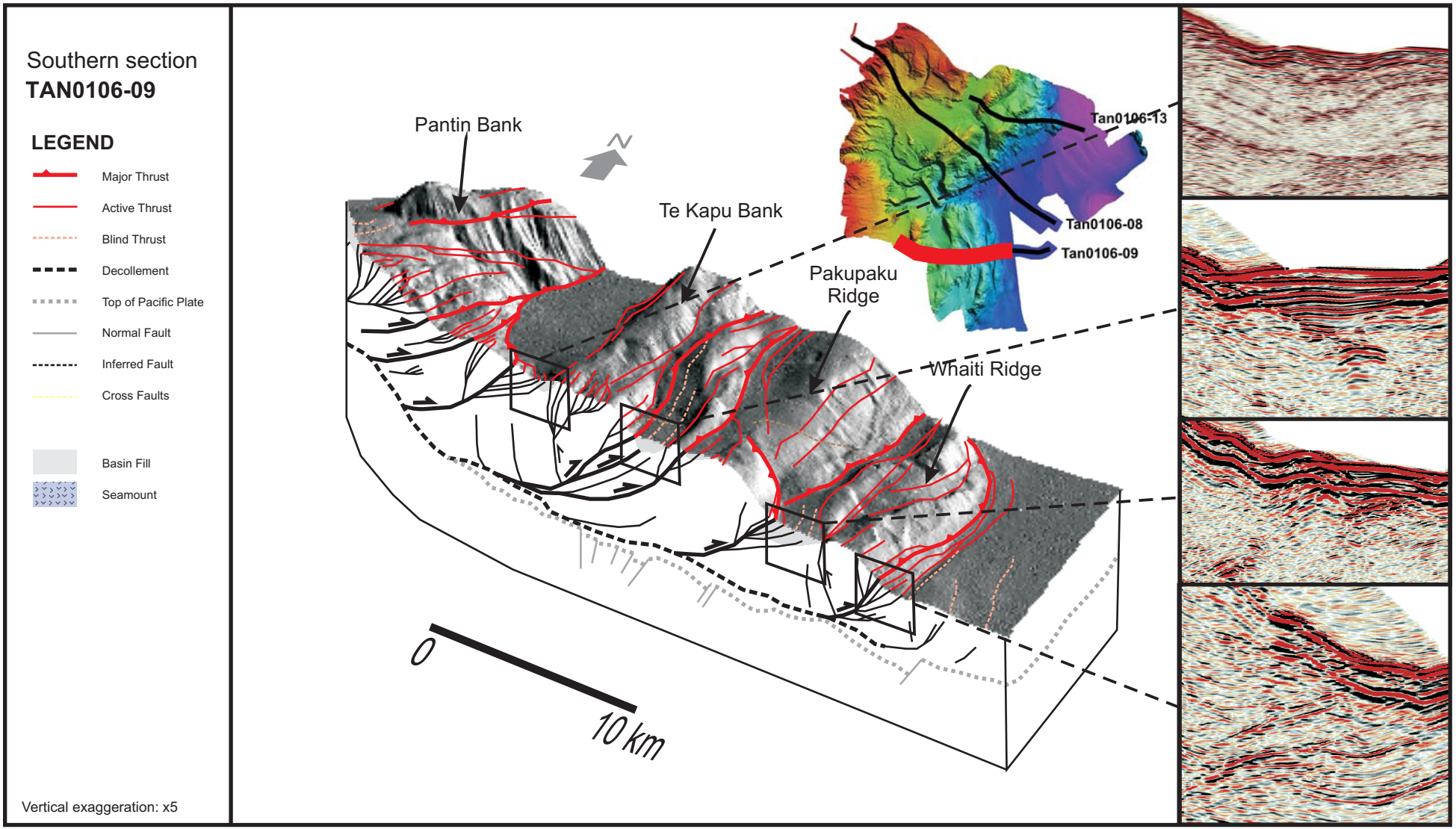

Figure 5.3 3D schematic block diagram of seismic profile TAN0106-09 combined with swath bathymetry DEM. DEM is illuminated from 045° at 45°, VE = x5. Uninterpreted seismic profile inserts show detail of (i), (ii) and (iii) various examples of wedge slope basin stratigraphy with thrust faults propagating into the sediment fill, and (iv) thrust propagation into the trench-fill sequence at the deformation front.

Figure 5.4 Structural geomorphology map of the Poverty Indentation, Northern Hikurangi Margin, New Zealand. Please see the folded map in the map pocket inserted at the back cover of this thesis.

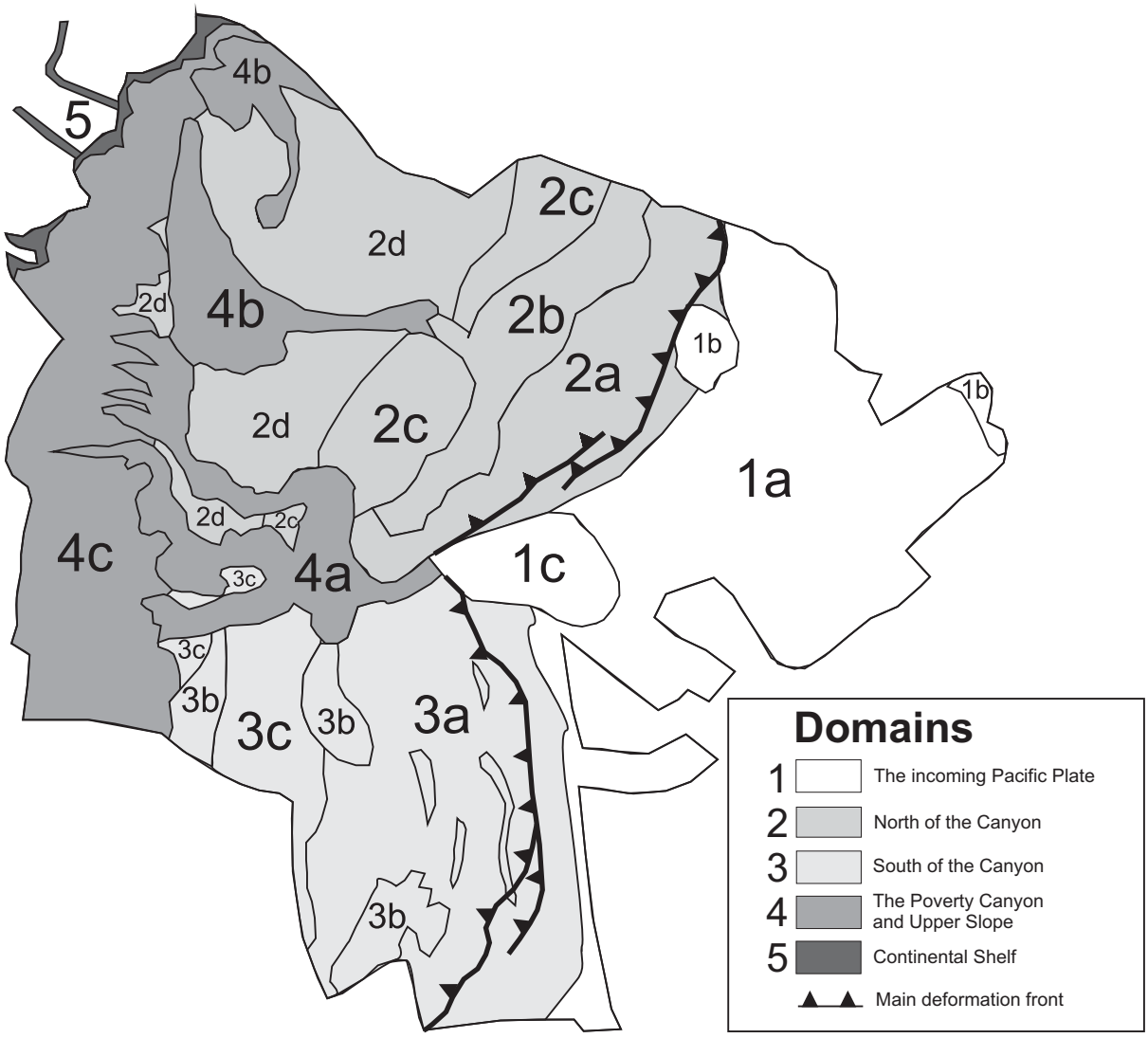

Figure 5.5 Domains and sub-domains within the Poverty Indentation.

1a = The Hikurangi Trough and Plateau
1b = Seamounts
1c = Poverty Canyon mouth

2a = Lower slope frontal wedge to deformation front
2b = Lower slope basins and sediment fill
2c = North and South Paritu Ridge Complex
2d = Paritu Basin

3a = Lower slope accretionary wedge
3b = Lower trench slope basins
3c = Pantin Bank and Ritchie Trough
3d = Prograding clinoform wedge

4a = Poverty Canyon
4b = The Poverty debris avalanche and Tuaheni Landslide Complex
4c = Poverty Gullies

CHAPTER 6: POVERTY TRANSECT PLATE MOTION BUDGET, POVERTY BAY INDENTATION

Abstract

Structural and stratigraphic analyses of the frontal part of the Hikurangi margin wedge, East Coast North Island, New Zealand, yield quantitative data on: (i) the timing of inception of thrust faults and folds; (ii) on the growth and mechanics of frontal accretion; and (iii) on the amounts and rates of horizontal shortening. The data also place constraints on the partitioning of geological strain across the entire northern Hikurangi Margin. Analysis is focussed on the southern part of the Poverty Indentation, offshore Gisborne, where there is a reasonably well formed accretionary wedge, compared to the rest of the northern section of the margin where high erosion rates and limited sediment supply make quantifying plate motions difficult. This region is located just north of the central and northern section boundaries at the very northern edge of the extensive accretionary wedge to the south, and is also influenced significantly by the subduction of large seamounts on the Pacific Plate Hikurangi Plateau.

Rates of shortening vary on the six different horizons identified in seismic reflection profiles across the lower margin. Shortening rates increase down-section from ~24% to ~46%. Using dates extrapolated from sedimentary sequences on the northern wall of the Hikurangi Channel to the south, rates have been determined at 4.3 mm/yr for horizon 3 (aged ~0.8 Ma), and 2.6 mm/yr for horizon 4 (aged ~2.03 Ma). These relatively low rates do not appear to reflect the high rate of deformation observed in the apparent frontal thrust activity in seismic reflection profiles, but the large age ranges between horizons allow for the possibility that deformation is very recent and rapid rather than spread out over time. Recovery from seamount impact and subduction may have a significant role to play also, and may inhibit establishing with greater accuracy the shortening rates across the frontal margin without more detailed age control being available for the upper sedimentary packages. Shortening rates on the upper margin horizons show activity as having decreased significantly post Miocene, ceasing altogether during the last ~ 0.4 Ma in the Pleistocene.

6.1 INTRODUCTION

In the offshore section of the Hikurangi margin deformation is partitioned in response to the oblique subduction system, with very little transcurrent motion on the plate interface (e.g. Webb and Anderson, 1998). Total plate motion accommodation, particularly accounting for the contractional or plate normal component, across the plate boundary is still not well constrained due to the added complexity of the extension in the Taupo Volcanic Zone and the lack of thrust fault daylighting on land, with >80% of the plate normal convergence across the plate boundary thought to be accrued on the subduction thrust (e.g. Nicol and Beavan, 2003; Wallace et al., 2004; Nicol et al., 2007).

This chapter attempts to further address the issue of quantifying the rate of shortening and plate normal motion across the plate boundary zone for the central to northern section of the margin by investigating offshore seismic data and stratigraphy in the Poverty Indentation, offshore Gisborne. It aims to add to the currently very limited knowledge of frontal wedge fault activity on the northern section of the Hikurangi margin, as outlined in Nicol et al. (2007). It is hypothesised that the lack of surface thrust faults and thrust activity on land is in response to a significant component of contraction currently being taken up in the frontal wedge offshore, inboard of the Hikurangi Trough.

6.1.1 Oblique subduction partitioning

In some oblique subduction systems the relative plate motion is partitioned between trench-parallel and trench-normal (orthogonal) deformation of the overriding plate, and slip on the subduction interface (Walcott, 1978; Barnes et al., 1998; Webb and Anderson, 1998; Mazzotti et al., 1999; Chemenda et al., 2000; Gutscher, 2001; Martinez et al., 2002; Upton et al., 2003). Additionally, these types of margins usually exhibit a wide zone of deformation characterised by block rotations and complex interactions between contractional, extensional and strike-slip faulting (Fitch, 1972; Yu et al., 1993; Upton et al., 2003). This is particularly true of the Hikurangi subduction margin in New Zealand where slip vectors indicate full partitioning with very little transcurrent motion on the plate interface, which instead is being accommodated by faults in the overlying Australian Plate (e.g. Webb and Anderson, 1998). Block rotations are evident in the Hikurangi margin (Wallace et al., 2004), as is significant extension west of the Hikurangi margin, reflected in the presence of the Taupo Volcanic Zone (TVZ) and strike-slip in the North Island Dextral Fault Belt (NIDFB) (Beanland and Haines,

1998). It is observed that a weak subduction interface is required for both the extension and partitioning of velocity components to occur in a subduction zone of a similar geometry to the Hikurangi margin (Upton et al., 2003) and as convergence obliquity increases, the cumulative rate of strike-slip displacement within the forearc increases (Barnes et al., 1998).

Total plate motion accommodation (De Mets et al., 1990; De Mets et al., 1994; Beanland et al., 1998) across the Pacific and Australian plates in the northern North Island is still not well understood despite successful attempts to address the total plate motion budget in the southern part of the North Island with onshore (Nicol and Beavan, 2003) and offshore (Barnes and Mercier de Lepinay, 1997; Barnes et al., 1998) data. This difficulty is in part due to: (i) the extension occurring within TVZ adding an estimated extra 10 mm/yr to the relative plate motion across the plate boundary zone, evident and quantified in GPS velocity data (Wallace et al., 2008); and (ii) the lack of surface propagated thrust faults across the forearc onshore. While there is certainly uplift and folding onshore, the contractional deformation in the overriding plate does not appear to be as significant a component as it should be, given the incoming plate vector of <50 mm/yr. While many have suggested various models for the distribution of plate motion across the more northern part of the margin with the extensional regime using onshore geodetic and geological data (Wallace and Beavan, 2006), the thrust component of the plate motion still remains largely unaccounted for and inclusion of the offshore section of the margin would significantly aid constraint. There is a need for quantifying the plate motion for kinematic models and earthquake hazard, not just for global understanding of such systems and seismic hazard, but with particular focus here on subduction-related tsunami hazards for the east coast of the North Island (Fuakao, 1979; Satake and Tanioka, 1999; Polet and Kanamori, 2000; Downes and Stirling, 2001) and implications for possible underplating affecting the back arc and Taupo Volcanic Zone (Watkins et al., 1981; Maruyama and Liou, 1989; Webb and Anderson, 1998; Park et al., 2002). Other subduction margins where strains have been quantified include Cascadia (McCrory, 1996; Adam et al., 2004), Aleutians (Doser and Lomas, 2000) and Nankai (Mazzotti et al., 1999).

To identify the strain rates and spread of accommodation of the plate motion, research requires excellent imaging of offshore structures, stratigraphic control and integration of geology and contemporary geodetic data. Quantifying plate motions across the subduction

system is something few others have been able to achieve elsewhere until very recently (e.g. Adam et al., 2004), particularly not with the inclusion of offshore data.

6.1.2 Strain across the Hikurangi margin

The major issue for the northern section of the Hikurangi margin is that the observed folding and insignificant activity on thrust faults onshore in the forearc between the NIDFB and the offshore accretionary prism is not sufficient (Nicol and Beavan, 2003) to account for consistent distribution of the contraction component of the total plate motion. While the long-term regional pattern of uplift is ongoing, significant activity on many onshore structures appears to have ceased prior to ~120ka e.g. (Leith, 2003). We propose in this chapter that there has been a shift in the distribution of strain across the margin and much of the contraction component is currently being taken up in the thrust front offshore at the Hikurangi Trough.

The Hikurangi margin (Figure 6.1A) is a southward continuation of the Tonga-Kermadec subduction system. Outboard of the Hikurangi trench the subducting plate incorporates the Hikurangi Plateau, a section of anomalously thick Mesozoic age oceanic crust (10-15 km) comprised of an accumulation of seamount ridges, lava flows and Cretaceous sedimentary basins (Davy and Wood, 1994). To the west of the Hikurangi Trench, where the Pacific Plate is subducting beneath the Australian Plate, a very wide frontal accretionary wedge has developed in response to, and records, several phases of deformation and off-scraping of sediment (Lewis, 1980; Chanier and Ferrière, 1991; Lewis and Pettinga, 1993; Collot et al., 1996b; Barnes et al., 1998; Barnes et al., 2002).

The Hikurangi margin is unique from other accretionary wedge-forming subduction margins due to the combination of the increased thickness of the subducting oceanic plate (Smith et al., 1989; Davy and Wood, 1994; Wood and Davy, 1994), the varying oblique nature of convergence (Collot et al., 1996b) and the vast thickness of Quaternary trench fill sediments (>2-3 km) (Carter et al., 2002). Deformation in the overriding plate is dominantly controlled by the subduction of the oceanic plate and will reflect the rates of subduction, the angle at which the subducting plate is converging with the overriding plate, the amount of slip between plates, volume of sediments being underplated and presence or absence of seamounts (Nicol and Beavan, 2003). The central sector of the Hikurangi Margin is classified as a convergent compressive margin as the moderate subduction rate (50 mm/yr) and the high

sedimentation rate from both transport of South Island material from the Hikurangi Channel and material from the East Coast have formed a significant accretionary prism (Lewis and Pettinga, 1993). In contrast, the northern sector can be classified as a convergent extensional margin due to sediment starvation in the region and high rates of tectonic erosion, despite accretion (Pelletier et al., 1994; Collot et al., 1996b; Chanier et al., 1999).

Previous research has quantified the deformation across the southern Hikurangi margin with strain partitioned widely across the forearc (Barnes et al., 1998; Nicol and Beavan, 2003). In the northern section, there is little upper plate deformation recorded onshore from contemporary GPS data east of the North Island Dextral Fault Belt (NIDFB) (Wallace et al., 2004; Douglas et al., 2005). This may imply that much of the margin normal plate motions must be accommodated in the continental margin offshore, and/or fully on the subduction interface. In the most northern part of the northern sector, backarc extension contributes a relative motion of up to 60 mm/yr total between the wedge and the incoming Pacific Plate (Darby and Meertens, 1995; Chanier et al., 1999; Upton et al., 2003; Wallace et al., 2004).

6.2 POVERTY INDENTATION

The study area for this research encompasses a feature known as the Poverty Indentation (Figure 6.1B). This is a large canyon system and associated re-entrant in the Hikurangi Margin located just north of the boundary between the central sector and the northern sector. The transition between the characteristics of the two sectors is evident in the study area with the developed accretionary wedge and gentler slopes in the southern half contrasting with the steep slopes and numerous failures to the north of the canyon system. This is a reasonably well formed accretionary wedge and ideal for this study, compared to the rest of the northern section of the margin where, while there is still accretion developing, high erosion rates and limited sediment supply make quantifying plate motions difficult.

In the upper slope section of the margin prograding clinoforms in significant basin fill overlie a buried inactive thrust system with some more recent activity evident on shelf faults (i.e. Lachlan Fault (Barnes et al., 2002)). Recent activity is also observed at the transition into the lower margin, but with reduced or no evidence of recent deformation across the majority of the section. Inverted structures are common, particularly in the lower basin fill sequence buried beneath the shelf. In the lower slope section of the margin most anticlinal structures in

the southern domain of the indentation are bounded by a single thrust and backthrust. Propagation of thrusts into the footwall are at a shallow, superficial level (only just propagating into the top 0.5 sTWT of sediment) and do not appear to add significantly to the structure and extent of the anticlines in the southern region. Families of small normal faults are common, particularly on the trailing limb of anticlines and in the hanging wall of propagating thrusts. Landslide scars are often isolated and very shallow on the accretionary front but concentrated on east-facing leading limb slopes of anticlines, facing towards the trench.

6.3 DATA AND METHODS

New data are used in this chapter to attempt to constrain the plate motion rates for the offshore cross section of the margin. The data include two spliced sections in order to provide a composite seismic cross-section normal to the margin and south of the Poverty Canyon system. The upper margin is represented here by multi-channel seismic (MCS) data from the 2005 Ministry of Economic Development (MED) voyage CM05 (hi-fold, deep penetration industry) on the M/V Pacific Titan (Figure 6.1B). Recording parameters for the CM05 survey include a Bolt (1500 & 1900 Long Life) airgun array source with shot spacing of 37.5 m and receiver spacing of 12.5 m. Sample rate and record length are 2000 ms and 8000/12000 ms respectively. The lower margin is represented by a section from the National Institute of Water and Atmosphere (NIWA) voyage TAN0106 (low fold) in 2001 on the R/V Tangaroa (Figure 6.1B). The source for the TAN0106 survey is a 45/105 ci GI gun with a shot spacing of 25.0 m and receiver spacing of 12.5 m. Sample rate and record length are 1 ms and 8 s respectively. Both surveys are presented using The Kingdom Suite (TKS) seismic interpretation software.

The frontal slope section and the mid-slope major anticlinal ridge of the margin are represented by line TAN0106-09. The continental shelf and upper slope basins of the margin are represented by line CM05-23.

Stacking velocities (*Vrms*) were obtained for the transect from data obtained for the MED lines and used to depth convert the sections. While *Vrms* can be used directly to obtain interval velocities (*Vint*) for line CM05-23, *Vrms* from MED line CM05-01 (Figures 6.1B and

6.2) were used as a proxy for the front section of line TAN0106-09 due to it lacking velocity values (streamer was too short).

In the section processing, *Vrms* are used to calculate *Vint* by a derivative of the Dix equation (Dix, 1955):

$$V\,\mathrm{int}_n = \frac{\sqrt{\left(Vrms_n{}^2 \times T_n\right) - \left(Vrms_{n-1}{}^2 \times T_{n-1}\right)}}{\Delta T_n}$$

where *Vint* equals the interval velocity of the sediments, in metres per second, between the chosen reflecting horizon and the following one, *Vrms* equals the stacking velocity for the reflecting horizon in metres per second, and *T* equals time in milliseconds to that horizon.

In the MED seismic lines, time/stacking velocities were recorded at regular interval slices along the profiles. Vertically down these slices, both time and stacking velocity were recorded at consistent strong reflecting horizons. These were labelled Horizons 1 through 25, with Horizon 2 representing the sea floor. This data was then inserted into an Excel spread sheet to obtained *Vint* and thickness values between each horizon. Table 6.1 (below) shows an example of a line of data from one vertical slice through a profile. Through both seismic profiles a total of 16 time/velocity slices were used - 6 for TAN0106-09, and 9 for CM05-23.

Horizon	Time (ms)	Vrms m/s	Vint m/s	Thickness (m)
1	0	1497	1497	70
2	93	1497	1678.083456	149
3	270	1618	1911.655484	166
4	444	1739	2936.377721	874
5	1039	2496	3556.663721	333
6	1226	2685	3863.830312	402
7	1434	2886	3888.074068	1032
8	1965	3188	4058.586967	2762
9	3326	3570	4326.356205	1265
10	3911	3693	5152.143849	5028
11	5863	4235	5344.37318	2565

Table 6.1 Example of Excel spread sheet calculations for converting time into *Vint* interval velocities and thickness, using *Vrms* stacking velocities. For the first row, Horizon 1, *Vint* = SQRT(((D4^2*C4)-(D3^2*C3))/(C4-C3)) and Thickness = ROUND((((C4-C3)*E3)/2000),0), where C = Time; D = *Vrms*; and E = *Vint* columns respectively. Note that the décollement and subduction interface region observed in seismic profiles can be identified in this table as a jump in *Vint* between Horizons 9 and 10 (highlighted).

Depth conversion of the seismic sections was then achieved using both DepthCon2000 and Globe Claritas (e.g. Figure 6.3). Shortening values for strain across the seismic sections were

calculated using both line and area balance methods of a sequence of stratigraphic horizons undergoing linear strain:

$$e = (l - l_o)l_o$$

where a negative value of e is a shortening, l_o equals the original length, and l equals the new length (e.g. Park, 1997).

6.4 AGE CONSTRAINTS FOR THE MARGIN SEDIMENTARY SEQUENCE

Estimates of age correlations for MED line CM05-23 can be extrapolated through the Hawke Bay-1 well (BP Shell Aquitaine and Todd Petroleum Development Ltd, 1976) and previous research by (Barnes et al., 2002; Paquet, 2007) outlined in Chapter 2, despite crossing several active shelf fault structures. Estimated age correlations for the trench fill sequence at the base of the Poverty Indentation and incorporated into the deformation front is even more difficult to pin down. These age correlation can not be achieved by using Hawke Bay-1 and continental shelf sample stations as the source region for the trench-fill sediments are dominantly from the south up the Hikurangi Trough and are therefore accreted Pacific Plate sediments without a direct stratigraphic correlation to the over-riding plate sequence. These sediments occupy a completely different geological setting and can not be directly correlated. An important reason for not using MED line CM05-01, as has been referred to in Nicol et al. (2007), is that the trench-end of this line does not directly intersect any of the trench GeodyNZ seismic lines. Dates for frontal wedge sediments on CM05-01 (Nicol and Uruski, 2005) have previously been inferred from the Hawke Bay-1 well and Lachlan Ridge sediments (Barnes et al., 2002) on the shelf.

The ability to assign age constraints for the trench-fill sequence in TAN0106-09 have required extensive extrapolation across a wide geographic region using the sequences exposed in the northern wall of the Hikurangi Channel, offshore Wairarapa, by Barnes and Mercier de Lepinay (1997), who used a gravity core, two dredge samples and the stratigraphic succession established on the Chatham Rise (Barnes, 1994). In 1993, the joint French and New Zealand GeodyNZ-Sud voyage was conducted around the East Coast, North Island on the RV L'ATALANTE (Lewis and Pettinga, 1993; Collot et al., 1995b; Collot et al., 1995a; Collot et al., 1996b; Collot et al., 1996a; Lewis et al., 1997; Barnes et al., 1998; Lewis et al., 1998). Using the ages determined in line GeodyNZ-P38 from the 1997 research (Barnes and Mercier

de Lepinay, 1997) (Figure 6.4A) we were able to follow the horizons north up the margin front to the Poverty Indentation study area and correlate the ages to the horizons for the trench fill sequence in TAN0106-09 (Figures 6.4B and 6.4C). Correlations have provided dating constraints for Horizons 3 and 4 at approximately 0.8 Ma and 2.03 Ma respectively (Figure 6.4A). Dated horizons able to be brought into the Poverty region (but not intersecting with TAN0106-09) also include Horizon 5, dated approximately at 5.1 Ma (from Barnes and Mercier de Lepinay, 1997) and interpreted to be the base of the Pliocene (Figure 6.4A). We introduce two new horizons, labelled KB1 and KB2 to enable more accurate follow-through with the horizon picks (Figure 6.4A). Horizons 4 and 5 can be used to approximate the ages of KB1 and KB2, assuming constant sedimentation rates and seismic velocity. KB1 is therefore inferred to be around 2.7 Ma, and KB2 around 3.5 Ma. The 'New Vents' Sonne voyage profiles (Bialas et al., 2007) show consistent stratigraphy to what was traced up the GeodyNZ lines – reinforcing our horizon picks. For correlation of these horizons to the horizons used in the MED velocity slices, please refer to Appendix 3.

6.5 ESTIMATING RATES OF SHORTENING ACROSS PROFILES

The derived errors for calculations include as realistic assumptions and estimates as possible and derive rates for an average value. The main potential sources of error for estimating shortening are likely to be a result of misinterpreting horizons, thrust faults and duplexing of sections where there is the potential for missing pieces of the correlated horizons. Accurately determining the intersections between shallow-dipping horizons and shallow-dipping thrusts is difficult and could lead to plenty of error in offset and initial length. Other errors also include ranges of values for sediment velocities obtained from the seismic section (combined to produce an average) and measurement error. Calculations have been carried forward where possible, significantly reducing compounded rounding errors. The errors have been derived to encompass as much of the expected variation of the values as possible, although it is acknowledged that, given the large uncertainty associated with some measurements and data extrapolation, it is possible that some errors have been overlooked. The rate errors are independent of the errors associated with estimated dates for the dated horizons and extrapolation of these horizons up the margin front and tied across seismic profiles, with the error calculated for the shortening /strain calculation for any given horizon. Therefore, the

following rates and interpretations should be acknowledged as only an insight and guide to shortening and contractional activity on the Poverty sector of the northern frontal wedge.

6.5.1 Lower margin (TAN0106-09)

While it is clear that the frontal anticlinal structures incorporate the trench fill sequence and horizons are able to be followed reasonably comfortably across the first 3-4 structures, it soon becomes impossible to follow these horizons any further and the packages become acoustically chaotic (Figure 6.5). A change to Australian Plate sediments in the mid-slope anticlinal ridge (c.f. Barnes et al., 2009) at the back of TAN0106-09 (Figure 6.5) is defined by another change in acoustic character and leads to the assumption that up to that point the sediments are still derived from the trench fill sequence, although highly deformed.

The décollement appears to be well defined but affected by numerous normal faults in the subducting Pacific Plate so there is a reasonable amount of relief on the subduction interface (Figure 6.5). Resolution of the décollement becomes difficult away from the thrust front due to the presence of multiples in the TAN0106 data but correlation from neighbouring MED and GeodyNZ lines constrains the décollement to rise at a steady rate from 6 seconds two-way-time (TWT) up to 4 seconds TWT.

A subducted sequence of plateau turbidites is interpreted as underlying the frontal thrust wedge and occupying space accommodated by normal faults occurring in the subducting Pacific plate (Figure 6.5).

Line balance of the main identified horizons across the first three thrust fault structures in the frontal wedge reveals approximate percentages of shortening, with approximate rates of shortening for aged horizons 3, 4 and KB1:

3.4 ± 0.3km (24%) shortening on horizon 3 in 0.8 Ma = ~4.3 mm/yr

5.1 ± 0.4 km (27%) shortening on horizon A

5.3 ± 0.5 km (27%) shortening on horizon 4 in 2.03 Ma = ~2.6 mm/yr

8.3 ± 0.4 km (36%) shortening on horizon B

9.2 ± 0.6 km (38%) shortening on horizon KB1 in ~2.7 Ma = ~3.4 mm/yr

13.5 ± 0.7 km (46%) shortening on horizon KB2 in ~3.5 Ma = ~3.8 mm/yr

Area balance of the suspected trench-fill sequence now incorporated into the accretionary wedge across the frontal three main thrust faults of TAN0106-09, indicates a linear overall shortening of around 47%, with an approximate 43.5 km extent of trench-fill (area ~308 km^2) now shortened into just over 20 ± 1.5 km. Area balance of the section between the frontal three thrust structures and the inferred transition between accreted trench-fill sequence and Australian Plate sediments beneath Pantin Bank reveals a shortening of around 35% with 87.9 ± 2.1 km extent (area ~615 km^2) of trench-fill sequence now incorporated into 30 ± 1.5 km of the accretionary wedge.

6.5.2 Upper margin (CM05-23)

The décollement is very well defined in this section (Figure 6.5) with very little apparent relief on the subduction interface and a steady downwards slope (~1^o) to the northwest. It appears that the décollement may have once split towards the southeast, with a large percentage of the motion taken up on the main thrust through the over-riding wedge beneath the South Paritu Ridge anticline. Activity has since ceased on this anticline according to the green horizon (Late Pliocene - see following paragraphs) and the majority of the motion on the décollement in this region appears to bypass CM05-23 altogether with little or no activity on any structures in this section.

Ages for the continental shelf horizons are extrapolated from both the Hawke Bay-1 drill hole (BP Shell Aquitaine and Todd Petroleum Development Ltd, 1976), and cores and dredge/rock samples interpreted and extrapolated along the shelf by Barnes at al. (2002), Paquet et al. (Paquet, 2007; 2009), and Mountjoy (2009). The blue-labelled horizon reflector (refer to Figure 6.2) has been dated in the Castlecliffian stage during the Pleistocene (~1.1 Ma). Quantification of shortening along this horizon was approximated using direct line balance. Shortening rates are not significant at 0.6 ± 0.2 km shortening (~0.5 mm/yr) and most of this relating to only two structures – an active thrust fault just outboard of the Lachlan Thrust beneath the continental shelf, and thrust-related growth on the first major anticline when approaching the margin front from the shore (Figure 6.5).

Major structures are pre-Miocene with very little deformation after the mid Castlecliffian horizon except for that on the active nearshore/shelf structures (Figure 6.5). Some activity on the eastern-most anticline (South Paritu Ridge) on this section is evident post the c. 1.1 Ma

horizon, with activity being inferred to have ceased post the green horizon (~ 0.4 Ma) due to the subsequent onlap geometries above this horizon. Rapid subsidence and/or sea level rise is also inferred to have taken place since the end of the Miocene as the c. 1.1 Ma horizon represents a significant erosion period with a substantial accommodation space opening up to allow formation of prograding clinoforms (e.g. Christie-Blick and Driscoll, 1995; Christie-Blick et al., 2007) (Figure 6.5).

6.6 RATES OF HORIZONTAL SHORTENING ACROSS THE PLATE BOUNDARY

The mid to upper slope of the Poverty Indentation is largely inactive (see Chapter 3) and rates of shortening across dated horizons reflect that, with less than 2% contraction activity (Figure 6.6). In the frontal wedge, the first three main anticlinal-forming thrust faults share a shortening rate of <4.3 mm/yr but representing up to 47% shortening of the trench-fill sequence (Figure 6.6).

Results are not definitive, but we note that the rates of shortening are representing a minimum because the onset of deformation can not be determined with a high degree of confidence. There are two possible explanations for this low rate of shortening:

1) the frontal thrusts are not as active as they appear, with contraction/shortening taken up more on the subduction interface and largely bypassing the wedge.

2) the rate observed is an average over that period of time, with actual current shortening only initiating in more recent time and consequently would represent a much higher rate.

If shortening represented by the deformation in the frontal wedge is representative of only a small proportion of the total plate convergence rate, this leads in to the idea of duplexing and underplating further into the subduction zone i.e. Under inner Hikurangi margin, NIDFB and TVZ (Litchfield, 2001). Shortening could be occurring in the lower part of the upper plate beneath the Raukumara range, hence driving the uplift rates observed in that region (Litchfield, 2001).

Explanation 2 appears to be more likely, given the observed level of current activity in the frontal wedge structures. Unfortunately there is no way to prove this currently without age

control of the slope basins in the accretionary wedge. Tectonic convergence resulting in seamount subduction continually modifies this sector of the margin with recovery from seamount impact and subduction likely to have a significant role to play here, and may inhibit further attempts to constrain/determine shortening rates without more detailed age control on the upper sediment packages in the incorporated trench fill sequence.

Realistically, both explanations are valid and a combination of the two is most likely, particularly if the contractional activity across the frontal wedge is only a very recent occurrence. Slope basins across this frontal wedge are very limited, with apparently very recent growth strata (Figure 6.5), and warrant further investigation into timing of deformation of this sequence.

6.7 CONCLUSIONS

In this chapter we have attempted to constrain the temporal rates of shortening across the frontal slope of the Hikurangi margin. This analysis has not provided a conclusive determination, with rates of shortening across the continental slope appearing to be minimal, ranging from ~0.5 mm/yr in the upper slope to ~4.3 mm/yr across the deformation front. However, geomorphology and seismic structure indicate a much higher rate. It appears that the frontal thrusts are currently taking up a significant amount of the total shortening across the margin, but that this may only be a recent development and not reflected properly in shortening rates given the limited age control. The age control required is the onset of deformation in the frontal part of the wedge, of which the growth strata of the limited slope basins on the wedge, may provide key clues to this timeline. The plate décollement beneath this sector of the margin may be very actively accommodating slip, producing higher strain on the frontal wedge and allowing the margin normal convergence to bypass the mid-slope and upper slope regions on the subduction interface. This may also lead to duplexing and underplating beneath the Raukumara ranges, driving the observed uplift rates in that region.

References

Adam, J., Klaeschen, D., Kukowski, N. and Fleuh, E., 2004. Upward delamination of Cascadia Basin sediment infill with landward frontal accretion thrusting caused by rapid glacial age material flux. Tectonics, 23.

Barnes, P.M., 1994. Pliocene-Pleistocene depositional units on the continental slope off central New Zeland: control by slope currents and global climate cycles. Marine Geology, 117: 155-175.

Barnes, P.M. and Mercier de Lepinay, B., 1997. Rates and mechanics of rapid frontal accretion along the very obliquely convergent southern Hikurangi margin, New Zealand. Journal of Geophysical Research, 102(B11): 24,931-24,952.

Barnes, P.M., Mercier de Lepinay, B., Collot, J.-Y., Delteil, J. and Audru, J.-C., 1998. Strain partitioning in the transition area between oblique subduction and continental collision, Hikurangi Margin, New Zealand. Tectonics, 17(4): 534-557.

Barnes, P.M., Nicol, A. and Harrison, T., 2002. Late Cenozoic evolution and earthquake potential of an active listric thrust complex above the Hikurangi subduction zone, New Zealand. GSA Bulletin, 114(11): 1379-1405.

Barnes, P.M., Lamarche, G., Bialas, J., Henrys, S., Pecher, I.A., Netzeband, G., Greinert, J., Mountjoy, J.J., Pedley, K.L. and Crutchley, G., 2009. Tectonic and Geological Framework for Gas Hydrates and Cold Seeps on the Hikurangi Subduction Margin, New Zealand. Marine Geology, in press.

Beanland, S. and Haines, J., 1998. The kinematics of active deformation in the North Island, New Zealand, determined from geological strain rates. New Zealand Journal of Geology and Geophysics, 41: 311-323.

Beanland, S., Melhuish, A., Nicol, A., Ravens, J.M. and Anonymous, 1998. Structure and deformational history of the inner forearc region, Hikurangi subduction margin, New Zealand. New Zealand Journal of Geology and Geophysics, 41(4): 325-342.

Bialas, J., Greinert, J., Linke, P. and Pfannkuche, O., 2007. FS Sonne Fahrtbericht / Cruise Report SO 191 New Vents, Leibniz-Institut für Meereswissenschaften, Kiel, Germany.

BP Shell Aquitaine and Todd Petroleum Development Ltd, 1976. Well completion report Hawke Bay-1. 667, New Zealand Ministry of Commerce.

Carter, L., Manighetti, B., Elliot, M., Trustrum, N. and Gomez, B., 2002. Source, sea level and circulation effects on the sediment flux to the deep ocean over the past 15 ka off eastern New Zealand. Global and Planetary Change, 33(3-4): 339-355.

Chanier, F. and Ferrière, J., 1991. From a passive to an active margin; tectonic and sedimentary processes linked to the birth of an accretionary prism (Hikurangi Margin, New Zealand). Bulletin de la Societe Geologique de France, 162(4): 649-660.

Chanier, F., Ferriere, J. and Angelier, J., 1999. Extensional deformation across an active margin, relations with subsidence, uplift, and rotations; the Hikurangi subduction, New Zealand. Tectonics, 18(5): 862-876.

Chemenda, A., Lallemand, S. and Bokun, A., 2000. Strain partitioning and interplate friction in oblique subduction zones: Constraints provided by physical modelling. Journal of Geophysical Research, 105(B3): 5567-5582.

Christie-Blick, N. and Driscoll, N.W., 1995. Sequence Stratigraphy. Annual Review of Earth and Planetary Sciences, 23: 451-478.

Christie-Blick, N., Pekar, S.F. and Madof, A.S., 2007. Is there a role for sequence stratigraphy in chronostratigraphy? In: B. McGowran (Editor), Special Issue of Stratigraphy on Chronostratigraphy, pp. 1-39.

Collot, J.-Y., Delteil, J., Lewis, K. and l'equipe scientifique, 1995a. De la fosse de Kermadec a la termi-naision sud du fosse d'Hikurangi: Resultat de la campagne de cartographie multifaisceaux GEO-DYNZ-SUD, Leg 1. Comptes Rendus de L'Academie des Sciences - Series IIA - Earth and Planetary Science, 320: 295-302.

Collot, J.-Y., Delteil, J., Herzer, R., Wood, R., Lewis, K. and Shipboard Party, 1995b. Sonic Imaging reveals new plate boundary structures offshore New Zealand. Eos Trans. AGU, 76(1): 4-5.

Collot, J.-Y., Davy, B., Lamarche, G. and Anonymous, 1996a. Forearc structures and tectonic regimes at the oblique collision zone between the Hikurangi Plateau and the southern Kermadec arc. Eos, Transactions, American Geophysical Union, 77(22): 121.

Collot, J.-Y., Delteil, J., Lewis, K.B., Davy, B., Lamarche, G., Audru, J.-C., Barnes, P., Chanier, F., Chaumillon, E., Lallemand, S.E., Mercier de Lepinay, B., Orpin, A., Pelletier, B., Sosson, M., Toussaint, B. and Uruski, C., 1996b. From oblique subduction to intra-continental transpression; structures of the southern Kermadec-Hikurangi margin from multibeam bathymetry, side-scan sonar and seismic reflection. Marine Geophysical Researches, 18(2-4): 357-381.

Darby, D.J. and Meertens, C.M., 1995. Terrestrial and GPS measurements of deformation across the Taupo back arc and Hikurangi forearc regions in New Zealand. Journal of Geophysical Research, 100(B5): 8221-8232.

Davy, B. and Wood, R., 1994. Gravity and magnetic modelling of the Hikurangi Plateau. Marine Geology, 118(1-2): 139-151.

De Mets, C., Gordon, R.G., Argus, D.F. and Stein, S., 1990. Current plate motions. Geophysical Journal International, 101: 425-478.

De Mets, C., Gordon, R.G., Argus, D.F. and Stein, S., 1994. Effect of recent revisions to the geomagnetic reversal time scale on estimates of current plate motions. Geophysical Research Letters, 21(20): 2191-2194.

Dix, C.H., 1955. Seismic velocities from surface measurements. Geophysics, 20(1): 68-86.

Doser, D.I. and Lomas, R., 2000. The transition from strike-slip to oblique subduction in southeastern Alaska from seismological studies. Tectonophysics, 316(1-2): 45-65.

Douglas, A., Beavan, J., Wallace, L. and Townend, J., 2005. Slow slip on the northern Hikurangi subduction interface, New Zealand. Geophysical Research Letters, in press.

Downes, G. and Stirling, M.W., 2001. Groundwork for development of a probabilistic tsunami hazard model for New Zealand, ITS 2001 Proceedings, pp. 293-301.

Fitch, T.J., 1972. Plate convergence, transcurrent faults and internal deformation adjacent to southeast Asia and the Western Pacific. Journal of Geophysics Research, 77: 4432-4460.

Fuakao, Y., 1979. Tsunami earthquakes and subduction processes near deep-sea trenches. Journal of Geophysical Research, 84(B5): 2303-2314.

Gutscher, M.-A., 2001. An Andean model of interplate coupling and strain partitioning applied to the flat subduction zone of SW Japan (Nankai Trough). Tectonophysics, 333(1-2): 95-109.

Leith, K.J., 2003. The role of deep-seated landsliding in the geomorphic evolution of the Esk Valley, Hawke's Bay: An innovative approach to hazard evaluation. M.Sc Thesis, University of Canterbury, Christchurch, 220 pp.

Lewis, K., Collot, J.-Y. and Lallemand, S., 1998. The dammed Hikurangi Trough: a channel-fed trench blocked by subducting seamounts and their wake avalanches (New Zealand-France GeodyNZ Project). Basin Research, 10(4): 441-468.

Lewis, K.B., 1980. Quaternary sedimentation on the Hikurangi oblique-subduction and transform margin, New Zealand. Special Publication of the International Association of Sedimentologists(4): 171-189.

Lewis, K.B. and Pettinga, J.R., 1993. The emerging, imbricate frontal wedge of the Hikurangi Margin. Sedimentary Basins of the World, 2: 225-250.

Lewis, K.B., Collot, J.-Y., Davy, B., Delteil, J., Lallemand, S. and Uruski, C., 1997. GeodyNZ Team 1997:North Hikurangi GeodyNZ swath maps: depths, texture and

geological interpretation, NIWA Chart Miscellaneous Series 72. National Institute of Water and Atmospheric Research Ltd, Wellington.
Litchfield, N.J., 2001. Dynamics of the Hikurangi subduction margin as recorded by river terraces in the eastern North Island, New Zealand, Institute of Geological & Nuclear Sciences Information Series, Report: 50, pp. 80.
Martinez, A., Malavieille, J., Lallemand, S. and Collot, J.-Y., 2002. Strain partitioning in an accretionary wedge, in oblique convergence: analogue modelling. Bulletin de la Societe Geologique de France, 173(1): 17-24.
Maruyama, S. and Liou, J.G., 1989. Possible depth limit for underplating by a seamount. Tectonophysics, 160(1-4): 327-337.
Mazzotti, S., Henry, P., Le Pichon, X. and Sagiya, T., 1999. Strain partitioning in the zone of transition from Nankai subduction to Izu-Bonin collision (Central Japan): implications for an extensional tear within the subducting slab. Earth and Planetary Science Letters, 172(1-2): 1-10.
McCrory, P.A., 1996. Tectonic model explaining divergent contraction directions along the Cascadia subduction margin, Washington. Geology, 24(10): 929-932.
Mountjoy, J.J., 2009. Submarine canyon evolution: Quantifying geomorphic processes on New Zealand's active continental margin. PhD Thesis, University of Canterbury.
Nicol, A. and Beavan, J., 2003. Shortening of an overriding plate and its implications for slip on a subduction thrust, central Hikurangi Margin, New Zealand. Tectonics, 22(6): 1070.
Nicol, A. and Uruski, C., 2005. Structural Interpretation and Cross Section Balancing, East Coast Basin, New Zealand. Unpublished Petroleum Report PR3184, Ministry of Economic Development New Zealand.
Nicol, A., Mazengarb, C., Chanier, F., Rait, G., Uruski, C. and Wallace, L., 2007. Tectonic evolution of the active Hikurangi subduction margin, New Zealand, since the Oligocene. Tectonics, 26(3).
Paquet, F., 2007. Morphostructural evolution of active margin basins: the example of the Hawke Bay forearc basin, New Zealand. Ph.D. Thesis, University of Canterbury, Christchurch, 263 pp.
Paquet, F., Proust, J.-N., Barnes, P.M. and Pettinga, J.R., 2009. Inner-Forearc Sequence Architecture in Response to Climatic and Tectonic Forcing Since 150 ka: Hawke's Bay, New Zealand. Journal of Sedimentary Research, 79(3): 97-124.
Park, J.-O., Tsuru, T., Takahashi, N., Hori, T., Kodaira, S., Nakanishi, A., Miura, S. and Kaneda, Y., 2002. A deep strong reflector in the Nankai accretionary wedge from multichannel seismic data: Implications for underplating and interseismic shear stress release. Journal of Geophysical Research, 107(B4).
Park, R.G., 1997. Foundations of Structural Geology. Chapman & Hall, London.
Pelletier, B., Collot, J.Y., Lamarche, G., Delteil, J., Lewis, K., Davy, B., Lallemand, S., Chanier, F. and Anonymous, 1994. Combined influence of strike-slip and collision tectonics on tectonic erosion of the southern Kermadec-Northern Hikurangi Margin (New Zealand). Eos, Transactions, American Geophysical Union, 75(44, Suppl.): 671.
Polet, J. and Kanamori, H., 2000. Shallow subduction zone earthquakes and their tsunamigenic potential. Geophysical Journal International, 142(3): 684.
Satake, K. and Tanioka, Y., 1999. Sources of tsunami and tsunamigenic earthquakes in subduction zones. Pure and Applied Geophysics, 154: 467-483.
Smith, E.G.C., Stern, T. and Reyners, M., 1989. Subduction and back-arc activity at the Hikurangi convergent margin, New Zealand. Pure and Applied Geophysics, 129(1-2): 203-231.

Upton, P., Koons, P.O. and Eberhart-Phillips, D., 2003. Extension and partitioning in an oblique subduction zone, New zealand: Constraints from three-dimensional numerical modeling. Tectonics, 22(6): 1-14.

Walcott, R.I., 1978. Present tectonics and late Cenozoic evolution of New Zealand. Geophysical Journal of the Royal Astronomical Society, 52: 137-164.

Wallace, L., Beavan, J., McCaffrey, R. and Darby, D.J., 2004. Subduction zone coupling and tectonic block rotations in the North Island, New Zealand. Journal of Geophysical Research, 109.

Wallace, L. and Beavan, J., 2006. A large slow slip event on the central Hikurangi subduction interface beneath the Manawatu region, North Island, New Zealand. Geophysical Research Letters, 33(11).

Wallace, L., Ellis, S. and Mann, P., 2008. Tectonic block rotation, arc curvature, and back-arc rifting: Insights into these processes in the Mediterranean and the western Pacific. IOP Conf. Series: Earth and Environmental Science, 2.

Watkins, J.S., Moore, J.C., Shipley, T.H., Bachman, S.B., Butt, A., Didyk, B.M., Leggett, J.K., Lundburg, N., McMillen, K.J., Niitsuma, N., Shephaerd, L.E., Stephan, J.F. and Stradner, H., 1981. Accretion, underplating, subduction and tectonic evolution, Middle America trench, southern Mexico: results of DSDP Leg 66. Oceanologica Acta SP 213-224;.

Webb, T.H. and Anderson, H.J., 1998. Focal mechanisms of large earthquakes in the North Island of New Zealand: slip partitioning at an oblique active margin. Geophysical Journal International, 134(1): 40-86.

Wood, R. and Davy, B., 1994. The Hikurangi Plateau. Marine Geology, 118(1-2): 153-173.

Yu, G., Wesnousky, S.G. and Ekstrom, G., 1993. Slip partitioning along major convergent plate boundaries. Pure and Applied Geophysics, 140: 183-210.

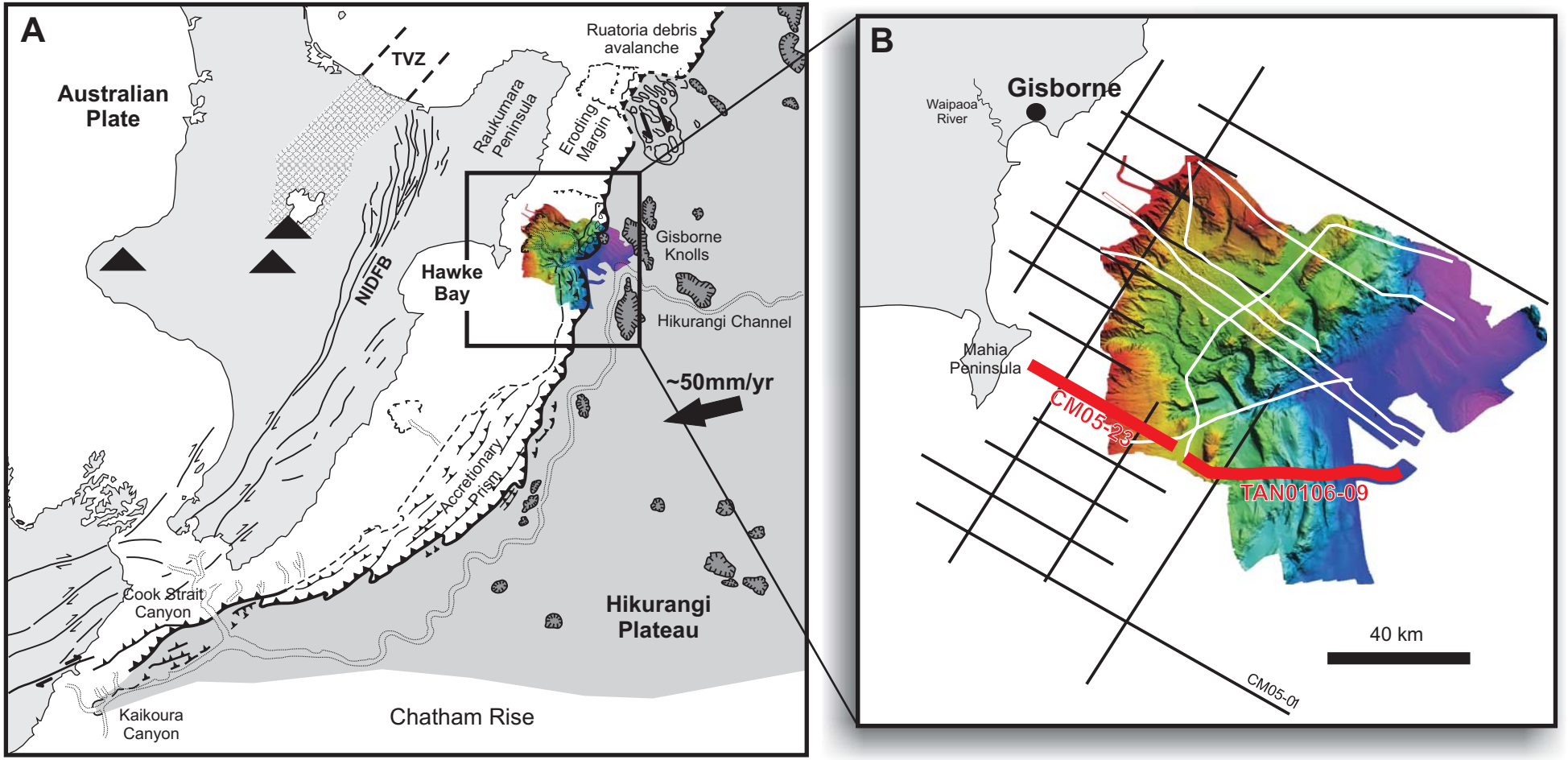

Figure 6.1 A: The New Zealand plate boundary through the Hikurangi margin and showing seamounts distributed across the Hikurangi Plateau, including the Gisborne Knolls (Modified from Lewis et al. 1998, Davy & Wood 1994, Foster & Carter 1997, Cole 1990). NIDFB = North Island Dextral Fault Belt; TVZ = Taupo Volcanic Zone. Convergence vector PAC-AUS is indicted by the black arrow and rate of ~50mm/yr.

B: The Poverty Indentation study region DEM and location of seismic lines from MED and NIWA. Lines in red mark the two seimic survey lines presented in this paper - CM05-23 and TAN0106-09. Velocity data from line CM05-01 to the south was used as a proxy for the trench-fill stratigraphic sequence in Line TAN0106-09 to enable depth conversion.

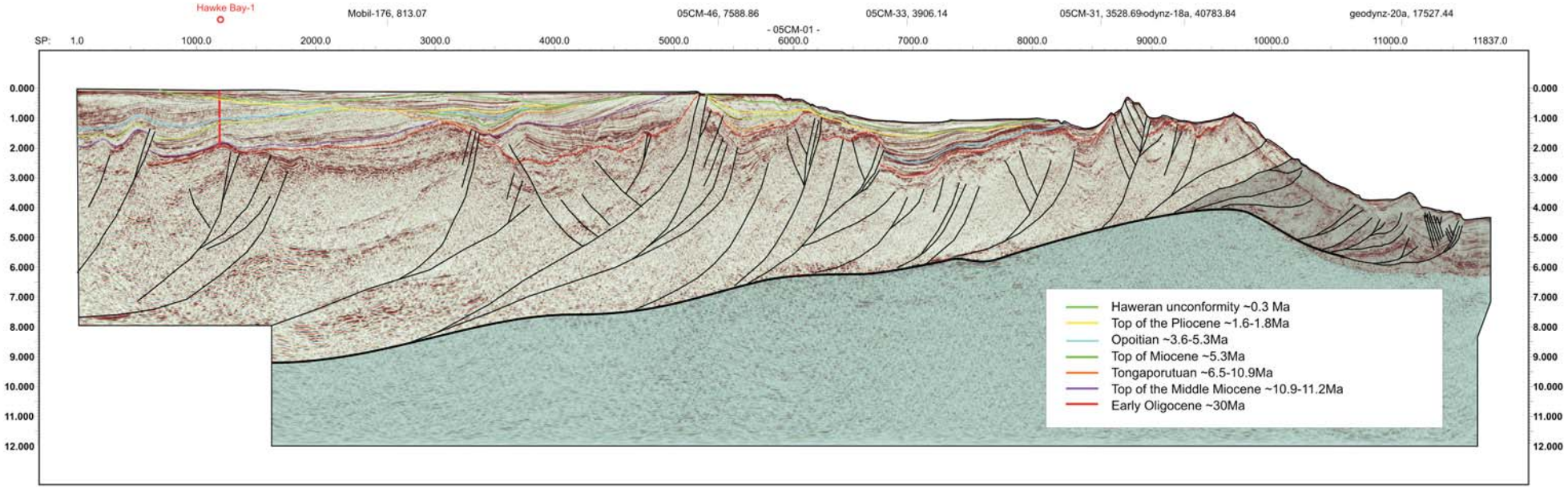

Figure 6.2 Structural and stratigraphic interpretation of Ministry of Economic Development (MED) seismic profile CM05-01. Dated stratigraphic horizons correlated from Hawke Bay-1 well (BP Shell Acquitane and Todd Petroleum Development Ltd., 1976) and core/dredge samples and previous research from the Hawke Bay continental shelf (Barnes et al., 2002; Paquet, 2007). Location of Hawke Bay-1 well indicated by the vertical red line. Green shaded region represents the subducting Pacific Plate, with the grey shaded region covering the approximate extent of trench-fill sequence incorporated into the accretionary wedge.

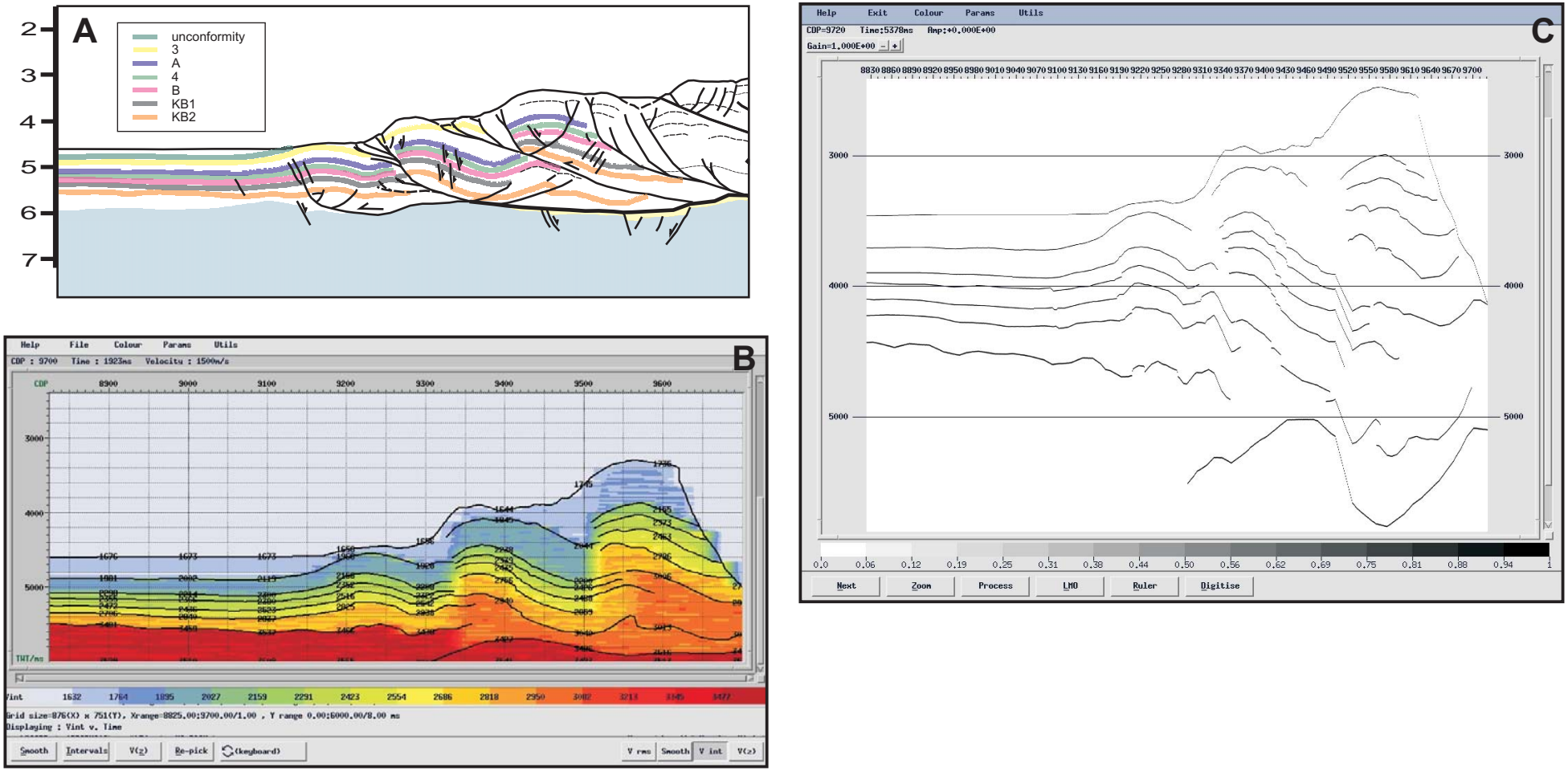

Figure 6.3 A: Two-way-time seismic profile of TAN0106-09 with key stratigraphic horizons.

B: Interpreted time horizons from A overlain on an image representing interval velocities (coloured) of the frontal wedge and deformation front on seismic line TAN0106-09 as extrapolated from 05CM/CM05-01.

C: Depth profile with interpreted horizons of the front section of seismic line TAN0106-09 (depth measured in metres).

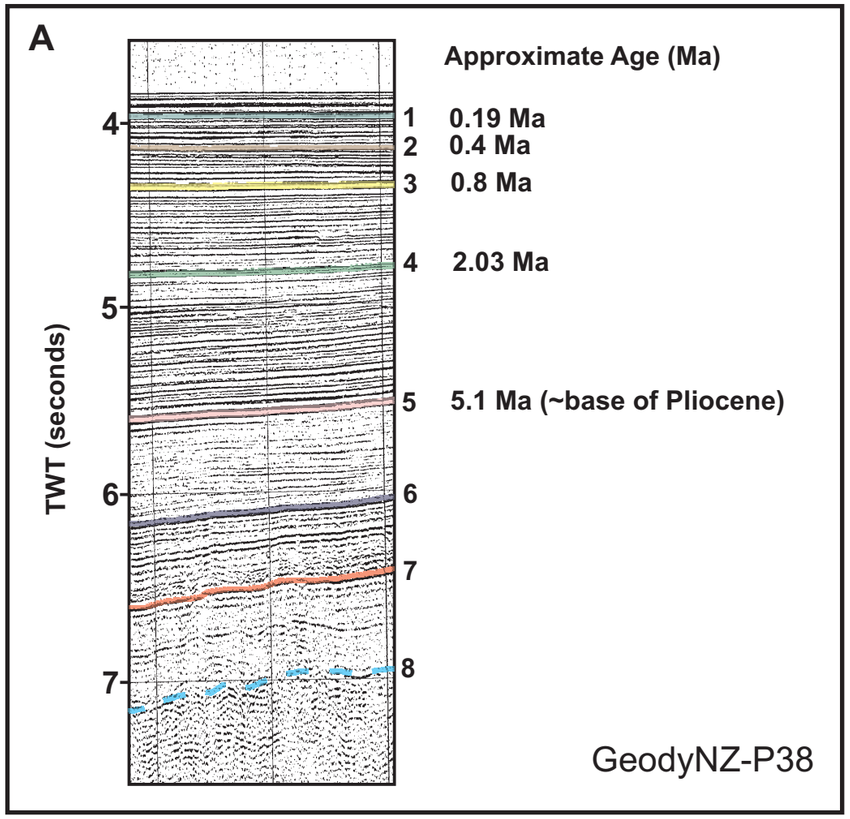

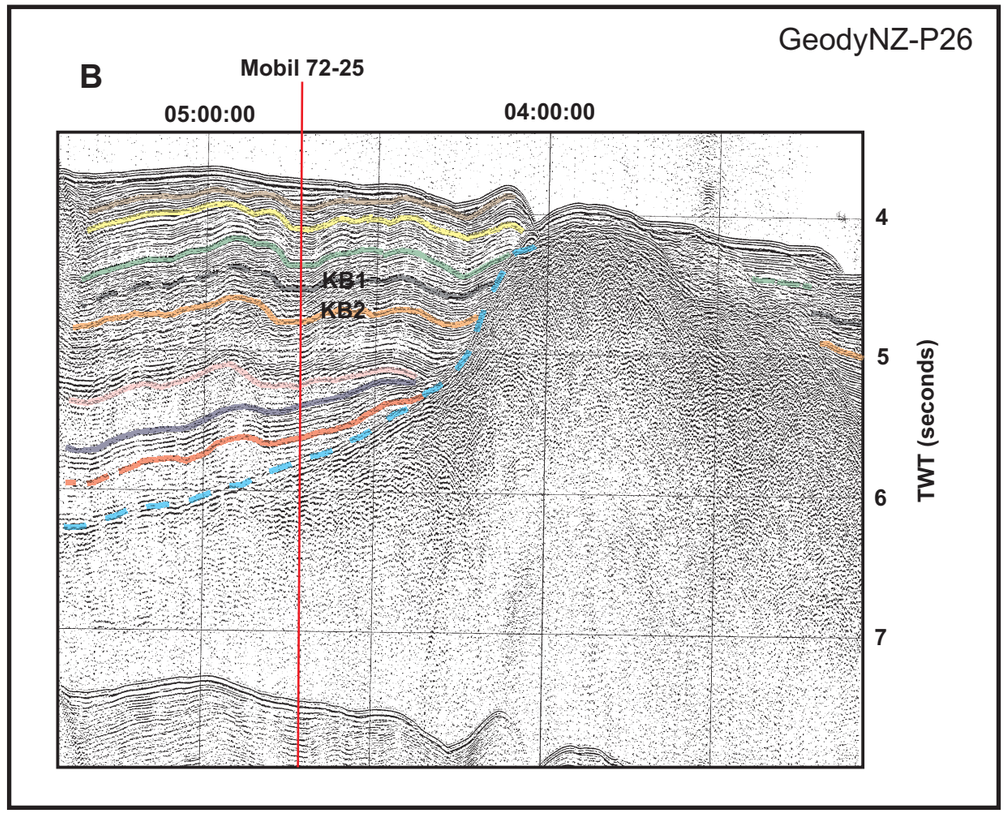

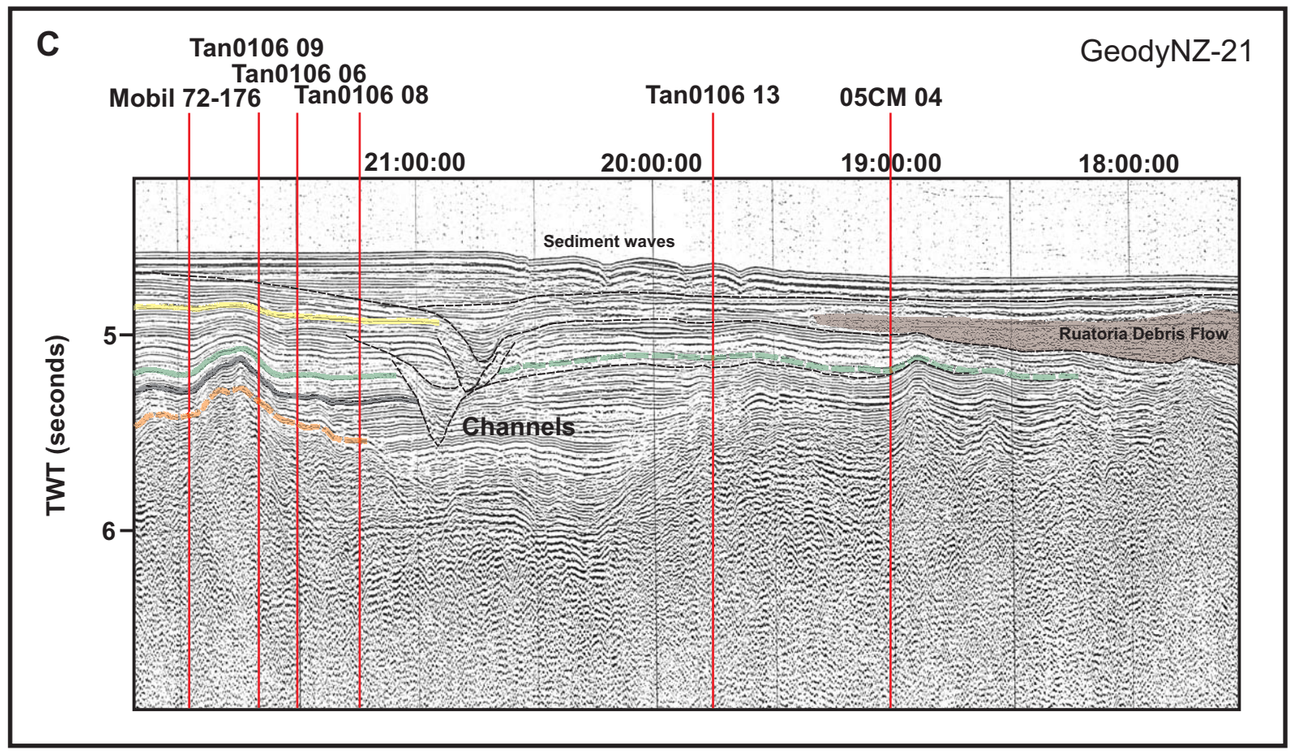

Figure 6.4 A: Horizons 1 to 8 interpreted by Barnes and Mercier de Lepinay (1997) on GeodyNZ-P38.

B:Dated horizons on GeodyNZ seismic profile Geodynz-P26 intersecting with sesimic profile Mobil 72-25 (tie line). Horizons KB1 and KB2 created to assist seismic reflection picks.

C: Seismic profile GeodyNZ-21 (P21) with intersections of Poverty seismic data, including TAN0106-09.

For locations of these seismic lines, readers are referred to NIWA Chart Miscellaneous Series 72 (Lewis et al. 1997).

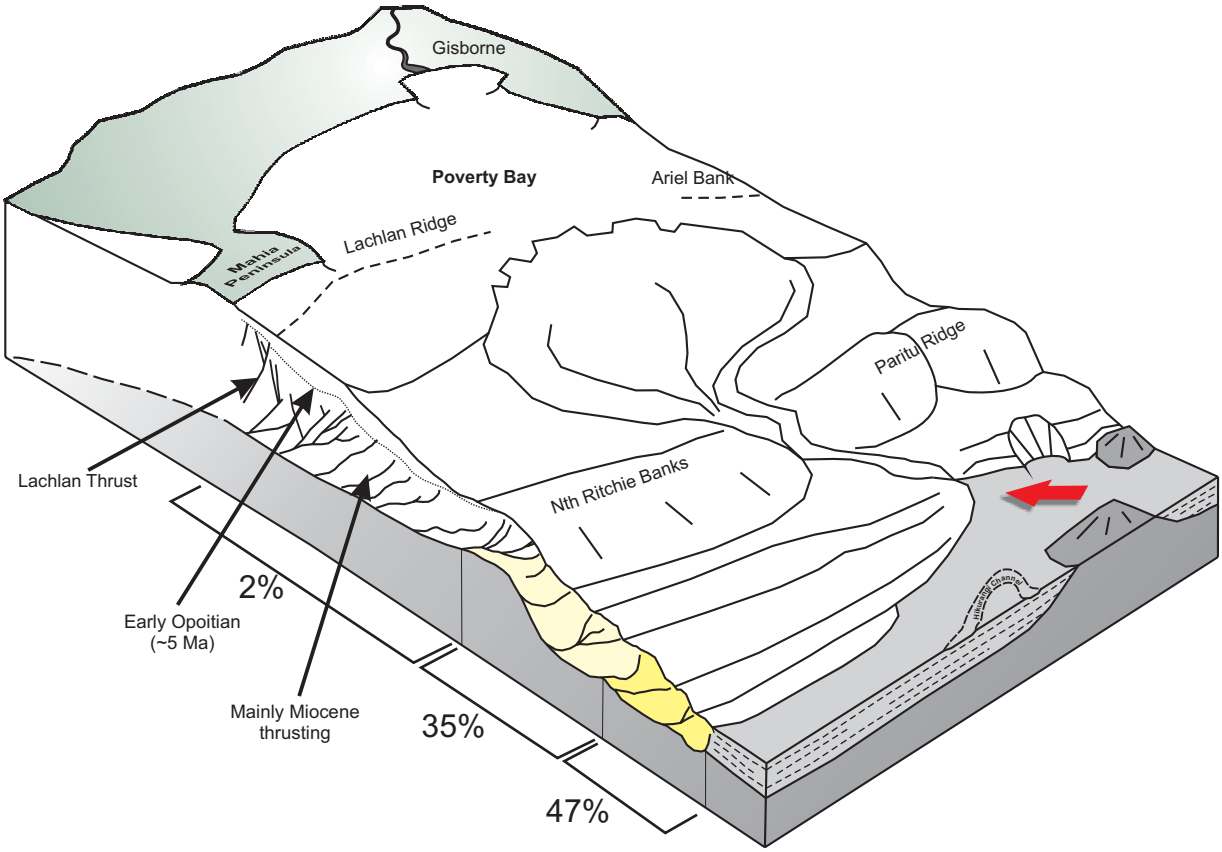

Figure 6.6 Percentage of horizontal shortening across the plate boundary post-Pliocene in the Poverty Bay region. Diagram is representative and not to scale.

CHAPTER 7: SEAMOUNT SUBDUCTION IN THE POVERTY INDENTATION, NEW ZEALAND: INSIGHTS FROM NUMERICAL AND ANALOGUE MODELLING

7.1 INTRODUCTION

Worldwide, many convergent plate boundaries are influenced by the subduction of large seafloor asperities from a variety of origins. High-relief features on the subducting plate may include ridges formed by ancient, long defunct spreading axes, hot-spot chains, remnant arcs, active volcanic arcs, ridges adjacent to transform faults or upfaulted oceanic slices (e.g. Lallemand et al., 1990). Discrete seamount subduction is less common and falls into three main categories, including guyot subduction (flat-topped seamounts characteristic of Japanese convergent margins), conical, and elongate seamount subduction. Seamounts come in a variety of geometries and sizes and this will be reflected in the differing effects on the morpho-structure of the margin due to the geometry and relief characteristics of the asperity combined with the geology and rheology of the overriding plate and subduction interface. Seamount subduction appears to play a significant role in the tectonic erosion observed along convergent margins, with the resulting tectonic deformation strongly influencing morphology and seismicity of the margin (Dominguez et al., 1998a; Dominguez et al., 2000).

Analogue sandbox experiments have been used to effectively model margin convergence with either accretion development or tectonic erosion, complementing marine bathymetric observations along convergent margins. In particular, sandbox experiments have been used to model the effects of seamount and ridge subduction on the styles of deformation, including overprinting, within accretionary wedges (Malavieille, 1984; Malavieille et al., 1991; Lallemand et al., 1992; Kukowski et al., 1994; Dominguez et al., 1998b; Dominguez et al., 1998a; Gutscher et al., 1998; Dominguez et al., 2000). These physical experiments have shown that the inboard accretionary wedge thickens and shortens with the forward propagation of the basal décollement as the incoming seamount approaches the deformation front and is introduced into the subduction zone. The accretionary wedge thickening leads to a change in the taper angle, with reactivation of pre-existing thrusts and retreat of the frontal segment (Lallemand et al., 1992). Back-thrusting and conjugate strike-slip faulting also may

develop inboard of the leading slope of the seamount, with the basal décollement deflected upward onto the leading slope as it subducts, creating a large shadow zone behind the seamounts trailing slope (Dominguez et al., 2000). The wedge thickens directly above the asperity, generating a slope break in topography and leading to the creation of an indentation.

7.1.1 The Poverty Indentation

The Poverty Indentation is a large (~4000 km^2) structural re-entrant in the northern Hikurangi Margin, New Zealand (Figure 7.1). The subducting Pacific Plate in this region is dominated by the Hikurangi Plateau, an anomalously thick (~15 km) triangular-shaped section of oceanic crust that is studded with Mesozoic-aged seamounts (Davy and Wood, 1994; Wood and Davy, 1994) (Figure 7.1A). The Pacific Plate relative convergence (PAC-AUS) is oblique, ranging from 30^o obliquity (with respect to the deformation front) in the north at a rate of ~50mm/yr, to 80^o obliquity and a rate of 37 mm/yr at the SE tip of the North Island (Walcott, 1978; Walcott, 1987; De Mets et al., 1990; De Mets et al., 1994; Wallace et al., 2004) (Figure 7.1A). Kinematic GPS modelling indicate that current relative rates of convergence between the Central Hikurangi block (see Wallace et al., 2004, Figure 10) and the Pacific Plate decrease southwards from ~ 60 mm/yr off East Cape to 45 mm/yr off southern Hawke Bay (Wallace et al., 2004; Wallace et al., 2008). The convergence at the northern Hikurangi Margin is more orthogonal than the PAC-AUS vector due to the extension of the Taupo Volcanic Zone (TVZ) and the subsequent rotation of the East Coast (c.f. Beavan et al., 2002). Effectively, this means that at the deformation front, a subducting seamount will be expected to experience an orthogonal collision path into the margin.

Previous research (e.g. Lewis and Pettinga, 1993; Collot et al., 1996; Lewis et al., 1998) has identified the Poverty Indentation as being primarily the result of subducting seamounts impacting against the weak water-laden rocks of the margin. The indentation axis is incised by the Poverty Canyon system (Figure 7.1B), a 70 km long entrenched channel representing the only significant sediment transport pathway to directly reach the trough (structural trench) for nearly 300 km along the margin (Lewis et al., 1998). The Poverty Indentation is currently being approached on the outboard side of the trench axis, across the subducting Pacific Plate, by a number of elongate seamounts including the Gisborne Knolls and the Mahia Seamount. Also, currently at the deformation front, subduction of the much smaller conical Puke Seamount has been initiated on the indentation's northern margin (Figure 7.1). Evidence

points to at least three main seamount subduction events within the Poverty Indentation, each with different margin responses (Pedley et al. 2009; Chapter 3, this thesis):

i) older substantial seamount impact that drove the first-order perturbation in the margin, since approximately ~1-2 Ma

ii) subducted seamount(s) now beneath Pantin and Paritu Ridge complexes, initially impacting on the margin approximately ~0.5 Ma, and

iii) incipient seamount subduction of the Puke Seamount at the current deformation front.

7.1.2 Investigating seamount subduction on the Hikurangi margin

Analogue sandbox models previously developed for the Hikurangi margin and other convergent margins can be applied to both the accretionary wedge forming processes, and the effects of seamount subduction on the margin as a whole. The Ruatoria debris avalanche (Figure 7.1A), located north of the Poverty Indentation, has been well studied in terms of relatively recent (~170,000 years ago) and largely unmodified effects of seamount subduction on the northern end of the Hikurangi margin (e.g. Lewis, 1997; Collot et al., 2001; Lewis et al., 2004). In the Poverty Indentation the effects of seamount subduction on the seafloor morphology, and on the internal deformation of the accretionary wedge is at a more evolved stage of seamount subduction than the Ruatoria event. The Poverty Indentation exhibits effects of multiple seamount impacts over time, with significant sedimentary modification and morpho-structural overprinting affecting the same region of the frontal wedge.

We present here a detailed investigation into how the indentation compares to global research on other convergent margins affected by seamount subduction. We investigate the margin response and whether we can identify the same, or similar, morphologic and structural effects with multiple seamounts impacting on the same region of a margin before it has had a chance to re-establish the accretionary frontal wedge. To date, research on other convergent margins has investigated discrete seamount subduction events, where there are few if any complex overprint effects on the margin front from successive seamount subduction episodes and little modification from sedimentary processes (e.g. Fryer and Smoot, 1985; Dominguez et al., 1998b; Park et al., 1999). The Poverty Indentation is to date the only documented seamount derived re-entrant with an established canyon system incised down its axis.

To observe and compare morphologic and structural features of the Poverty Indentation with other examples of seamount subduction, we will first present the observed features in the indentation, graphically compare it to a sandbox model prepared for the Hikurangi margin, compare it to published analogue and numerical experiments, both theoretical and representing other margins, and finally, compare it to other convergent margins with documented seamount subduction.

7.2 INVESTIGATING THE POVERTY INDENTATION

In 2001, the National Institute of Water and Atmospheric Research Ltd. (NIWA) collected over 4000 km^2 of 13 kHz swath bathymetry (SIMRAD EM300) across the entire Poverty Indentation covering the rugged slope topography from the continental shelf edge to the trench floor, encompassing depths ranging from 48 to 3547 m at a resolution of 10 and 25 m grids. This high quality bathymetric data is complemented by a range of high quality multi-channel seismic lines, enabling a detailed and integrated investigation of both the detailed seafloor morphology and the subsurface structural response to seamount subduction (Pedley et al., 2009) (refer to map of data in Figure 2.3, Chapter 2).

The Poverty Indentation is located just north of the transition from the wide central sector to the narrower, steeper northern sector of the Hikurangi Margin (see Figure 7.1A) and as such, the study area expresses some morphology characteristics of both the overall northern and central sectors. The variation in structural morphology between these two sectors is evident with the development of a lower slope accretionary wedge south of the Poverty Canyon, contrasting with the steep slopes and numerous gravitational collapse features present on the lower slope north of the canyon (Figure 7.1B).

The Poverty Indentation is a first order asymmetric morpho-structural re-entrant formed into the frontal wedge slope and penetrating from the trench floor to shelf edge across the entire forearc slope. The axis of the indentation is defined by the branched Poverty Canyon system (Figure 7.2). The most marked morpho-structural expression of the indentation is at the toe of the forearc slope, where the trench forming re-entrant is delineated by an over-steepened scarp forming the northern margin of the indentation, oriented at ~065/245^o (Figure 7.2). South of the Poverty Canyon, the northern end of the accretionary wedge has been dragged inwards into the indentation creating a distinctive arcuate lower slope accretionary wedge

oriented ~165/345^{o} in the north, and swinging back around to ~030/210^{o} towards the south (Figure 7.2). The northern sector of the indentation has a frontal slope with an average width of 50-60 km, while the southern sector accretionary wedge widens progressively southward to more than 100 km off Hawke Bay (see Figure 7.1A).

The Hikurangi Trough opens out into a 150 km long by 20-30 km wide depocentre, containing 1.5-2 km of sediment fill at the toe of the Poverty Indentation (Figure 7.2). This depocentre is bounded to the east by the Mahia Seamount and the Gisborne Knolls, with the Hikurangi Channel incising between them and extending away from the margin, out on to the Hikurangi Plateau (Figure 7.2). The Mahia Seamount stands up to ~1250 m high above the seafloor, measuring 25 km wide by 50 km long. The Gisborne Knolls, directly north across the Hikurangi Channel, consists of two main seamounts, the largest in the south measuring 19 km by 50 km and 1000 m high from the seafloor. This seamount extends another 1.5 km (1.3 s TWT) into the trench fill sequence to the top of the subducting Pacific Plate. The smaller Gisborne Knoll to the north measures 10 km by 27 km and extends ~500 m above the seafloor (Figure 7.2). The northern edge of the indentation is currently undergoing impact by the Puke Seamount, a small 7 km wide by 600 m high roughly conical seamount that appears to extend under the deformation front another 8 km and to a depth of 900 m (0.8 s TWT) (Figure 7.2). Directly out from the Poverty Canyon mouth, the largely buried seamount of the Poverty Knoll extends only 100 m above the trench floor but measures 1.6 km (1.4 s TWT) down to the top of the Pacific Plate (Figure 7.2). In all, there are five seamounts within 60 km of the deformation front of the Poverty Indentation that will impact within the next 1.2 Ma assuming current plate convergence rates of ~50 mm/yr (De Mets et al., 1994; Wallace et al., 2004).

Beneath the Poverty Indentation, seismic reflection profiles reveal in two-way-time (TWT) the presence of seamounts expressed as “topographic highs” on the subducting Pacific Plate currently residing under the Paritu Ridge complex on the northern side of the indentation and Pantin Bank on the southern side (Figure 7.3). Previous research directly south of the indentation has also identified a seamount ridge beneath the Ritchie Ridge complex (Barnes et al., 2002; Barnes et al., 2009) (refer to Figure 7.1). These ridges rise 1-1.7 s TWT above the subducting plate and extend 85-95 km along the margin (Figure 7.3A). On the surface, the Paritu Ridge complex and Pantin Bank topographies mirror the geometry of the seamounts at depth, with the morpho-structurally dominant and distinctive mid-slope ridge complexes

contrasting with the succession of asymmetric thrust-propagated anticlines developing in the accretionary wedge (Figure 7.3B).

7.3 MODELLING SEAMOUNT SUBDUCTION

Numerical and analogue experiments have been used to effectively model margin convergence with either accretion development or tectonic erosion, complementing marine bathymetric observations along convergent margins. In particular, sandbox experiments have been used to model the effects of seamount and ridge subduction on the styles of deformation, including overprinting, within accretionary wedges (Malavieille, 1984; Malavieille et al., 1991; Lallemand et al., 1992; Kukowski et al., 1994; Dominguez et al., 1998b; Dominguez et al., 1998a; Gutscher et al., 1998; Dominguez et al., 2000).

7.3.1 The Coulomb Wedge Theory

Davis et al's (1983) Coulomb wedge model describes accretionary wedges as evolving in terms of a homogeneous wedge of deformable non-cohesive Coulomb material that is compressed by a push from its wide end and slides along a rigid base. This material deforms until a critical taper is reached, where the wedge will then slide stably. This means that, for a wedge of accretionary material with a given inclination at the base of the wedge, there is a characteristic critical topographic slope angle. Below this critical value, the wedge will not slide when pushed, but will instead deform internally until the topographic slope becomes steep enough to obtain a critical taper. Above the critical value, the wedge will be prone to slumping and erosion and will slide without compressional deformation (Davis et al., 1983). The Coulomb wedge model thus predicts that the first consequence of impact by a seamount as it undergoes subduction is a compressive thickening of the wedge toe above the inboard seamount flank, as the topographic slope becomes under-critical (Lallemand and Le Pichon, 1987) (see Figure 7.10A). As the seamount passes under the shortened and steepened wedge, the wedge becomes over-critical, increasing dramatically as the seamount is fully subducted, leading to severe erosion and slumping in the wake of its passage. The path of the seamount underneath the wedge will be distinguished in the topographic slope by a moving zone of shortening, followed by a zone of listric faulting (Lallemand and Le Pichon, 1987).

7.3.2 Sandbox Experiment

In March, 1995 Dr K.B. Lewis (NIWA), Dr S. Lallemand and S. Dominguez (Montpellier) conducted a series of previously unpublished sandbox experiments in order to model the formation of the Ruatoria debris avalanche, directly north of the Poverty Indentation (for reference to similar experiments, refer to Dominguez et al., 1998b; Dominguez et al., 2000). The NZ3 version of the unpublished sandbox experimental models is used in this study to graphically compare my own interpretations of the structures and margin response from the model to observations of the seafloor response in the Poverty Indentation. This sandbox model is presented as a simplistic model of an accretionary wedge, impacted by a single seamount and is used here to model what effect the initial indentation-forming seamount might have had on the margin and how it compares to effects of subsequent seamount impacts on the same locality. In the immediate Poverty study area, the accretionary wedge has been subjected to multiple and relatively frequent seamount impacts in the past, with a resulting significantly steeper margin front, erosion and more structural complexity than that which is developed in the models. This means that the surface morphologic expression will be harder to identify than that developed in models, making a direct comparison more difficult for this section of the margin. The reason for using this model is to identify whether the fundamental responses of a margin to seamount collision and subduction can still be recognised, despite a history of successive seamount impacts and modification by the evolving canyon system. The sandbox model used has a convergence obliquity of 40^{o} representing the Pacific Plate relative convergence to the Australian Plate for this section of the margin (as was known at the time), however, modern GPS vectors show almost orthogonal localised relative movement from the separate Central Hikurangi block to the Pacific Plate (Wallace et al., 2004) due to combined current convergence effects of backarc extension and large scale crustal rotation of the east coast of North Island (see Beavan et al., 2002; Wallace et al., 2008). With orthogonal convergence at the deformation front, the seamount path may still produce an asymmetrical re-entrant, when the seamount is elongate and orientated at an oblique angle across the margin, as is the case with the Hikurangi seamounts, with effects on the margin likely to be more analogous to ridge subduction than conical seamount subduction (e.g. Dominguez et al., 1998b; Schnurle et al., 1998). This seamount probably collided with the margin front ~1.6 Ma, when extension in the Taupo Volcanic Zone and strike-slip faulting first initiated in the North Island Dextral Fault Belt around 2 Ma (e.g. Nicol et al., 2007). It's also expected that due to the rotation of the East Coast block through time since 2 Ma, the deformation front would likely have been at a different relative position to the initial indentation-forming

seamount than its current position, relative to the currently subducting Puke Seamount, or the approaching Mahia and Gisborne Seamounts.

Four experiments (NZ1 – 4) of oblique subduction were undertaken at the Montpellier laboratory. The NZ3 experiment (Figure 7.4) is presented here as an analogue for the creation for the Poverty Indentation and has the following characteristics (Table 7.1):

initial taper	10^o (surface slope because the basal plate is horizontal)
basal friction	low
backstop	high friction, rigid vertical wall
wedge	deformable backstop dipping 30^o and 6 cm thick near the rigid backstop (wall) composite initial wedge 32 cm wide including a 4 cm wide weak vertical zone (glass beads)
convergence **obliquity**	40^o
sediment input	(oceanic sediment cover) 1 cm thick
sediment output	("basal erosion") 0.5 cm thick
seamount	Hikurangi Plateau-type or "Mahia-type" (elongate seamount with a ratio ~2:1, long axis orientation approximately 70^o to the margin front)
base sheet	mylar - on which the subducting sediments are able to be pulled beneath the over-riding wedge
scale	1 cm in the experiment is approximately equivalent to 1 km in nature

Table 7.1 Sandbox experiment NZ3 characteristics.

7.3.3 Sandbox Model Interpretations

My interpretations of this model are as follows - in sequential order from the first stages of seamount impact to full subduction beneath the margin:

Experiment NZ3 initiates progressive formation of the accretionary wedge with footwall imbricate thrust slices forming in the front of the 20 cm (= 20 km) wide pre-existing sand wedge (Figure 7.5A). In the initial stages of seamount collision, the frontal thrusts of the

accretionary wedge are passively uplifted with only minor deformation, but this is rapidly followed by a bending of the deformation front fabric around the leading slope of the seamount (Figure 7.5A).

New imbricate thrusts propagate up between the previous structural fabric, leading to a concentration of faults directly inboard of the leading slope of the seamount (Figures 7.5B & 7.6). A zone of collapse is then initiated between the seamount leading slope and the zone of uplift, where the accretionary wedge slope has over-steepened to a critical angle (dependant on a range of factors, i.e. pore pressures, stress, material strength) (Figures 7.5B & 7.6). An oblique fault network, diverging away from the seamount, develops directly inboard of the headwall of the collapse zone, following the slip lines defined by the major stress component (convergent, into the margin) and have a transverse-normal sense of motion (Figures 7.5B & 7.6).

The subducting seamount generates a shadow zone in its wake where frontal accretion is inhibited and sediments are dragged into subduction, leading to the formation of a large indentation in the margin (Figure 7.5C). This indentation has asymmetrical geometry consisting of a straight steep side on the acute edge roughly parallel to the convergence vector, and an arcuate gentle slope on the obtuse edge, most likely influenced by the oblique orientation of the seamount relative to the deformation front (but in this sandbox model, also influenced by the oblique nature of the convergence).

On both sides of the indentation, frontal accretion continues with greater stepping-out on the arcuate edge (Figures 7.5D & 7.7). Uplift of the margin slope topography continues on into the over-riding plate sediments and the oblique fault network extends also into this region (Figures 7.5D & 7.7).

Beneath the surface, the décollement is deflected up and over the seamount, emerging at the surface in the middle of the collapse zone, and migrating to the base of the collapse scar once the seamount has passed into the margin and is more deeply subducted (Figures 7.5E & 7.7). Large transverse faults in the over-riding plate curve towards the head of the indentation, connecting with the smaller scale diverging oblique fault network (Figures 7.5E & 7.8). Erosion into the collapse scar is dictated by the indentation geometry, with preferential incision into the axis region encouraged by continued plate convergence (Figures 7.5E, F & 7.8).

Uplift continues into the backstop until the subducting plate is deep enough so that any uplift is no longer able to be expressed in the surface topography, angle of subduction increases or the seamount is thought to be eroded and/or underplated (e.g. Dominguez et al., 2000) (Figure 7.5F).

7.4 COMPARISON OF MODELS WITH THE POVERTY INDENTATION

Comparisons of convergent margins with sandbox models reveal some important similarities in the complex structural deformation and morphological features of a seamount-formed indentation. In the Poverty Indentation there are three stages of seamount subduction: subducted (and responsible for the over-arching geometry of the indentation), currently subducting (underneath Pantin Bank and the Paritu Ridge complex), and in the initial stages of impact (Puke Seamount). To compare the indentation with models, we need to address features of all three of these events as separate effects on the margin.

The Poverty Indentation presents a challenge in modelling the initial indentation-forming seamount subduction event. Comparisons of the over-arching geometry of the Poverty Indentation with sandbox models of both orthogonal and oblique seamount subduction, suggest a closer comparison with oblique convergence, which produces an asymmetrical re-entrant (Dominguez et al., 1998b; Dominguez et al., 1998a; Dominguez et al., 2000), despite current convergence in this system being orthogonal. Further challenges to modelling the effects of seamount subduction on the Poverty Indentation include the effects of multiple impacts over time and the development and modification of the re-entrant by the Poverty Canyon system.

Sandbox models of convergent margins undergoing seamount subduction appear to share some common morphological and structural responses independent of the obliquity of convergence and the geometry of the seamount (e.g. Dominguez et al., 1998b; Dominguez et al., 2000). All sandbox experiments have shown that accretionary wedges thicken and contract when the forward propagation of the basal décollement ceases or is perturbed (Lallemand et al., 1992). This wedge thickening leads to a local taper change, with reactivation of pre-existing thrusts and retreat of the frontal segment.

7.4.1 Models applied to current initial seamount impact

Subduction of the Puke Seamount at the northern end of the Poverty Indentation deformation front (Figure 7.9B) correlates well to the Coulomb wedge model of initial topographic and structural response of the frontal wedge to impact by a seamount (Figure 7.10A and 7.10B(i)). The structural features detailed below also conform to what would be expected for traditional orthogonal convergence (e.g. Dominguez et al., 1998a; Dominguez et al., 2000), consistent with the current relative convergence of the Central Hikurangi Block over the Pacific Plate (Wallace et al., 2004).

In the sandbox models, the development of sets of oblique thrust and strike-slip faults cross-cutting the fundamental structural fabric of the deformation front thrust faults are accompanied by a set of strike-slip and normal faults developing orthogonal to the deformation front, directly inboard of a subducting seamount in the initial stages of impact (see Figures 7.5B-F to 7.8). This relationship of cross-cutting fault sets can be observed where the Puke Seamount is currently in the early stages of being subducted and correlates well to the observed features illustrated in the initial stages of subduction in the sandbox models (Figure 7.9B). A set of normal/strike-slip faults are developing orthogonal to the deformation front and directly inboard of the Puke Seamount, while the deformation front itself is responding to the increased compressional stress by propagation of a closely-spaced series of thrusts in the zone of increased contraction between the Puke Seamount and the frontal wedge. Oblique cross-cutting faults are also developing south of the seamount at an angle to the deformation front, bisecting the margin parallel faults (Figure 7.9B).

7.4.2 Models applied to seamounts currently subducting

Details of seafloor structures resulting from current subduction of seamounts beneath the mid-slope ridge complexes at the Poverty Indentation are inconclusive when compared to sandbox models, as those experiments model effects from much larger scale seamount impacts, forming margin re-entrants. The seamounts currently beneath the mid-slope ridge complexes are no longer indentation-forming, and are instead “rolled-over” by the accretionary wedge. This type of seamount subduction does, however, correlate well to the Coulomb wedge model (Figure 7.10A). Seamount subduction beneath both the Paritu Ridge complex and the northern end of Ritchie Ridge has produced wedge topography that is “under-critical” inboard of the subducting seamounts, and “over-critical” in the trailing slope over the outboard flanks of the seamounts (Figure 7.10B(ii) and (iii)). It is effectively the change in basal friction that drives these observed changes, resulting from the décollement having to steepening up over the

leading slope of the seamount. While the critical wedge is in a different 2-dimensional plane to the seamount trajectory through this oblique convergence experiment, this Coulomb wedge theory of critical slope is supported superficially by interpretations in sandbox models, with the primary features of uplift ahead of or above the seamount, and collapse in the wake of the seamount. Local 3-dimensional topography and wedge tapers are probably evolving more complexly than can be expressed fully in 2-D Coulomb wedge theory. This is, however, not an unusual case of seamount subduction, and while difficult to observe in analogue models, can be compared effectively with other convergent margins - see Section 7.5.1.

7.4.3 Models applied to the initial indentation-forming seamount subduction event

The overall geometry and geomorphology of the wider indentation appears to conform to the geometry accompanying the structure observed in the sandbox models after the seamount has passed completely through the deformation front (Figure 7.9A). The main morphological features correlating with the sandbox models include: i) the axial re-entrant down which the Poverty Canyon now incises; ii) the re-establishment of an accretionary wedge to the south of the indentation axis, accompanied by out-stepping, deformation front propagation into the trench fill sequence, particularly towards the mouth of the canyon; iii) the linear north margin of the indentation with respect to the more arcuate shape of the southern accretionary wedge; and, iv) the set of faults cutting obliquely across the deformation front near the mouth of the canyon (Figure 7.9A).

A challenge to identifying these main morphological correlations from the original indentation-forming seamount subduction is how much the subsequent effects of canyon development and slope modification have had on the geometry of the indentation. It is well known that surface-water erosion by river and wave systems are capable of removing large quantities of sediment from the toe of the slope, leading to substantial mass movement (e.g. Crozier, 1986; Hampton et al., 2004; Shultz, 2007). The Poverty Canyon mouth opens out at an oblique angle to the deformation front, with current-generated scour holes and large sediment waves (5 km across) directly in front of the northern deformation front. This front is over-steepened and highly eroded, as well as being relatively straight for about 30 km. As first thought, from a structural point of view, this straightness, over-steepening and erosion could be attributed to the scraping of the passage of a large seamount on an oblique path into the margin, as observed in sandbox models for oblique subduction, and also suggested as having occurred in the Ruatoria debris avalanche, further north (Collot et al., 2001; Lewis et al.,

2004). However, it is also possible that this feature may have been exaggerated due to turbidity current activity down the Poverty Canyon during the last glacial low-stand ca. 18 ka BP (Lewis, 1973; Orpin et al., 2006). This is relatively recent activity in terms of the structural response of the deformation front, hence a possible explanation for the lack of significant fault scarps or thrust-bounded anticlines across the toe of slope, north of Poverty Canyon (Figure 7.9A).

The Riwha Landslide and scar face in the northern deformation front also shows a geometry consistent with a past seamount subduction event as observed in sandbox models (Figure 7.9C). The northern edge of the scar is roughly parallel to the plate convergence vector labelled on Figure 7.9C. It is very similar in morphology to the Ruatoria debris avalanche (e.g. Lewis, 1997; Lewis et al., 1998; Collot et al., 2001; Lewis et al., 2004), north of the Poverty Indentation, but on a much smaller scale with a debris avalanche block run-out of ~4 km (Figure 7.9C). Uplift and gravitational collapse is currently occurring in the head wall of the scar, as evidenced by the numerous slump scarps extending ~1 km directly behind the head wall and extending in a widening zone nearly 7 km to the south west (Figure 7.9C).

The late stages of seamount subduction in the sandbox models show the onset of substantial erosion into the collapse zone scar (refer to Figures 7.5E, F & 7.8) and are important as a possible analogue for post-subduction modification resulting in the canyon, gullies and debris flows. It is also quite possible that the gullies forming from the shelf-break may have been partially controlled by the diverging oblique fault network and over-steepening at the head of the collapse zone as is interpreted in the model (Figures 7.5F & 7.8).

7.5 POVERTY INDENTATION COMPARED TO OTHER CONVERGENT MARGINS

Models and observations presented on other convergent margins around the world affected by seamount subduction share many similarities in the seafloor topographic and structural response. The difference in margin responses to seamount subduction appear to be characterised by the obliquity of plate convergence (orthogonal to almost margin parallel), the size and shape of the seamount (i.e. conical vs. elongate) and whether the margin is dominated by tectonic erosion or a substantial accretionary wedge.

7.5.1 Seamount subduction

Well studied convergent margins undergoing seamount subduction include: the Japan Trench (Lallemand et al., 1989), the Nankai margin (Yamazaki and Okamura, 1989), the Kuril Trench (Cadet et al., 1987), the Sumatra margin (Moore and Curray, 1980), the New Hebrides Trench (Fisher et al., 1991), the Tonga Trench (Ballance et al., 1989), the Hikurangi margin (Lewis, 1997), the Costa Rican margin (von Huene et al., 1995), and the Mediterranean Ridge (von Huene et al., 1997). Seamount subduction along all of these margins results in localised wedge uplift and subduction of sediment around the seamount (e.g. Yamazaki and Okamura, 1989; Masson et al., 1990; Park et al., 1999; Park et al., 2003). The seamounts are stronger and less deformable than the inner accretionary wedge lithology and are therefore not offscraped onto inner trench slopes, remaining relatively intact during subduction, until possible underplating well under the margin (e.g. Moore and Curray, 1980; Hühnerbach et al., 2005; Sak et al., 2009).

While the wider Hikurangi margin is overall classified as a sediment-rich margin, the Poverty Indentation expresses two different styles of margin being sediment-rich and accretionary to the south, and sediment-starved and erosional to the north. Many of the observed structural and geomorphic features of the Poverty Indentation correlate well both with other sediment-rich convergent margins where seamount subduction is prevalent, particularly the Nankai and Sumatra margins (e.g. Masson et al., 1990; Moore et al., 1990; Bangs et al., 2005; Moore et al., 2009), and the sediment-starved Costa Rican margin (e.g. von Huene et al., 1995; Dominguez et al., 1998a; Hühnerbach et al., 2005; Sak et al., 2009).

The general structural style of the southern section of the Poverty Indentation deformation front is very similar to the Nankai margin, south-western Japan, with proto-thrusts, out-of-sequence thrust activity and megasplay faults, although there appears to be a higher percentage of trough sediment subducted at Nankai (e.g. Park et al., 1999; Moore et al., 2009). The Nankai margin is also interpreted to be over-critical (Lallemand and Le Pichon, 1987). A comparison of the internal accretionary wedge deformation observed in seismic profile inboard of the Nankai Trough, (Park et al., 1999), to the subducting seamounts beneath the South Paritu Ridge and the southern accretionary wedge, reveals many similarities but also some key differences (Figure 7.11). In the Nankai profile, the accretionary wedge has rolled over the seamount and is developing in its wake, as is occurring in the accretionary wedge, south of the Poverty Canyon (Figure 7.11). This differs from the seamount beneath the South Paritu Ridge on the north side of the Poverty Canyon (Figure 7.10B(ii)), where the

margin front is still very steep and erosional behind the seamount. Elongate seamount subduction in the Poverty Indentation has produced corresponding ridge features in the overlying topography (see Figure 7.3B), rather than the discrete circular bulge arising from conical seamount and guyot subduction at Nankai (Park et al., 1999) (Figure 7.11B). These elongate "Mahia-type" (ratio of 2:1) seamounts present on the subducting Hikurangi Plateau appear to produce structural and topographic response in the accretionary wedge that correlates best with a combination of conical and ridge subduction as effectively short ridges, with many similarities to the Gagua Ridge and elongate seamount observed in the Ryukyu accretionary wedge (Dominguez et al., 1998b). Due to the obliquity of convergence in both settings, the trend of the indentation, in the wake of the seamount, tends to be elongated roughly parallel to the relative plate motion, due to the shortening and uplift from the seamount being directed at an angle through the accretionary wedge sediments.

In Sumatra, landward convergence is common and an increase in plate dip at the deformation front differs from both the Nankai and Hikurangi margins. The Sumatra margin is undergoing oblique convergence, with a pronounced backstop structure arising from slip partitioning (e.g. Moore and Curray, 1980; Malod et al., 1995; Kopp et al., 2001). In the Sumatran margin over-steepening and erosion of the frontal wedge slope occurs at the earliest stages of seamount subduction (Moore and Curray, 1980). This is comparable to the Hikurangi margin, but only occurs at latter stages of subduction along the Nankai margin (Park et al., 1999).

The Costa Rican margin is also affected by multiple seamount impacts but is dominated by tectonic erosion with rapid convergence and limited sediment input (e.g. von Huene et al., 2004; Hühnerbach et al., 2005; Sak et al., 2009). Seamount subduction effects on the Costa Rican margin are similar to those experienced on sediment-rich margins, producing significant re-entrant scars and collapse following uplift and subduction into the margin front. However, these scarring effects appear to be more pronounced at the Costa Rican margin (Hühnerbach et al., 2005) due to the small accretionary wedge and the conical geometry of the seamounts (i.e. compared to the more elongate seamounts present at Hikurangi and Nankai). The area of margin slope affected by seamount subduction on the Costa Rican margin seems comparable to the shelf to trench extent of both the Poverty Indentation and re-entrant associated with the Ruatoria debris avalanche on the Hikurangi margin. The Hikurangi margin is therefore unusual in this respect in that its indentations are of a larger scale than those observed on other sediment-rich margins (e.g. Nankai and Sumatra). The key to this may be

the change to the steep erosional slope of the northern sector of the Hikurangi margin, making it more comparable to the Costa Rican margin.

The Puke Seamount impact on the northern edge of the Poverty Indentation deformation front can be compared with the seamounts impacting at the Java Trench (Masson et al., 1990). Masson's analyses of seamounts impacting on the Javan deformation front shows substantial indenting, even in the earliest stages of seamount subduction (Masson et al., 1990, their Figures 3 and 11). However, the Puke Seamount is not creating as much of an indentation in the frontal wedge sediments as is observed in Java. Although the toe of slope is riding up over the advancing slope of the Puke Seamount, as imaged in seismic profile (Figure 7.10B(iii)), the frontal wedge inboard of Puke Seamount is largely absorbing the deformation with very little shortening (see Figure 7.9B). This is most likely due to the over-steepened margin front and the relatively small size of the Puke Seamount compared to the frontal wedge. Generally, it appears that seamounts will be more likely to be "rolled-over" if the margin slope is under-steepened and of comparable "height" to the seamount. Collapse of the margin front is more likely to occur when the margin front is over-steepened and/or is of smaller relative "height" to the seamount.

7.5.2 Submarine canyon systems

While submarine canyon systems are certainly present on other convergent margins undergoing seamount subduction (e.g. Taylor and Smoot, 1984; Fryer and Smoot, 1985; Aubouin, 1989; Dominguez et al., 1998a), the link between the formation of some of these canyons related to seamount impact-derived margin re-entrants is not well explored, and there appears to be no other documented shelf to trench extending canyon system developing in the axis of such a re-entrant, as in the Poverty Indentation.

In the Coast Rican margin, two small (initiating mid-slope) diverging canyons are controlled by the landward propagation of the uplift ahead of the subducting seamount, where they bend around the seamount flanks (Dominguez et al., 1998a, their Figures 8 and 10). Extensive canyon development is observed widely across the margin from the shelf edge, into the upper slope of seamount re-entrants. These are not evolved, heavily incised canyon systems like that observed in the Poverty Indentation, and are instead more indicative of incipient drainage and gullying (Dominguez et al., 1998a). Divergence of shelf to upper slope canyons as a result of seamount uplift is also present in the Japan margin, inboard of the Daiichi-Kashima guyot

(flat-topped seamount) (Dominguez et al., 1998a, their Figure 11). However, the major shelf to trench Hidaka Canyon across the intersection of the Japan and Kuril Trenches is apparently controlled by island-arc structure and not by the subducting seamounts on the oceanic plate (Aubouin, 1989).

Extensive submarine canyon systems across the Bonin fore-arc appear to be independent of seamount subduction (Taylor and Smoot, 1984). However, Klaus and Taylor (1991) note that structural lows in an outer-arc high, present at the base of this margin, have determined the initial locus points of canyon formation, with a major jog in the canyon axis, linear tributaries, and a prominent lineament all trending NW-NNW, also reflecting the outer-arc high basement influence on canyon morphology. This suggests that perhaps a direct investigation and link into seamount subduction effects on canyon development has just not yet been made for this margin, although it is also clear that these features, while perhaps responding to seamount subduction, do not appear to be incising into the axis of any indentations as a subsequence of impact.

7.6 CONCLUSIONS

The Poverty Indentation is a first order structural re-entrant in the Hikurangi margin, formed by the process of repeated seamount subduction. The indentation has evolved sequentially through time as a result of the progressive encroachment, collision, and finally subduction of an initial large seamount, followed by numerous smaller seamounts into the Hikurangi Margin. These multiple smaller seamount impacts have subsequently modified the indentation, and are part of a process continuing through to the present time.

Comparisons with models and other convergent margins reveal many similarities, but also some important differences.

Similarities - All margins and models show:

1) singular or multiple seamount impacts.
2) topographic response as uplift and shortening directly inboard of the seamount(s).
3) morphologic indentations produced in the margin front as a result of seamount subduction.

4) either collapse in the wake of a seamount, or roll-over and re-establishment of the accretionary wedge. This is dependent on the size of the asperity and the style of the margin.

Differences:

1) At Poverty, there is evidence of multiple seamount impacts in the same indentation, each with more mature effects on the margin.
2) The subduction of an obliquely-oriented seamount into the accretionary wedge produces asymmetrical and elongate indentations, even with orthogonal convergence.
3) The Poverty Indentation contains both an accretion-style and an erosion-style margin with corresponding variations in the effects of seamount subduction on the those margin morphologies.
4) The distinctive elongate seamounts subducting at Poverty produce structures and morphologic effects that are a hybrid between observed effects of conical seamount subduction and ridge subduction on other margins.
5) The Ruatoria and Poverty indentations on the Hikurangi margin appear to be on the larger end of the scale than many indentations observed at other margins (i.e. extending fully from shelf edge to trench floor).
6) The Poverty Indentation is the only documented seamount impact-derived indentation with a fully developed shelf to trench canyon system incising into its axis.

References

Aubouin, J., 1989. Some aspects of the tectonics of subduction zones. Tectonophysics, 160(1-4): 1-3, 7-21.

Ballance, P.F., Scholl, D.W., Vallier, T.L., Stevenson, A.J., Ryan, H. and Herzer, R.H., 1989. Subduction of a Late Cretaceous seamount of the Louiseville Ridge at the Tonga Trench: A model of normal and accelerated tectonic erosion. Tectonics, 8(5): 953-962.

Bangs, N.L., Shipley, T.H., Moore, G.F., Moore, C., Gulick, S.P.S., Kuramoto, S., Nakamura, Y. and Park, J.-O., 2005. The 3-D architecture of the Nankai trough accretionary wedge and the development of the seismogenic zone. Margins Newsletter, 14: 1-5.

Barnes, P.M., Nicol, A. and Harrison, T., 2002. Late Cenozoic evolution and earthquake potential of an active listric thrust complex above the Hikurangi subduction zone, New Zealand. GSA Bulletin, 114(11): 1379-1405.

Barnes, P.M., Lamarche, G., Bialas, J., Henrys, S., Pecher, I.A., Netzeband, G., Greinert, J., Mountjoy, J.J., Pedley, K.L. and Crutchley, G., 2009. Tectonic and Geological Framework for Gas Hydrates and Cold Seeps on the Hikurangi Subduction Margin, New Zealand. Marine Geology, in press.

Beavan, J., Tregoning, P., Bevis, M., Kato, T. and Meertens, C.M., 2002. Motion and rigidity of the Pacific Plate and implications for plate boundary deformation. Journal of Geophysical Research, 107(B10).

Cadet, J.-P., Kobayashi, K., Aubouin, J., Boulègue, J., Deplus, C., Dubois, J., von Huene, R., Jolivet, L., Kanazawa, T., Kasahara, J., Koizumi, K., Lallemand, S., Nakamura, Y., Pautot, G., Suyehiro, K., Tani, S., Tokuyama, H. and Yamazaki, T., 1987. The Japan Trench and its juncture with the Kuril Trench: cruise results of the Kaiko project, Leg 3. Earth and Planetary Science Letters, 83(1-4): 267-284.

Collot, J.-Y., Delteil, J., Lewis, K.B., Davy, B., Lamarche, G., Audru, J.-C., Barnes, P., Chanier, F., Chaumillon, E., Lallemand, S.E., Mercier de Lepinay, B., Orpin, A., Pelletier, B., Sosson, M., Toussaint, B. and Uruski, C., 1996. From oblique subduction to intra-continental transpression; structures of the southern Kermadec-Hikurangi margin from multibeam bathymetry, side-scan sonar and seismic reflection. Marine Geophysical Researches, 18(2-4): 357-381.

Collot, J.-Y., Lewis, K., Lamarche, G. and Lallemand, S., 2001. The giant Ruatoria debris avalanche on the northern Hikurangi margin, New Zealand; results of oblique seamount subduction. Journal of Geophysical Research, B, Solid Earth and Planets, 106(9): 19,271-19,297.

Crozier, M.J., 1986. Landslides: causes, consequences and environment.

Davis, D., Suppe, J. and Dahlen, F.A., 1983. Mechanics of fold-and-thrust belts and accretionary wedges. Journal of Geophysical Research, 88: 1153-1172.

Davy, B. and Wood, R., 1994. Gravity and magnetic modelling of the Hikurangi Plateau. Marine Geology, 118(1-2): 139-151.

De Mets, C., Gordon, R.G., Argus, D.F. and Stein, S., 1990. Current plate motions. Geophysical Journal International, 101: 425-478.

De Mets, C., Gordon, R.G., Argus, D.F. and Stein, S., 1994. Effect of recent revisions to the geomagnetic reversal time scale on estimates of current plate motions. Geophysical Research Letters, 21(20): 2191-2194.

Dominguez, S., Lallemand, S.E., Malavieille, J. and von Huene, R., 1998a. Upper plate deformation associated with seamount subduction. Tectonophysics, 293(3-4): 207-224.

Dominguez, S., Lallemand, S., Malavieille, J. and Schnurle, P., 1998b. Oblique subduction of the Gagua Ridge beneath the Ryukyu accretionary wedge system: Insights from marine observations and sandbox experiments. Marine Geophysical Researches, 20: 383-402.

Dominguez, S., Malavieille, J. and Lallemand, S., 2000. Deformation of accretionary wedges in response to seamount subduction - insights from sandbox experiments. Tectonics, 19(1): 182-196.

Fisher, M.A., Collot, J.-Y. and Geist, E.L., 1991. Structure of the collision zone between Bouganville Guyot and the accretionary wedge of the New Hebrides Island Arc, Southwest Pacific. Tectonics, 10(5): 887-903.

Fryer, P. and Smoot, N.C., 1985. Processes of seamount subduction in the Mariana and Izu-Bonin trenches. Marine Geology, 64(1-2): 77-90.

Gutscher, M.-A., Kukowski, N., Malavieille, J. and Lallemand, S., 1998. Material transfer in accretionary wedges from analysis of a systematic series of analog experiments. Journal of Structural Geology, 20(4): 407-416.

Hampton, M.A., Griggs, G.B., Edil, T.B., Guy, D.E., Kelley, J.T., Komar, P.D., Mickelson, D.M. and Shipman, H.M., 2004. Processes that govern the formation and evolution of coastal cliffs. . In: M.A. Hampton and G.B. Griggs (Editors), Formation, Evolution,

and Stability of Coastal Cliffs — Status and Trends, U.S. Geological Survey Professional Paper, pp. 7-38.

Hühnerbach, V., Masson, D.G., Bohrmann, G., Bull, J.M. and Weinrebe, W., 2005. Deformation and submarine landsliding caused by seamount subduction beneath the Coasta Rica continental margin - new insights from high-resolution sidescan sonar data. In: D.M. Hodgson and S.S. Flint (Editors), Submarine Slope Systems: Processes and Products. Geological Society, Special Publications, London, pp. 195-205.

Klaus, A. and Taylor, B., 1991. Submarine canyon development in the Izu-Bonin forearc: A SeaMARC II and seismic survey of Aoga Shima Canyon Marine Geophysical Researches, 13(2): 131-152.

Kopp, H., Flueh, E.R., Klaeschen, D., Bialas, J. and Reichert, C., 2001. Crustal structure of the central Sunda margin at the onset of oblique subduction. Geophysical Journal International, 147: 449-474.

Kukowski, N., Huene, R., Malavieille, J. and Lallemand, S.E., 1994. Sediment accretion against a buttress beneath the Peruvian continental margin at 12Â° S as simulated with sandbox modeling. International Journal of Earth Sciences, 83(4): 822-831.

Lallemand, S. and Le Pichon, X., 1987. Coloumb wedge model applied to the subduction of seamounts in the Japan Trench. Geology, 15: 1065-1069.

Lallemand, S., Culotta, R. and Von Huene, R., 1989. Subduction of the Daiichi Kashima Seamount in the Japan Trench. Tectonophysics, 160(1-4): 231-233.

Lallemand, S., Collot, J.-Y., Pelletier, B., Rangin, C. and Cadet, J.-P., 1990. Impact of oceanic asperities on the tectogenesis of modern convergent margins. Oceanologica Acta, Special 10: 56-69.

Lallemand, S., Malavieille, J. and Calassou, S., 1992. Effects of oceanic ridge subduction on accretionary wedges: experimental modelling and marine observations. Tectonics, 11(6): 1301-1313.

Lewis, K., Collot, J.-Y. and Lallemand, S., 1998. The dammed Hikurangi Trough: a channel-fed trench blocked by subducting seamounts and their wake avalanches (New Zealand-France GeodyNZ Project). Basin Research, 10(4): 441-468.

Lewis, K.B., 1973. Erosion and deposition on a tilting continental shelf during Quaternary oscillations of sea level. New Zealand Journal of Geology and Geophysics, 16: 281-301.

Lewis, K.B. and Pettinga, J.R., 1993. The emerging, imbricate frontal wedge of the Hikurangi Margin. Sedimentary Basins of the World, 2: 225-250.

Lewis, K.B., 1997. The succession of seamount impacts and giant avalanches on the Hikurangi margin. In: D.N.B. Skinner (Editor), Geological Society of New Zealand 1997 annual conference; programme and abstracts Geological Society of New Zealand Lower Hutt pp. 99.

Lewis, K.B., Lallemand, S. and Carter, L., 2004. Collapse in a Quaternary shelf basin off East Cape, New Zealand: evidence for passage of a subducted seamount inboard of the Ruatoria giant avalanche. New Zealand Journal of Geology and Geophysics, 47: 415-429.

Malavieille, J., 1984. Modelisation experimentale des chevauchements imbriques: Application aux chaines de montagnes. Bulletin de la Societe Geologique de France, 7: 129-138.

Malavieille, J., Larroque, C., Lallemand, S. and Stephan, J.-F., 1991. Experimental modelling of accretionary wedges. Terra Nova Abstracts, 3: 367.

Malod, J.A., Karta, K., Beslier, M.O. and Zen Jr, M.T., 1995. From normal to oblique subduction: Tectonic relationships between Java and Sumatra. Journal of Southeast Asian Earth Sciences, 12(1/2): 85-93.

Masson, D.G., Parson, L.M., Milsom, J., Nichols, G., Sikumbang, N., Dwiyanto, B. and Kallagher, H., 1990. Subduction of seamounts at the Java Trench: a view with long-range sidescan sonar. Tectonophysics, 185(1-2): 51-65.

Moore, G.F. and Curray, J.R., 1980. Structure of the Sunda Trench lower slope off Sumatra from multichannel seismic reflection data. Marine Geophysical Researches, 4: 319-340.

Moore, G.F., Shipley, T.H., Stoffa, P.L., Karig, D.E., Taira, A., Kuramoto, S., Tokuyama, H. and Suyehiro, K., 1990. Structure of the Nankai trough accretionary zone from multichannel seismic reflection data. Journal of Geophysical Research, 95(B6): 8753-8765.

Moore, G.F., Park, J.-O., Bangs, N.L., Gulick, S.P.S., Tobin, H.J., Nakamura, Y., Sato, S., Tsuji, T., Yoro, T., Tanaka, H., Uraki, S., Kido, Y., Sanada, Y., Kuramoto, S. and Taira, A., 2009. Structural and seismic stratigraphic framework of the NanTroSEIZE Stage 1 transect. Proceedings of the Integrated Ocean Drilling Program, 314/315/316.

Nicol, A., Mazengarb, C., Chanier, F., Rait, G., Uruski, C. and Wallace, L., 2007. Tectonic evolution of the active Hikurangi subduction margin, New Zealand, since the Oligocene. Tectonics, 26(3).

Orpin, A., Alexander, C., Carter, L., Kuehl, S. and Walsh, J.P., 2006. Temporal and spatial complexity in post-glacial sedimentation on the tectonically active, Poverty Bay continental margin of New Zealand. Continental Shelf Research, 26(17-18): 2205-2224.

Park, J.-O., Tsuru, T., Kaneda, Y., Kono, Y., Kodaira, S., Takahashi, N. and Kinoshita, H., 1999. A subducting seamount beneath the Nankai accretionary prism off Shikoku, southwestern Japan. Geophysical Research Letters, 26(7): 931-934.

Park, J.-O., Moore, G.F., Tsuru, T., Kodaira, S. and Kaneda, Y., 2003. A subducted oceanic ridge influencing the Nankai megathrust earthquake rupture. Earth and Planetary Science Letters, 217(1-2): 77-84.

Pedley, K.L., Barnes, P.M., Pettinga, J.R. and Lewis, K., 2009. Seafloor structural geomorphic evolution of the accretionary frontal wedge in response to seamount subduction, Poverty Indentation, New Zealand. Marine Geology, In Press, Corrected Proof.

Sak, P.B., Fisher, D.M., Gardner, T.W., Marshall, J.S. and LaFemina, P.C., 2009. Rough crust subduction, forearc kinematics, and Quaternary uplift rates, Costa Rican segment of the Middle American Trench. GSA Bulletin, 121(7/8): 992-1012.

Schnurle, P., Liu, C.-S., Lallemand, S.E. and Reed, D.L., 1998. Structural insight into the south Ryukyu margin: effects of the subducting Gagua Ridge. Tectonophysics, 288(1-4): 237-250.

Shultz, W.H., 2007. Landslide susceptibility revealed by LIDAR imagery and historical records, Seattle, Washington. Engineering Geology, 89(1-2): 67-87.

Taylor, B. and Smoot, N.C., 1984. Morphology of Bonin fore-arc submarine canyons. Geology, 12: 724-727.

von Huene, R., Bialas, J., Flueh, E.R., Cropp, B., Csernok, T., Fabel, E., Hoffman, J., Emeis, K.-C., Holler, P., Jeschke, G., Leandro, M.C., Perez Fernandez, I., Chavarria, S.J., Florez, H.A., Escobedo, Z.D., Leon, R. and Barrios, L.O., 1995. Morphotectonic features of the Coast Rican Pacific margin surveyed during the Sonne 76 cruise. Geological Society of America Abstracts Special Paper, 295: 291-307.

von Huene, R., Restona, T., Kukwskia, N., Dehghanib, G.A., Weinrebe, W. and IMERSE Working Group, 1997. A subducting seamount beneath the Mediterranean Ridge. Tectonophysics, 271(3-4): 249-261.

von Huene, R., Ranero, C.R. and Watts, P., 2004. Tsunamigenic slope failure along the Middle America Trench in two tectonic settings. Marine Geology, 203(3-4): 303-317.

Walcott, R.I., 1978. Present tectonics and late Cenozoic evolution of New Zealand. Geophysical Journal of the Royal Astronomical Society, 52: 137-164.

Walcott, R.I., 1987. Geodetic Strain and the Deformational History of the North Island of New Zealand during the Late Cainozoic. Philosophical Transactions of the Royal Society of London. Series A, Mathematical and Physical Sciences, 321(1557): 163-181.

Wallace, L., Beavan, J., McCaffrey, R. and Darby, D.J., 2004. Subduction zone coupling and tectonic block rotations in the North Island, New Zealand. Journal of Geophysical Research, 109.

Wallace, L., Ellis, S. and Mann, P., 2008. Tectonic block rotation, arc curvature, and back-arc rifting: Insights into these processes in the Mediterranean and the western Pacific. IOP Conf. Series: Earth and Environmental Science, 2.

Wood, R. and Davy, B., 1994. The Hikurangi Plateau. Marine Geology, 118(1-2): 153-173.

Yamazaki, T. and Okamura, Y., 1989. Subducting seamounts and deformation of overriding forearc wedges around Japan. Tectonophysics, 160(1-4): 207-217.

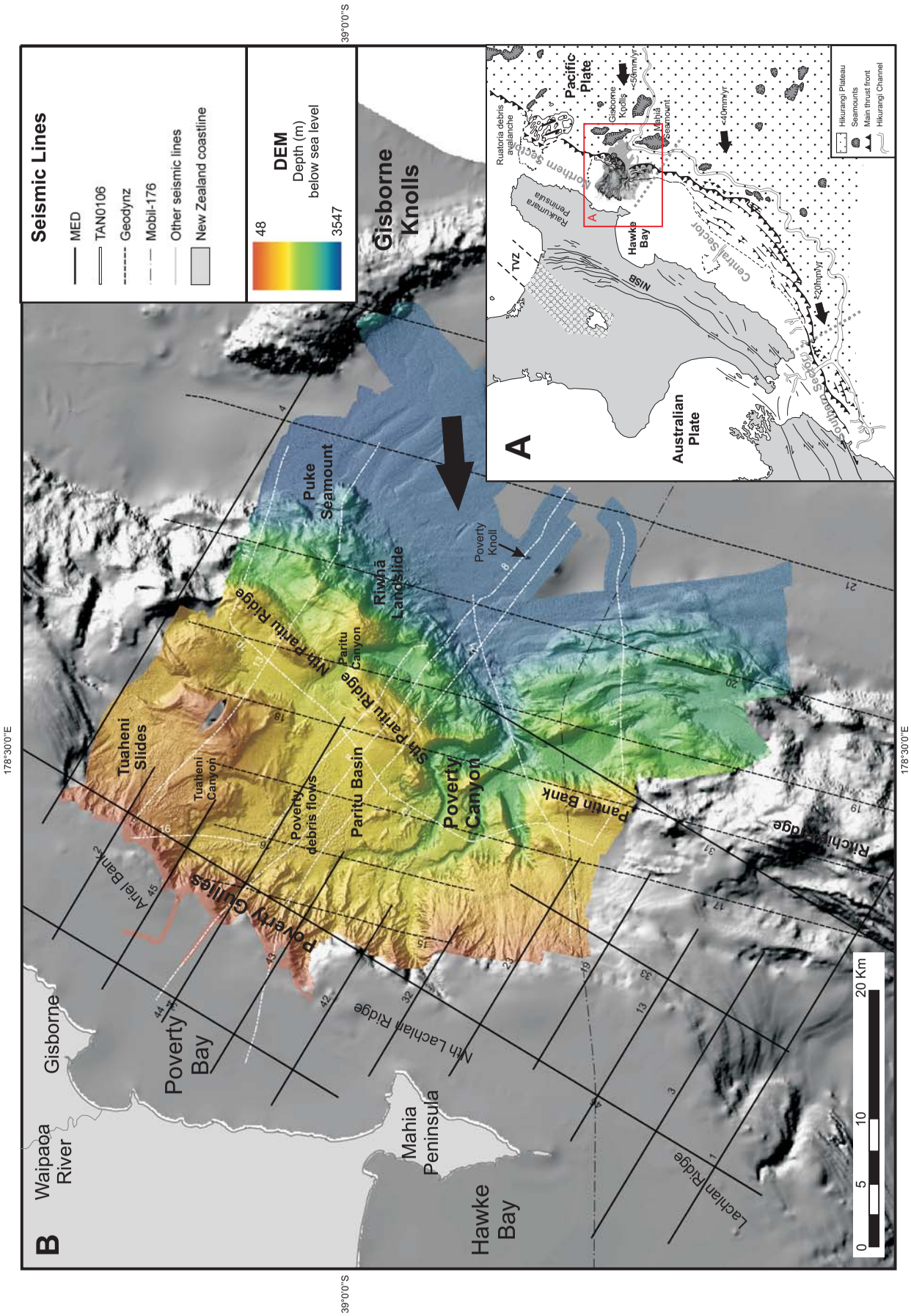

Figure 7.1 A: The Hikurangi margin and location of the Poverty Indentation, highlighting the central and northern sectors of the margin (separated by the grey dotted line), the Ruatoria debris avalanche, extent of the Hikurangi Plateau (stippled) and Hikurangi Channel, and the presence of seamounts directly outboard of the margin front (dark grey). Modified after Lewis et al. 1998.

B: The Poverty Indentation with DEM coverage (coloured swath image) and available seismic lines. Named morpho-structural features discussed in text are labelled.

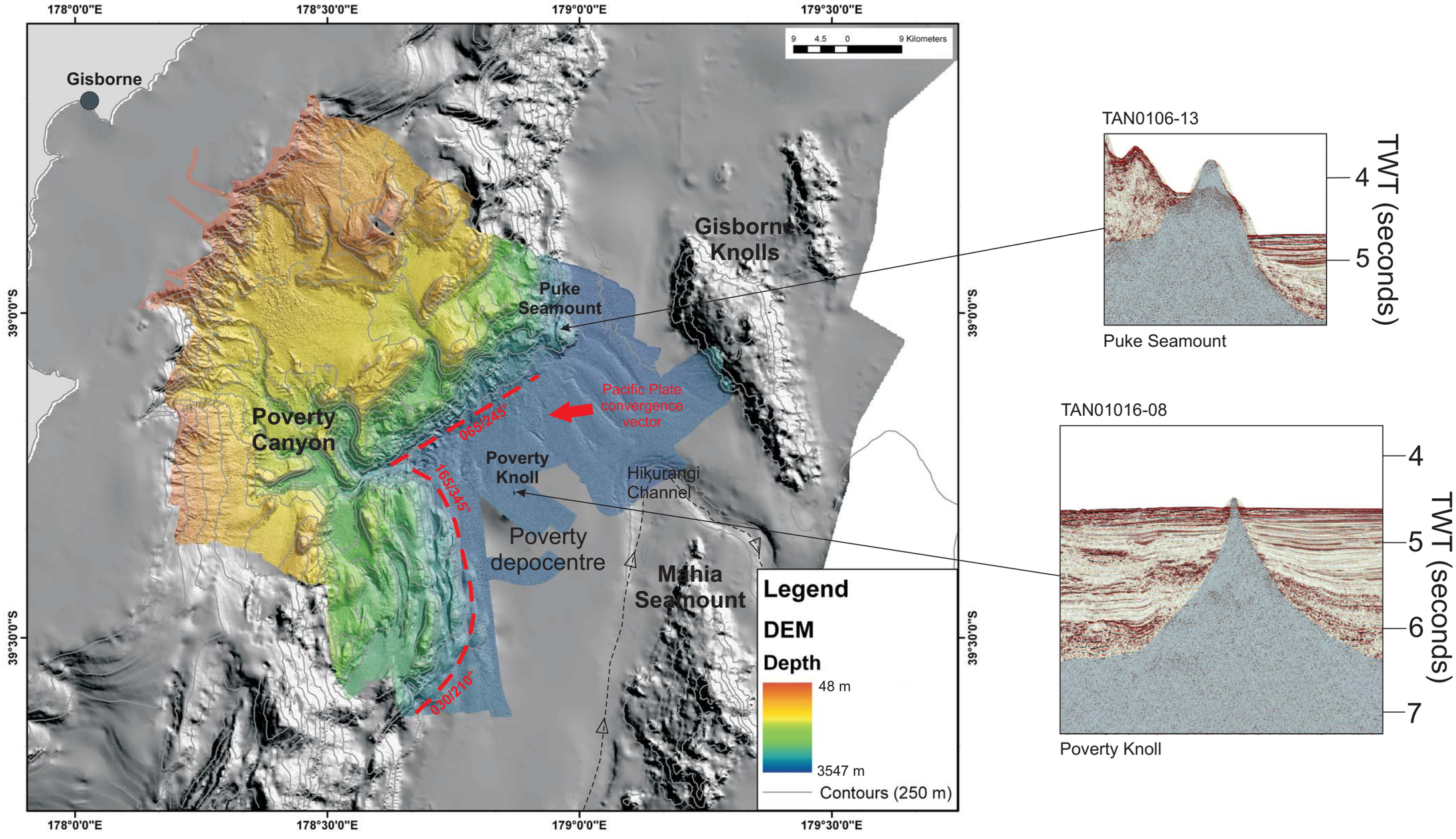

Figure 7.2 Morpho-structural expressions and seamounts encroaching on the Poverty Indentation. Red dashed line and trends indicate the approximate orientation of the deformation front. Vertical exaggeration = x5.

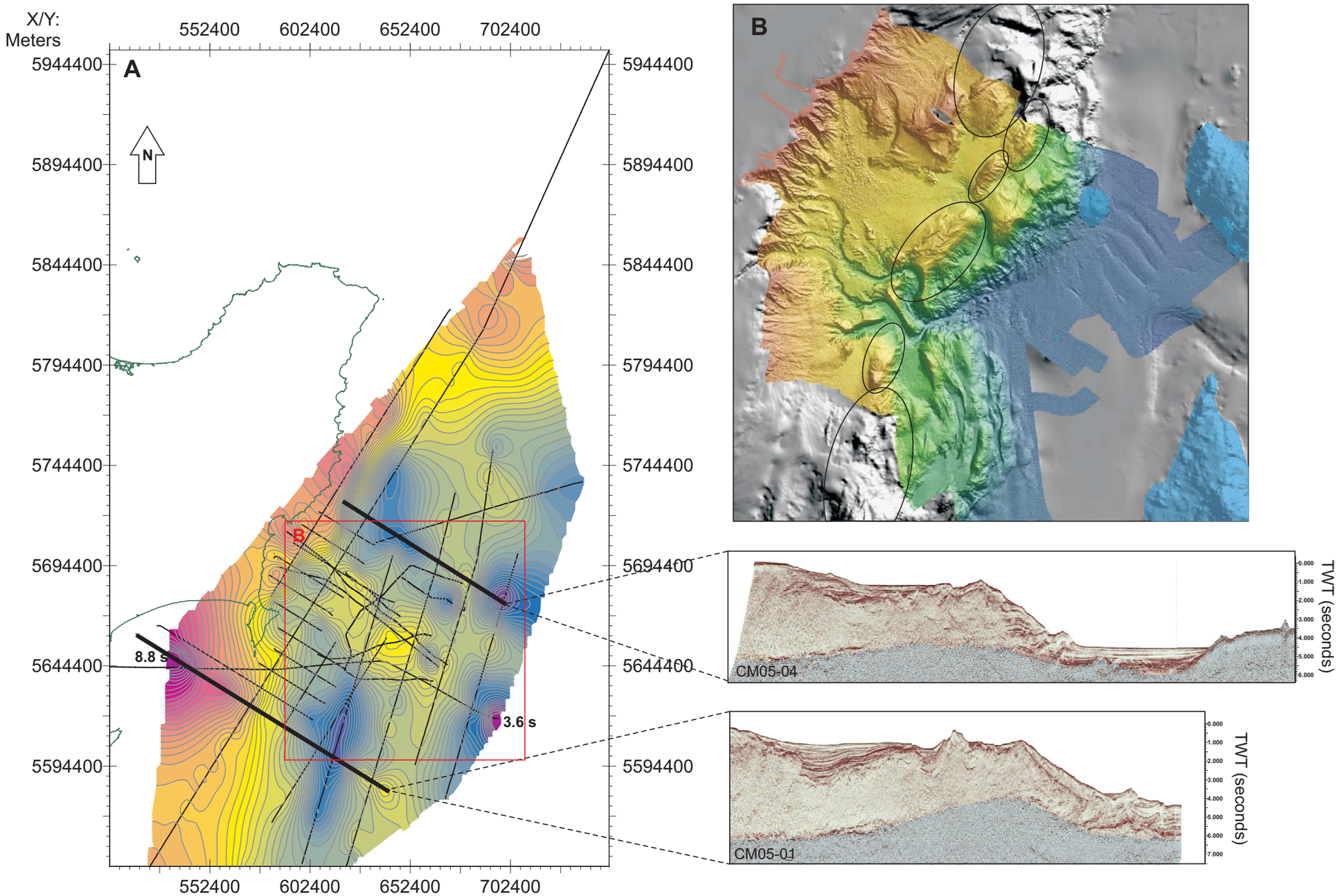

Figure 7.3 A: Contour map of the relief on the Pacific Plate in TWT (seconds).Note that due to these being time profiles, rather than depth converted, velocity pull-up will result in apparent highs beneath ridges resulting from the slower velocity of water compared to sediment and rock. Depth conversions from one section (discussed in Chapter 6) and in other research reveals that these highs are valid, although may not be as pronounced as expressed in these time profiles. Seismic lines are indicated in black. Contours (in grey) are spaced 0.1 seconds apart from 3.6 to 8.8 seconds. Contours extrapolated using seismic profiles from voyages GeodyNZ, TAN0106 and CM05. Outline of the East Coast, North Island is in green. Seismic profiles through lines CM05-04 and CM05-01reveal the correlation between the time relief on the subducting plate and the expressions of the large mid-slope ridges.

B: Location of the mid-slope ridge anticlines (ellipses) adjacent to and inboard of the Poverty Indentation. Known seamounts are highlighted in blue. DEM is lit from 045° at 45°. Vertical exaggeration = x5

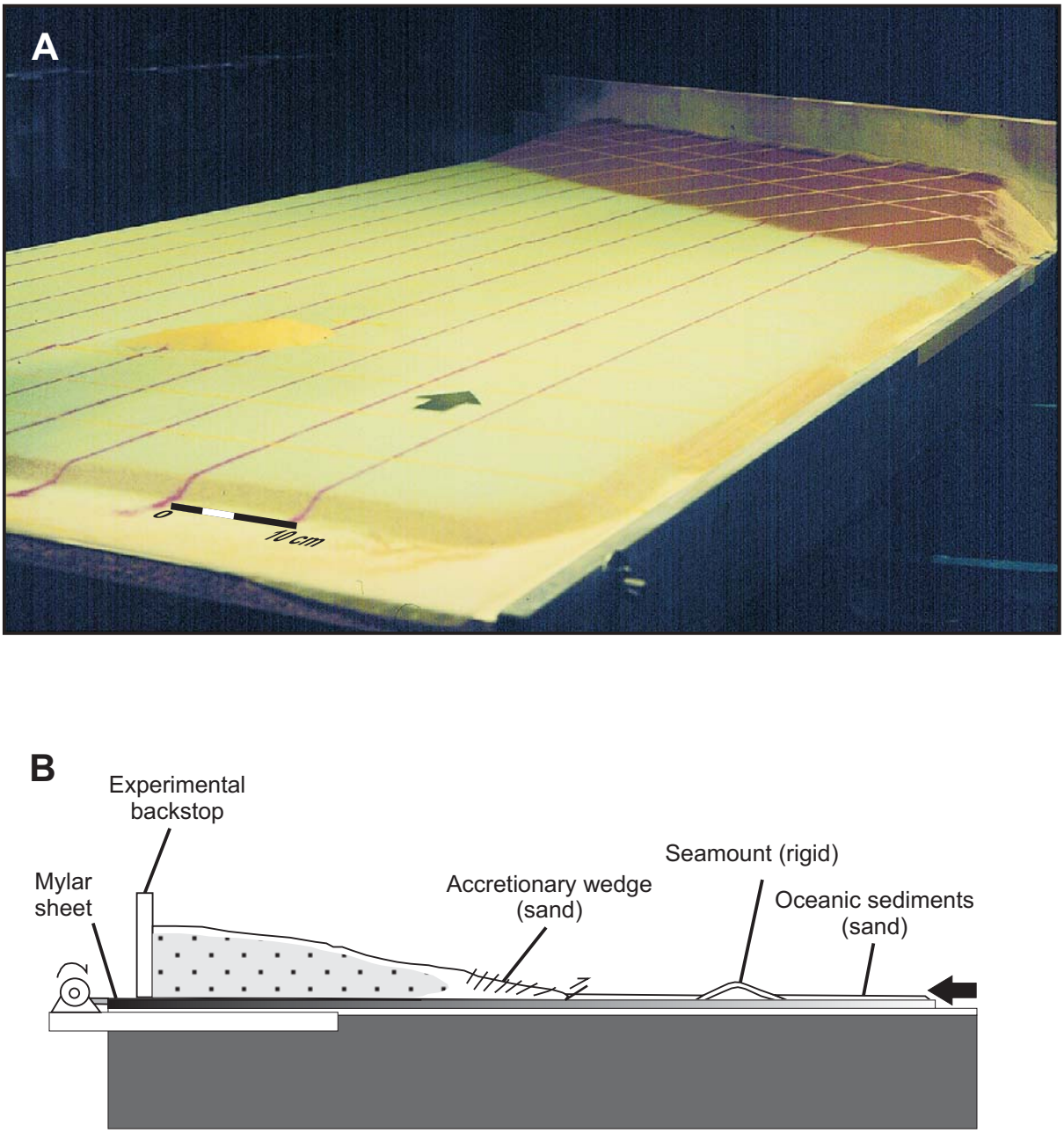

Figure 7.4 A: Slide photograph of the NZ3 experiment setup with green sand representing the subducting oceanic Pacific Plate, brown representing the over-riding Australian Plate, and yellow representing a "Mahia-type" elongate seamount (ratio approximately 2:1) located on the subducting plate. Convergence is at 40° obliquity. Deformation squares measure 10 cm x 10 cm.

B: Schematic cross-section of the experimental set-up showing internal structure during initial stage before seamount impact (modified after Dominguez et al., 1998).

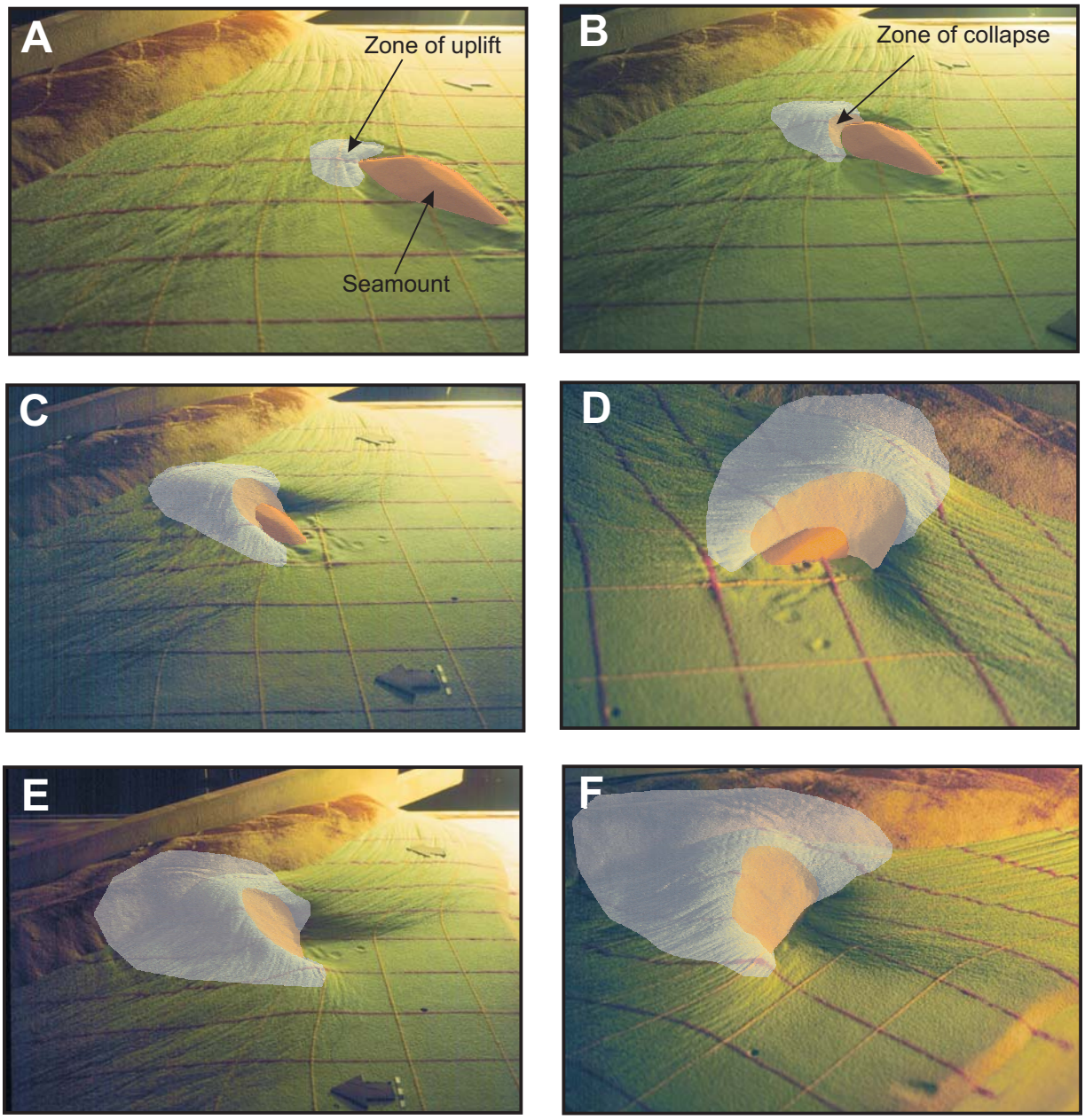

Figure 7.5 Seamount subduction sequence of events in experiment NZ3.

A: Initial seamount impact with the accretionary wedge.

B: Uplift occurs directly inboard (in front of the seamount along the line of convergence) of the leading seamount slope as the margin sediments are forced inwards.

C: A large indentation develops in the margin, accompanied by increasing uplift.

D: The seamount has almost disappeared beneath the wedge sediments.

E: The seamount has been completely engulfed by the margin, leaving a significant indentation. A small accretionary wedge is redeveloping in the wake of the seamount.

F: Uplift continues on into the over-riding plate sediments.

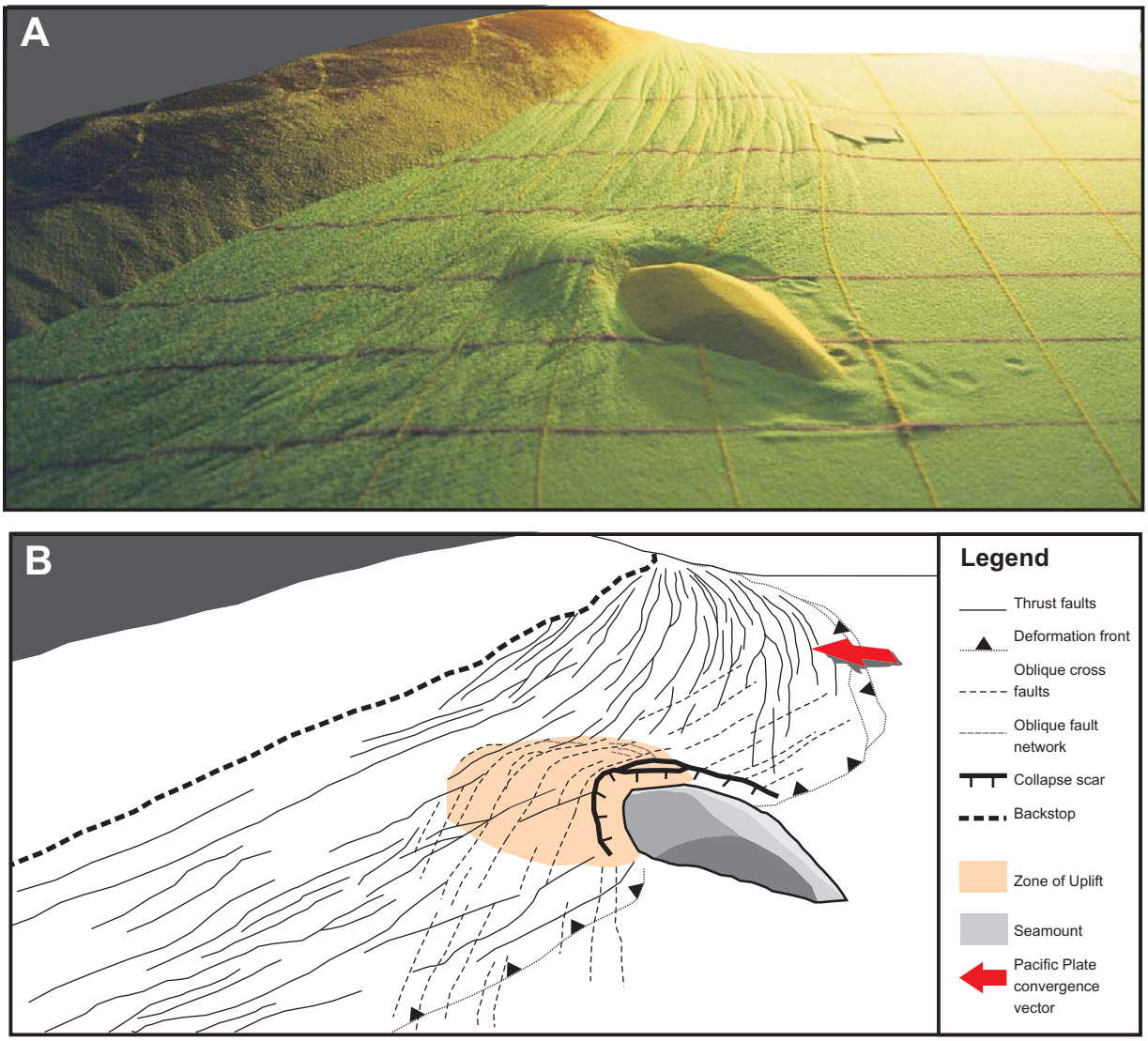

Figure 7.6 Initial seamount (in grey) collision with the accretionary wedge.

A: Photograph of sandbox experiment NZ3.

B: Structural interpretation of sandbox experiment. Uplift and a collapse zone develop directly inboard of the leading seamount slope with an oblique fault network (brown lines)forming above the collapse head wall. Some oblique cross faults (dashed lines) develop in the accretionary wedge, leading out and away from the leading edge of the seamount.

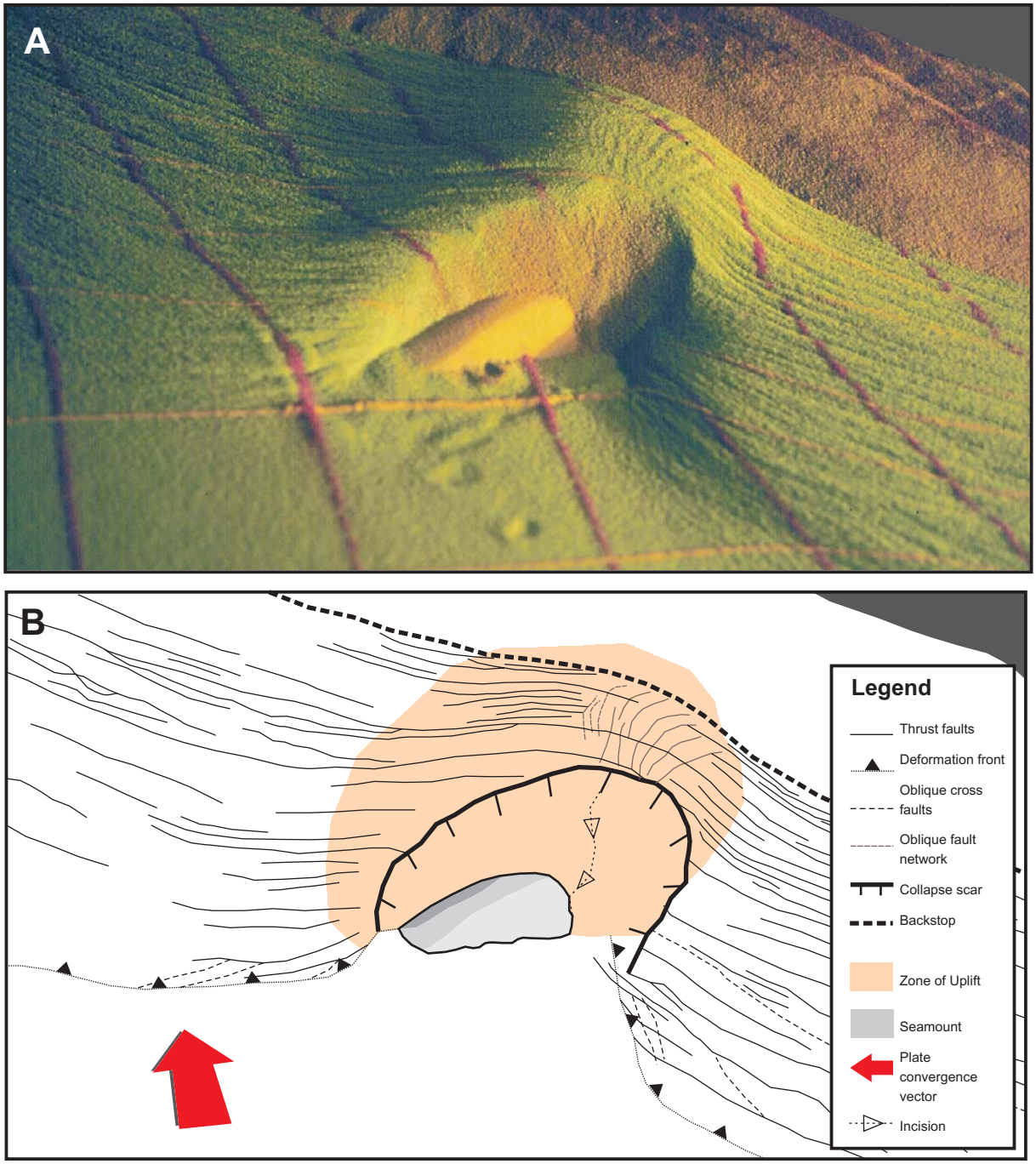

Figure 7.7 A: Photograph of sandbox experiment NZ3.

B: Structural interpretation of seamount collision in sandbox experiment. Uplift continues into the accretionary wedge, inboard of the seamount, with further propagation of the oblique fault network (brown lines) and an increase in the region affected by collapse. Erosion by incision into the collapse scar face initiates in the axis of the indentation.

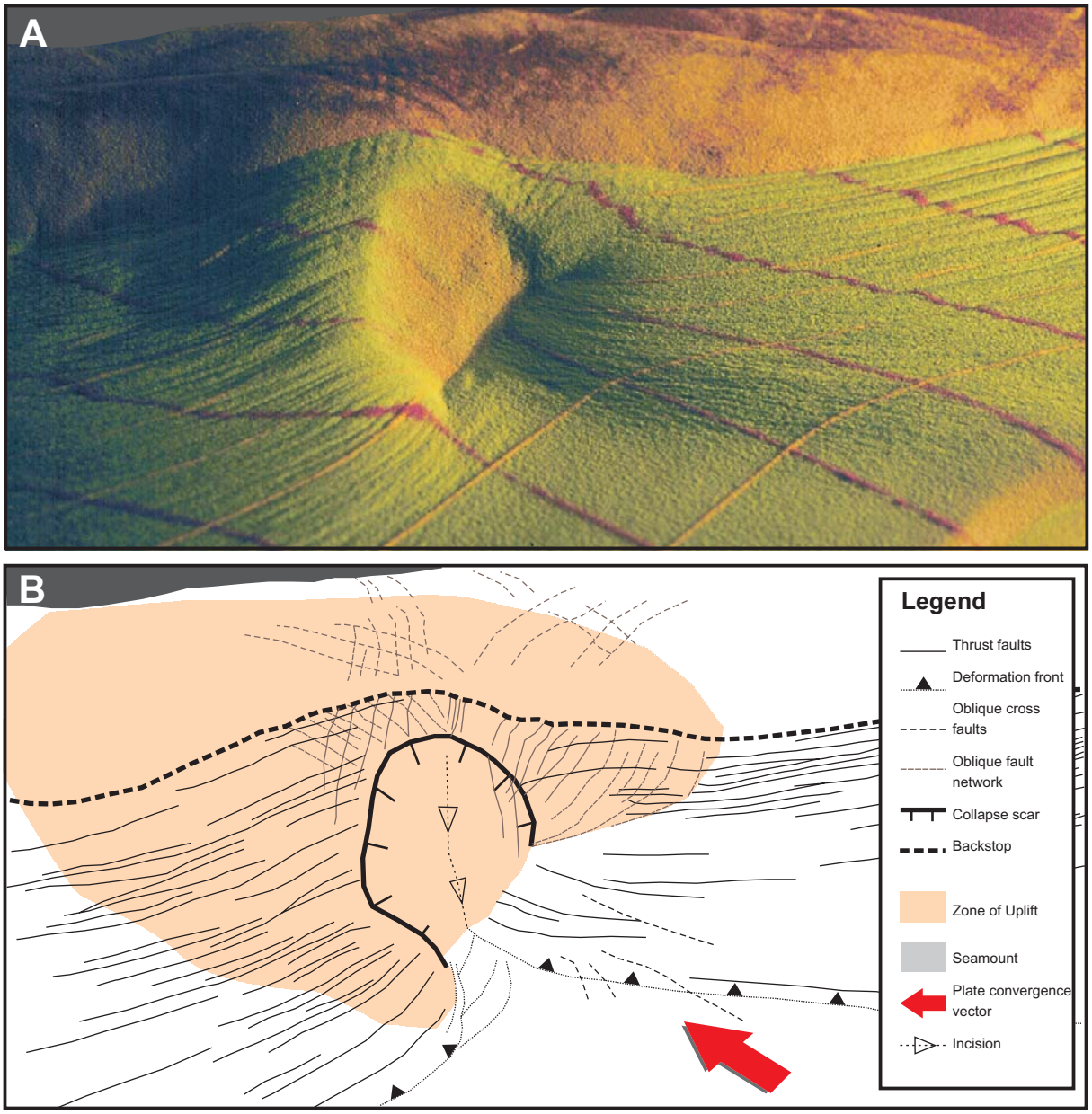

Figure 7.8 A: Photograph of sandbox experiment NZ3.

B: Structural interpretation of sandbox experiment immediately after the seamount has subducted under the frontal wedge. Uplift extends into the over-riding plate sediments, accompanied by the development of an extensive oblique fault network (brown lines). Incision into the axis of the indentation becomes more pronounced. Thrust faults develop outboard from the basal slope of the collapse scar.

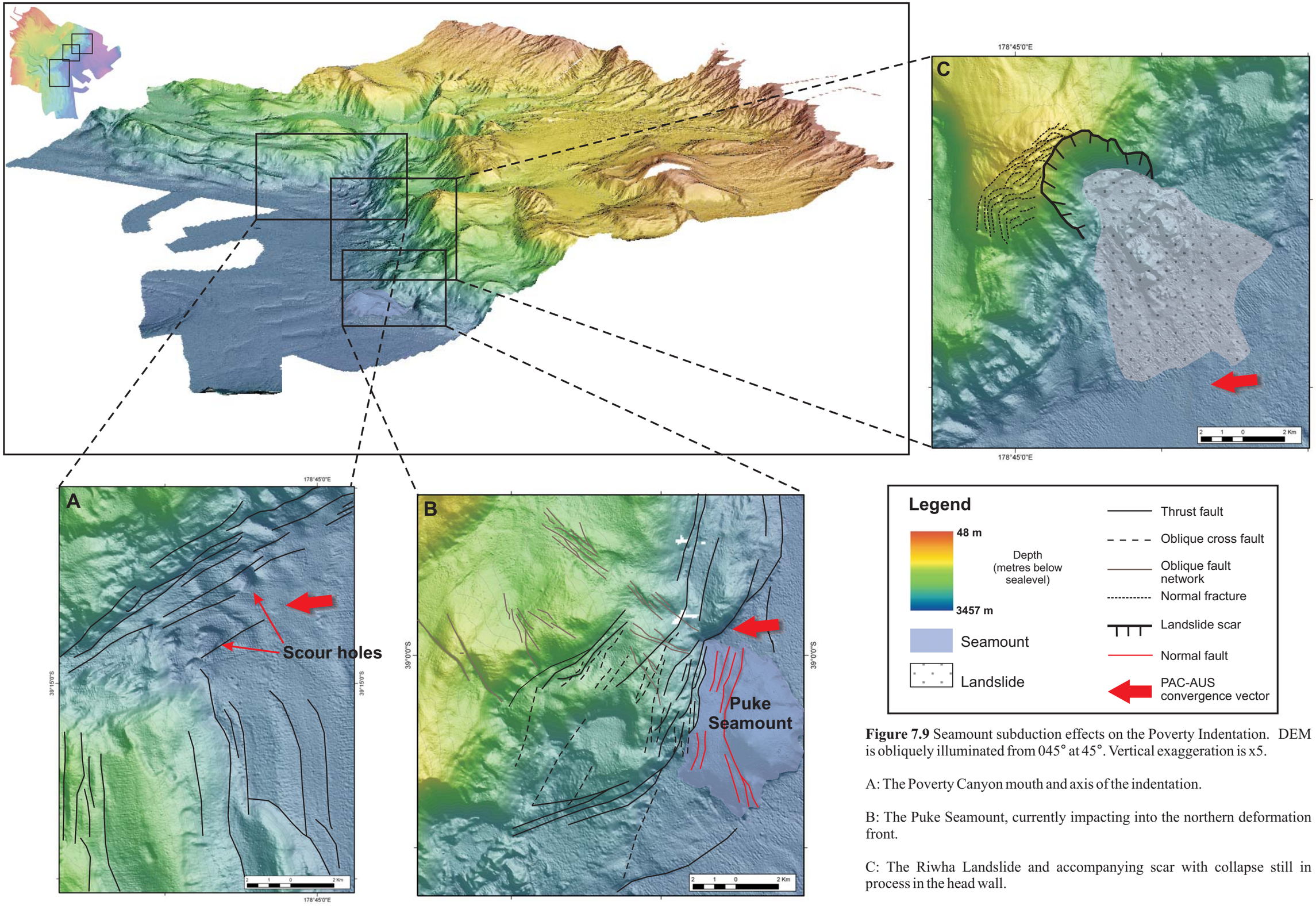

Figure 7.9 Seamount subduction effects on the Poverty Indentation. DEM is obliquely illuminated from 045° at 45°. Vertical exaggeration is x5.

A: The Poverty Canyon mouth and axis of the indentation.

B: The Puke Seamount, currently impacting into the northern deformation front.

C: The Riwha Landslide and accompanying scar with collapse still in process in the head wall.

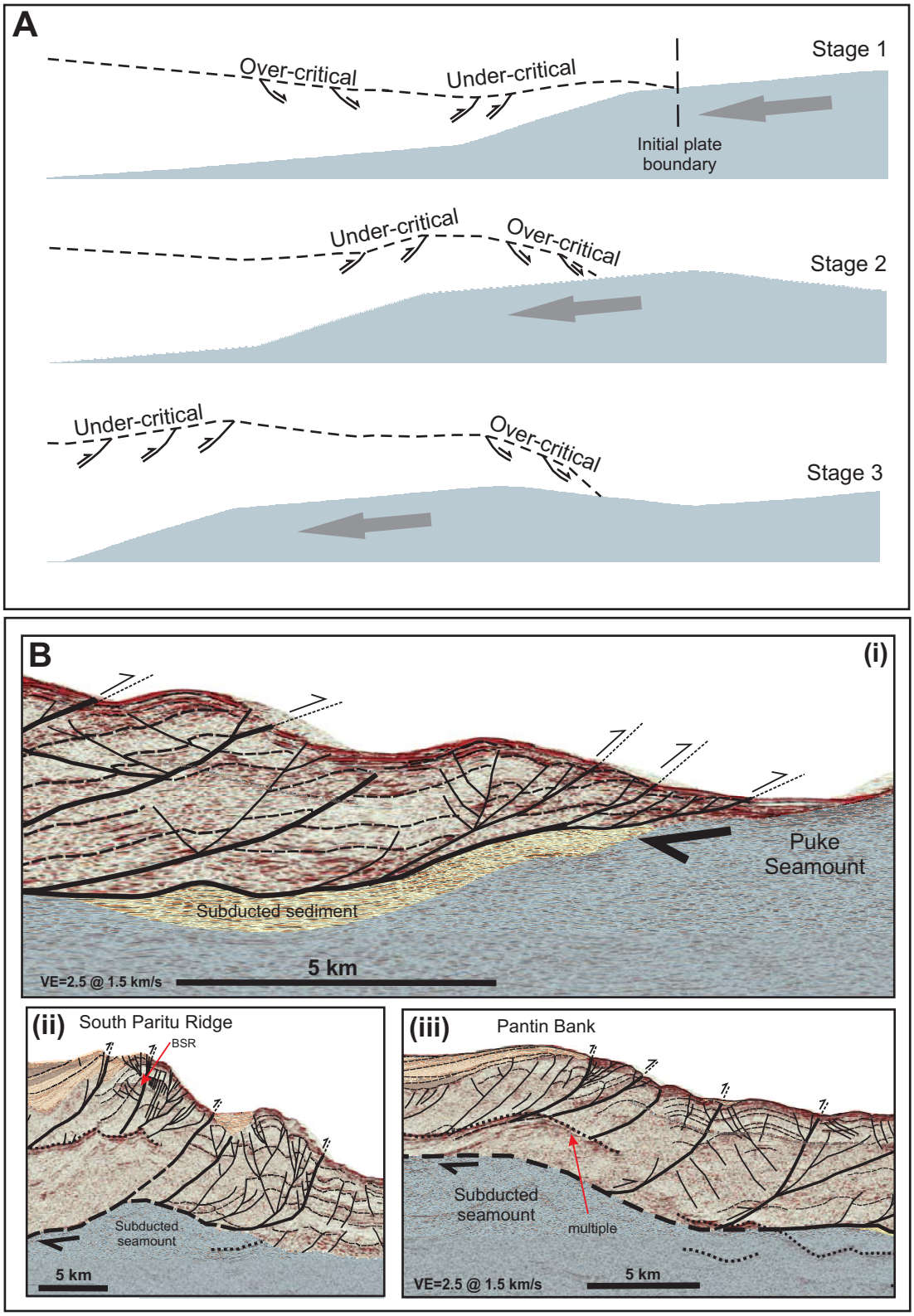

Figure 7.10 A: Progressive 2D model of seamount subduction beneath a convergent margin characterised by tectonic erosion. Modified from Lallemand and Le Pichon (1987). Stages show transient increase in the angle/inclination of the wedge lower boundary as a seamount subducts. Under-critical slope implies shortening and thickening, whereas over-critical slope implies erosion.

B: Examples of seamount subduction in the Poverty Indentation with deformation response in the over-riding sediment wedge. Note that the local topography and wedge tapers are probably evolving quite complexly in a 3D arrangement. (i) Initial stages of seamount impact by Puke Seamount, (ii) seamount subduction under South Paritu Ridge, and (iii) seamount subduction under Pantin Bank (northern end of Ritchie Ridge).

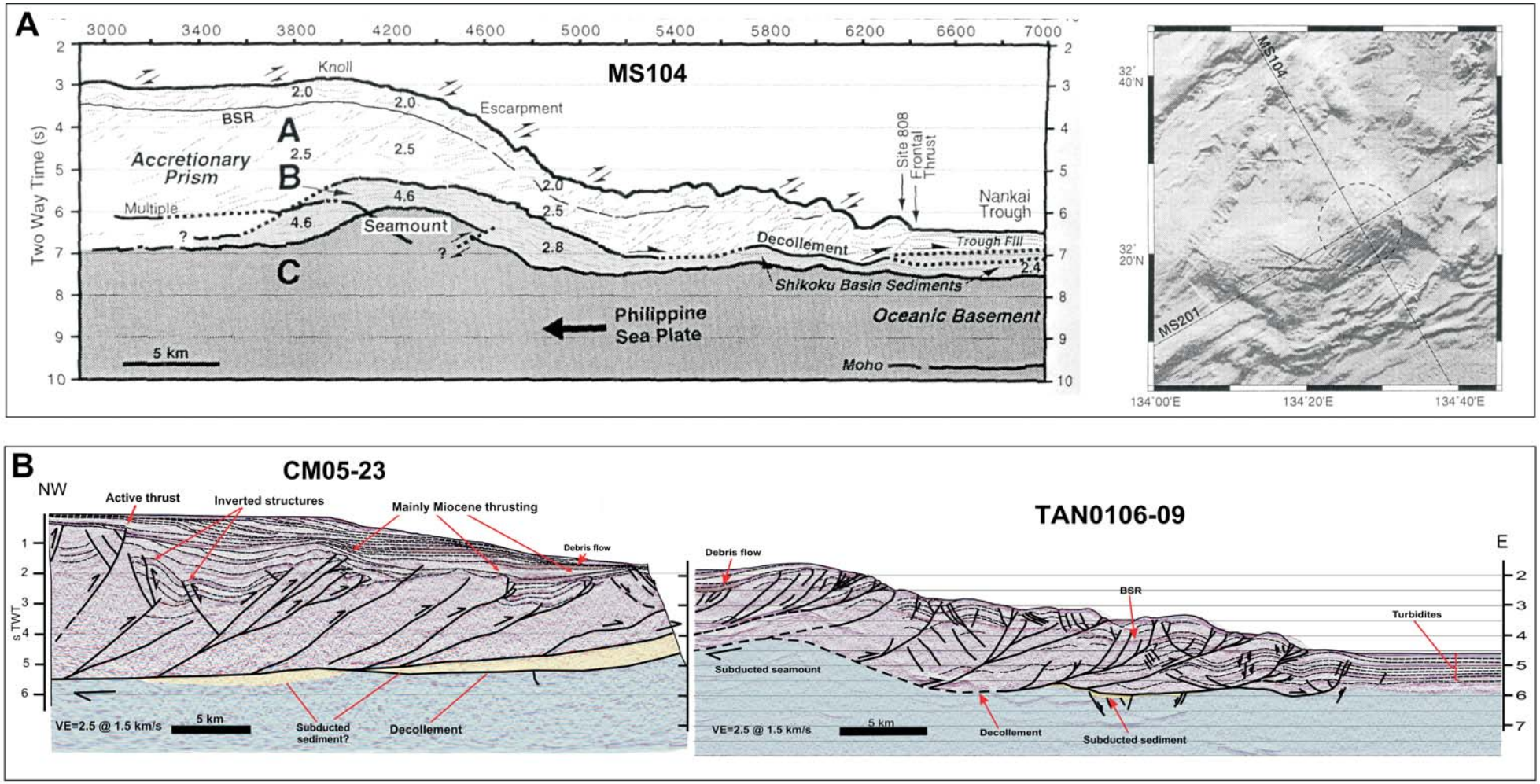

Figure 7.11 A: Time-migrated seismic profile showing seamount subduction beneath the Nankai accretionary wedge. Dashed circle on the shaded seafloor topography on the right shows approximate area in which a circular topographic bulge is observed (from Park et al., 1999).

B: Time-migrated seismic profiles of seamount subduction beneath the Poverty accretionary wedge, south of the Poverty Canyon.

CHAPTER 8: CONCLUSIONS

8.1 SUMMARY OF THE POVERTY INDENTATION

The Poverty Indentation is a complex morphological feature on the Hikurangi margin. It is a first order structural re-entrant extending across the margin slope, formed by the process of seamount subduction. The indentation has evolved sequentially through time as a result of the progressive encroachment, collision, and finally subduction of an initial large seamount, followed by numerous smaller seamounts into the Hikurangi Margin. These multiple smaller seamount impacts have subsequently modified the indentation and these effects can all be effectively modelled using sandbox experiments. Further modification and evolution of the indentation is complicated by the development of a large canyon system down the axis of the re-entrant, accompanied by the formation of an extensive gully system beneath the shelf-slope break, mass movement debris flows, landslides and slumps, and formation of numerous slope basins. The indentation has two distinct styles of frontal wedge with a steep margin front north of the canyon, characterised by erosion and collapse. South of the canyon, the frontal wedge is forming a well-developed accretionary wedge.

Interpretations suggest that: i) seamount impact significantly influences the structure/tectonic evolution, and submarine geomorphology of the inboard slope of the Hikurangi subduction zone, including the generation of large-scale gravitational collapse features; ii) the large gully systems located at the upper shelf slope boundary represent the source areas for the mega debris flows recognised; iii) there exists a complex interaction between the evolving thrust-driven submarine ridges, ponded slope basins and the structural geometry and evolution of the near-surface fault zones (imbrication); and iv) the submarine canyons may initiate complex patterns of fault zone segmentation and displacement transfer within the accretionary slope.

8.1.1 Seamount subduction and formation of the indentation

We infer that several subducting seamounts have significantly influenced the structural evolution and submarine geomorphology of the margin, and relate to the generation of large-scale gravitational collapse features and significant modification of the across-slope sediment transport system.

Evidence points to at least three main seamount subduction events within the Poverty Indentation, each with different margin responses:

i) older substantial seamount impact that drove the first-order perturbation in the margin, since approximately ~1-2 Ma

ii) subducted seamount(s) now beneath Pantin and Paritu Ridge complexes, initially impacting on the margin approximately ~0.5 Ma, and

iii) incipient seamount subduction of the Puke Seamount at the current deformation front.

Margin tectonic activity is partitioned into three main regions from continental shelf to trench floor. Activity is concentrated in the frontal wedge, with inactivity in the mid-upper slope and activity restricted to a few key structures on the continental shelf. Accretion is developing north of Puke Seamount, erosion and over-steepening dominant north of the Poverty Canyon in the axis of the indentation, and a well-developed accretionary wedge is developing south of Poverty Canyon. Ongoing modification of the Indentation appears to be driven by:

i) continued smaller seamount impacts at the deformation front, and currently subducting beneath the mid-lower slope,
ii) low and high sea-level stands accompanied by variations on sediment flux from the continental shelf,
iii) over-steepening of the deformation front and mass movement, particularly from the shelf edge and upper slope.

8.1.2 The development of the Poverty Canyon system

Development of the Poverty Canyon system and excavation of a margin-wide prograding clinoform sequence into the first-order re-entrant following initial seamount impact has provided a major conduit for sediment from the continental shelf directly to trench floor. We infer development of the margin-wide clinoform sequence over the last ~1 Myrs. A simplistic summary of inferred development of the Poverty Canyon is as follows:

i) initial incision into the axis of the indentation following indentation-forming seamount impact ~1 Ma

ii) incipient canyon eroding into the clinoform sequence ~1 - 0.5 Ma, and

iii) full-scale development of a three branched canyon system and extensive erosion of the local clinoform sequence by gullying and landsliding

8.1 FUTURE RESEARCH DIRECTIONS

This study is in a field of research that is in its infancy. Submarine geomorphology focussed on the combination of high resolution multibeam swath bathymetry and multi-channel seismic data is likely to become a major area of research in future years, and it is intended that aspects of this project will provide a foundation for further studies in this area. Additionally, it has become apparent that there is a significant amount of research to be done to better understand active tectonic margin submarine landscapes, in particular the complex relationship between all influences (e.g. tectonic, subducting asperities, seismic, sedimentary) on margin evolution. In this section I propose some directions for future studies, considered in terms of science questions, general methodologies and data requirements.

Current correlations to known sediment sample stations are limited so additional rock/dredge samples and deep-level cores would greatly benefit further study in the Poverty Indentation. Consequently, a large proportion of future research on the Poverty Indentation depends on obtaining that data. Possible future study directions are as follows:

i) Detailed correlation of sedimentary packages, landslide features and activity down the canyons and other sediment conduits within the indentation using cores and sediment samples.

The current network of sediment samples is very limited so a fuller coverage of rock and dredge samples across the indentation, particularly targeting sediment conduits, landslide scars and sediment veneers on growing anticlines (growth strata). Some deeper level cores, penetrating into the base of the Paritu Basin, Lower Paritu Basin and other smaller slope basins would greatly assist investigation into the evolution of such basins and the timing of sediment activity and tectonic effects, particularly the effects of seamount subduction. Constraining timing of certain events and relative ages would require targeting of very specific families of stratigraphic and structural relationships.

ii) Age correlation of the trench-fill sequence via deep-level cores down to the volcaniclastics and top of the Pacific Plate.

This would not only be immensely helpful for the Poverty Indentation situation, it would also open up a huge amount of potential research across the northern Hikurangi margin, and greatly add to research already achieved in the central and southern sectors of the margin. Current estimates of the rates of shortening across the northern sector of the Hikurangi margin front are still very limited, so acquiring cores with good age correlation would really assist our understanding of plate motion budgets across the entire margin and further our understanding of how much plate motion is carried on the subduction interface. This data would also significantly reduce the errors in horizon calculations, enabling more accurate identification of stratigraphy in the frontal wedge and recognising the timing of onset and duration of deformation in different parts of the wedge.

iii) Investigation of the slope north of Poverty Indentation to the Ruatoria debris avalanche.

The region of frontal wedge and slope between these two seamount subduction-formed indentations is also frequented by seamount subduction and is also highly erosional, sediment starved and over-steepened. Currently, there exists no high-quality bathymetry for this sector, and high quality seismic profiles are limited. A brief observation of seismic line CM05-46 which intersects the slope of this section of the margin and runs parallel to the deformation front, reveals some not insignificant relief on the subducting Pacific Plate that deserves further investigation.

iv) Investigate the generation of tsunami in a subduction zone setting and how the different generation mechanisms affect the scale and characteristics of the tsunami produced.

What sort of tsunami hazard might we expect from seamount subduction and associated collapse along the Hikurangi margin? I had intended to investigate this question in this thesis but it was outside the focus of this particular research and not warranted within the limits of this thesis.

APPENDIX 1 - MANUSCRIPT REPRINT

Pedley, K.L., Barnes, P.M., Pettinga, J.R. and Lewis, K., 2009. Seafloor structural geomorphic evolution of the accretionary frontal wedge in response to seamount subduction, Poverty Indentation, New Zealand. Marine Geology, In Press.

APPENDIX 2 - MANUSCRIPT REPRINT

Barnes, P.M., Lamarche, G., Bialas, J., Henrys, S., Pecher, I.A., Netzeband, G.L., Greinert, J., Mountjoy, J.J., Pedley, K.L. and Crutchley, G., 2009. Tectonic and Geological Framework for Gas Hydrates and Cold Seeps on the Hikurangi Subduction Margin, New Zealand. Marine Geology, In Press.

APPENDIX 3 - DEPTH CONVERSION

APPENDIX 4 - SEISMIC PROFILES